






Universitat Autònoma de Barcelona

**Development of antibody-based antitumor therapies based on Trastuzumab:
antibody-drug conjugates, immunocytokines and fragment conjugates**

Joan Miret Minard

ADVERTIMENT. L'accés als continguts d'aquesta tesi queda condicionat a l'acceptació de les condicions d'ús establertes per la següent llicència Creative Commons:  http://cat.creativecommons.org/?page_id=184

ADVERTENCIA. El acceso a los contenidos de esta tesis queda condicionado a la aceptación de las condiciones de uso establecidas por la siguiente licencia Creative Commons:  <http://es.creativecommons.org/blog/licencias/>

WARNING. The access to the contents of this doctoral thesis it is limited to the acceptance of the use conditions set by the following Creative Commons license:  <https://creativecommons.org/licenses/?lang=en>

Development of antibody-based antitumor therapies based on Trastuzumab: antibody-drug conjugates, immunocytokines and fragment conjugates

A dissertation submitted in partial fulfillment of the requirements for the degree of:

Doctor of Philosophy in Biotechnology

Universitat Autònoma de Barcelona

Department of Chemical, Biological and Environmental Engineering

Group of Cellular Engineering and Bioprocesses

Supervisors:

Dr. Jordi Joan Cairó Badillo, Dr. Martí Lecina Veciana and

Dr. Antoni Casablanças Mira

Joan Miret Minard

October 2019



JORDI JOAN CAIRÓ BADILLO, Professor Titular del Departament d'Enginyeria Química, Biològica i Ambiental de la Universitat Autònoma de Barcelona, ANTONI CASABLANCAS MIRA, Tècnic Superior de suport a la recerca de la Universitat Autònoma de Barcelona, i MARTÍ LECINA VECIANA, Professor contractat doctor a l'Institut Químic de Sarrià de la Universitat Ramon Llull.

CERTIFIQUEM:

Que el graduat Joan Miret Minard ha dut a terme sota la nostra direcció, als laboratoris del Departament d'Enginyeria Química, Biològica i Ambiental de la Universitat Autònoma de Barcelona, el treball que, amb el títol de "Development of antibody-based antitumor therapies based on Trastuzumab: antibody-drug conjugates, immunocytokines and fragment conjugates", es presenta en aquesta memòria, la qual consisteix la seva Tesi per optar al grau de Doctor en Biotecnologia.

I perquè en prengueu coneixement i tingui els efectes que corresponguin, presentem davant de l'Escola de Doctorat de la Universitat Autònoma de Barcelona l'esmentada Tesi, signada aquesta certificació a

Bellaterra, Juliol de 2019

Jordi Joan Cairó Badillo

Antoni Casablanças Mira

Martí Lecina Veciana

Agraïments

I sí, sembla mentida però finalment, després de gairebé quatre anys molt intensos i dels quals tindrè sempre un gran record, ha arribat el moment d'anar tancant això.

Voldria començar donant les gràcies a totes aquelles persones que d'alguna manera o altra han tingut un impacte directe en la realització d'aquesta tesi. En primer lloc, m'agradaria agrair molt especialment als directors Jordi J. Cairó, Toni Casablanca i Martí Lecina haver-me donat l'oportunitat de poder participar en aquest projecte, durant el qual m'han guiat i donat suport en tot moment, sempre tenint la porta del despatx oberta i baixant a ajudar a peu de canó al laboratori quan feia falta. Amb vosaltres he après molt a nivell científic i també personal.

Moltes gràcies també a tots els companys del GECIB/projecte FHP, grans persones, científics i professionals amb qui ha estat un privilegi poder compartir vivències dins i fora del lab, especialment al Ramón, que ha estat una referència constant des del moment que vaig entrar al grup i a qui dec, com a mínim, la part de producció del Trastuzumab; a la Mercè i el Marc, dos animals (en el més bon sentit de la paraula) amb qui hem lluitat el món dels ADCs, sense ells aquest treball no hagués estat possible; i a l'Iván i el Pere, dos grans companys a qui també he d'agrair ajudes en fermentacions i mil coses més.

Voldria esmentar també el Jordi Prat, amb les seves converses combinant saviesa i humor polèmic a parts iguals, i l'Oscar, un gran manetes.

També vull agrair la dedicació i esforç als diferents alumnes que m'han ajudat durant aquest temps, no tot ha anat sempre com volíem però crec que en general hem après bastant i ens ho hem passat prou bé: l'Aida, la Daniela, la Claudia, la Cristina, el Guillem, l'Anna, el Lluç, l'Álvaro, el Guille, l'Isaac, la Bea, la Maria, la Sara i el Víctor. Gràcies també als altres alumnes amb qui no he treballat directament però que han passat pel grup i amb qui també hem acabat compartint reunions, dinars, etc, penso especialment en el Joan Triquell i la Mariona.

Tampoc em voldria oblidar d'altres persones del Departament com la Rosi, la Pili i el Manuel, o les secretàries, que fan que tot funcioni.

Voldria agrair també totes aquelles persones externes al grup que han contribuït també a la feina de la tesi: al Dr. Quim Vives per haver-me obert les portes del BST, i al seu grup de teràpies avançades per la bona acollida que em va donar, especialment la Clémentine Mirabel, per totes les hores que vam passar amb la proliferació dels limfòcits. Gràcies també a la Dra. Ibane Abasolo del VHIR, finalment hem pogut desenvolupar un bon assaig *in vivo*; també a la Dra. Sarah Cianferani i el seu equip del LSMBO, per tots els experiments en espectrometria de masses.

Voldria també tenir un record per a tots els amics i amigues de Barcelona, alguns d'ells exiliats a l'estranger (em deixo gent i l'ordre no és rellevant: Sergio, Dani, Èric, Carol, Alejandro, Xavi, Ànnia, Dídac, Joan, Miquel, Alba...), ara ja no hi haurà l'excusa de la tesi per no quedar més sovint (potser m'hauré d'inventar una nova excusa...).

I finalment, moltes gràcies a la família, especialment als meus pares i als noobs del Roger i el Gabriel, pel suport mostrat durant tot aquest temps.

En resum, moltes gràcies a tots.

Summary

The thesis is focused on the development of antibody based therapeutic molecules for the treatment of HER2 positive breast cancer. The generated molecules consist in antibody-drug conjugates (ADCs) including whole antibody and antibody fragment conjugates, and an immunocytokine, all of these molecules being based on the model monoclonal antibody Trastuzumab. This work comprises the whole production and characterization process of the molecules, going from the cloning of the genetic sequences of the antibody molecules to the *in vitro* analysis of their antiproliferation activity, and, for one of the developed candidates, an *in vivo* assessment of its therapeutic potential was also performed.

In a first step, the reference antibody Trastuzumab was produced using the mammalian cell line HEK293, its production being characterized in shake flasks as well as in 5L and 50L single use culture strategies. An operation sequence was defined for recovering and purifying the product, obtaining purity levels in the order of 99% and physicochemical characterization tools were implemented in order to assess the quality of the product. The production, purification and characterization strategies developed for Trastuzumab were applied to the other antibody-derived molecules later produced.

In a first attempt to develop a Trastuzumab antibody-derived molecule with an enhanced therapeutic activity, Trastuzumab was fused to the cytokine interferon- α 2, forming an immunocytokine. This construct, however, did not result in an improved antiproliferative activity with respect to Trastuzumab, as assessed in an *in vitro* 2D proliferation assay. It did not result neither in an activation of the immune system, as analyzed in an *in vitro* lymphocyte proliferation assay.

An increased potency of the antiproliferative activity of Trastuzumab was achieved by heterogeneously conjugating it to the cytotoxic drugs DM1 and vcMMAE, with drug-antibody ratios (DARs) of 3.1 and 4, respectively, applying two of the main

reference conjugation strategies found in commercially approved ADCs: conjugation to endogenous lysine residues of the antibody (DM1), and conjugation to endogenous interchain cysteine residues after a partial reduction step (vcMMAE). After successfully implementing the conjugation strategies and DAR characterization tools, site-directed conjugation strategies (yielding homogeneous products that have therapeutic advantages in the form of a wider therapeutic window) were attempted.

Three different strategies were implemented for the homogeneous conjugation of Trastuzumab. In a first simple and straightforward strategy, Trastuzumab was conjugated to vcMMAE with an aimed DAR of 8, by applying a complete reduction of the antibody. High DARs, however, can result in instability and impaired *in vivo* therapeutic efficacy of the ADC. Therefore, the homogeneous conjugation for a DAR of 2 was attempted by inserting a cysteine in the sequence of Trastuzumab and conjugating the vcMMAE drug to it, obtaining a DAR of 1.79. An innovative alternative strategy to obtain an homogeneous ADC with a DAR of 2 was also developed, consisting in the cysteine conjugation of an independently produced light chain, which is then assembled with independently produced heavy chains, forming an homogeneous ADC with a DAR of 2.

The heterogeneous and homogeneous conjugation strategies implemented for whole Trastuzumab antibody were also applied to Trastuzumab-based scFv antibody fragments, resulting in conjugation processes with a low recovery yield due to precipitation issues.

The different generated ADCs had their antiproliferation activity tested in 2D *in vitro* models using the breast cancer model SKBR3 cell line, confirming their antitumor potential. 3D culture models were also generated, showing a higher resistance to the developed drugs than the 2D display. Finally, the therapeutic effect of the homogeneous ADC formed by the chains assembly was tested on a developed mouse

model *in vivo*, displaying a strong antitumor response, and therefore validating the whole developed ADC production process.

Resum

La tesi està centrada en el desenvolupament de molècules terapèutiques basades en anticossos per al tractament de càncer de mama HER2 positiu. Les molècules generades consisteixen en anticossos conjugats a drogues (ADCs) i una immunocitoquina, totes aquestes molècules basades en l'anticòs monoclonal model Trastuzumab. Aquest treball comprèn el procés producció i caracterització de les molècules, partint del clonatge de les seqüències dels anticossos i anant fins l'anàlisi *in vitro* de la seva activitat antiproliferativa, i, per a un dels candidats desenvolupats, analitzant també el seu potencial terapèutic *in vivo*.

Com a primer pas, l'anticòs de referència Trastuzumab ha estat produït mitjançant la línia cel·lular HEK293, s'ha caracteritzat la producció a escala matràs així com en sistemes d'un sol ús de 5 i 50 litres. També s'ha definit una seqüència d'operacions per a la recuperació i purificació del producte, amb la qual s'ha obtingut una puresa de l'ordre del 99%. Així mateix, s'han implementat eines per a la caracterització fisicoquímica del producte obtingut. Les estratègies de producció, purificació i caracterització desenvolupades per a l'anticòs Trastuzumab han estat aplicades a la resta de molècules derivades d'anticòs, produïdes posteriorment.

En un primer intent per a desenvolupar molècules derivades de Trastuzumab amb una activitat terapèutica incrementada, l'anticòs Trastuzumab ha estat fusionat a la citoquina interferó- $\alpha 2$, en forma d'immunocitoquina. Aquest constructe, però, no ha generat una activitat antiproliferativa més potent que la del Trastuzumab, ni tampoc ha resultat en una activació del sistema immunitari. Ambdues activitats han estat analitzades en assajos *in vitro*.

L'increment de la potència antiproliferativa de l'anticòs Trastuzumab ha estat aconseguïda a través de la seva conjugació a les drogues citotòxiques DM1 i vcMMAE, amb ràtios droga-anticòs (DAR) de 3.1 i 4, respectivament. Aquesta estratègia implica l'aplicació de dos dels principals mètodes de conjugació de

referència, utilitzats en ADCs aprovats comercialment: conjugació a residus endògens de l'anticòs de lisina (DM1) i de cisteïna, després d'una reducció parcial (vcMMAE). També s'han aplicat estratègies de conjugació dirigida, les quals generen ADCs homogenis, que presenten un índex terapèutic més favorable.

Tres estratègies diferents han estat implementades per la conjugació homogènia de l'anticòs Trastuzumab. En una primera estratègia, l'anticòs ha estat conjugat a la droga vcMMAE amb un DAR objectiu de 8, mitjançant una reducció completa de l'anticòs. DARs elevats, però, poden causar inestabilitat de la molècula i perjudicar-ne l'efecte *in vivo*. Així, s'ha realitzat la conjugació homogènia amb un DAR objectiu de 2, a través de la inserció d'una cisteïna a la seqüència del Trastuzumab, la qual ha estat conjugada al vcMMAE, amb un DAR resultant d'1.79. També s'ha desenvolupat una estratègia innovadora per tal d'obtenir un ADC homogeni amb un DAR de 2, basada en la conjugació del residu de cisteïna de cadenes lleugeres produïdes independentment, després unides a cadenes pesades també produïdes independentment: s'obté un ADC homogeni amb un DAR de 2.

Les estratègies de conjugació heterogènies i homogènies implementades per a l'anticòs Trastuzumab sencer han estat també aplicades a fragments scFv, en aquest cas, han resultat en processos amb un baix rendiment de recuperació a causa de la poca estabilitat dels conjugats.

Els diversos ADCs generats en aquest treball han estat analitzats en models *in vitro* 2D amb la línia cel·lular SKBR3, model de càncer de mama, amb els quals s'ha confirmat el seu potencial anticancerós. També s'han desenvolupat models 3D, els quals han estat més resistents que els models 2D. Finalment, l'efecte terapèutic de l'ADC homogeni format per la unió de les cadenes independents ha demostrat una forta activitat terapèutica en un model de ratolí *in vivo*, validant, així, el procés de producció d'ADCs desenvolupat.

Resumen

La tesis se centra en el desarrollo de moléculas terapéuticas basadas en anticuerpos monoclonales para el tratamiento de cáncer de mama HER2 positivo. Las moléculas generadas consisten en anticuerpos conjugados a drogas (ADCs) y una inmunocitoquina, todas ellas basadas en el anticuerpo monoclonal modelo Trastuzumab. Este trabajo comprende el proceso de producción y caracterización de las moléculas, partiendo del clonaje de las secuencias de los anticuerpos, y llegando hasta el análisis *in vitro* de su actividad antiproliferativa, y, para uno de los candidatos desarrollados, analizando también su potencial terapéutico *in vivo*.

Como primer paso, el anticuerpo de referencia Trastuzumab ha sido producido mediante la línea celular HEK293, caracterizándose su producción a escala matraz así como en sistemas de un solo uso de 5 y 50 litros. Se ha definido una secuencia de operaciones para la recuperación y purificación del producto, con la cual se ha conseguido una pureza aproximada del 99%. Asimismo, se han implementado herramientas para la caracterización fisicoquímica del producto obtenido. Las estrategias de producción, purificación y caracterización desarrolladas para el anticuerpo Trastuzumab han sido aplicadas al resto de moléculas derivadas, producidas posteriormente.

En un primer intento para desarrollar moléculas derivadas de Trastuzumab con una actividad terapéutica incrementada, el anticuerpo Trastuzumab ha sido fusionado a la citoquina interferón- α 2, generando una inmunocitoquina. Este constructo, no obstante, no ha causado un incremento en la actividad antiproliferativa del Trastuzumab, ni tampoco ha resultado en una activación del sistema inmunitario, ambas actividades siendo analizadas en ensayos *in vitro*.

El incremento de la potencia antiproliferativa del anticuerpo Trastuzumab ha sido conseguido conjugándolo a las drogas citotóxicas DM1 y vcMMAE, con ratios droga-anticuerpo (DAR) de 3.1 y 4, respectivamente. Esta estrategia implica la aplicación

de dos de los principales métodos de conjugación de referencia, utilizados en ADCs aprobados comercialmente: conjugación a residuos endógenos del anticuerpo de lisina (DM1) y de cisteína, posteriormente a una reducción parcial (vcMMAE). También se han aplicado estrategias de conjugación dirigida, las cuales generan ADCs homogéneos, que presentan un índice terapéutico más favorable.

Tres estrategias diferentes han sido implementadas para la conjugación homogénea del anticuerpo Trastuzumab. En una primera estrategia, el anticuerpo ha sido conjugado a la droga vcMMAE con un DAR objetivo de 8, mediante una reducción completa del anticuerpo. DARs elevados, no obstante, pueden causar inestabilidad de la molécula, perjudicando su efecto *in vivo*. Así, se ha realizado la conjugación homogénea con un DAR de 2, a través de la inserción de una cisteína a la secuencia del Trastuzumab, la cual ha sido conjugada a vcMMAE, obteniendo un DAR de 1.79. También se ha desarrollado una estrategia innovadora para obtener un ADC homogéneo con un DAR de 2, basada en la conjugación del residuo de cisteína de cadenas ligeras producidas independientemente, después unidas a cadenas pesadas también producidas independientemente, obteniendo un ADC homogéneo con un DAR de 2.

Las estrategias de conjugación heterogéneas y homogéneas implementadas para el anticuerpo Trastuzumab entero han sido también aplicadas a fragmentos scFv, dando lugar a procesos de conjugación de bajo rendimiento de recuperación a causa de la inestabilidad de los conjugados.

Los diferentes ADCs generados en este trabajo han sido analizados en modelos *in vitro* 2D con la línea celular SKBR3, modelo de cáncer de mama, con los cuales se ha confirmado su potencial anticancerígeno. También se han desarrollado modelos 3D, los cuales han presentado más resistencia que los modelos 2D. Finalmente, el efecto terapéutico del ADC homogéneo formado por la unión de las cadenas independientes ha demostrado una fuerte actividad terapéutica en un modelo de

ratón *in vivo*, validando, de esta forma, el proceso de producción de ADCs desarrollado.

Abbreviations

ADC: Antibody Drug Conjugate

CDR: Complementarity-Determining Region

CFSE: Carboxy-Fluorescein Diacetate Succinimidyl Ester

CMV: Cytomegalovirus

DAR: Drug Antibody Ratio

DCU: Digital Control Unit

DEPC: Diethyl Pyrocarbonate

DhAA: Dehydroascorbic Acid

DM1: Mertansine or (N2'-deacetyl-N2'-(3-mercapto-1-oxopropyl)-maytansine)

DMA: Dimethyl Acetamide

DMSO: Dimethyl sulfoxide

ER: Estrogen Receptor

ErbB: erythoblastic leukemia viral oncogene B

EGF: Epidermal Growth Factor

EGFR: Epidermal Growth Factor Receptor

ELISA: Enzyme Linked Immunosorbent Assay

FITC: Fluorescein Isothiocyanate

ICK: Immunocytokine

IL: Interleukin

IPTG: Isopropyl- β -D1 thiogalactopyranoside

IRES: Internal Ribosome Entry Site

HBEGF: Heparin Binding Epidermal Growth Factor

HER2: Human Epidermal Receptor 2

HIC: Hydrophobic Interaction Chromatography

HPLC: High Performance Liquid Chromatography

HRG: Heregulin

kDa: kilo Dalton

LAL: Limulus amoebocyte lysate

LAMP: Lysosomal Associated Membrane Protein I

mAb: monoclonal antibody

MAPK: Mitogen Activated Protein Kinase

MCS: Multi-Cloning Site

mRNA: messenger Ribonucleic acid

MS: Mass Spectrometry

MSC: Mesenchymal Stromal Cells

MTS: 3-(4,5-dimethylthiazol-2-yl)-5-(3-carboxymethoxyphenyl)-2-(4-sulfophenyl)-2H-tetrazolium

NHS: N-Hydroxy Succinimide

NK : Natural Killer

NRG-1: epigen neuregulin-1

PAB: *p*-aminobenzylcarbamate

PMA: Phorbol 12-myristate 13-acetate

PBMNC: peripheral blood mononuclear cells

PCR : Polymerase Chain Reaction

PI3K: Phosphoinositide 3-Kinase

PR: Progesterone Receptor

RTK: Receptor Tyrosine Kinase

SDS-PAGE: Sodium Dodecyl Sulfate Polyacrylamide Gel Electrophoresis

SEC: Size Exclusion Chromatography

SMCC: Succinimidyl-4-(N-maleimidomethyl)cyclohexane-1-carboxylate

TCEP: tris(2-carboxyethyl) phosphine

TGF α : Transforming Growth Factor α

TMB : 3,3',5,5'-Tetramethylbenzidine

TNF α : tumor necrosis factor α

ULA: Ultra-low attachment

UV/Vis: Ultraviolet visible

vcMMAE: valine-citrulline Monomethyl Auristatin E

V_{LC}: variable region of the light chain of the antibody

V_{HC}: variable region of the heavy chain of the antibody

INDEX

Agraïments	4
Summary	7
Resum	10
Resumen	12
Chapter 1. Introduction	27
1.1. Breast cancer	27
1.1.1. Broad implications of cancer: definition, impact and treatment.....	27
1.1.2. Breast cancer: impact, physiology and subtypes	30
1.1.3. Human Epidermal Receptor 2 (HER2) positive breast cancer	32
1.1.4. Non-directed therapies against breast cancer	36
1.1.5. Directed therapies against breast cancer.....	38
1.2. Monoclonal antibodies for cancer therapy	41
1.2.1. Therapeutic monoclonal antibodies.....	41
1.2.2. Antibody fragments.....	50
1.2.3. Immunocytokines (ICKs).....	52
1.2.4. Antibody Drug Conjugates (ADCs).....	54
1.2.5. Preclinical models for analyzing therapeutic mAb and derived molecules	70
1.3. Justification of the thesis project	71
1.4. References.....	72
2. Objectives	87
3. Results (I): Development of Trastuzumab production, purification and physicochemical characterization	90

3.1. Introduction.....	90
3.2. Trastuzumab sequence construction and cloning.....	99
3.3. Trastuzumab production, purification and physicochemical characterization establishment.....	102
3.3.1. Cell line characterization: growth and production assessment	102
3.3.2. Purification assay.....	103
3.3.3. Physicochemical characterization of produced Trastuzumab.....	104
3.4. Production in bioreactor platforms.....	115
3.4.1. Production in 5L single use wave bioreactor	115
3.4.2. Production in 50L single use STR bioreactor	116
3.5. Conclusions.....	117
3.6. References.....	118
Chapter 4. Results (II): Development of an Immunocytokine fusion protein based on Trastuzumab and Interferon	124
4.1. Introduction.....	124
4.2. Assessment of antiproliferation and immunomodulation activity tests of IFN α 2	129
4.2.1. Antiproliferation assay: MTS assay	130
4.2.2. Immunomodulation: Lymphocyte proliferation assay	131
4.3. Trastuzumab-IFN α 2 sequence construction and production	133
4.4. Product characterization:.....	136
4.4.1. Confirmation of the correct structure formation of the obtained product: SDS-PAGE.....	136

4.4.2. Antigen recognition capacity of both immobilized and cell surface antigen	137
4.4.3. Antiproliferative activity assessment of Trastuzumab-IFN α 2.....	139
4.5. Conclusions.....	139
4.6. References.....	140
Chapter 5. Results (III): ADCs: Heterogeneous conjugation of Trastuzumab.....	144
5.1. Introduction.....	144
5.2. Trastuzumab conjugation to DM1.....	153
5.2.1. Conjugation process definition	153
5.2.2. Physicochemical characterization of the conjugated product	154
5.2.2.1. DAR: UV/Vis, MS.....	155
5.2.2.2. Antigen recognition capacity: ELISA and flow cytometry	157
5.2.2.3. Aggregates and free drug determination.....	158
5.3. Trastuzumab conjugation to vcMMAE.....	160
5.3.1. Conjugation process definition	160
5.3.2. Characterization of the conjugated product	161
5.3.2.1. DAR: HIC-HPLC.....	161
5.3.2.2. Antigen recognition capacity: ELISA.....	162
5.3.2.3. Aggregates and free drug determination.....	163
5.4. Conclusions.....	165
5.5. References.....	166
Chapter 6. Results (IV): ADCs: Homogeneous conjugation of Trastuzumab with vcMMAE	171
6.1. Introduction.....	171

6.2. Homogeneous conjugation of Trastuzumab with a DAR of 8:	181
6.2.1. Conjugation process definition	181
6.2.2. Physicochemical characterization of the conjugated product.....	182
6.3. Construction and site-directed conjugation of Trastuzumab_cys114 thiomab	184
6.3.1. Trastuzumab_cys114 construction	184
6.3.2. Conjugation of Trastuzumab_cys114: generation of an homogeneous thiomab ADC	189
6.4. Construction and conjugation of an homogeneous Trastuzumab ADC without genetic modification: conjugation and assembly of independently produced heavy and light antibody chains	196
6.4.1. Heavy and light chains sequence obtention	196
6.4.2. Chains assembly assessment.....	201
6.4.3. Conjugation of the light chain and assembly of the ADC.....	203
6.5. Conclusions.....	209
6.6. References.....	210
Chapter 7. Results (V): Generation and conjugation of antibody fragments based on Trastuzumab.....	217
7.1. Introduction.....	217
7.2. scFv production in <i>Escherichia coli</i>	220
7.2.1. Sequence construction and cloning	220
7.2.2. Production, purification and characterization	222
7.3. scFv production in HEK293 and heterogeneous conjugation	227
7.3.1. Sequence construction and cloning	227

7.3.2. Production, purification and characterization	228
7.3.3. Conjugation and characterization	231
7.4. scFv_cys111: production in HEK293 and homogeneous conjugation	234
7.4.1. Sequence definition, construction and cloning.....	234
7.4.2. Production, purification and characterization	237
7.4.3. Conjugation and characterization	239
7.5. Conclusions.....	242
7.6. References.....	243
Chapter 8. Results (VI): biological activity assessment of the generated ADCs.....	246
8.1. Introduction.....	246
8.2. 2D <i>in vitro</i> assays with SKBR3 cell line:	252
8.2.1. MTS antiproliferation activity assay development and ADCs assessment	252
8.3. 3D <i>in vitro</i> assays with SKBR3 cell line:	258
8.3.1. 3D culture with SKBR3: assessed methodologies	258
8.4. <i>In vivo</i> assay: tumor model with SKBR3 cell line	265
8.4.1. Model mice generation	265
8.5. 2D <i>in vitro</i> assays with BT474 cell line:.....	267
8.6. 3D <i>in vitro</i> assays with BT474 cell line:.....	268
8.7. <i>In vivo</i> assay: tumor model with BT474 cell line	271
8.7.1. Model mice generation	271
8.7.2. <i>In vivo</i> ADC validation.....	272
8.5. Conclusions.....	275
8.6. References.....	276

Chapter 9. Concluding remarks and future work	283
Chapter 10. Materials and methods	290
10.1. Biologic material.....	290
10.1.1. Mammalian cell lines.....	290
10.1.2. Bacterial strains	292
10.2. Culture media	292
10.2.1. Culture media for mammalian cell lines	292
10.2.2. Culture media for bacterial strains.....	293
10.3. Maintaining and assessment of the biologic material	298
10.3.1. Mammalian cell line maintenance	298
10.3.2. Mycoplasma contamination assessment of mammalian cell lines	301
10.3.3. Bacterial strains maintaining.....	302
10.4. Culture systems	303
10.4.1. Culture systems for mammalian cell lines.....	303
10.4.2. Bacterial strains	307
10.5. Cell culture analysis.....	310
10.5.1. Cell counting and viability assessment.....	310
10.6. Plasmid vectors	311
10.6.1. Initial (base) vectors	311
10.6.2. Vector derived from pRESpuro3: pTRIpuro3.....	314
10.6.3. Expression vectors constructed in this thesis	315
10.7. Molecular biology techniques	315
10.7.1. Extraction and obtaining of plasmid DNA	315

10.7.2. Separation and purification of the genetic material: DNA electrophoresis	317
10.7.3. DNA quantification through spectrophotometry.....	320
10.7.4. Polymerase chain reaction (PCR)	320
10.7.5. DNA enzymatic modifications	323
10.7.6. DNA dephosphorylation.....	325
10.7.7. Ligation of DNA fragments	326
10.7.7. Introduction of genetic material into organisms	327
10.7.8. Sequencing of DNA.....	329
10.8. Antibody purification.....	330
10.8.1. Solid-liquid separation.....	330
10.8.2. Cell disruption	332
10.8.3. Microfiltration	332
10.8.4. Concentration.....	333
10.8.5. Chromatography	334
10.9. Protein characterization.....	337
10.9.1. Molecular weight and purity: SDS-PAGE.....	337
10.9.2. Concentration determination: SDS-PAGE and spectrophotometry....	338
10.9.3. Antigen binding assessment.....	339
10.9.4. Aggregates determination and free drug determination: Size-Exclusion Chromatography-HPLC.....	343
10.9.5. Mass and glycosylation pattern determination: Mass Spectrometry (MS)	344
10.9.6. Endotoxin content test: LAL method	344

10.10. Antibody/fragment conjugations	345
10.10.1. Heterogeneous conjugation with DM1	345
10.10.2. Heterogeneous conjugation with vcMMAE	348
10.10.3. Homogeneous conjugation with vcMMAE.....	350
10.11. Characterization drug-antibody ratio (DAR) in conjugated ADCs	358
10.11.1 DAR determination: UV spectroscopy.....	359
10.11.2. DAR determination: Hydrophobic Interaction Chromatography.....	360
10.11.3. DAR determination: Mass Spectrometry assay (MS)	363
10.12. Biological activity assessment of protein and ADC products	365
10.12.1. MTS antiproliferation assay.....	365
10.12.2. Lymphocyte proliferation assay	367
10.12.4. 3D Model generation	372
10.12.6. <i>In vivo</i> assay.....	379
10.13. References.....	382
Chapter 11. Appendix.....	386
11.1 Appendix I. Genetic and protein sequences	386
11.2. Appendix II. Oligonucleotides.....	389
11.3 Appendix III. Mass Spectrometry profiles	391

Chapter 1. Introduction

Chapter 1. Introduction

1.1. Breast cancer

1.1.1. Broad implications of cancer: definition, impact and treatment

Cancer is a generic term that includes several diseases characterized by the growth of abnormal cells beyond their usual boundaries, based on an uncontrolled division and loss of differentiation. It is one of the most spread diseases in the world, being the second leading cause of global death globally and accounting for 8.8 million deaths in 2015 (WHO, 2018), and an increase to 19.3 million cases per year expected for 2025. The majority of cancer cases occur in low- and middle-income countries, and this trend is expected to increase by 2025 (Block et al., 2015). Moreover, it has a big economic impact in the society, the direct medical cost for cancer being estimated at \$80.2 billion only in the US in 2015 (“Economic Impact of Cancer,” 2018). Cancer development is originated by damage or mutation of proto-oncogenes that are involved with the regulation of the cell proliferation and differentiation, as well as tumor suppressor genes that code for proteins related to the generation of signals that inhibit cell growth and/or stimulate apoptosis (Pérez-Herrero et al., 2015). Environmental as well as hereditary causes lie behind these mutations (Arnold et al., 2012). Cancer cells form tumors that, in their solid form, interact with different cell types that collectively allow the tumor growth and progression (Figure 1.1) (Hanahan et al., 2011).

Chapter 1. Introduction

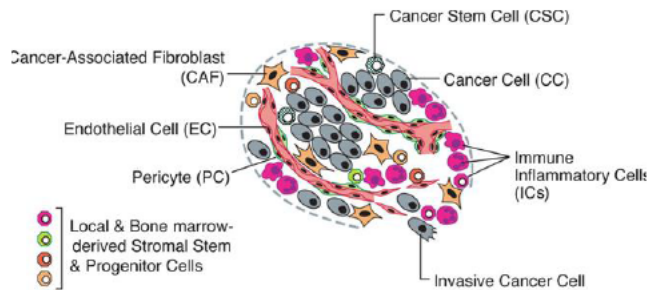


Figure 1.1: Depiction of a tumor with cancer cells and other cell types found in the tumor microenvironment (Hanahan et al., 2011).

There are several types of cancers, the most important in terms of affected people being: lung, colorectal, prostate, stomach and liver for men; and breast, colorectal, lung, cervix and stomach for women (WHO, 2018). Depending on the cell type in which they start, they can be classified into different subtypes (Table 1.1).

Table 1.1: cancer types and origin

Cancer types	Cancer origin
Carcinoma	Skin or tissues that line or cover internal organs.
Sarcoma	Connective or supportive tissues such as bone, cartilage, fat, muscle or blood vessels.
Leukaemia	Blood forming tissue such as the bone marrow and causes abnormal blood cells to be produced and go into the blood
Lymphoma and myeloma	Cells of the immune system
Brain and spinal cord cancers	Central nervous system

Chapter 1. Introduction

Treatment of cancer includes several main strategies, which are summarized in table 1.2. Conventional treatments include surgery, radiotherapy and chemotherapy, this last method being the trademark medical treatment for cancer since it was approved around 60 years ago (Baudino, 2015). However, both radiotherapy and chemotherapy are non-targeted, potentially affecting non-cancerous cells and generating strong secondary effects on the patient. Alternative treatments in which a more selective and effective approach is attempted include targeted therapy, which can include hormone therapy and immunotherapy (see Table 1.2 and Figure 1.2).

Table 1.2: therapies for cancer treatment

Therapy	Characteristics
Surgery	First line of attack against cancer, tumor is removed from the body
Radiotherapy	Use of high doses of radiation to kill cancer cells and shrink tumors
Chemotherapy	Chemical drugs are used to kill cancer cells
Targeted therapy	Cancer cells are specifically targeted, with molecules such as antibodies:
Hormone therapy	Inhibits the growth of cancers that rely on hormones to grow
Immunotherapy	The immune system is activated in order to attack tumor cells

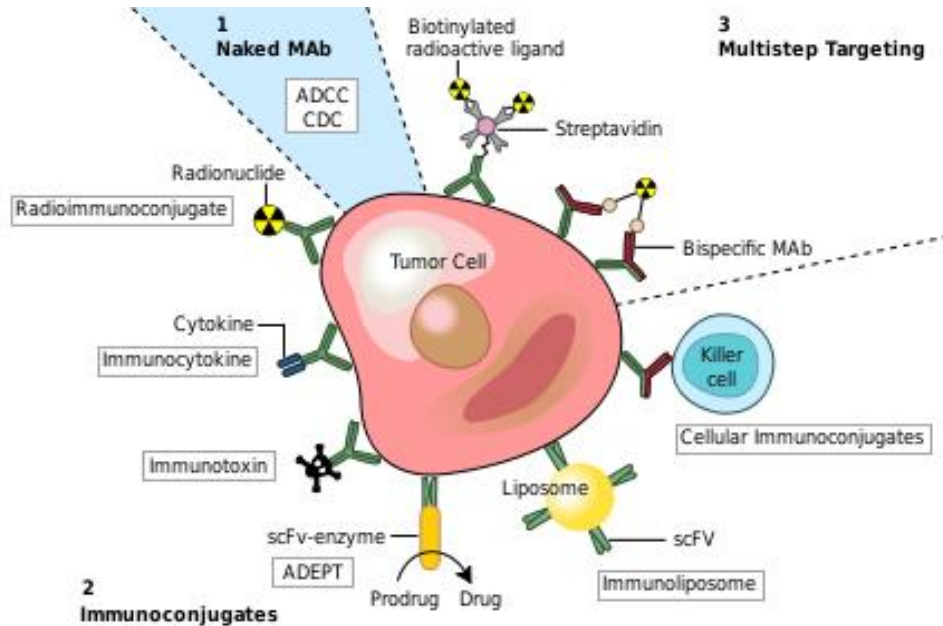


Figure 1.2. Schematic representations of different antibody-derived molecules potentially applied for targeted cancer therapies. Obtained from (Paul Carter, 2001).

In relation to this topic, the thesis work presented will focus on targeted therapies, which are based on molecules that allow a specific targeting of the tumor cells, mainly: monoclonal antibodies (and molecules derived from them, such as antibody-drug conjugates (ADCs), or immunotoxins (Akbari et al., 2017)) and small molecule inhibitors (which include several molecules such as hormones) (Baudino, 2015). Cancer is treated according to different parameters such as the type of cancer and its stage of development (“Stages of cancer | Cancer Research UK,” 2017).

1.1.2. Breast cancer: impact, physiology and subtypes

Breast cancer is the most prevalent cancer in women, in both developed and developing countries (Society, 2011), with an estimated 1.7 million newly diagnosed cases worldwide in 2012 alone (Kalimutho et al., 2015). It accounted for 41% of total cancer cases in women in the US in 2012 (Siegel et al., 2013). Survival to breast

Chapter 1. Introduction

cancer is not evenly distributed: there is an estimated 5-year survival of 80% in high income countries, while in developing countries it drops to below 40% (Coleman et al., 2008). Its classification and prognosis have historically relied on the analysis of both tumor morphology and molecular markers (mainly estrogen receptors (ER), progesterone receptor (PR) and human epidermal receptor 2 (HER2) (Kalimutho et al., 2015).

Since it is a heterogeneous disease, breast tumors can be classified into four main molecular subtypes: luminal A, luminal B, HER2+, and basal-like (Guiu et al., 2012). The luminal subtype is characterized by a high expression of receptors for estrogen (ER) and progesterone (PR), while HER2+ tumors are negative for ER and PR, but express high levels of HER2. The basal-like class of breast tumors comprises the triple-negative breast cancers (TNBCs) and is defined by lack of ER, PR, and HER2 expression (Tudoran et al., 2015). Each type is summarized on Table 1.3.

Table 1.3: breast tumor types and characteristics

Breast tumor type	Characteristics
Luminal A	PR/ER positive. They are often low grade and treatable with hormonal therapies. They generally exhibit the best outcomes among all subtypes.
Luminal B	Usually ER positive, and may be associated with either HER2 overexpression or high levels of Ki67. Treatable by hormonal therapy, but they frequently relapse and present a poor clinical outcome (Canello et al., 2013).

HER2+	HER2 overexpressed. Aggressive. Treated with monoclonal antibodies Trastuzumab or pertuzumab or small-molecule kinase inhibitor lapatinib (Schnitt, 2010).
Basal-like / Triple negative	ER, PR, HER2 negative. Treatable only with chemotherapy and radiotherapy.

Breast cancer treatment is designed on the basis of this classification, luminal tumors having a more favorable prognosis, while TNBC patients (Onitilo et al., 2009) and HER2 positive patients (Tolaney et al., 2015) (Gutierrez & Schiff, 2011) have been historically affected by a poor prognosis.

1.1.3. Human Epidermal Receptor 2 (HER2) positive breast cancer

HER2 positive breast tumors, as previously stated, are defined by presenting an overexpression of the HER2 gene. The human Epidermal Growth Factor Receptor 2 (HER2) can be known as HER-2/*neu* (*neu* in rodents (Wieduwilt et al., 2008)) or ErbB2, although HER2 remains the most commonly used designation (Cooke, 2000). It is a member of the ErbB family of cell surface receptor tyrosine kinases (RTKs), which takes part in the transmission of signals involved in controlling normal cell growth and differentiation (Rubin & Yarden, 2001). ErbB gene symbol is derived from the homologous erythroblastic leukemia viral oncogene B (Vennström et al., 1982). The HER2 receptor is a 185 kDa type 1 transmembrane glycoprotein, encoded by the HER2 gene, a proto-oncogene located on the long arm of chromosome 17 (Coussens et al., 1985).

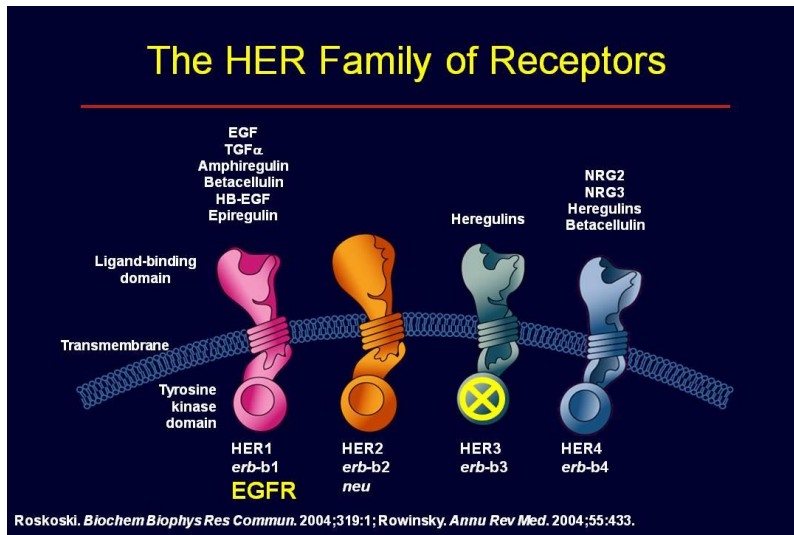


Figure 1.3: HER family of receptors. Obtained from (Roskoski, 2014).

The ErbB family (Figure 1.3) consists of four members: HER1 (also EGFR (Epidermal Growth Factor Receptor) or ERBB1), HER2 (*Neu* or ERBB2), HER3 (ERBB3) and HER4 (ERBB4). All of four receptors have three domains: Ligand binding, Transmembrane and Tyrosine kinase domains (Roskoski, 2014).

All members of the HER Family, with the exception of HER2, have several known ligands, and at least 11 of which have been identified: Epidermal Growth Factor (EGF), Transforming Growth Factor-alpha (TGF- α), amphiregulin, betacellulin, Heparin Binding-EGF (HBEGF), epiregulin, epigen, neuregulin-1 (NRG-1)/Heregulin (HRG), NRG-2, NRG-3 and NRG-4 (Baselga et al., 2009). Ligand binding induces either homodimer formation between two identical HER receptors, or heterodimer formation between two different HER receptors (Cooke, 2000).

The extracellular domain of HER proteins can exist in a closed inhibited conformation or an open active one. The ligand binding induces a conformational change in their extracellular domain that in turn induces the active conformation and promotes their dimerization and consequent trans-phosphorylation (Moasser, 2007).

Chapter 1. Introduction

Dimerization activates the tyrosine kinase activity of the intracellular domain, which provokes the activation of several downstream signalling pathways, such as MAPK (Mitogen Activated Protein Kinase) or Akt-PI3K (Protein Kinase B-phosphoinositide 3-kinase) pathway, which control several processes, including cell proliferation, survival, migration, invasion and differentiation. Related to a tumour environment, this also leads to tumour cell survival (Baselga et al., 2009).

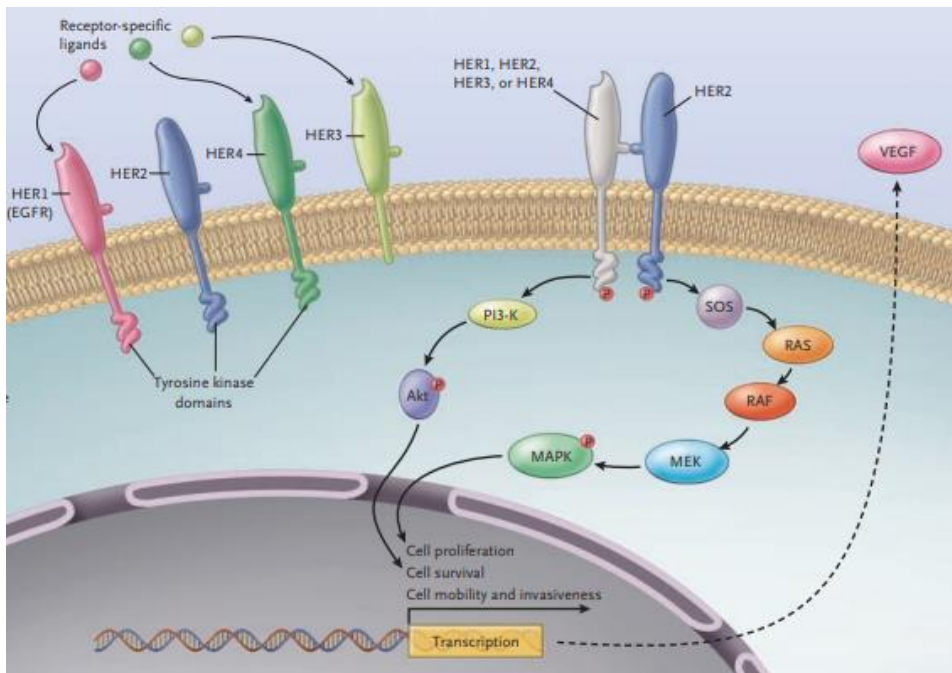


Figure 1.4. HER receptors cellular activity. Obtained from (Hudis, 2007).

HER2, unlike the other HER-family receptors, constitutively exists in an active conformation. Consistent with this fact, it lacks an endogenous ligand (Garrett et al., 2003), being considered an “orphan receptor”. This lack of ligand binding activity causes it to partner with other receptors of the family in order to perform its signalling activity (Moasser, 2007). Of these associations, the HER2-HER3 heterodimer is considered the most potent HER-dimer with regards to the strength of interaction, ligand induced tyrosine phosphorylation and downstream signalling

Chapter 1. Introduction

(Franklin et al., 2004). This can be related to the fact that HER2 lacks ligand binding activity while HER3, unlike the other members of the family, lacks ATP binding within its catalytic domain. Individually they are, therefore, incomplete signalling molecules. Several studies have shown that the interaction between HER2 and HER3 generates the most active signalling heterodimer of the family and it is essential for many biological and developmental processes (Britsch et al., 1998; Sliwkowskiso et al., 1994; Tzahar et al., 1996).

The HER2 protein can be deregulated via different mechanisms, including point mutations occurring in the tyrosine kinase domain and protein overexpression, generally resulting from HER2 gene amplification, which represents the most widely known mechanism underlying HER2 deregulation in many cancers. Overexpression can cause the appearance of an abnormally high number of monomers on the cell membrane, which favours receptor interaction and results in constitutively activated signal transduction. HER2 overexpression and/or amplification were initially discovered in approximately a third of human breast cancers and were associated with more aggressive tumour behaviour and poorer outcomes (Slamon et al., 1987). Further studies showed that HER2/*neu* (*c-erbB-2*) is amplified and/or overexpressed in some 18-25% of human breast cancers, depending on different factors such as the diagnostic technique used (Baselga et al., 2009). Numerous studies have shown that this event is associated with a more aggressive phenotype. In particular, HER2/*neu* overexpressing tumors are known to be refractory to various types of chemo- and endocrine therapy (often associated with down-regulation of the estrogen receptor; ER) and to be associated with shortened overall survival (Wilso et al., 2002).

Other studies have reported HER2 overexpression and/or amplification in a variety of other cancer types, including gastric, colorectal, salivary gland, bladder, ovarian, stomach, oesophagus, colon, kidney, prostate and lung cancers (Scholl et al., 2001). In these different types of solid tumours, a correlation of the HER2 status in the

primary tumour and the paired distant metastatic lesions was observed, thus supporting the key role of HER2 deregulation in tumour progression and spreading (Martin et al., 2014).

The important biological role of HER2 in the signaling network that drives epithelial cell proliferation, together with its extracellular accessibility and its overexpression in some human tumors led to considering HER2 as an appropriate target for tumor-specific therapies (Molina et al., 2001).

1.1.4. Non-directed therapies against breast cancer

Breast cancer is treated using different strategies, depending on the subtype of the disease and the stage of development of each case. Conventional therapies include surgery, radiotherapy and chemotherapy. Surgery is carried out in order to remove the tumor by surgical means. It involves breast conserving surgery or mastectomy. Surgery is applied more predominantly in patients at early stages of development of the tumor. Of all the patients diagnosed with breast cancer in England during 2013-14, 81% of them had surgery to remove their primary tumor as part of their primary cancer treatment (NCRAS, 2018).

Radiotherapy is a treatment based on using ionizing radiation that focused on the tumor site, therefore targeting all the cells localized into the tumor microenvironment (Baudino, 2015). In breast cancer it is often applied following surgery, although it can also be independently applied. When applied following breast conserving surgery, in regional or localized cancers, long-term survival is the same as with mastectomy (Miller et al., 2016). Approximately 56% of breast cancer patients received radiation therapy in the US in 2014-15 (American Cancer Society, 2015).

Another conventional treatment strategy consists on the use of chemotherapy. Chemotherapy relies in a systemic application (i.e., treating the whole body) of molecules that attack fast dividing cells, which are characteristic of cancer. Therefore, these molecules are intended to target elements of the cell related to the cellular division or DNA synthesis. Common drug types used in chemotherapy include: alkylating agents, topoisomerase inhibitors, anthracyclines, plant alkaloids or pyrimidine and purine metabolites (Baudino, 2015). In the case of breast cancer, the most common chemotherapy drugs for breast cancer treatment include anthracyclines, such as doxorubicin and epirubicin, taxanes, such as paclitaxel and docetaxel, 5-fluorouracil, cyclophosphamide, and carboplatin (Table 1.4). Most often, combination of 2 or 3 of these drugs are used. In the case of advanced breast cancer, drugs are not used in combination, they are more often individually used. However, some combinations, such as paclitaxel plus carboplatin, are commonly used (American Cancer Society, 2017).

Table 1.4. Most common drugs used for breast cancer chemotherapy

Anthracyclines (doxorubicin, epirubicin)
Taxanes (paclitaxel, docetaxel)
5-fluorouracil
cyclophosphamide
carboplatin
Taxanes (paclitaxel, docetaxel)

Chemotherapy and radiotherapy can be used together in different ways, such as neoadjuvant therapy (pre-surgery), adjuvant therapy (following surgery), and concomitant therapy (without surgery intervention). Combining the two treatments allows attacking the tumor cells from different approaches and can prevent the appearance of resistance to each treatment (Tanvetyanon et al., 2005). Neoadjuvant

therapies are used to reduce the size of the tumor and thus facilitate the following surgery, whereas adjuvant therapies are applied to kill the cells that may have not been removed by surgery.

However, these therapies face several drawbacks, mainly related to the generation of side-effects, which include pain, nausea, diarrhea, cardiotoxicity, hair loss, darkened or dry skin and depression of the immune system (Baudino, 2015). Since they are not targeted to the cancer cells, the effects of the chemotherapy can also be suffered by the healthy non-cancerous cells. Therefore, the therapeutic window of these kinds of treatments is also limited. Moreover, the cells that are not killed by these treatments often end up by acquiring resistance to the treatment, and cause a more aggressive cancer (Baudino, 2015). These issues can be overcome by using directed therapies.

1.1.5. Directed therapies against breast cancer

Directed therapies are based on molecules which are specifically targeted to the tumor site. This results in lower side effects with respect to conventional non-directed therapies. Directed therapies include several strategies, mainly the ones based on monoclonal antibodies (mAb) and those based on small inhibitor molecules.

Monoclonal antibodies are molecules that bind to a specific antigen, thus conferring selectivity to the therapy. They can be used as a therapy in itself: by binding to the antigen, they inhibit the activity of the antigen (and, thus, the proliferation of the cell, when the antigen is a receptor for hormones that promote cell proliferation). Another mechanism of action of monoclonal antibodies is the activation of antibody derived cellular response (ADCC), by which they activate the response of the immune system against their target cell (explained in section 1.2.2).

Chapter 1. Introduction

This therapeutic ability of monoclonal antibodies can be further strengthened by using them as a vehicle for delivering potent antitumor molecules to the tumor site. This category includes molecules such as antibody drug conjugates (ADCs), which are antibodies conjugated to highly cytotoxic payloads; and immunocytokines (ICKs), in which antibodies are fused to cytokines that can have a direct antiproliferation effect on the targeted tumor cell and also activate the immune system against it.

There are several other directed therapies derived from monoclonal antibodies, which take advantage of their selectivity for a specific antigen, which are related to the field of immunotherapy (Gotwals et al., 2017). Examples of this can be found in the form of engineered T cells: early trials relied on expression of cloned cell receptors (TCR) with targeted affinity, more recently, artificial receptors such as chimeric antigen receptors (CAR), which consist of a specificity-conferring antibody extracellular domain coupled to one or more intracellular co-stimulatory domains, have been engineered into T cells, resulting in CAR-T cells (Fesnak et al., 2017). Therefore, CAR-T cells generated from patient T cells are targeted to attack the tumor (see Figure 1.5). Two cases of approved CAR-T therapies already exist in the market (Zheng et al., 2018).

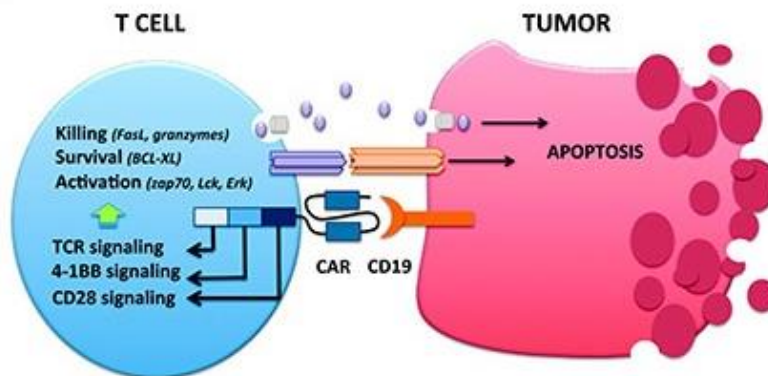


Figure 1.5: CAR-T cell mechanism of action. CAR receptor recognizes the CD19 antigen expressed by the tumor cell, activating signals that induce the T cell to attack the tumor. Obtained from (Enblad et al., 2015).

Chapter 1. Introduction

Targeted delivery of anticancer therapeutic agents is also being tested through means independent from antibodies, mainly related to the nanomedicine field (Mattos-arruda et al., 2016). These vehicles include engineered virus particles (Yildiz et al., 2011), liposomes, and nanoparticles from different materials such as nanodiamond and graphene (Jiang et al., 2015).

Other molecules non-related to antibodies are also included in the domain of directed therapies. These consist in small inhibitor molecules that selectively bind to specific receptors of the target cell, and exert an inhibitory effect upon binding to them (Baselga et al., 2009).

In the case of breast cancer, the targeted therapy to be applied depends on the subtype of cancer. Focusing on the HER2+ subtype, the approved available treatments include the antibody Trastuzumab (commercial name: Herceptin), the antibody Pertuzumab (Perjeta), the ADC ado-trastuzumab emtansine (Kadcyla or T-DM1), the tyrosine kinase inhibitor Lapatinib (Tykerb), and the tyrosine kinase inhibitor Neratinib (Nerlynx) (American Cancer Society, 2018).

Trastuzumab is a humanized monoclonal antibody that targets the HER2 receptor, and it is often given along with chemotherapy although it can also be used alone (especially when chemotherapy has already been tried). It can be used both in early and late-stage breast cancer. When started before or after surgery to treat early breast cancer, this drug is usually given for a total of 6 months to a year. For advanced breast cancer, treatment is given for as long as the drug is helpful. Pertuzumab (Agus et al., 2005) is also a humanized monoclonal antibody that also targets HER2 (albeit at a different subdomain than Trastuzumab) that can be given with Trastuzumab and chemotherapy, either before surgery to treat early-stage breast cancer, or to treat advanced breast cancer. Trastuzumab emtansine (T-DM1) is used in advanced breast cancers, when chemotherapy and Trastuzumab have already been used. Lapatinib is

used to treat advanced breast cancer and might be used along with certain chemotherapy drugs or Trastuzumab. Neratinib is used to treat early stage breast cancer after a woman has completed one year of Trastuzumab and is usually given for one year (American Cancer Society, 2018).

1.2. Monoclonal antibodies for cancer therapy

1.2.1. Therapeutic monoclonal antibodies

Antibodies (Abs) are glycoproteins that belong to the immunoglobulin (Ig) superfamily which play an important role in the immune system, being secreted by B cells to identify or neutralize foreign organisms or antigens. They are formed by two heavy and two light chains and are classified into different isotypes dependent on the type of heavy chain they contain. Therapeutic monoclonal antibodies (mAbs) are normally of the γ -immunoglobulin (or IgG) isotype (Figure 1.6).

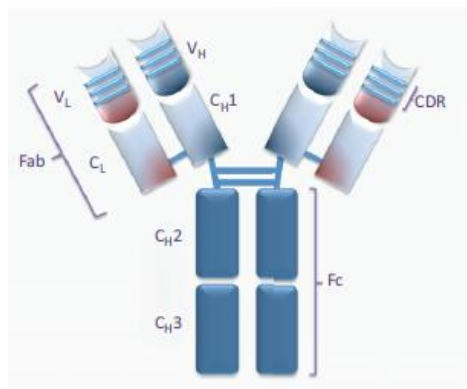


Figure 1.6: Schematic representation of an IgG. Adapted from (Buss et al., 2012).

This isotype of antibodies are large molecules of approximately 150 kDa, which are formed by heavy and light chains interconnected by disulphide bonds. The heavy chains contain a variable domain (V_H), a hinge region and three constant domains (C_H1, C_H2 and C_H3). The light chains contain one variable (V_L) and one constant (C_L)

Chapter 1. Introduction

domains. The structure can also be separated into the Fragment antigen binding (Fab) region that is composed of one variable and one constant domain of both the heavy and the light chain and the fragment crystallizable (Fc) domain, which is composed by two constant domains (C_{H2} and C_{H3}) (Figure 1.6). The specificity of antibodies is driven by their variable domains, which can be further subdivided into hypervariable regions (or complementary-determining regions (CDR), which bind to the antigen directly and framework regions which serve as a scaffold for the CDR to contact the antigen (Buss et al., 2012).

The immune response to an antigen or organism is normally polyclonal in nature, however, in 1975 it was described for the first time the *in vitro* production of murine mAbs from hybridomas (Köhler & Milstein, 1975). In the late 1980s, murine mAbs were already in clinical trials, with the first one being approved in 1986 (muromonab-CD3) (Leavy, 2010). However, murine mAbs presented several drawbacks, including: causing allergic reactions and the induction of anti-drug antibodies; presenting a relatively short-life compared to human IgG (Ober et al., 2001); and being poor recruiters of effector function, antibody-dependent cellular cytotoxicity (ADCC) and complement-dependent cytotoxicity (CDC) (Stern & Herrmann, 2005).

In order to overcome these limitations, chimeric mouse-human mAbs were developed. This was achieved by grafting the whole antigen-specific variable domain of a mouse Ab onto the constant domains of a human Ab using genetic engineering techniques, obtaining molecules that were ~65% human (Morrison et al., 1984). Despite presenting an extended half-life in man and generating less immunogenicity, these antibodies still induce the generation of anti-drug antibodies (Presta, 2006). This led to the development of humanized mAbs, through the grafting of just the murine hypervariable regions onto a human antibody framework, yielding molecules that are around 95% human (Jones et al., 1986). Humanization of an antibody, however, can be a laborious process and present limitations. Currently, fully human

Chapter 1. Introduction

mAbs can be generated through the application of phage display technology (McCafferty et al., 1990), and the use of transgenic mouse strains expressing human variable domains (Lonberg et al., 1994). The different types of mAbs are summarized in Table 1.5 and depicted in Figure 1.7.

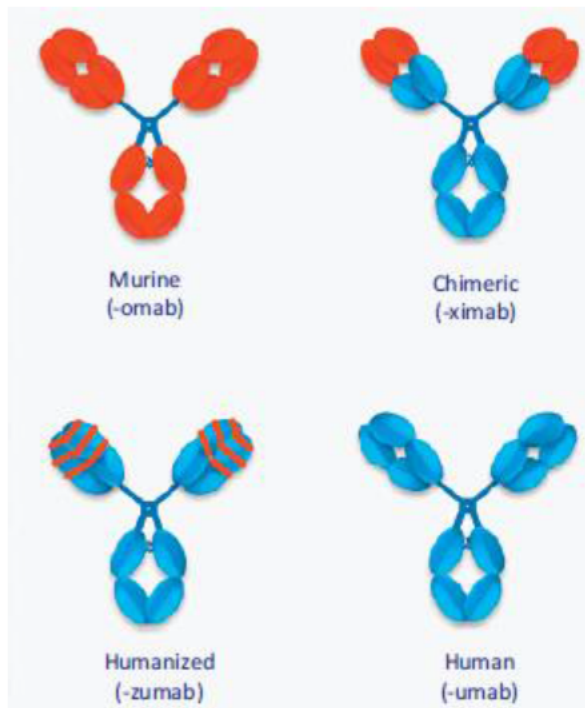


Figure 1.7: Depiction of the structure of different types of mAb (murine, chimeric, humanized and human). Obtained from (Buss et al., 2012).

Table 1.5: antibody types and features

Antibody type	Features
Murine	<ul style="list-style-type: none">• Produced through “hybridoma” technology• Generates allergic reactions• Induces the generation of anti drug antibodies• Low half-life• Nomenclature: suffix -omab

Chapter 1. Introduction

Chimeric	<ul style="list-style-type: none">• Genetically engineered: variable region of murine mAb grafted into human IgG framework (about 65% human)• Induces the generation of anti drug antibodies• Nomenclature: suffix -ximab
Humanized	<ul style="list-style-type: none">• Genetically engineered: hypervariable CDR region of murine mAb grafted into human IgG framework (about 95% human)• Improved immunogenic and effector response in humans• Grafting process can be laborious• Nomenclature: suffix -zumab
Human	<ul style="list-style-type: none">• Produced through:<ul style="list-style-type: none">○ Phage display technology○ Transgenic humanized mice• Nomenclature: suffix -umab

As of 10 May 2018, the Food and Drug Administration of the United States (FDA) has approved 80 therapeutical monoclonal antibodies, 17 of which were approved in 2017 (its record high for a single year). 7 of these 17 mAbs were related to oncology indications (H. H. Cai, 2018). One of the approved monoclonal antibodies with a higher impact in terms of cancer treatment is the anti-HER2 mAb Trastuzumab (Herceptin), which has had an important role in the breast cancer treatment since it was approved by the FDA in 1998 (Dall et al., 2018; Hartkopf et al., 2014).

Several monoclonal antibody modifications have been studied in order to improve their therapeutic efficacy, including engineering the Fc fraction and developing bispecific antibodies. The Fc fraction mediates the ADCC and CDC response by binding to Fc γ receptors (Fc γ Rs) expressed on immune effector cells, eventually

leading to the killing of the target cell. Modifications into the amino acids of the Fc that interact with Fc γ Rs, as well as into the glycosylation of these domains, have been applied in order to improve the activity of the Fc region with regards to the ADCC/CDC triggering (Strohl, 2009). Fc engineering has also been directed to extending the half-life of the antibody, by introducing mutations that improve the binding of the Fc to the Fc neonatal receptors (FcRn), which is responsible of the long half-life of mAbs (Hinton et al., 2006).

Bispecifics consist on antibody constructs that have multiple, functionally different, binding domains that allow for interaction with two target antigens (Figure 1.8).

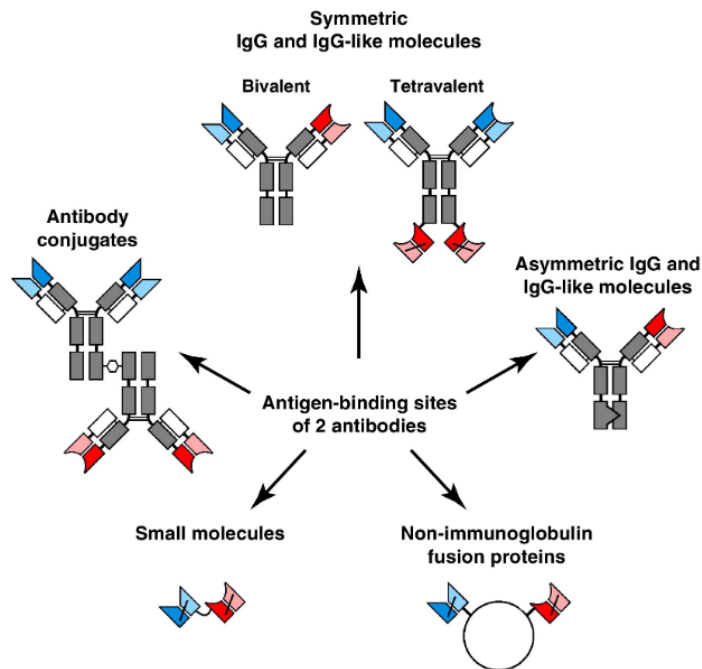


Figure 1.8. Schematic representation of several antibody formats, including different bispecific displays. Obtained from (Kontermann et al., 2015)

A common strategy of bispecific antibodies relies in simultaneously targeting an antigen of the site of the target disease, and an effector cell. This was the case of the

Chapter 1. Introduction

first approved bispecific antibody catumaxomab, which targets CD3 antigen of T cells and epithelial cell antigen molecule-positive carcinoma EpCAM (Linke et al., 2010).

Other important antibody modifications consist in antibody fragments, which consist in using parts of the antibody instead of the whole antibody as therapeutic tools. Thanks to the modular nature and multi domain structure of immunoglobulins, they can be customized or engineered to produce antibodies with desired pharmacologic properties for specific applications (Alibakhshi et al., 2017), leading to the optimization of properties such as tissue penetration, affinity, half-time and distribution (Schroeder et al., 2010). Antibody fragments will be more thoroughly explained in section 1.2.2.2.

Monoclonal antibodies can also have their therapeutic activity enhanced through their combination with other effector molecules. Their use as vehicles for delivering potent cytotoxic drugs to the site of the disease, yielding Antibody Drug Conjugates (ADCs) has represented an important breakthrough for the therapeutic treatment of cancer, with 4 ADC currently approved by the FDA.

1.2.1.1. Trastuzumab

Trastuzumab (commercial name: Herceptin) is a humanized monoclonal antibody (P Carter et al., 1992) developed by Genentech, which selectively binds to the HER2 receptor on the C-terminal portion of the extracellular domain (ECD) (Cho et al., 2003); it was constructed by grafting the complementary-determining regions (CDRs) from the murine mAb 4D5 into a human kappa IgG1 to avoid a human anti-mouse antibody (HAMA) response in patients (Nahta et al, 2006). Trastuzumab has antitumor activity against HER2-positive human breast cancer cells in laboratory models (Baselga et al, 1998) and is active for the treatment of women with HER2-overexpressing breast cancers (Slamon et al., 2001). Based on Trastuzumab clinical efficacy, this antibody was approved in 1998 for clinical use for HER2 overexpressing

metastatic breast cancer (Molina et al., 2001), and it was later approved for HER2 positive gastric and gastroesophageal junction (GEJ) adenocarcinomas (Davidson et al., 2016).

The working mechanisms of Trastuzumab are not completely understood, but its binding to the HER2 receptor causes a diminishing of the tumor growth and activates the immune system activity against the tumor (ADCC, Antibody Dependent Cell Associated Cytotoxicity). Its proposed action mechanisms (Figure 1.9) include:

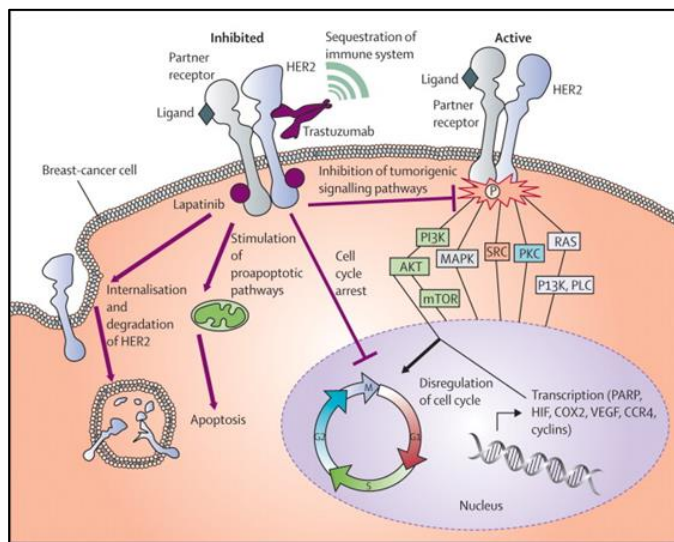


Figure 1.9: Mechanism of action of Trastuzumab and Lapatinib therapies for HER2-expressing breast cancer (Cho et al., 2003).

1) Trastuzumab sensitises cells to apoptotic agents: it is currently unclear whether or not Trastuzumab induces apoptosis in tumours *in vivo* (Gennari et al., 2004), (Mohsin et al., 2005) but it does sensitise tumour cells to apoptosis-inducing agents. Trastuzumab also enhances TRAIL-induced apoptosis, (Cuellar et al., 2001) and prevents cells from repairing DNA damage caused by chemotherapy or irradiation (Pietras et al., 1994).

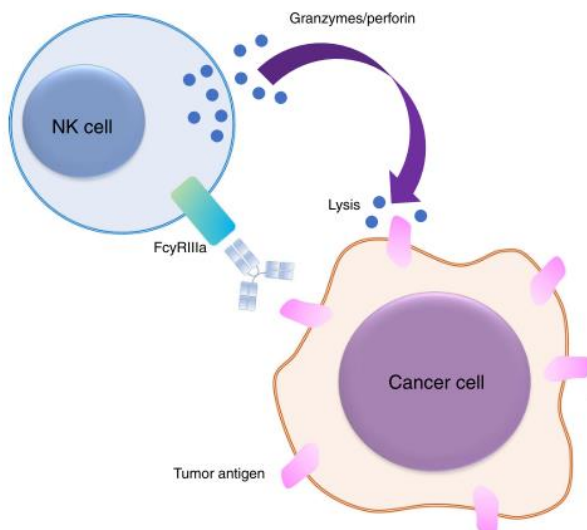
2) HER2 Extracellular domain (ECD)-shedding inhibition: HER2 is cleaved by proteins containing Metalloprotease A domains: the extracellular domain is shed and the truncated kinase domain (p95-HER2) retains the ability to form heterodimers with

Chapter 1. Introduction

HER3 (Molina et al., 2002), and can be phosphorylated and activated. Higher levels of ECD-shedding *in vivo* correlate with a poor prognosis and decreased responsiveness to endocrine therapy and chemotherapy in patients with advanced breast cancer. Trastuzumab inhibits ECD-shedding *in vitro* (Molina et al., 2001), and *in vivo*, the serum ECD levels of HER2 are lower in Trastuzumab-treated patients compared to those not treated with Trastuzumab (Ko et al., 2004).

3) Inhibition of angiogenesis: HER2 overexpression correlates with elevated levels of vascular endothelial growth factor (VEGF) and increased angiogenesis (Konecny et al., 2004). Angiogenesis consists in the growth of new blood vessels from pre-existing ones and is essential for tumour growth (Izumi et al., 2002). Trastuzumab *in vivo* treatment of xenograft mice models results in lower angiogenesis levels (Zhang et al., 2010).

4) Antibody-dependent cell-mediated cytotoxicity (ADCC): Trastuzumab activates Antibody-dependent Cell-mediated Cytotoxicity (ADCC) via recruitment of natural killer (NK) cells to the tumour. The NK cells express an Fc γ receptor (Fc γ -R) which binds to the Fc domain on Trastuzumab (Clynes et al., 2000).



Chapter 1. Introduction

Figure 1.10: Representation of the mechanism of action of the ADCC response mediated by an antibody against a cancer cell, attracting natural killer (NK) cells to the tumor site. Obtained from: (Nagayama et al., 2017).

5) Reduction of signalling through Protein kinase B (Akt) and Mitogen Activated Protein Kinase (MAPK). Trastuzumab disrupts HER2-Src tyrosine kinase interaction, which lowers the Phosphatase and Tensin Homologue (PTEN) phosphorylation, thus increasing its activity. PTEN is a tumor suppressor protein. This results in a dephosphorylation of Akt and the inhibition of proliferation (Nagata et al., 2004).

Therapeutic effect of Trastuzumab was confirmed in the first phase III clinical trial, in women with HER2+ metastatic breast cancer. Higher respondent rates and increased time to disease progression when Trastuzumab was added to standard chemotherapy were observed. Follow-up data revealed prolonged survival (median survival, 25.1 versus 20.3 months), and a 20 per cent reduction in risk of death compared with standard chemotherapy alone (Slamon et al., 2001). Cardiac dysfunction was the main observed toxic side-effect, which has been addressed through several measures including monitoring of cardiac function and minimising of cardiovascular risk factors (Jones et al., 2009). Later, in 2006, Trastuzumab was also approved for adjuvant treatment of early stage HER2+ disease after phase III trials showed that Trastuzumab reduced the risk of recurrence (Piccart-Gebhart et al., 2005). This was confirmed in a follow-up study of the same trial, which revealed that after a follow-up of 11 years, random assignment to 1 year of Trastuzumab significantly reduced the risk of a disease-free survival event and death compared with observation (Cameron et al., 2017).

Trastuzumab conjugated to the maytansinoid cytotoxic drug DM1, forming an ADC, has also been approved for therapeutic use for metastatic breast cancer patients that do not respond to Trastuzumab or that despite being initially responsive ultimately experience disease progression (Lambert et al., 2014).

Apart from the approved mAb and ADC, Trastuzumab derived molecules such as CAR-Ts (Zhao et al., 2009) and antibody fragments (Selis et al., 2016) are also being investigated as potential therapeutic candidates.

1.2.2. Antibody fragments

Due to their modular structure, as previously stated, parts of antibodies can also be used as functional entities since they retain some of the functions of the whole molecule and can even be preferable to using the complete antibody with regards to some issues caused by the Fc region (Deonarain et al., 2015). Despite the fact of being important for its effector function in activating the ADCC/CDC immune response and for the antibody half-life, the Fc region can also be associated to some drawbacks. These include: the long half-life associated to neonatal Fc receptor (FcRn) recycling increases normal tissue exposure, giving more time for off-target payload releasing leading to side-effects (Litvak-Greenfeld et al., 2012); Fc-gamma receptor (Fc γ R) mediated cross reaction with immune or endothelial cells can also cause toxicity; the overall large size of an IgG provides a physical barrier to tumour penetration (R. K. Jain, 1990); steric blocking that might inhibit receptor dimerization, often needed for internalization or epitope access (de Goeij et al., 2014). Eliminating the Fc domain from the antibody, predominantly by genetical engineering, results in antigen-binding fragments (Fab), single chain fragment variable (scFv) and other multiple formats derived from antibodies, including nanobodies and multivalent antibody fragments such as diabodies, triabodies, tetrabodies and minibodies (Alibakhshi et al., 2017). They are depicted in Figure 1.11.

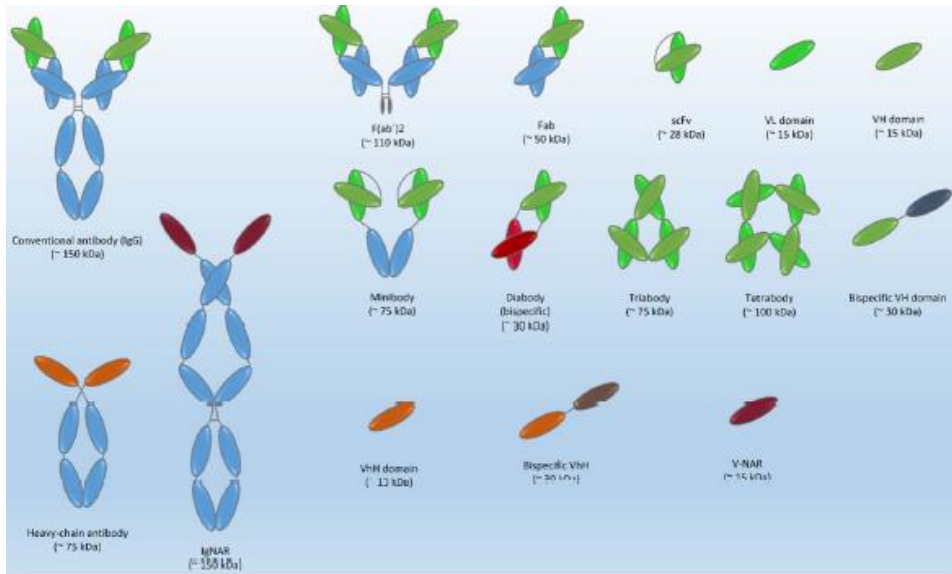


Figure 1.11: Several fragment antibody formats. Adapted from Alibakhshi et al., 2017.

Fab and scFv were the first developed fragments and are the most used fragments in the literature.

1.2.2.1. Fragment antigen binding (Fab) and single chain fragment variable (scFv)

Antigen-binding fragments (Fab) are the oldest form of antibody used in medicine (Nelson, 2010). They were first made by enzymatic cleavage of an intact antibody with the protease papain, resulting in two Fab fragments from a whole antibody. Each Fab fragment has a molecular weight of about 50 kDa and is formed by one VH and one VL chain linked by disulfide bonds and contains a single antigen-binding site (Andrew & Titus, 2001). As of May 2017, there were 5 therapeutic Fabs approved by the FDA (Animal Cell Technology Industrial Platform, 2017).

Single chain fragment variable (scFv) consist of a single polypeptide chain (molecular weight of approximately 25 kDa) formed by the variable regions of an antibody heavy and light chains joined with a short flexible peptide linker. The linker is usually based on glycine and serine residues, which render it flexible and resistant to proteases.

scFv have a monovalent structure with a good affinity for a single antigen (Ahmad et al., 2012). Several scFv fragments are employed in clinical trials as promising therapeutic or diagnostic fragments (Elvin et al., 2013). As of November 2018, only one scFv had been approved by the FDA, which is binatumomab, a bispecific T-cell engager (BiTE) consisting of the fusion of two scFv, directed against CD19 and CD3 (Santos et al., 2018). scFvs, as well as other fragments and whole antibodies, can have their activity enhanced by their conjugation to effector molecules such as cytotoxic drugs or by their fusion to other proteins such as toxins or cytokines (Deonarain et al., 2015).

1.2.3. Immunocytokines (ICKs)

Another way of improving the therapeutic potential of antibodies is mediating their fusion to effector proteins such as cytokines, forming an immunocytokine (ICK) or antibody-cytokine fusion protein. In this configuration, the antibody serves as a vehicle for delivering a cytokine to the site of the disease. Cytokines are molecules that play an important role in the immune system, being regulators and mediators of both the innate and the adaptive immune system (Kontermann, 2012). Immunotherapy with immunostimulatory cytokines was initially established for interferons and IL-2 (Baxevanis et al., 2009), IFN α being the first recombinant cytokine approved for the treatment of cancer. Cytokines as therapeutic agents, however, can cause severe side effects, and at the same time, their accumulation in the target site can be insufficient (Kontermann, 2012). Therefore, their targeted delivery through their fusion with antibodies has been proposed as a way to overcome these issues (Dela Cruz et al., 2004).

1.2.3.1. Structural elements and action mechanism of cytokines

Immunocytokines are composed by an antibody or antibody-derived fraction and the cytokine payload, fused by a peptide linker. Therefore, several structures can be

found in the immunocytokines, depending on the antibody format: fusions with whole immunoglobulins, or with fragments such as Fab, scFv and other derivate fragments. Differences in the structure of the immunocytokine can also be caused by the cytokine itself: many cytokines are monomeric (Interleukin 2, IL-2), while others are homodimeric (interferon gamma, IFN γ) or homotrimeric (tumor necrosis factor, TNF), and there are also some immunocytokines that are composed by two different polypeptide chains (IL-12) (Kontermann, 2012), connected by a flexible peptide linker (Peng et al., 1999). Combining two different cytokines in the same construct, for example by fusing them at N and C-terminal has also been attempted (Kontermann, 2012). Some of the immunocytokine formats are depicted in Figure 1.12.

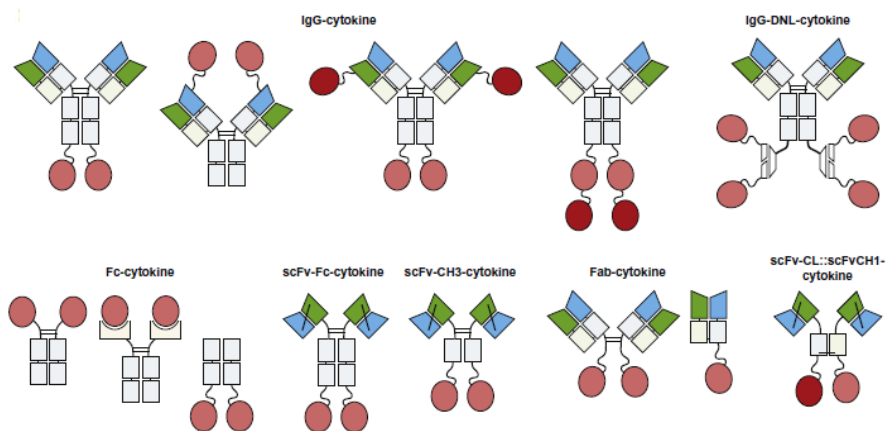


Figure 1.12: different immunocytokine antibody formats. Obtained from (Kontermann, 2012).

The fusion construct format has a direct impact on the therapeutic activity of the immunocytokine: antibody fragment based immunocytokines will lack the ADCC/CDC response driven by the Fc region of the antibody. The therapeutic antitumor activity of the immunocytokine is also defined by the cytokine, which can have a direct cytotoxic effect on the target cells (IFN- α , TNF α , FasL) and/or have a stimulatory effect over the immune system.

Despite the fact that many different antibody-cytokine fusion proteins have been investigated, relatively few have entered clinical phases (featuring mostly IL2, TNF and IL12 as immunomodulatory payloads), and only recently they have been able to reach Phase III clinical trials (Hutmacher et al., 2018). The high molecular mass of immunocytokines can reduce therapeutic efficacy by impairing vascular evasion and tissue penetration (Kontermann, 2012). Another issue can be generated immunogenicity associated to the linkers used to connect the cytokine and the antibody and also to using non-human or humanized antibody moieties (Kontermann, 2012).

1.2.4. Antibody Drug Conjugates (ADCs)

Antibody drug conjugates (ADCs) are one of the most prominent spearheads of the anticancer therapeutic field (Diamantis et al., 2016). They consist of cytotoxic drugs covalently linked to antibodies that specifically recognize antigens overexpressed in tumors or other diseases (Figure 1.13).

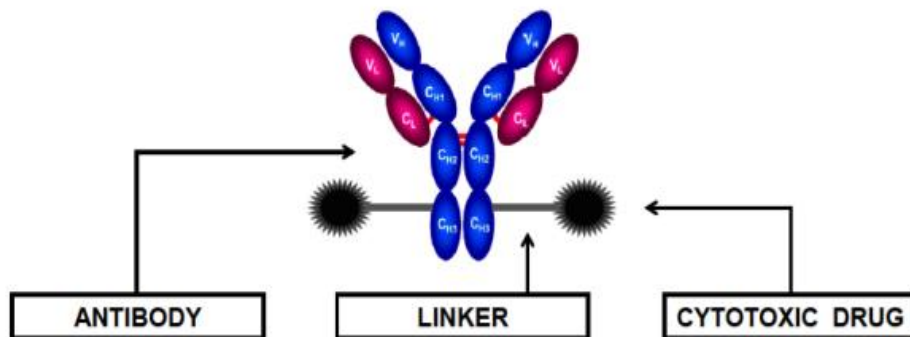


Figure 1.13: scheme of the structure of an ADC with its three main elements: antibody, linker, and cytotoxic drug (Wooge, 2014).

Targeting cytotoxic agents to the tumor site represents an improvement with respect to chemotherapy, which can cause severe side-effects due to off-target

cytotoxicity. Thus, a broader therapeutic window is obtained with ADCs (Figure 1.14).

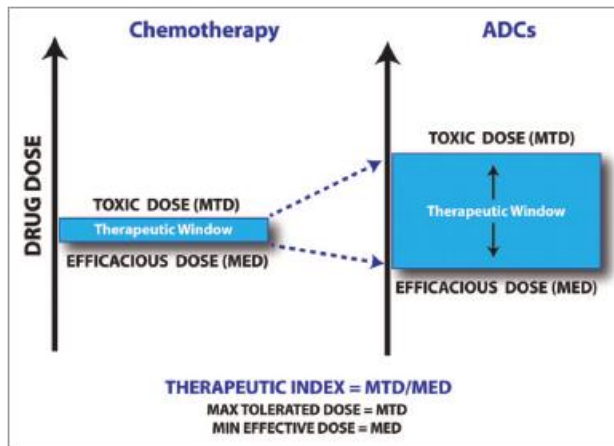


Figure 1.14: therapeutic index improved by ADCs with respect chemotherapy treatment. Obtained from (Panowski et al., 2014).

ADCs are the translation of the “magic bullet” theory described by Paul Ehrlich in 1913 (Ehrlich, 1913), referring to the selective delivery of toxic agents to target cells causing disease. In 1958, the first ADC was generated, consisting of methotrexate conjugated to a leukemia cell-targeting antibody (Mathe et al., 1958). The first ADC clinical trial in humans was performed using an anticarcinoembryonic antigen (anti-CEA) antibody-vindesine conjugate in 1983 (Ford et al., 1983), and promising results were reported. However, poor target antigen selection, immunogenicity derived from the use of murine or chimeric antibodies, and low potency drugs, hindered the success of the first ADCs (Panowski et al., 2014). Technological advances on antibodies (including antibody humanization) led to an increasing in ADC studies. The first-generation ADCs consisting of chimeric or humanized antibodies were tested in the 1990s (Tsuchikama & An, 2016). Finally, further efforts towards practical therapeutics led to the first FDA-approved ADC brentuximab vedotin (Adcetris) in 2011 (Younes et al., 2010) (previous to that, another ADC, gemtuzumab ozogamicin

Chapter 1. Introduction

(Mylotarg) had been approved in 2000 but later withdrawn from market in 2010 due to a lack of clinical benefit and high fatal toxicity rate compared to standard chemotherapy (ten Cate et al., 2009)).

Currently, there are 4 FDA-approved ADCs in the market (Figure 1.15), and a high number of them (around 60 (Chalouni et al., 2018)) are in clinical trials (Tables 1.6 and 1.7 report some of the ADCs that are in phase II and III). The numbers of ADCs entering clinical trials has steadily increased over the past years, and a higher number of approved ADCs is expected in the future.

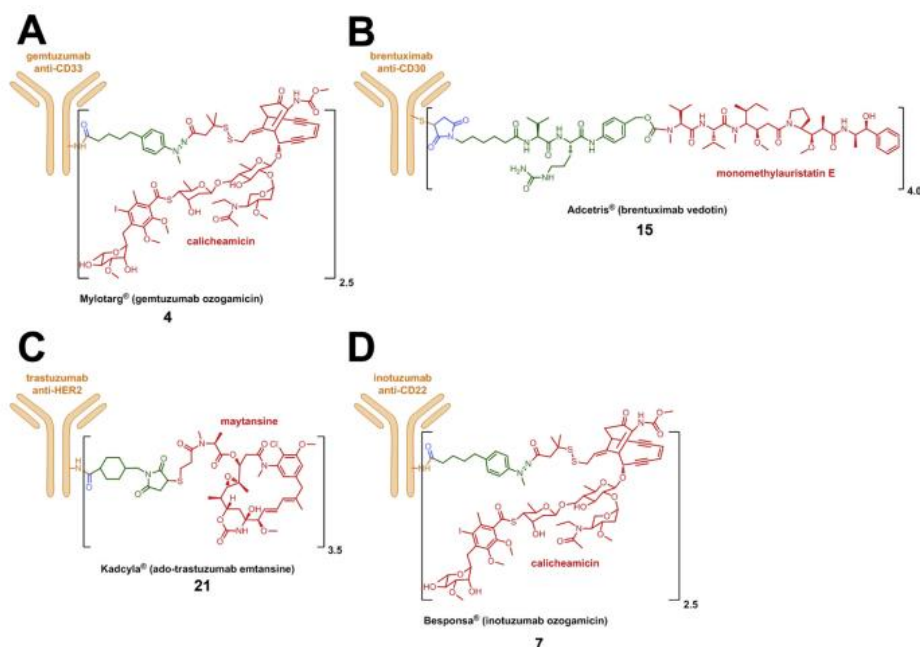


Figure 1.15: representation of the 4 approved ADCs. A) Mylotarg; B) Adcetris; C) Kadcyla; D) Besponsa. Obtained from (Joubert et al., 2017).

Chapter 1. Introduction

Table 1.6 ADCs in clinical phase III (beginning 2018) (adapted from (Lambert et al., 2018))

ADC	Company	Antigen	Indication	Drug compound	Conjugation strategy
Mirvetuximab Soravtansine (IMGN853)	Immunogen	FR α	Ovarian cancer	DM4 (Maytansinoid)	Heterogeneous (Lysines)
Sacituzumab govitecan (IMMU-132)	Immunomedics (licensed to Seattle genetics)	TROP-2	Triple negative breast cancer, urothelial and other cancers	SN-38	Heterogeneous (Cysteines)
Vadastuximab talirine (SGN-CD33A)	Seattle genetics	CD33	Acute myeloid leukemia	PBD dimers	Homogeneous (cysteine addition)
Depatuxizumab mafodotin	Abbvie	EGFR	Glyoblastoma and other EGFR+ tumors	MMAF (Auristatin)	Heterogeneous (cysteine)
Rovalpituzumab tesirine (Rova-T)	Abbvie	DLL3	Small Cell Lung Cancer	PBD dimers	Heterogeneous (cysteines)

Table 1.7 ADCs in clinical phase II (beginning 2018) (adapted from (Lambert et al., 2018))

ADC	Company	Antigen	Indication	Drug	Conjugation strategy
AGS-16C3F	Astellas	ENPP3	Renal cell carcinomas	MMAF	Heterogeneous (cysteines)
Anetumab Ravtansine (BAY94-9343)	Bayer	Mesothelin	Mesothelioma and other solid tumors	DM4	Heterogeneous (Lysines)
Naratuximab emtansine (IMGN529)	Immunogen	CD37	Diffuse large B-Cell Lymphoma and Follicular Lymphoma	DM1	Heterogeneous (Lysines)
Rovalpituzumab tesirine (Rova-T)	Abbvie	DLL3	Small Cell Lung Cancer	PBD dimers	Heterogeneous (cysteines)

Chapter 1. Introduction

Denintuzumab Mafodotin (SGN-CD19a)	Seattle genetics	CD19	Diffuse large B-Cell Lymphoma and Follicular Lymphoma	MMAF	Heterogeneous (Cysteines)
Depatuzumab mafodotin	Abbvie	EGFR	Glyoblastoma and other EGFR+ tumors	MMAF (Auristatin)	Heterogeneous (cysteine)
BMS986148	Bristol-Myers Squibb	Mesothelin	Solid tumors	<i>Not available</i>	<i>Not available</i>
Indatuximab Ravtansine (BT-062)	Biotest	CD-138	Multiple myeloma	DM4	Heterogeneous (Lysines)
Glembatumumab Vedotin (CDX-011)	Celldex Therapeutics	Transmembrane glycoprotein	Breast cancer and melanoma	MMAE	Heterogeneous (cysteines)
Labetuzumab govitecan (IMMU-130)	Immunomedics	CEACAM-5	Colorrectal cancer	SN-38	Heterogeneous (cystines)
Polatuzumab Vedotin (RG7596)	Genentech/ Roche	CD79b	Diffuse large B-Cell Lymphoma and Follicular Lymphoma	MMAE	Homogeneous (cysteine addition)
PSMA-ADC	Progenics	Prostate Specific Membrane Antigen (PSMA)	Prostate cancer	MMAE	Heterogeneous (Cysteines)
SAR408701	ImmunoGen/ Sanofi	CEACAM-5	Solid tumors	DM4	Heterogeneous (Lysines)
Coltuximab ravtansine (SAR-3419)	Immunogen/ Sanofi	CD19	Diffuse large B-Cell Lymphoma	DM4	Heterogeneous (Lysines)
Tisotumab vedotin (HUMAX-TF-ADC)	Genmab/ Seattle Genetics	Tissular Factor (TF)	Solid tumors	MMAE	Heterogeneous (cysteines)
SAR 566658	Immunogen	CA6	Triple Negative Breast cancer and other CA6+ tumors	DM4	Heterogeneous (Lysine)

From an economical perspective, the ADC market is anticipated to grow in the upcoming years, reaching an estimated value of \$8 billion in the next five years (Sharma, 2018), and representing one of the most developed biologic drugs by biopharma companies (Figure 1.16).

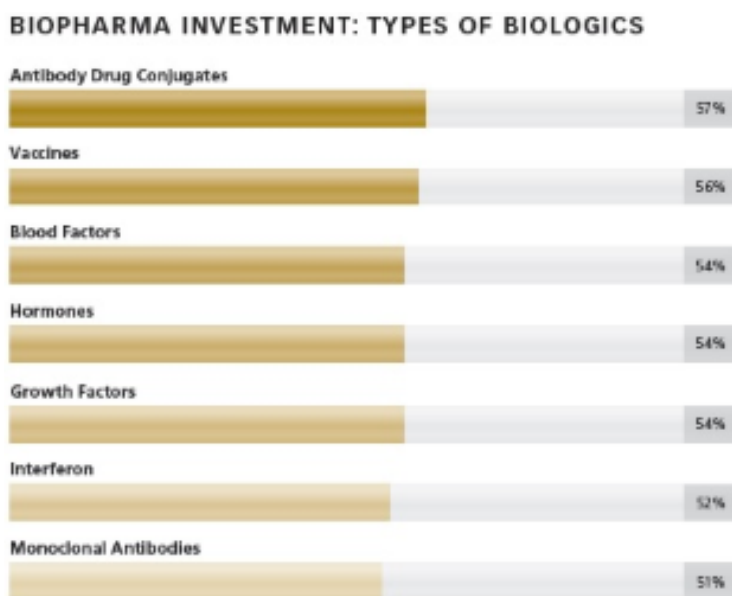


Figure 1.16. Percentage of biopharma companies that develop the listed products ((Ferraro, 2016).

1.2.4.1. ADCs: action mechanism and structural elements

ADCs are formed by an antibody moiety covalently linked to a cytotoxic drug (payload) by a linker, as previously presented in Figure 1.13. The general mechanism of action of an ADC consists in its binding to the cancer cell surface-expressed antigen. Then, the ADC is internalized through endocytosis, and processed in the lysosomes, where the cytotoxic payload is released and then released inside the cell

Chapter 1. Introduction

in a bioactive form. This allows the payload to exert its function, normally disrupting DNA or microtubules, or inhibiting RNA polymerase or topoisomerase. A general mechanism of action is depicted in Figure 1.17.

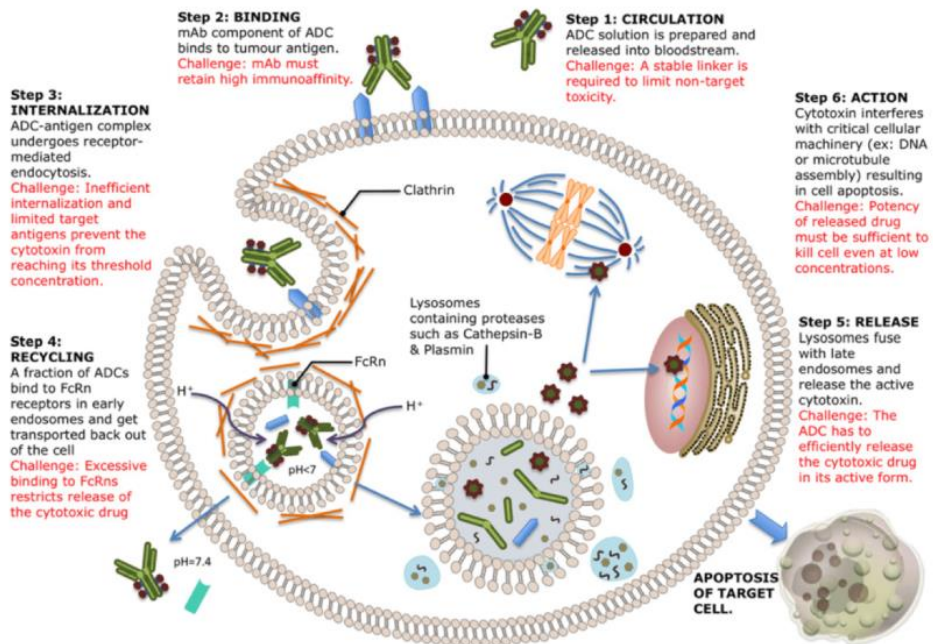


Figure 1.17: action mechanism depiction and explanation of an ADC, and challenges associated with ADC design (Peters & Brown, 2015).

Taking into account their action mechanism, it is important that the ADCs antibodies have enough affinity and specificity for the target antigen. In this regard, it is also crucial that the selected antigen is predominantly expressed in the target cells while having a minimal expression on healthy cells, thus minimizing off-target driven side-effects and broadening the window therapy. It is also important for the antibody to avoid the generation of immunogenicity and have a long half life in human blood

stream. This can be achieved by using humanized or fully human antibodies (Tsuchikama et al., 2016).

1.2.4.1.1. Payload

Regarding the payload, it is important that it is a potent molecule, and that, ideally, they have inherent selectivity for target cells. It must be considered that a very low proportion of the injected payload molecules will exert its function into the target cell: some approximations state that less than 2% of administered drug load molecule enter the target cells due to loss of drug at each step of the ADC action mechanism (biodistribution, binding to antigen, internalization, release of payload, intracellular stability of payload, and payload binding to target (Teicher et al., 2011)), therefore, potent drugs are needed, with cytotoxic activity ideally in the picomolar range (Tsuchikama et al., 2016). Related to this fact, payloads can attain non-target cells through nonspecific pinocytosis or mediating interaction with the Fc region of the antibody (Lencer et al., 2005). Moreover, payload can be released due to degradation during the circulation into the bloodstream. These issues render attractive the use of antimetabolic agents as payloads, since they are generally less toxic to noncancerous cells than to cancerous cells (Tsuchikama et al., 2016). These include calicheamicin, auristatins (such as monomethyl auristatin E, MMAE) and maytansinoids (such as DM1) (all three used in FDA-approved ADCs), and new classes of antimetabolic compounds such as duocarmycins, pyrrolobenzodiazepine dimers (PBDs), amanitins and tubulysin analogs (Chari et al., 2014) (Pérez-Herrero et al., 2015). Table 1.8 summarizes the most used payloads in ADCs in development.

Table 1.8 Targets and action mechanisms of the main payloads used in ADCs

Target	Payloads	Action mechanism
DNA repair ways	Calicheamicins	They bind to the minor groove of DNA of the tumor cell, where they form diradical

Chapter 1. Introduction

species that end up by causing the excision of the DNA chains in different locations (Smith & Nicolaou, 1996).

Duocarmicines	They bind to A-T rich regions of DNA.
---------------	---------------------------------------

Pirrolobenzodiazepines(PBD)	They bind to G residues of DNA.
-----------------------------	---------------------------------

Microtubule formation	Auristatins	They stop the cell cycle in phase G2/M. They interfere with microtubule formation during mitosis by binding to β subunits of α - β tubulin. Therefore, GTP hydrolysis is avoided in the β -tubulin subunit, causing the excessive growth of the microtubules (Francisco et al., 2003) (Figure 1.15).
------------------------------	-------------	---

Maitansines	They stop the cell cycle at G2/M phase. They interfere with tubulin microtubules formation during mitosis by blocking the polymerization of tubulin dimers and avoid mature microtubules formation. Moreover, already formed mature
-------------	---

microtubules depolymerize when the GTP, which is bound to β -tubulin subunits, is hydrolyzed. (Lopus et al., 2010) (Figure 1.15).

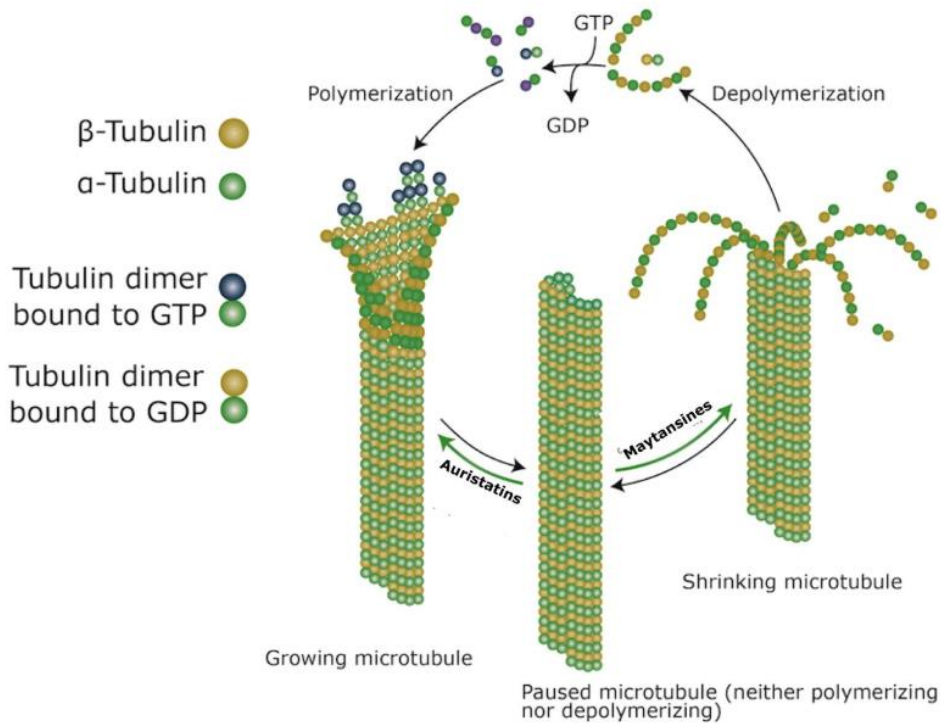


Figure 1.18. Effect of auristatins and maytansines cytotoxic drugs on tubulin microtubules (Peters et al., 2015).

1.2.4.1.2. Linker and conjugation strategies

The linker element of the ADC is also crucial for its success. In order to have the best outcome in terms of therapeutic window and therapeutic efficacy of the ADC, the linker should comply several requirements, including: being stable enough to allow the circulation of the ADC through the bloodstream without being cleaved and

releasing the payload; being able to rapidly cleave in the lysosome in the target cell, allowing the payload to have its cytotoxic effect; being hydrophilic, since hydrophobic linkers promote the aggregation of the ADC, resulting in loss of therapeutic function and generation of immunogenicity (Tsuchikama et al., 2016). Current linkers can be classified into two categories: cleavable and non-cleavable (Panowski et al., 2014). Cleavable linkers can be divided into three main groups: acid labile, protease cleavable linkers and disulfide linkers. Acid labile linkers are stable in blood at neutral pH but break at acidic pH found in lysosomes. Protease cleavable linkers are also stable in plasma but are designed to be cleaved by specific proteases found in lysosomes of cancer cells. Another class of linkers are the ones that conjugate through disulfide linkage, exploiting the high level of intracellular reduced glutathione to release the free drug inside the cell (Panowski et al., 2014). The linker and conjugation strategy applied in an ADC determine their main classification into conventional heterogeneous ADCs or homogeneous ADCs.

1.2.4.2. ADC conjugation strategies: heterogeneous

Heterogeneous ADCs are a mixture of products that differ in the site and stoichiometry of conjugation (Behrens et al., 2015). This strategy includes the conventional conjugation methodology, which is based on using solvent accessible amino acids lysine and cysteines derived from the reduction of the interchain disulfide bonds in the antibody (Panowski et al., 2014). In both heterogeneous cases, the process affords a mixture of ADC species with variable Drug-Antibody Ratios (DARs) and different conjugation sites. Generally, a broad distribution of the DAR leads to reduced efficacy. High DAR can increase potency and the risk of aggregation, clearance rate and premature release of the cytotoxic drug during circulation (Tsuchikama et al., 2016).

Lysine conjugation is based on an amide coupling: solvent accessible lysine residues are conjugated to linkers containing activated carboxylic acid esters. Since there are

Chapter 1. Introduction

about 80 lysine residues on a typical antibody and about 10-20 residues (depending on the source: (Chari, 2008), (Panowski et al., 2014)) are chemically accessible, the outcome results in a multiple ADC species with variable DARs and conjugation sites: linker drug per antibody can range from 0-8 (Hamblett et al., 2004). Furthermore, some lysine residues that are critical in antibody-antigen interaction may be modified, resulting in reduced binding affinity (Tsuchikama et al., 2016). The heterogeneity of the product also renders consistency in ADC production challenging.

Despite the above mentioned drawbacks, lysine conjugation has yielded 3 of the 4 FDA-approved ADCs. These consist in gemtuzumab ozogamicin (Mylotarg), trastuzumab-emtansine (Kadcyla) and inotuzumab ozogamicin (Besponsa). Gemtuzumab ozogamicin is an anti-CD33 ADC approved for acute myelogenous leukemia treatment. The payload consists in the calicheamicin ozogamicin. Inotuzumab ozogamicin shares the same payload than Mylotarg and is directed to the antigen CD22, being approved to treat acute lymphoblastic leukemia. Kadcyla consists of the previously described anti-HER2 antibody Trastuzumab conjugated to the maytansinoid microtubule inhibitor DM1, with a DAR of 3.5. This ADC was approved in 2013 for metastatic HER2+ breast cancer patients who had relapsed after Herceptin (Trastuzumab) treatment. Phase III clinical trial results showed that Kadcyla significantly prolonged progression-free and overall survival with less toxicity than the standard treatment of lapatinib plus capecitabine (Lambert et al., 2014).

The second conventional heterogeneous conjugation method consists of using solvent accessible cysteines from the reduced interchain disulfide bonds of the antibody. In IgG1, the most commonly used form in modern ADC, there are 4 interchain and 12 intrachain disulfide bonds. The 4 interchain bonds can be reduced and generate 2, 4, 6 or 8 free thiols while maintaining the intrachain disulfide bridges

unaltered. This conjugation strategy leads to products with species with DARs ranging from 0-8. It has been used in FDA-approved ADC brentuximab-vedotine, an anti-CD30 ADC with a DAR of 4, for treating relapsed or refractory Hodgkin's lymphoma.

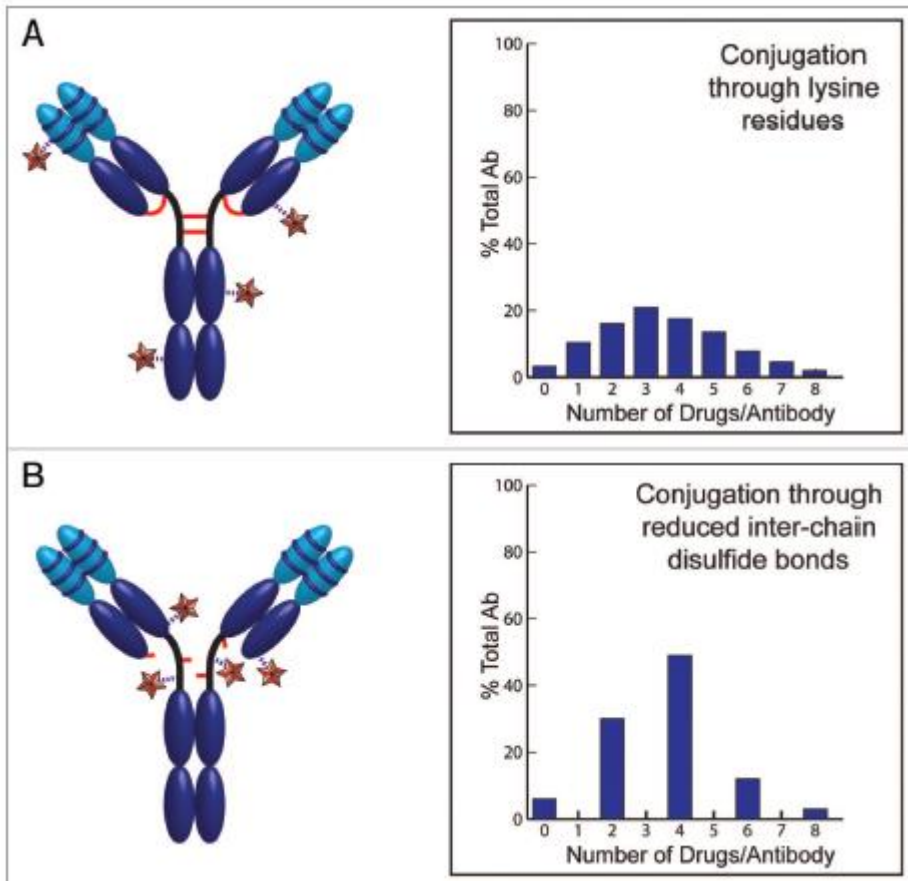


Figure 1.19: conjugation mediating classical lysine and cysteine residues. Adapted from (Panowski et al., 2014).

Some of the drawbacks of heterogeneous ADCs can be overcome by alternative conjugation strategies in which homogeneous products are obtained.

1.2.4.2. ADC conjugation strategies: homogeneous

Homogeneous ADCs contain a specific number of conjugated drugs at defined sites on the antibody (Jain et al., 2015). This allows obtaining a product in which there is only one specie with the same number of drugs per antibody and at the same location, therefore eliminating naked antibody species (with low therapeutic activity) and high-loaded species, which tend to aggregate and produce toxic side-effects. This can lead to improvements in ADCs properties such as stability, potency and safety, rendering the therapeutic windows of homogeneous ADCs wider when compared to conventional heterogeneous benchmarks (Jackson, 2016) (Figure 1.20).

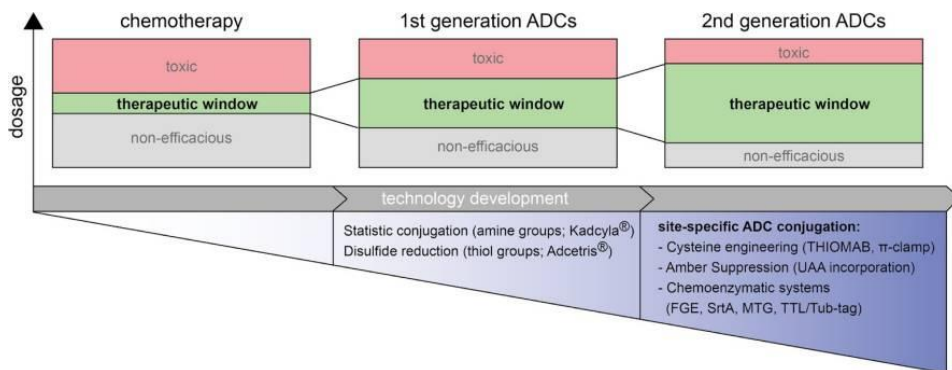


Figure 1.20: therapeutic index improved by homogeneous ADCs with respect heterogeneous ADC and chemotherapy treatment. Adapted from (Schumacher et al., 2016).

Homogeneous ADCs can be obtained through different strategies (Figure 1.21 and table 1.9), the most relevant including:

- A) **Thiomabs:** The typical cysteine-based homogeneous conjugation process relies on a genetically modified antibody which normally contains a single point mutation where one of the amino acids of the antibody is substituted by a cysteine, to which the cytotoxic drug will be conjugated in a selective manner (Sochaj et al., 2015).

- B) **Antibodies with unnatural amino acids:** These are antibodies which contain unnatural amino acids in concrete locations. They are homologous to Thiomabs, but contain unnatural amino acids instead of cysteines. These amino acids have specific side-chains that allow them to be conjugated in a site-directed way, since the applied conjugation chemistry will not react with the rest of the amino acids of the antibody.
- C) **Enzymatic conjugations:** Site-directed conjugations can be driven by enzymes that selectively modify antibodies with unique functional groups.
- D) **Linker-based approaches:** Site-directed conjugations can also be performed through linker-based processes. In this case, the processes are chemically driven and differ from previously described processes in that they are focused on linker modifications.

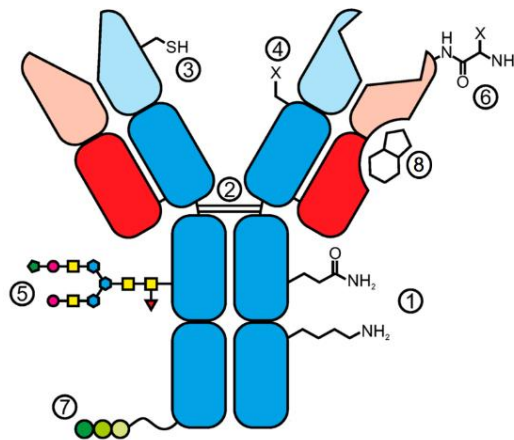


Figure 1.21. Depiction of an antibody marked with different conjugation sites and strategies, explained in Table 1.9. Figure obtained from (Dennler et al., 2015).

Table 1.9. Summary of ADC conjugation strategies (related to Figure 1.18)

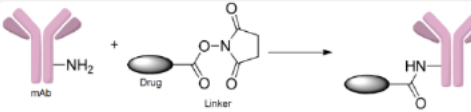

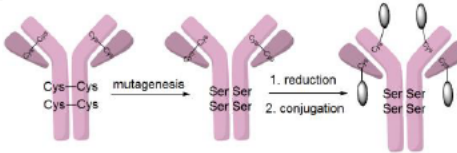
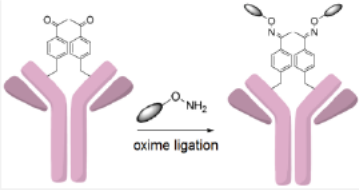

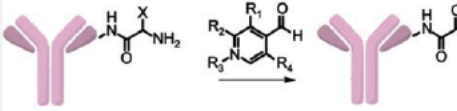
Site	Conjugation target	Type	Example
Natural amino acids	Lysines (Yao et al., 2016): amine group	Endogenous	
Fig. 1.18 (1-3)	Native cysteines (Yao et al., 2016): thiol group	Endogenous	
	Added cysteines (thiomab)	Modified	
Unnatural amino acids	p-acetylfenylalanine (pAcPhe)	Modified	
Carbohydrates	Glucanes	Modified	
Fig. 1.18 (5)			
N-terminal	α -amino group	Endogenous	 <p>Pyridoxal 5'-phosphate: R₁-OH, R₂-CH₃, R₃-H, R₄-CH₂OPO₃²⁻</p>
Fig. 1.18 (6)			



Fig. 1.18

(7)

Several homogeneous ADCs have entered clinical trials and reached late phases, thus, the possibility of seeing a homogeneous ADC in the market being very close (Beck et al., 2017).

1.2.5. Preclinical models for analyzing therapeutic mAb and derived molecules

Experimental therapeutic anticancer molecules need to be tested in order to check their efficacy and this can be achieved through several methodologies. In preclinical research, 2D *in vitro* tests and *in vivo* mice are standard procedures. In the last years, 3D culture models, comprising different methodologies, have been gaining importance.

2D *in vitro* cultures with cells growing as monolayer are routinely used for drug screening, and also allow to study the genetic and molecular mechanisms underlying cancer (Nyga et al., 2011). For the analysis of Trastuzumab and Trastuzumab ADC derived molecules, HER2+ breast cancer cell lines are used, including SKBR3, BT474 and JIM-T1 (Phillips et al., 2008), (Barok et al., 2011). However, the 2D approach does not reproduce the native *in situ* environment of cancer or normal tissues.

In vivo models provide the native 3D microenvironment in which the tumors reside. The most commonly used *in vivo* model is the human tumor xenograft which consists of inoculating human cancer cells or small fragments from cancer specimens either subcutaneously or orthotopically in other organs/tissues of the laboratory mouse and let the tumor grow. Mice used for xenografts are immunocompromised so they

do not reject human cells and include: athymic nude mice, severely compromised immunodeficient (SCID) mice or non-obese diabetic (NOD)/SCID humanized mice (Richmond & Su, 2008). Xenograft models have been useful in therapeutic testing, however, sometimes phase I clinical trials reveal a different behavior of the observed in mice, showing the fact that *in vivo* models may provide insufficient relevant information for translation to the clinic (Nyga et al., 2011).

3D culture models present several advantages over classical 2D cultures, including: morphology of the cells; differentiation, which is better characterized and evidenced in 3D cultures; viability, since cells in 3D culture are more viable and less prone to apoptosis than 2D cells, due to the stronger interactions between cells; drug metabolism; gene expression and protein synthesis. All of this makes 3D system more *in vivo* relevant than 2D (Gupta et al., 2016). 3D culture models comprise different displays, going from cancer cell spheroids to models comprising many cellular lines, or microfluidic devices. They are used in order to simulate more closely the tumor microenvironment, and offer a compromise between the 2D and the mice *in vivo* approaches. Strategies for generating 3D models include spheroids, which can be of one cell type or multicellular; using matrices and scaffolds (the last generation of which can be generated through bioprinting); and microfluidic related methods (Gupta et al., 2016).

1.3. Justification of the thesis project

As it has been explained in the previous sections, immunocytokines and antibody drug conjugates represent some of the most promising and effective therapies against cancer. The work that will be carried out in this thesis will focus on the development of production strategies for Trastuzumab derived molecules: immunocytokines and heterogeneous and homogeneous ADCs. The whole process of generation and validation of these molecules will be performed: starting from

cloning the DNA sequences for Trastuzumab expression and finishing with the *in vivo* validation of one of the produced ADCs.

1.4. References

- Agus, D. B., Gordon, M. S., Taylor, C., Natale, R. B., Karlan, B., Mendelson, D. S., ... Fyfe, G. (2005). Phase I clinical study of pertuzumab, a novel HER dimerization inhibitor, in patients with advanced cancer. *Journal of Clinical Oncology: Official Journal of the American Society of Clinical Oncology*, 23(11), 2534–2543. <https://doi.org/10.1200/JCO.2005.03.184>
- Ahmad, Z. A., Yeap, S. K., Ali, A. M., Ho, W. Y., Alitheen, N. B. M., & Hamid, M. (2012). scFv Antibody: Principles and Clinical Application. *Clinical and Developmental Immunology*, 2012, 1–15. <https://doi.org/10.1155/2012/980250>
- Akbari, B., Farajnia, S., Ahdi Khosroshahi, S., Safari, F., Yousefi, M., Dariushnejad, H., & Rahbarnia, L. (2017). Immunotoxins in cancer therapy: Review and update. *International Reviews of Immunology*, 36(4), 207–219. <https://doi.org/10.1080/08830185.2017.1284211>
- Alibakhshi, A., Abarghooi Kahaki, F., Ahangarzadeh, S., Yaghoobi, H., Yarian, F., Arezumand, R., ... de la Guardia, M. (2017). Targeted cancer therapy through antibody fragments-decorated nanomedicines. *Journal of Controlled Release*, 268(September), 323–334. <https://doi.org/10.1016/j.jconrel.2017.10.036>
- American Cancer Society. (2015). Cancer treatment & survivorship: facts & figures 2014-2015. <https://doi.org/404-320-3333>
- American Cancer Society. (2017). Chemotherapy for Breast Cancer. Retrieved December 8, 2018, from <https://www.cancer.org/cancer/breast-cancer/treatment/chemotherapy-for-breast-cancer.html>
- American Cancer Society. (2018). Targeted Therapy for Breast Cancer. Retrieved December 9, 2018, from <https://xpv.uab.cat/cancer/breast-cancer/treatment/,DanaInfo=.awxyCgftjm0Jz3t,SSL+targeted-therapy-for-breast-cancer.html>
- Andrew, S. M., & Titus, J. A. (2001). Fragmentation of Immunoglobulin G. In *Current Protocols in Immunology* (Vol. Chapter 2, p. Unit 2.8). Hoboken, NJ, USA: John Wiley & Sons, Inc. <https://doi.org/10.1002/0471142735.im0208s21>
- Animal Cell Technology Industrial Platform. (n.d.). Monoclonal Antibodies Approved by the EMA and FDA for Therapeutic Use – ACTIP. Retrieved December 17,

Chapter 1. Introduction

2018, from <https://xpv.uab.cat/products/monoclonal-antibodies-approved-by-the-ema-and-fda-for-therapeutic-use/>, DanaInfo=.awxyCehzpxly2s+

- Arnold, M., & Razum, O. (2012). Stem cell divisions, somatic mutations, cancer etiology, and cancer prevention. *Encyclopedia of Immigrant Health*, 1334(March), 351–358. https://doi.org/10.1007/978-1-4419-5659-0_116
- Barok, M., Tanner, M., Köninki, K., & Isola, J. (2011). Trastuzumab-DM1 causes tumour growth inhibition by mitotic catastrophe in trastuzumab-resistant breast cancer cells *in vivo*. *Breast Cancer Research*, 13(2), R46. <https://doi.org/10.1186/bcr2868>
- Baselga, J., Norton, L., Albanell, J., Kim, Y.-M., & Mendelsohn, J. (1998). Recombinant Humanized Anti-HER2 Antibody (Herceptine™) Enhances the Antitumor Activity of Paclitaxel and Doxorubicin against HER2/neu Overexpressing Human Breast Cancer Xenografts¹. *CANCER RESEARCH* (Vol. 58). Retrieved from <https://xpv.uab.cat/content/58/13/DanaInfo=.acbpfiwxl0Iklo4x3-85t5BV.D5+2825.full-text.pdf>
- Baselga, J., & Swain, S. M. (2009). Novel anticancer targets: Revisiting ERBB2 and discovering ERBB3. *Nature Reviews Cancer*. <https://doi.org/10.1038/nrc2656>
- Baudino, T. (2015). Targeted Cancer Therapy: The Next Generation of Cancer Treatment. *Current Drug Discovery Technologies*, 12(1), 3–20. <https://doi.org/10.2174/1570163812666150602144310>
- Baxevasis, C. N., Perez, S. A., & Papamichail, M. (2009). Cancer immunotherapy. *Critical Reviews in Clinical Laboratory Sciences*, 46(4), 167–189. <https://doi.org/10.1080/10408360902937809>
- Beck, A., Goetsch, L., Dumontet, C., & Corvaia, N. (2017). Strategies and challenges for the next generation of antibody-drug conjugates. *Nature Reviews Drug Discovery*, 16(5), 315–337. <https://doi.org/10.1038/nrd.2016.268>
- Behrens, C. R., Ha, E. H., Chinn, L. L., Bowers, S., Probst, G., Fitch-Bruhns, M., ... Jackson, D. Y. (2015). Antibody-Drug Conjugates (ADCs) Derived from Interchain Cysteine Cross-Linking Demonstrate Improved Homogeneity and Other Pharmacological Properties over Conventional Heterogeneous ADCs. *Molecular Pharmaceutics*, 12(11), 3986–3998. <https://doi.org/10.1021/acs.molpharmaceut.5b00432>
- Block, K. I., Gyllenhaal, C., Lowe, L., Amedei, A., Ruhul Amin, A. R. M., Amin, A., ... Zollo, M. (2015). Designing a broad-spectrum integrative approach for cancer prevention and treatment. *Seminars in Cancer Biology*, 35, S276–S304. <https://doi.org/10.1016/j.semcan.2015.09.007>

<https://doi.org/10.1021/bc900103p>

- Britsch, S., Li, L., Kirchhoff, S., Theuring, F., Brinkmann, V., Birchmeier, C., & Riethmacher, D. (1998). The ErbB2 and ErbB3 receptors and their ligand, neuregulin-1, are essential for development of the sympathetic nervous system, 1825–1836.
- Buss, N. A. P. S., Henderson, S. J., Mcfarlane, M., Shenton, J. M., & Haan, L. De. (2012). Monoclonal antibody therapeutics: history and future. *Current Opinion in Pharmacology*, 12(5), 615–622. <https://doi.org/10.1016/j.coph.2012.08.001>
- Cai, H. H. (2018). Therapeutic monoclonal antibodies approved by FDA in 2017. *MOJ Immunology*, 1(3), 2017–2019. <https://doi.org/10.15406/moji.2018.06.00198>
- Cameron, D., Piccart-Gebhart, M. J., Gelber, R. D., Procter, M., Goldhirsch, A., de Azambuja, E., ... Herceptin Adjuvant (HERA) Trial Study Team. (2017). 11 years' follow-up of trastuzumab after adjuvant chemotherapy in HER2-positive early breast cancer: final analysis of the HERceptin Adjuvant (HERA) trial. *The Lancet*, 389(10075), 1195–1205. [https://doi.org/10.1016/S0140-6736\(16\)32616-2](https://doi.org/10.1016/S0140-6736(16)32616-2)
- Cancello, G., Maisonneuve, P., Rotmensz, N., Viale, G., Mastropasqua, M. G., Pruneri, G., ... Colleoni, M. (2013). Progesterone receptor loss identifies luminal B breast cancer subgroups at higher risk of relapse. *Annals of Oncology*. <https://doi.org/10.1093/annonc/mds430>
- Carter, P. (2001). Improving the efficacy of antibody-based cancer therapies. *Nature Reviews Cancer*, 1(2), 118–129. <https://doi.org/10.1038/35101072>
- Carter, P., Presta, L., Gorman, C. M., Ridgway, J. B., Henner, D., Wong, W. L., ... Shepard, H. M. (1992). Humanization of an anti-p185HER2 antibody for human cancer therapy. *Proceedings of the National Academy of Sciences of the United States of America*, 89(10), 4285–4289. Retrieved from <http://www.ncbi.nlm.nih.gov/pubmed/1350088>
- Chalouni, C., & Doll, S. (2018). Fate of Antibody-Drug Conjugates in Cancer Cells. *Journal of Experimental & Clinical Cancer Research: CR*, 37(1), 20. <https://doi.org/10.1186/s13046-017-0667-1>
- Chari, R. V. J. (2008). Targeted Cancer Therapy: Conferring Specificity to Cytotoxic Drugs. *Accounts of Chemical Research*, 41(1), 98–107. <https://doi.org/10.1021/ar700108g>
- Chari, R. V. J., Miller, M. L., & Widdison, W. C. (2014). Antibody-Drug Conjugates: An Emerging Concept in Cancer Therapy. *Angewandte Chemie International Edition*, 53(15), 3796–3827. <https://doi.org/10.1002/anie.201307628>
- Cho, H. S., Mason, K., Ramyar, K. X., Stanley, A. M., Gabelli, S. B., Denney, D. W., & Leahy, D. J. (2003). Structure of the extracellular region of HER2 alone and in

Chapter 1. Introduction

- complex with the Herceptin Fab. *Nature*. <https://doi.org/10.1038/nature01392>
- Clynes, R. A., Towers, T. L., Presta, L. G., & Ravetch, J. V. (2000). Inhibitory Fc receptors modulate *in vivo* cytotoxicity against tumor targets. *Nature Medicine*. <https://doi.org/10.1038/74704>
- Coleman, M. P., Quaresma, M., Berrino, F., Lutz, J., Angelis, R. De, Capocaccia, R., ... Rachet, B. (2008). Cancer survival in five continents : a worldwide population-based study (CONCORD), 9(August). [https://doi.org/10.1016/S1470-2045\(08\)70179-7](https://doi.org/10.1016/S1470-2045(08)70179-7)
- Cooke, T. (2000). What is HER2? *European Journal of Oncology Nursing*, 4 (Suppl 2, 2–9). <https://doi.org/10.1054/ejon.2000.0072>
- Coussens, L., Yang-Feng, T. L., Liao, Y. C., Chen, E., Gray, A., McGrath, J., ... Ullrich, A. (1985). Tyrosine kinase receptor with extensive homology to EGF receptor shares chromosomal location with neu oncogene. *Science*. <https://doi.org/10.1126/science.2999974>
- Cuello, M., Ettenberg, S. a, Clark, a S., Keane, M. M., Posner, R. H., Nau, M. M., ... Lipkowitz, S. (2001). Down-regulation of the erbB-2 receptor by trastuzumab (herceptin) enhances tumor necrosis factor-related apoptosis-inducing ligand-mediated apoptosis in breast and ovarian cancer cell lines that overexpress erbB-2. *Cancer Research*.
- Dall, P., Koch, T., Göhler, T., Selbach, J., Ammon, A., Eggert, J., ... Cirrincione, U. (2018). Trastuzumab without chemotherapy in the adjuvant treatment of breast cancer : subgroup results from a large observational study, 1–7. <https://doi.org/10.1186/s12885-017-3857-5>
- Davidson, M., & Starling, N. (2016). Trastuzumab in the management of gastroesophageal cancer: patient selection and perspectives. *OncoTargets and Therapy*, 9, 7235–7245. <https://doi.org/10.2147/OTT.S100643>
- de Goeij, B. E., Peipp, M., de Haij, S., van den Brink, E. N., Kellner, C., Riedl, T., ... Parren, P. W. (2014). HER2 monoclonal antibodies that do not interfere with receptor heterodimerization-mediated signaling induce effective internalization and represent valuable components for rational antibody-drug conjugate design. *MAbs*, 6(2), 392–402. <https://doi.org/10.4161/mabs.27705>
- Dela Cruz, J. S., Huang, T. H., Penichet, M. L., & Morrison, S. L. (2004). Antibody-cytokine fusion proteins: innovative weapons in the war against cancer. *Clinical and Experimental Medicine*, 4(2), 57–64. Retrieved from <http://www.ncbi.nlm.nih.gov/pubmed/15672942>
- Dennler, P., Fischer, E., Schibli, R., Dennler, P., Fischer, E., & Schibli, R. (2015). Antibody Conjugates: From Heterogeneous Populations to Defined Reagents.

Chapter 1. Introduction

- Antibodies*, 4(3), 197–224. <https://doi.org/10.3390/antib4030197>
- Deonarain, M. P., Yahioğlu, G., Stamati, I., & Marklew, J. (2015). Emerging formats for next-generation antibody drug conjugates. *Expert Opinion on Drug Discovery*, 10(5), 463–481. <https://doi.org/10.1517/17460441.2015.1025049>
- Diamantis, N., & Banerji, U. (2016). Antibody-drug conjugates - An emerging class of cancer treatment. *British Journal of Cancer*, 114(4), 362–367. <https://doi.org/10.1038/bjc.2015.435>
- Economic Impact of Cancer. (2018). Retrieved August 15, 2018, from <https://www.cancer.org/cancer/cancer-basics/economic-impact-of-cancer.html>
- Ehrlich, P. (1913). Address in Pathology, ON CHEMIOTHERAPY: Delivered before the Seventeenth International Congress of Medicine. *British Medical Journal*, 2(2746), 353–359. Retrieved from <http://www.ncbi.nlm.nih.gov/pubmed/20766753>
- Elvin, J. G., Couston, R. G., & van der Walle, C. F. (2013). Therapeutic antibodies: Market considerations, disease targets and bioprocessing. *International Journal of Pharmaceutics*, 440(1), 83–98. <https://doi.org/10.1016/j.ijpharm.2011.12.039>
- Enblad, G., Karlsson, H., & Loskog, A. S. I. (2015). CAR T-Cell Therapy: The Role of Physical Barriers and Immunosuppression in Lymphoma. *Human Gene Therapy*, 26(8), 498–505. <https://doi.org/10.1089/hum.2015.054>
- Ferraro, A. (2016). Investment in Biopharma Facilities Continues. Retrieved February 28, 2019, from <https://www.pharmamanufacturing.com/articles/2016/investment-in-biopharma-facilities-continues/>
- Fesnak, A. D., Levine, B. L., & June, C. H. (2017). Engineered T Cells: The Promise and Challenges of Cancer Immunotherapy. *Nat Rev Cancer*, 16(9), 566–581. <https://doi.org/10.1038/nrc.2016.97>. Engineered
- Ford, C. H., Newman, C. E., Johnson, J. R., Woodhouse, C. S., Reeder, T. A., Rowland, G. F., & Simmonds, R. G. (1983). Localisation and toxicity study of a vindesine-anti-CEA conjugate in patients with advanced cancer. *British Journal of Cancer*, 47(1), 35–42. Retrieved from <http://www.ncbi.nlm.nih.gov/pubmed/6821632>
- Francisco, J. A., Cerveny, C. G., Meyer, D. L., Mixan, B. J., Klussman, K., Chace, D. F., ... Wahl, A. F. (2003). cAC10-vcMMAE, an anti-CD30-monomethyl auristatin E conjugate with potent and selective antitumor activity. *Blood*, 102(4), 1458–1465. <https://doi.org/10.1182/blood-2003-01-0039>
- Franklin, M. C., Carey, K. D., Vajdos, F. F., Leahy, D. J., De Vos, A. M., & Sliwkowski,

Chapter 1. Introduction

- M. X. (2004). Insights into ErbB signaling from the structure of the ErbB2-pertuzumab complex. *Cancer Cell*. [https://doi.org/10.1016/S1535-6108\(04\)00083-2](https://doi.org/10.1016/S1535-6108(04)00083-2)
- Garrett, T. P. J., Mckern, N. M., Lou, M., Elleman, T. C., Adams, T. E., Lovrecz, G. O., ... Parade, R. (2008). The Crystal Structure of a Truncated ErbB2 Ectodomain Reveals an Active Conformation , Poised to Interact with Other ErbB Receptors Cooperative Research Centre for Cellular Growth Factors CSIRO Health Sciences and Nutrition, *11*, 495–505.
- Gennari, R., Menard, S., Fagnoni, F., Ponchio, L., Scelsi, M., Tagliabue, E., ... Costa, A. (2004). Pilot study of the mechanism of action of preoperative trastuzumab in patients with primary operable breast tumors overexpressing HER2. *Clinical Cancer Research*. <https://doi.org/10.1158/1078-0432.CCR-04-0225>
- Gotwals, P., Cameron, S., Cipolletta, D., Cremasco, V., Crystal, A., Hewes, B., ... Dranoff, G. (2017). Prospects for combining targeted and conventional cancer therapy with immunotherapy. *Nature Reviews Cancer*, *17*(5), 286–301. <https://doi.org/10.1038/nrc.2017.17>
- Guiu, S., Michiels, S., André, F., Cortes, J., Denkert, C., Di Leo, A., ... Reis-Filho, J. S. (2012). Molecular subclasses of breast cancer: How do we define them? The IMPAKT 2012 working group statement. *Annals of Oncology*, *23*(12), 2997–3006. <https://doi.org/10.1093/annonc/mds586>
- Gupta, N., Liu, R., Patel, B., Solomon, D. E., Vaidya, B., & Gupta, V. (2016). Micro fluidics-based 3D cell culture models : Utility in novel drug discovery and delivery research. *Bioengineering and Translational Medicine*, (March), 63–81. <https://doi.org/10.1002/btm2.10013>
- Gutierrez, C., & Schiff, R. (2011). HER2: Biology, detection, and clinical implications. *Archives of Pathology and Laboratory Medicine*, *135*(1), 55–62. <https://doi.org/10.1043/2010-0454-RAR.1>
- Hamblett, K. J., Senter, P. D., Chace, D. F., Sun, M. M. C., Lenox, J., Cervený, C. G., ... Francisco, J. A. (2004). Effects of Drug Loading on the Antitumor Activity of a Monoclonal Antibody Drug Conjugate. *Clinical Cancer Research*, *10*(20), 7063–7070. <https://doi.org/10.1158/1078-0432.CCR-04-0789>
- Hanahan, D., & Weinberg, R. A. (2011). Hallmarks of Cancer: The Next Generation. *Cell*, *144*(5), 646–674. <https://doi.org/10.1016/J.CELL.2011.02.013>
- Hartkopf, A. D., Brendel, M. H., Wallwiener, M., Taran, F.-A., Brucker, S., & Grischke, E.-M. (2014). Trastuzumab Administration in Patients with Metastatic Breast Cancer - Experience of a Large University Breast Center. *Geburtshilfe Und Frauenheilkunde*, *74*(6), 563–568. <https://doi.org/10.1055/s-0034-1368244>

Chapter 1. Introduction

- Hinton, P. R., Xiong, J. M., Johlfs, M. G., Tang, M. T., Keller, S., & Tsurushita, N. (2006). An engineered human IgG1 antibody with longer serum half-life. *Journal of Immunology (Baltimore, Md. : 1950)*, 176(1), 346–356. Retrieved from <http://www.ncbi.nlm.nih.gov/pubmed/16365427>
- Hudis, C. A. (2007). Trastuzumab — Mechanism of Action and Use in Clinical Practice. *New England Journal of Medicine*, 357(1), 39–51. <https://doi.org/10.1056/NEJMra043186>
- Hutmacher, C., & Neri, D. (2018). Antibody-cytokine fusion proteins: Biopharmaceuticals with immunomodulatory properties for cancer therapy. *Advanced Drug Delivery Reviews*. <https://doi.org/10.1016/j.addr.2018.09.002>
- Izumi, Y., Xu, L., Di Tomaso, E., Fukumura, D., & Jain, R. K. (2002). Herceptin acts as an anti-angiogenic cocktail. *Nature*. <https://doi.org/10.1038/416279b>
- Jackson, D. Y. (2016). Processes for Constructing Homogeneous Antibody Drug Conjugates. *Organic Process Research & Development*, 20(5), 852–866. <https://doi.org/10.1021/acs.oprd.6b00067>
- Jain, N., Smith, S. W., Ghone, S., & Tomczuk, B. (2015). Current ADC Linker Chemistry. *Pharmaceutical Research*, 32(11), 3526–3540. <https://doi.org/10.1007/s11095-015-1657-7>
- Jain, R. K. (1990). Physiological barriers to delivery of monoclonal antibodies and other macromolecules in tumors. *Cancer Research*, 50(3 Suppl), 814s–819s. Retrieved from <http://www.ncbi.nlm.nih.gov/pubmed/2404582>
- Jiang, T., Sun, W., Zhu, Q., Burns, N. A., Khan, S. A., Mo, R., & Gu, Z. (2015). Furin-Mediated Sequential Delivery of Anticancer Cytokine and Small-Molecule Drug Shuttled by Graphene. *Advanced Materials*, 27(6), 1021–1028. <https://doi.org/10.1002/adma.201404498>
- Jones, A. L., Barlow, M., Barrett-Lee, P. J., Canney, P. A., Gilmour, I. M., Robb, S. D., ... Verrill, M. W. (2009). Management of cardiac health in trastuzumab-treated patients with breast cancer: updated United Kingdom National Cancer Research Institute recommendations for monitoring. *British Journal of Cancer*, 100(5), 684–692. <https://doi.org/10.1038/sj.bjc.6604909>
- Jones, P. T., Dear, P. H., Foote, J., Neuberger, M. S., & Winter, G. (1986). Replacing the complementarity-determining regions in a human antibody with those from a mouse. *Nature*, 321(6069), 522–525. <https://doi.org/10.1038/321522a0>
- Joubert, N., Denevault-Sabourin, C., Bryden, F., & Viaud-Massuard, M.-C. (2017). Towards antibody-drug conjugates and prodrug strategies with extracellular stimuli-responsive drug delivery in the tumor microenvironment for cancer

Chapter 1. Introduction

- therapy. *European Journal of Medicinal Chemistry*, 142, 393–415. <https://doi.org/10.1016/J.EJMECH.2017.08.049>
- Kalimutho, M., Parsons, K., Mittal, D., López, J. A., Srihari, S., & Khanna, K. K. (2015). Targeted Therapies for Triple-Negative Breast Cancer: Combating a Stubborn Disease. *Trends in Pharmacological Sciences*, 36(12), 822–846. <https://doi.org/10.1016/j.tips.2015.08.009>
- Ko, W. J., Schwab, B., Singer, C. F., Neumann, R., Brodowicz, T., Tomek, S., ... Zielinski, C. C. (2004). Monitoring of Serum Her-2 / neu Predicts Response and Progression- Free Survival to Trastuzumab-Based Treatment in Patients with Metastatic Breast Cancer. *Clinical Cancer Research*, 10, 1618–1624.
- Köhler, G., & Milstein, C. (1975). Continuous cultures of fused cells secreting antibody of predefined specificity. *Nature*, 256(5517), 495–497. <https://doi.org/10.1038/256495a0>
- Konecny, G. E., Meng, Y. G., Untch, M., Wang, H.-J., Bauerfeind, I., Epstein, M., ... Pegram, M. D. (2004). Association between HER-2/neu and vascular endothelial growth factor expression predicts clinical outcome in primary breast cancer patients. *Clinical Cancer Research: An Official Journal of the American Association for Cancer Research*, 10(5), 1706–1716. <https://doi.org/10.1158/1078-0432.CCR-0951-3>
- Kontermann, R. E. (2012). Antibody-cytokine fusion proteins. *Archives of Biochemistry and Biophysics*, 526(2), 194–205. <https://doi.org/10.1016/j.abb.2012.03.001>
- Kontermann, R. E., & Brinkmann, U. (2015). Bispecific antibodies. *Drug Discovery Today*, 20(7), 838–847. <https://doi.org/10.1016/J.DRUDIS.2015.02.008>
- Lambert, J. M., & Berkenblit, A. (2018). Antibody–Drug Conjugates for Cancer Treatment. *Annual Review of Medicine*, 69(1), 191–207. <https://doi.org/10.1146/annurev-med-061516-121357>
- Lambert, J. M., & Chari, R. V. J. (2014). Ado-trastuzumab Emtansine (T-DM1): An Antibody–Drug Conjugate (ADC) for HER2-Positive Breast Cancer. *Journal of Medicinal Chemistry*, 57(16), 6949–6964. <https://doi.org/10.1021/jm500766w>
- Leavy, O. (2010). Therapeutic antibodies: past, present and future. *Nature Reviews Immunology*, 10(5), 297–297. <https://doi.org/10.1038/nri2763>
- Lencer, W. I., & Blumberg, R. S. (2005). A passionate kiss, then run: exocytosis and recycling of IgG by FcRn. *Trends in Cell Biology*, 15(1), 5–9. <https://doi.org/10.1016/j.tcb.2004.11.004>
- Linke, R., Klein, A., & Seimetz, D. (2010). Catumaxomab: clinical development and future directions. *MAbs*, 2(2), 129–136. Retrieved from

Chapter 1. Introduction

<http://www.ncbi.nlm.nih.gov/pubmed/20190561>

- Litvak-Greenfeld, D., & Benhar, I. (2012). Risks and untoward toxicities of antibody-based immunoconjugates. *Advanced Drug Delivery Reviews*, *64*(15), 1782–1799. <https://doi.org/10.1016/j.addr.2012.05.013>
- Lonberg, N., Taylor, L. D., Harding, F. A., Trounstine, M., Higgins, K. M., Schramm, S. R., ... Huszar, D. (1994). Antigen-specific human antibodies from mice comprising four distinct genetic modifications. *Nature*, *368*(6474), 856–859. <https://doi.org/10.1038/368856a0>
- Lopus, M., Oroudjev, E., Wilson, L., Wilhelm, S., Widdison, W., Chari, R., & Jordan, M. A. (2010). Maytansine and cellular metabolites of antibody-maytansinoid conjugates strongly suppress microtubule dynamics by binding to microtubules. *Molecular Cancer Therapeutics*, *9*(10), 2689–2699. <https://doi.org/10.1158/1535-7163.MCT-10-0644>
- Martin, V., Cappuzzo, F., Mazzucchelli, L., & Frattini, M. (2014). HER2 in solid tumors: More than 10 years under the microscope; Where are we now? *Future Oncology*. <https://doi.org/10.2217/fo.14.19>
- Mathe, G., TRAN BA, L. O. C., & BERNARD, J. (1958). [Effect on mouse leukemia 1210 of a combination by diazo-reaction of amethopterin and gamma-globulins from hamsters inoculated with such leukemia by heterografts]. *Comptes Rendus Hebdomadaires Des Seances de l'Academie Des Sciences*, *246*(10), 1626–1628. Retrieved from <http://www.ncbi.nlm.nih.gov/pubmed/13537412>
- Mattos-arruda, L. De, Shen, R., Reis-filho, J. S., Sloan, M., Cancer, K., Sloan, M., ... Avenue, Y. (2016). Cancer nanomedicine: progress, challenges and opportunities. *Nat Rev Clin Oncol.*, *13*(9), 566–579. <https://doi.org/10.1038/nrc.2016.108.Cancer>
- McCafferty, J., Griffiths, A. D., Winter, G., & Chiswell, D. J. (1990). Phage antibodies: filamentous phage displaying antibody variable domains. *Nature*, *348*(6301), 552–554. <https://doi.org/10.1038/348552a0>
- Miller, K. D., Siegel, R. L., Lin, C. C., Mariotto, A. B., Kramer, J. L., Rowland, J. H., ... Jemal, A. (2016). Cancer treatment and survivorship statistics, 2016. *CA: A Cancer Journal for Clinicians*, *66*(4), 271–289. <https://doi.org/10.3322/caac.21349>
- Moasser, M. M. (2007). The oncogene HER2: Its signaling and transforming functions and its role in human cancer pathogenesis. *Oncogene*. <https://doi.org/10.1038/sj.onc.1210477>
- Mohsin, S. K., Weiss, H. L., Gutierrez, M. C., Chamness, G. C., Schiff, R., Digiovanna, M. P., ... Chang, J. C. (2005). Neoadjuvant trastuzumab induces apoptosis in

Chapter 1. Introduction

- primary breast cancers. *Journal of Clinical Oncology : Official Journal of the American Society of Clinical Oncology*.
<https://doi.org/10.1200/JCO.2005.00.661>
- Molina, M. A., Codony-Servat, J., Albanell, J., Rojo, F., Arribas, J., & Baselga, J. (2001). Trastuzumab (Herceptin), a humanized anti-HER2 receptor monoclonal antibody, inhibits basal and activated HER2 ectodomain cleavage in breast cancer cells. *Cancer Research*. <https://doi.org/11406546>
- Molina, M. A., Sáez, R., Ramsey, E. E., Molina, M. A., Sa, R., Ramsey, E. E., ... Lluch, A. (2002). NH 2 -terminal Truncated HER-2 Protein but not Full-Length Receptor Is Associated with Nodal Metastasis in Human Breast Cancer Advances in Brief NH 2 -terminal Truncated HER-2 Protein but not Full-Length Receptor Is Associated with Nodal Metastasis in Hum, *8*(February), 347–353.
- Morrison, S. L., Johnson, M. J., Herzenberg, L. A., & Oi, V. T. (1984). Chimeric human antibody molecules: mouse antigen-binding domains with human constant region domains. *Proceedings of the National Academy of Sciences of the United States of America*, *81*(21), 6851–6855. Retrieved from <http://www.ncbi.nlm.nih.gov/pubmed/6436822>
- Nagata, Y., Lan, K. H., Zhou, X., Tan, M., Esteva, F. J., Sahin, A. A., ... Yu, D. (2004). PTEN activation contributes to tumor inhibition by trastuzumab, and loss of PTEN predicts trastuzumab resistance in patients. *Cancer Cell*. <https://doi.org/10.1016/j.ccr.2004.06.022>
- Nagayama, A., Ellisen, L. W., Chabner, B., & Bardia, A. (2017). Antibody–Drug Conjugates for the Treatment of Solid Tumors: Clinical Experience and Latest Developments. *Targeted Oncology*, *12*(6), 719–739. <https://doi.org/10.1007/s11523-017-0535-0>
- Nahta, R., Yu, D., Hung, M. C., Hortobagyi, G. N., & Esteva, F. J. (2006). Mechanisms of disease: Understanding resistance to HER2-targeted therapy in human breast cancer. *Nature Clinical Practice Oncology*. <https://doi.org/10.1038/ncponc0509>
- National Cancer Registration & Analysis Service and Cancer Research UK: “Chemotherapy, Radiotherapy and Tumour Resections in England: 2013-2014” workbook. (2017). Retrieved December 8, 2018, from http://www.ncin.org.uk/cancer_type_and_topic_specific_work/topic_specific_work/main_cancer_treatments
- Nelson, A. L. (2010). Antibody fragments: hope and hype. *MAbs*, *2*(1), 77–83. Retrieved from <http://www.ncbi.nlm.nih.gov/pubmed/20093855>
- Nyga, A., Cheema, U., & Loizidou, M. (2011). 3D tumour models: novel *in vitro* approaches to cancer studies. *Journal of Cell Communication and Signaling*,

Chapter 1. Introduction

5(3), 239–248. <https://doi.org/10.1007/s12079-011-0132-4>

- Ober, R. J., Radu, C. G., Ghetie, V., & Ward, E. S. (2001). Differences in promiscuity for antibody-FcRn interactions across species: implications for therapeutic antibodies. *International Immunology*, *13*(12), 1551–1559. Retrieved from <http://www.ncbi.nlm.nih.gov/pubmed/11717196>
- Onitilo, A. A., Engel, J. M., Greenlee, R. T., & Mukesh, B. N. (2009). Breast cancer subtypes based on ER/PR and Her2 expression: Comparison of clinicopathologic features and survival. *Clinical Medicine and Research*, *7*(1–2), 4–13. <https://doi.org/10.3121/cmr.2008.825>
- Panowski, S., Bhakta, S., Raab, H., Polakis, P., & Junutula, J. R. (2014). Site-specific antibody drug conjugates for cancer therapy. *MABs*, *6*(1), 34–45. <https://doi.org/10.4161/mabs.27022>
- Peng, L. S., Penichet, M. L., & Morrison, S. L. (1999). *Antitumor Activity IL-12 Bioactivity and Demonstrates Protein Retains Antibody Specificity and A Single-Chain IL-12 IgG3 Antibody Fusion*. *J Immunol References* (Vol. 250). Retrieved from <http://www.jimmunol.org/content/163/1/http://www.jimmunol.org/content/163/1/250.full#ref-list-1>
- Pérez-Herrero, E., & Fernández-Medarde, A. (2015). Advanced targeted therapies in cancer: Drug nanocarriers, the future of chemotherapy. *European Journal of Pharmaceutics and Biopharmaceutics*, *93*, 52–79. <https://doi.org/10.1016/j.ejpb.2015.03.018>
- Peters, C., & Brown, S. (2015). Antibody-drug conjugates as novel anti-cancer chemotherapeutics. *Bioscience Reports*, *35*(4), e00225–e00225. <https://doi.org/10.1042/BSR20150089>
- Phillips, G. D. L., Li, G., Dugger, D. L., Crocker, L. M., Parsons, K. L., Mai, E., ... Sliwkowski, M. X. (2008). Targeting HER2-Positive Breast Cancer with Trastuzumab-DM1, an Antibody–Cytotoxic Drug Conjugate. *Cancer Res*, *68*(22), 9280–9290. <https://doi.org/10.1158/0008-5472.CAN-08-1776>
- Piccart-Gebhart, M. J., Procter, M., Leyland-Jones, B., Goldhirsch, A., Untch, M., Smith, I., ... Herceptin Adjuvant (HERA) Trial Study Team. (2005). Trastuzumab after Adjuvant Chemotherapy in HER2-Positive Breast Cancer. *New England Journal of Medicine*, *353*(16), 1659–1672. <https://doi.org/10.1056/NEJMoa052306>
- Pietras, R. J., Fendly, B. M., Chazin, V. R., Pegram, M. D., Howell, S. B., & Slamon, D. J. (1994). Antibody to HER-2/neu receptor blocks DNA repair after cisplatin in human breast and ovarian cancer cells. *Oncogene*, *9*(7), 1829–1838. Retrieved from <http://www.ncbi.nlm.nih.gov/pubmed/7911565>

Chapter 1. Introduction

- Presta, L. G. (2006). Engineering of therapeutic antibodies to minimize immunogenicity and optimize function. *Advanced Drug Delivery Reviews*, 58(5–6), 640–656. <https://doi.org/10.1016/j.addr.2006.01.026>
- Richmond, A., & Su, Y. (2008). Mouse xenograft models vs GEM models for human cancer therapeutics. *Disease Models and Mechanisms*, 1(2–3), 78–82. <https://doi.org/10.1242/dmm.000976>
- Roskoski, R. (2014). The ErbB/HER family of protein-tyrosine kinases and cancer. *Pharmacological Research*, 79, 34–74. <https://doi.org/10.1016/j.phrs.2013.11.002>
- Rubin, I., & Yarden, Y. (2001). The basic biology of HER2. *Annals of Oncology*. https://doi.org/10.1093/annonc/12.suppl_1.S3
- Santos, M. L. dos, Quintilio, W., Manieri, T. M., Tsuruta, L. R., Moro, A. M., Santos, M. L. dos, ... Moro, A. M. (2018). Advances and challenges in therapeutic monoclonal antibodies drug development. *Brazilian Journal of Pharmaceutical Sciences*, 54(spe). <https://doi.org/10.1590/s2175-97902018000001007>
- Schnitt, S. J. (2010). Classification and prognosis of invasive breast cancer: from morphology to molecular taxonomy. *Modern Pathology : An Official Journal of the United States and Canadian Academy of Pathology, Inc.* <https://doi.org/10.1038/modpathol.2010.33>
- Scholl, S., Beuzeboc, P., & Pouillart, P. (2001). Targeting HER2 in other tumor types. *Annals of Oncology*. https://doi.org/10.1093/annonc/12.suppl_1.S81
- Schroeder, H. W., & Cavacini, L. (2010). Structure and function of immunoglobulins. *Journal of Allergy and Clinical Immunology*, 125(2), S41–S52. <https://doi.org/10.1016/j.jaci.2009.09.046>
- Schumacher, D., Hackenberger, C. P. R., Leonhardt, H., & Helma, J. (2016). Current Status: Site-Specific Antibody Drug Conjugates. *Journal of Clinical Immunology*, 36 Suppl 1, 100–107. <https://doi.org/10.1007/s10875-016-0265-6>
- Selis, F., Focà, G., Sandomenico, A., Marra, C., Di Mauro, C., Sacconi Jotti, G., ... Tonon, G. (2016). Pegylated Trastuzumab Fragments Acquire an Increased *in vivo* Stability but Show a Largely Reduced Affinity for the Target Antigen. *International Journal of Molecular Sciences*, 17(4), 491. <https://doi.org/10.3390/ijms17040491>
- Sharma, V. (2018). CPhI Annual Report 2018: ADCs Growth Driven by Lack of In-House Facilities, Oncology and Integrated CDMOs. Retrieved February 28, 2019, from <https://www.pharmoutsourcing.com/Featured-Articles/354437-CPhI-Annual-Report-2018-ADCs-Growth-Driven-by-Lack-of-In-House-Facilities-Oncology-and-Integrated-CDMOs/>

Chapter 1. Introduction

- Siegel, R., Desantis, C., Virgo, K., Stein, K., Mariotto, A., Smith, T., ... Fedewa, S. (2013). Cancer Treatment and Survivorship Statistics, 2012. <https://doi.org/10.3322/caac.21149>.
- Slamon, D. J., Clark, G. M., Wong, S. G., Levin, W. J., Ullrich, A., & Mcguire, W. L. (1987). Correlation Amplification. *Science*, 235(21), 0–5.
- Slamon, D. J., Leyland-Jones, B., Shak, S., Fuchs, H., Paton, V., Bajamonde, A., ... Norton, L. (2001). Use of Chemotherapy plus a Monoclonal Antibody against HER2 for Metastatic Breast Cancer That Overexpresses HER2. *New England Journal of Medicine*, 344(11), 783–792. <https://doi.org/10.1056/NEJM200103153441101>
- Sliwkowskiso, M. X., Schaefers, G., Akita, W., Lofgrens, J. A., Fitzpatrick, V. D., Nuijens, A., ... Iij, K. L. C. (1994). Coexpression of, 269(20), 14661–14665.
- Smith, A. L., & Nicolaou, K. C. (1996). The Eneidyne Antibiotics. *Journal of Medicinal Chemistry*, 39(11), 2103–2117. <https://doi.org/10.1021/jm9600398>
- Sochaj, A. M., Świdarska, K. W., & Otlewski, J. (2015). Current methods for the synthesis of homogeneous antibody-drug conjugates. *Biotechnology Advances*, 33(6), 775–784. <https://doi.org/10.1016/j.biotechadv.2015.05.001>
- Society, A. C. (2011). *Global Cancer Facts & Figures 2nd Edition*. Atlanta: American Cancer Society; 2011. <https://doi.org/10.1002/ijc.27711>
- Stages of cancer | Cancer Research UK. (n.d.). Retrieved December 8, 2018, from <https://xpv.uab.cat/about-cancer/what-is-cancer/>,DanalInfo=.awxyCgftjm01p4ro6syA3T9B3,SSL+stages-of-cancer
- Stern, M., & Herrmann, R. (2005). Overview of monoclonal antibodies in cancer therapy: present and promise. *Critical Reviews in Oncology/Hematology*, 54(1), 11–29. <https://doi.org/10.1016/j.critrevonc.2004.10.011>
- Strohl, W. R. (2009). Optimization of Fc-mediated effector functions of monoclonal antibodies. *Current Opinion in Biotechnology*, 20(6), 685–691. <https://doi.org/10.1016/j.copbio.2009.10.011>
- Tanvetyanon, T., Clark, J. I., Campbell, S. C., & Lo, S. S. (2005). Neoadjuvant therapy: An emerging concept in oncology. *Southern Medical Journal*. <https://doi.org/10.1097/01.SMJ.0000145313.92610.12>
- Teicher, B. A., & Chari, R. V. J. (2011). Antibody Conjugate Therapeutics: Challenges and Potential. *Clinical Cancer Research*, 17(20), 6389–6397. <https://doi.org/10.1158/1078-0432.CCR-11-1417>
- ten Cate, B., Bremer, E., de Bruyn, M., Bijma, T., Samplonius, D., Schwemmlin, M., ... Helfrich, W. (2009). A novel AML-selective TRAIL fusion protein that is

Chapter 1. Introduction

- superior to Gemtuzumab Ozogamicin in terms of *in vitro* selectivity, activity and stability. *Leukemia*, 23(8), 1389–1397. <https://doi.org/10.1038/leu.2009.34>
- Tolaney, S. M., Barry, W. T., Dang, C. T., Yardley, D. A., Moy, B., Marcom, P. K., ... Winer, E. P. (2015). Adjuvant Paclitaxel and Trastuzumab for Node-Negative, HER2-Positive Breast Cancer. *New England Journal of Medicine*, 372(2), 134–141. <https://doi.org/10.1056/NEJMoa1406281>
- Tsuchikama, K., & An, Z. (2018). Antibody-drug conjugates: recent advances in conjugation and linker chemistries. *Protein & Cell*, 9(1), 33–46. <https://doi.org/10.1007/s13238-016-0323-0>
- Tudoran, O., Virtic, O., Balacescu, L., Lisencu, C., Fetica, B., Balacescu, O., ... Gherman, C. (2015). Baseline blood immunological profiling differentiates between Her2– breast cancer molecular subtypes: implications for immunomediated mechanisms of treatment response. *OncoTargets and Therapy*, 8, 3415. <https://doi.org/10.2147/OTT.S91720>
- Tzahar, E., Waterman, H., Chen, X., Levkowitz, G. I. L., Karunakaran, D., Lavi, S., & Ratzkin, B. J. (1996). A Hierarchical Network of Interreceptor Interactions Determines Signal Transduction by Neu Differentiation Factor / Neuregulin and Epidermal Growth Factor, 16(10), 5276–5287.
- Vennström, B., & Michael Bishop, J. (1982). Isolation and characterization of chicken DNA homologous to the two putative oncogenes of avian erythroblastosis virus. *Cell*. [https://doi.org/10.1016/0092-8674\(82\)90383-X](https://doi.org/10.1016/0092-8674(82)90383-X)
- WHO | Cancer. (2018). Retrieved August 15, 2018, from <http://www.who.int/cancer/en/>
- Wieduwilt, M., & Moasser, M. (2008). The epidermal growth factor receptor family: Biology driving targeted therapeutics. *Cell Mol Life Sci*, 65(10), 1566–1584. <https://doi.org/10.1007/s00018-008-7440-8>
- Wilson, K. S., Roberts, H., Leek, R., Harris, A. L., & Geradts, J. (2002). Differential gene expression patterns in HER2/neu-positive and -negative breast cancer cell lines and tissues. *The American Journal of Pathology*, 161(4), 1171–1185. [https://doi.org/10.1016/S0002-9440\(10\)64394-5](https://doi.org/10.1016/S0002-9440(10)64394-5)
- Wooge, C. (2014). Successful Strategies in the Development and Technology Transfer of Antibody-Drug Conjugates. *ADC Review / Journal of Antibody-Drug Conjugates*, 2014(5). <https://doi.org/10.14229/jadc.2014.5.2.001>
- Yao, H., Jiang, F., Lu, A., & Zhang, G. (2016). Methods to design and synthesize antibody-drug conjugates (ADCs). *International Journal of Molecular Sciences*, 17(2). <https://doi.org/10.3390/ijms17020194>
- Yildiz, I., Shukla, S., & Steinmetz, N. F. (2011). Applications of viral nanoparticles in

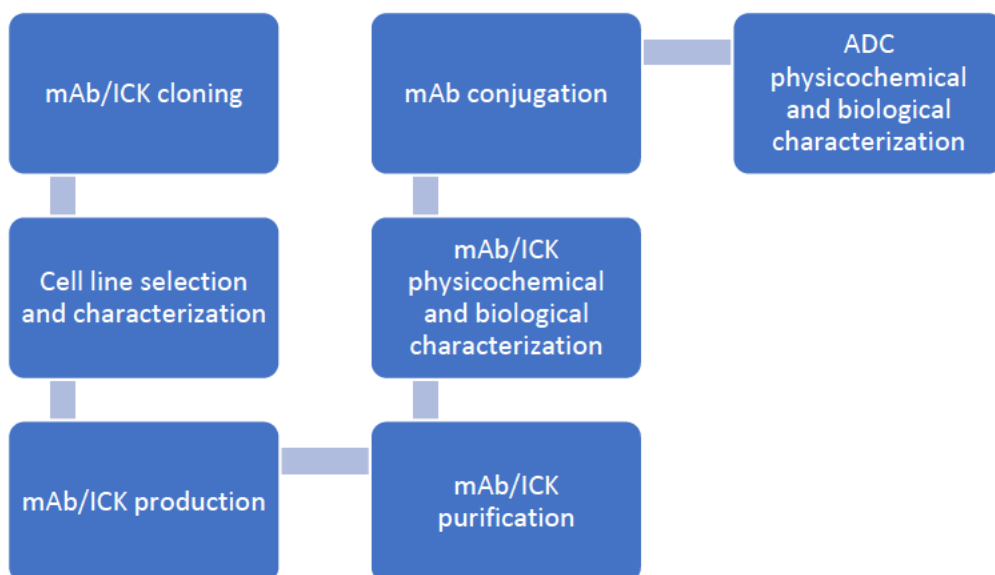
Chapter 1. Introduction

- medicine. *Current Opinion in Biotechnology*, 22(6), 901–908. <https://doi.org/10.1016/j.copbio.2011.04.020>
- Younes, A., Bartlett, N. L., Leonard, J. P., Kennedy, D. A., Lynch, C. M., Sievers, E. L., & Forero-Torres, A. (2010). Brentuximab Vedotin (SGN-35) for Relapsed CD30-Positive Lymphomas. *New England Journal of Medicine*, 363(19), 1812–1821. <https://doi.org/10.1056/NEJMoa1002965>
- Zhang, A., Shen, G., Zhao, T., Zhang, G., Liu, J., Song, L., ... Wu, Q. (2010). Augmented inhibition of angiogenesis by combination of HER2 antibody chA21 and trastuzumab in human ovarian carcinoma xenograft. *Journal of Ovarian Research*, 3(1), 1–8. <https://doi.org/10.1186/1757-2215-3-20>
- Zhao, Y., Wang, Q. J., Yang, S., Kochenderfer, J. N., Zheng, Z., Zhong, X., ... Morgan, R. A. (2009). A Herceptin-Based Chimeric Antigen Receptor with Modified Signaling Domains Leads to Enhanced Survival of Transduced T Lymphocytes and Antitumor Activity. *The Journal of Immunology*, 183(9), 5563–5574. <https://doi.org/10.4049/jimmunol.0900447>
- Zheng, P.-P., Kros, J. M., & Li, J. (2018). Approved CAR T cell therapies: ice bucket challenges on glaring safety risks and long-term impacts. *Drug Discovery Today*, 23(6), 1175–1182. <https://doi.org/10.1016/J.DRUDIS.2018.02.012>

2. Objectives

The work presented in this thesis has been performed in the Cellular Bioprocess and Engineering Group, the main aim of which is the development, optimization and scaling up of bioprocesses, based specially on mammalian cells. In particular, the work performed in the thesis is focused on the development of a production platform for therapeutic antibody-derived molecules: immunocytokines and antibody drug conjugates, based on the therapeutic anti-HER2 monoclonal antibody model Trastuzumab. The production platform comprises the antibody alone or antibody-fusion protein or antibody-drug conjugates conjugation, production, purification, and the implementation of tools for physicochemical and biological activity characterization. Several antibody formats and conjugation strategies will be assessed.

A summarized diagram of the proposed platform is depicted below:



The main objective can be divided in the following sub-objectives:

Chapter 2. Objectives

- Construction of Trastuzumab, which includes: cloning of the DNA sequences into the selected expression vector, transfection and selection of the producer HEK293 cell line, production, purification, and physicochemical and biological characterization of the product, for which several tools will be established, and will be later applied to the immunocytokine and antibody-drug conjugate products. The following list includes the characterized features and the tools implemented for their assessment:
 - Recognition capacity (Identity): ELISA and flow cytometry
 - Amount of the obtained product: SDS-PAGE
 - Purity and aggregate content: SDS-PAGE and HPLC-SEC
 - Security: endotoxin content test
 - Stability: HPLC-SEC
- Generation of an immunocytokine based on Trastuzumab: the antiproliferative activity of several cytokines will be assessed, and one of them will be selected and genetically fused to Trastuzumab. The fusion construct will then be produced, purified and both physicochemically and biologically characterized.
- Definition of conjugation strategies of Trastuzumab to the cytotoxic drugs DM1 and vcMMAE, in heterogeneous and homogeneous ways. Construction (applying the development sequence implemented for Trastuzumab) of the variant Trastuzumab_cys114 for the homogeneous conjugation with vcMMAE. Conjugation and physicochemical and biological characterization of the conjugate products will be performed. Additional characterization tools will be implemented:
 - Drug Antibody Ratio: UV spectroscopy, HIC-HPLC, Mass Spectrometry (MS)

Chapter 2. Objectives

- Safety: free drug assessment through SEC-HPLC

- Development of fragment conjugates: construction, production, and purification of a scFv and a scFv_cys111 anti-HER2 fragments based on Trastuzumab. The scFv fragment will be heterogeneously conjugated to DM1 and scFv_cys111 will be homogeneously conjugated to vcMMAE. Both fragment conjugates will then be physicochemically and biologically characterized.

- Development and evaluation of different methodologies for the assessment of the biological activity of the generated products. *In vitro* 2D and 3D models will be compared, and an *in vivo* model based on immunosuppressed mice will also be developed in order to validate the therapeutic effect of one of the selected antibody conjugated candidates.

3. Results (I): Development of Trastuzumab production, purification and physicochemical characterization

3.1. Introduction

In order to develop an antibody fused to a cytokine or an antibody drug conjugate production platform, the first step consists in producing the selected antibody of interest, which in this case corresponds to Trastuzumab. As it has been mentioned in the introduction chapter (see section 1.2.2.), Trastuzumab is approved for its use in breast cancer and metastatic cancer therapy and forms the antibody part of the commercially approved ADC Trastuzumab-emtansine (see section 1.2.10). As it is the case for all recombinant proteins, antibody production requires several steps that start with the obtaining of the codifying DNA sequence and end up with the purification and characterization of the product. The sequence followed in this chapter is depicted in Figure 3.1, and considerations for its several steps are commented below.

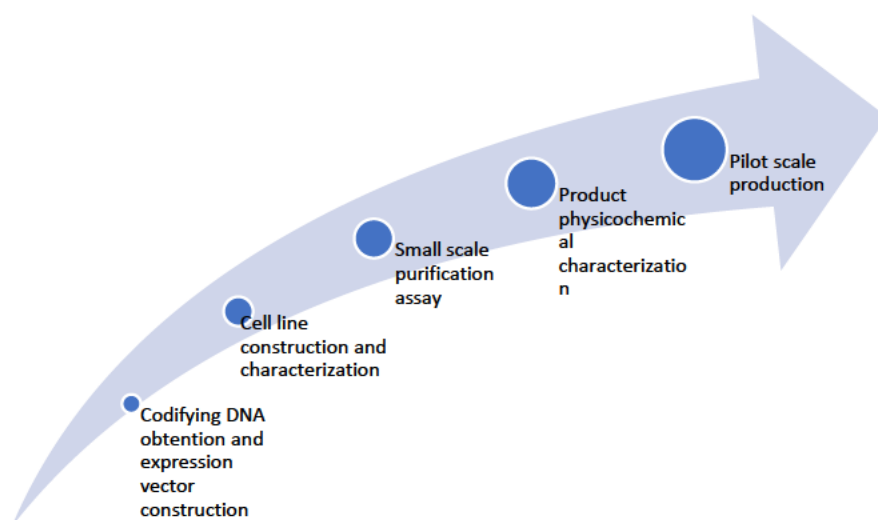


Figure 3.1. Sequence followed for Trastuzumab production, purification and physicochemical characterization.

- **DNA sequence obtention:** in order to express the therapeutic antibody Trastuzumab, it has to be considered that two DNA sequences are necessary, one for the heavy chain (HC) and another for the light chain (LC) that form the antibody (see section 1.2.1). DNA sequences from heavy and light trastuzumab chains were indirectly obtained from an online database and were then synthetically generated (see section 3.2). An important parameter when designing DNA sequences consists in taking into account the fact that the genetic code is degenerated, resulting in different codons codifying for each amino acid (Komar, 2016). In this regard, the codon usage bias (preferred codons for each amino acid of each species) and codon context (the codons that immediately precede or follow the preferred codons) have to be adapted to the expression host in order to maximize the transcription rate of the gene of interest. At this respect, the Codon Optimization On-line (COOL) software (Chin et al., 2014), were used for this purpose.
- **Expression vector construction:** in order to express the antibody, it is necessary to express its 2 chains. Regarding the expression vector, this can be achieved through different ways. One possibility is the expression of each chain in a different mRNA. The other possibility is the coexpression of both chains in the same mRNA, which is the one that has been used in this work (see section 3.2). This could be performed using a derivate of the commercial bicistronic pIRESpuro3 plasmid (Figure 3.2). The main elements of the pIRESpuro3 expression cassette include:
 - A cytomegalovirus (CMV) promoter with an enhancer sequence.
 - A multiple cloning site (MCS) sequence, in which the gene of interest is cloned.
 - An IVS synthetic intron (Intervening sequence) which improves the stability of the mRNA (Huang et al., 1990).

Chapter 3. Results (I)

- An Internal Ribosome Entry Site (IRES) sequence for expressing 2 genes in the same mRNA by allowing the entry of the ribosome inside the codifying mRNA (Jackson et al., 1990).
- A gene codifying for the puromycin-acetyltransferase gene (*pac*), which acts as a selection marker by conferring resistance to the eukaryotic antibiotic puromycin, which is used to stably select the transfected cells (Paik et al., 1985) .

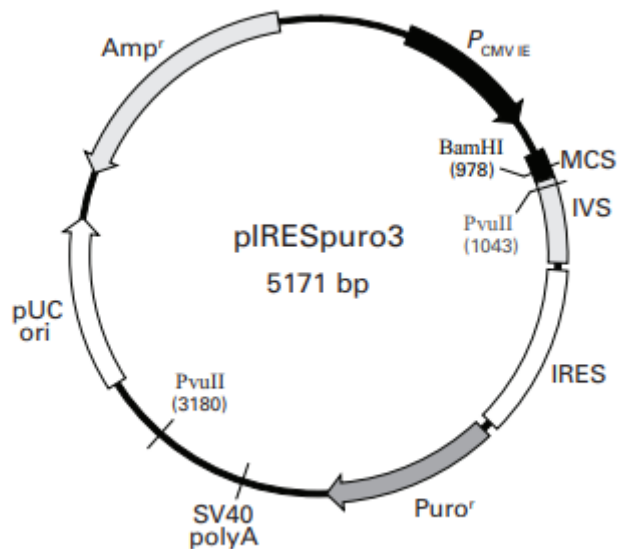


Figure 3.2. Graphic map of pIRESpuro3 commercial plasmid. Obtained from (Clontech, 2010).

As it has been seen, the IRES element allows the expression of two genes in the same mRNA. This fact presents several advantages:

- Since the plasmid does not have a replication origin, all the selected cells contain the whole expression cassette integrated in their genome: the selection marker, necessary for cell survival, will only be expressed when the promoter of the

Chapter 3. Results (I)

expression cassette (therefore, the whole expression cassette) is also integrated.

- The cells containing the expression marker will also express the target gene of interest, therefore, all the selected cells will produce the protein of interest.
- Coexpressing the gene of interest with the selection marker allows avoiding undesirable issues that appear when other expression strategies are used. For example, when two different promoters are used, there can be resistant cells that do not express the protein of interest due to epigenetic silencing (Mariati et al., 2014).
- **Host cell line:** Once the expression vector is constructed, the next step consists in its transfection to the host cell line. The cell line used in this work for Trastuzumab and all the different Trastuzumab derived antibody molecules production has been HEK293 (Human Embryonic Kidney 293). Most therapeutic recombinant proteins are currently produced with CHO (Chinese Hamster Ovarium) cell line (Butler et al., 2014), with commercial Trastuzumab (Herceptin) also being produced with this cell line (Li et al., 2010). However, human cell lines such as HEK293 have been gaining importance in the last years, with several commercially approved therapeutic proteins being produced in human cell lines (Dumont et al., 2016). With respect to CHO cell line, they present the main advantage of performing human glycosylation on the produced protein, avoiding some immunogenic glycosylation produced by CHO cells (Dumont et al., 2016). Moreover, other characteristics of HEK293 that render them viable production hosts include:
 - Easily genetically modified (Kim et al., 2012), with a high transfection efficiency (Thomas et al., 2005).
 - Easy growth in suspension cultures, reaching high densities.

Chapter 3. Results (I)

- Growth in media that do not contain bovine serum (chemically defined media allow better reproducibility and safety profiles than media containing human derived molecules) (Liste-Calleja et al., 2014).

Once the cell line has been selected, its characterization in terms of growth rate and maximum cell density achieved in small scale cultures (Erlenmeyer) are performed, prior to the scale-up to bioreactor culture.

- **Recombinant protein production in bioreactors: single use technologies.** In the production phase, cells are typically cultured in a bioreactor in controlled conditions of temperature, pH and pO_2 mediating automatized control systems managed from the Digital Control Unit (DCU). Normally, some of the parameters controlled by the DCU are monitored on-line through the corresponding probes (oxygen, pH, temperature), and other off-line variables are also monitored, such as counting of viable cells or metabolite analysis. Classical bioreactor culture processes are carried out in stainless steel bioreactors, however, the use of single use bioreactors in the biopharmaceutical industry has hugely incremented in the last years (Kaiser et al., 2015). Single use bioreactors are mostly based bag technology made of FDA-approved plastics (Löffelholz et al., 2013), and present several advantages (Kaiser et al., 2015):
 - Reduced cleaning procedures.
 - Lack of validation issues (cleaning, sterilization, etc.).
 - Lower investment costs.
 - Easier to adapt to changing process demands.

Chapter 3. Results (I)

- Less contamination risks (including avoiding cross-contamination issues).

The breakthrough of this technology was paved by the wave-technology, based on disposable bags mounted on rocking devices (the WAVE bioreactor was introduced in 1996 (Shukla et al., 2013)). The success of this technology led the way to the appearance of stirred bioreactors based on the bag technology, with higher working volumes, up to the m³ scale (Kaiser et al., 2015). In this work, both single use technologies (wave and stirred bioreactor) have been used.

- **Downstream: recovery and purification of the product.** Once the product has been produced, it has to be recovered through a series of steps forming the downstream process. Downstream sequences for monoclonal antibody production processes have been established in the biopharmaceutical industry, consisting in the following general steps compliant with FDA quality requirements (Shukla et al., 2017; Xenopoulos, 2015):
 - Cell culture harvest
 - Centrifugation: it is the first common step for separating the culture broth, where the antibody is secreted, from the cells. However, complete removal of cells and cell debris, which must be removed prior to chromatography, cannot be achieved (Shukla et al., 2007).
 - Depth filtration: applied in order to remove cellular debris. Depth filtration consists in using a porous medium that is capable of retaining particulates throughout its matrix rather than just on its surface. Depth filters typically consist of a fibrous bed of cellulose or polypropylene fibers along

Chapter 3. Results (I)

with a filter aid (diatomaceous earth) and binder (Khanal et al., 2018), therefore, not having an absolute pore size rating.

- Membrane filtration: normally of 0.45 or 0.2 μm of absolute pore size rating, it ensures the removal of solid particulates from the cell culture harvest supernatant.
- Capture chromatography: protein A chromatography. It is an affinity chromatography based on protein A ligand, which has a strong affinity for the constant fraction of the heavy chain of most IgGs. It serves as the capture step of the process, and can yield around 99% purity starting from the cell culture supernatant (Shukla et al., 2007). Further polishing steps can remove levels of host cell protein contaminants, DNA and product-related species (high molecular weight aggregates and low molecular weight clipped species) and assure viral safety.
- Low pH viral inactivation: due to regulatory requirements (Shukla et al., 2007), a low pH treatment is applied in order to inactivate virus content. Since the elution from the protein A chromatography is performed with an acid pH, the eluted solution is adjusted to $\text{pH} < 3.8$ and incubated assuring the viral inactivation.
- Polishing chromatography steps: these steps are aimed at reducing host cell protein impurities, high molecular weight aggregates, low molecular clipped species, and DNA and leached protein A that remain after the protein A chromatographic step. Usually 2 to 3 subsequent chromatography steps are typically employed, consisting in cation-exchange chromatography (CEX), anion-exchange chromatography (AEX) and hydrophobic chromatography (HIC) (Marichal-Gallardo et al., 2012).
- Viral filtration: applied to complement the low pH- viral inactivation step.

Chapter 3. Results (I)

- Ultrafiltration / Diafiltration: step to exchange the buffer to the formulation buffer.

For smaller scale productions and purifications, as it is the case of this thesis work, modifications of this downstream sequence can be applied.

- **Characterization of the product:** Once purified, the product needs to be characterized. Biotechnological therapeutics, particularly monoclonal antibodies, can have numerous quality attributes that can potentially affect the safety and/or efficacy of the product (Rathore, 2009). The European Medicine's Agency (EMA) regarding "Production and Quality Control of Monoclonal Antibodies" states that "the mAb should be characterized thoroughly", including several parameters such as molecular weight or size, disulfide bridge integrity, aggregates, and glycosylation pattern (EMA, 2016). Physicochemical and functional characterization need to be performed in order to assure that the product is able to correctly perform its functions. Immunological properties of the antibody, such as determining the binding ability to its target antigen, also have to be performed (EMA, 2016). The characterization of several of these parameters will be performed in this work:

- Concentration
- Purity
- Molecular weight
- Structure: the formation of the interchain disulfide bridges of the antibody are critical for the correct structure formation and stability of the antibody (McAuley et al., 2008).
- Antigen recognition capacity. The antibody ability to recognize its target antigen will be assessed in two different ways: ability to bind to an immobilized antigen and ability to bind to a cell surface antigen, for which several cell lines have been used:

Chapter 3. Results (I)

- SKBR3: it is a breast cancer model cell line which overexpresses the target antigen of Trastuzumab antibody (HER2).
 - MCF7: breast cancer model cell line that does not overexpress the HER2 antigen.
 - Hybridoma (KB-26.5): hybridomas are cell lines formed by fusing an immortal B cancer cell with an antibody-producing B cell. It does not express the HER2 antigen.
- Aggregates: the active monoclonal antibody will be found in a monomer form, while aggregates can affect the biological activity of the mAb, are irreversible, have the potential to cause side effects (Wang et al., 2018) and, from a conjugation point of view, are more prone to precipitation once conjugated and render more difficult obtaining a conjugated product with the desired proprieties (see chapter 5).
 - Glycosylation pattern: glycosylation is one of the most common post-translational modifications (PTMs) of proteins, and have an effect on a high number of functions of their protein carrier. In antibodies, glycosylation can affect their stability and in vivo efficacy, including pharmacokinetics and immunogenicity (Torkashvand et al., 2017). IgG1 antibodies are typically glycosylated on the Asparagine 297 residue of the heavy chain, with the light chain generally not being glycosylated.
 - Safety: endotoxin content test. Endotoxins (molecules that come from gram negative bacteria) can cause fever after intravenous administration or inhalation (they are pyrogens) (Franco et al., 2018). Therefore, their content in a therapeutic product has to be determined.

- Stability: the produced antibody has to remain stable along time, maintaining its function. One of the parameters that can be analyzed for stability determination is the aggregate content of the antibody sample.

Trastuzumab production is the base for the subsequent generation of the different ADCs later assessed in this thesis (chapter 5), and allows the implementation of several tools for antibody and ADC characterization that will also be used later.

3.2. Trastuzumab sequence construction and cloning

As it has been explained in the introduction, Trastuzumab is formed by two different protein subunits: the heavy chain (HC) and the light chain (LC). The DNA sequences of each chain that were used by Genentech for Trastuzumab production are not publicly available. However, their amino acid sequences are reported in the Drugbank database (Wishart et al., 2017). These amino acid sequences were used to obtain the DNA sequences by reverse translation. Then, the obtained DNA sequences were adapted to the HEK293 host codon usage, since due to the degeneration of the genetic code, multiple codons can be used to codify for a determined DNA sequence. This was performed using the Codon Optimization Online (COOL) software (Chin et al., 2014), which considers the individual codon usage and the codon context of a given sequence, thus obtaining a sequence similar to a natural sequence of the host organism. These sequences are contained in the Appendix I.

Up to this point, the obtained DNA sequences of each chain codified for the mature protein, therefore lacking a signal peptide, which was added to each chain sequence.

Chapter 3. Results (I)

Signal peptides are short sequences which are necessary in order to allow the secretion of a protein from a production host, and which are then cleaved from the mature protein (Martoglio & Dobberstein, 1998) (this is the reason why it was not included in the DrugBank sequence). Bibliographically obtained signal peptides described as highly efficient for Trastuzumab secretion (Haryadi et al., 2015) were used. Finally, the restriction sites NheI and AgeI were added to the LC sequence, while NotI and BamHI were added to the HC sequence, in order to clone them into the expression vector. Signal sequences are included in the sequences contained in the Appendix I. The designed DNA sequences were then chemically synthesized by the company GenScript (US), each one of them (LC and HC) in a commercial pUC57 plasmid vector (see section 10.6 of Materials and Methods).

As it has been explained in the introduction of this chapter, the expression of both chains of the antibody in an equilibrated manner has to be ensured. This can be achieved through different approaches regarding the chains cloning, which include:

1. Cloning the heavy chain and the light chain each one in a different vector.
2. Cloning both chains in the same vector, each one of them under the control of different promoters.
3. Cloning both chains in the same vector, both of them under the control of the same promoter, and, therefore, in the same mRNA.

The third strategy, consisting in cloning both chains in the same vector, presents several advantages with respect to approaches 1 and 2: only one plasmid is needed, and, by controlling the expression of both chains with only 1 promoter, a more equilibrated expression of the chains can be obtained, avoiding epigenetic silencing of one of the two promoters potentially resulting in decompensated LC:HC

Chapter 3. Results (I)

proportions (Ho et al., 2013). Therefore, this was the selected strategy for the expression of Trastuzumab.

In order to express LC and HC under the control of the same promoter, a tricistronic plasmid derived from the commercial pIRESpuro3 plasmid was used. As it has been explained in the introduction of this chapter, pIRESpuro3 is a bicistronic plasmid that allows the expression of a gene of interest and the antibiotic resistance selection marker (puroR) in a single mRNA, therefore ensuring that all the selected cells, resistant to the selective pressure, produce the protein of interest. The pIRESpuro3 vector, however, only allows the expression of one gene of interest. In order to allow the expression of the two chains from the same mRNA, the pIRESpuro3 vector was modified and converted in a tricistronic vector, named pTRIpuro3. This was achieved by cloning an extra IRES sequence (identical to the IRES sequence of pIRESpuro3) into the MCS of the pIRESpuro3 vector, thus generating a tricistronic vector as depicted in Figure 3.3 and detailed in (Román, 2018).

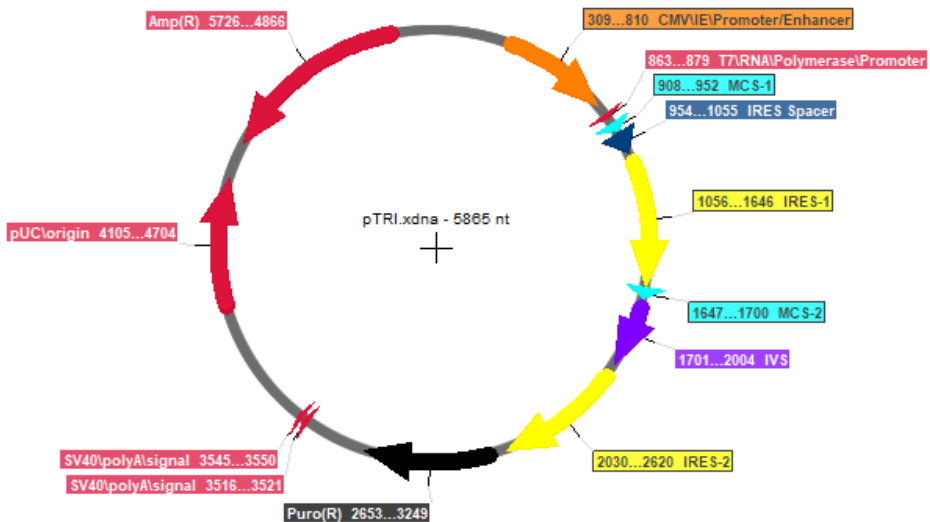


Figure 3.3 Map of generated pTRIpuro3 vector.

LC and HC were cloned from the original pUC57 vector to the pTRIpuro3 vector between NheI-AgeI and NotI-BamHI sites, respectively, resulting in the sequence shown in Figure 3.4. The pTRIpuro3 plasmid containing LC and HC was named pTRIpuro3_Tzmb.



Figure 3.4. Scheme of LC and HC distribution in under the control of the CMV promoter, separated by two IRES sequences with the puromycin resistance gene at the end.

3.3. Trastuzumab production, purification and physicochemical characterization establishment

3.3.1. Cell line characterization: growth and production assessment

Once constructed, pTRIpuro3_Tzmb was transfected to HEK293 cells (see section 10.7.6), resulting in HEK293_Tzmb cell line, and cell pools were selected with culture medium containing 10 mg/L of puromycin antibiotic (see section 10.2.1.1.). Once the cell pool had been established, cells were transferred to 125 ml shake flasks and their growth profile and production titers were assessed, as depicted in Figure 3.5. Values of maximum cell density (MCD) of $13.4 \cdot 10^6$ cell/ml were reached, and a final concentration of 9.1 mg/L of Trastuzumab product was obtained, with a maximum exponential growth rate of 0.0295 h^{-1} corresponding to a doubling time of 23.5 h. Trastuzumab concentration assessment is detailed later in the chapter, in section 3.3.3.1.

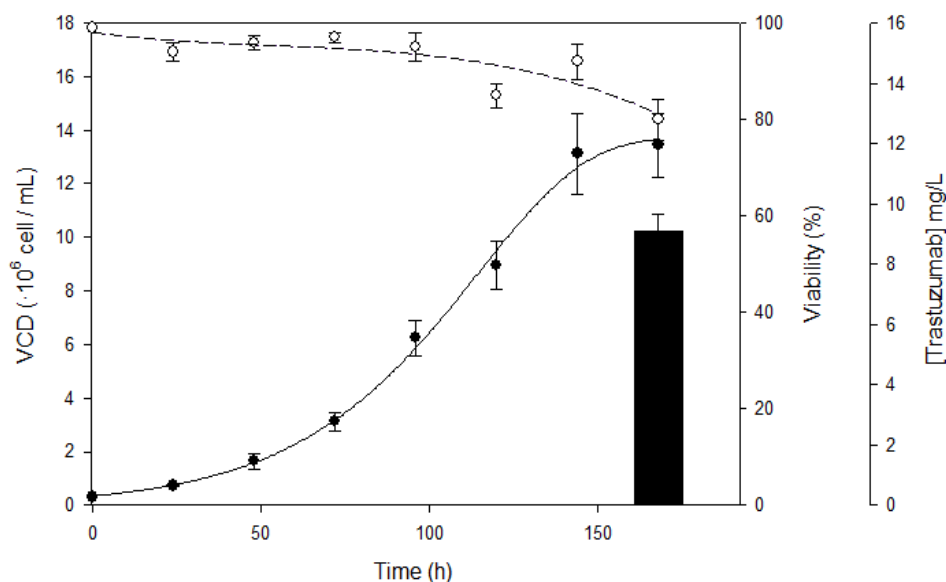


Figure 3.5. HEK293_Tzmb growth profile and Trastuzumab production titers in erlenmeyer culture. Error bars correspond to standard deviation of $n = 3$ replicates.

3.3.2. Purification assay

After the production cell line was characterized, a sequence for recovering and purification of the produced Trastuzumab was implemented. This initial recovery and purification sequence was implemented at a small scale (50 ml of initial broth culture), since the produced product came from shake flask productions. This sequence consisted in a first solid-liquid separation step performed by centrifugation, followed by a $0.45 \mu\text{m}$ microfiltration, an affinity chromatography with a Protein A resin (which selectively binds to the constant fraction of heavy chains IgGs), and a final dialysis step, in order to exchange the buffer of the eluted chromatography fraction from an acid one ($\text{pH} = 2.75$) to a buffer closer to a neutral pH (PBS), more adequate for the preservation of the product. This downstream

sequence is summarized in Figure 3.6. See section 10.8 for more detailed information on the specifics of the performance of this downstream process.



Figure 3.6. Scheme of the downstream process implemented for small scale purification of Trastuzumab.

This purification sequence had a global yield of 86% obtaining a product with a purity of >95%. The purity determination is detailed later in this chapter, in the section 3.3.3.1.

3.3.3. Physicochemical characterization of produced Trastuzumab

In order to analyze the quality of the produced Trastuzumab and characterize the obtained purified Trastuzumab samples, several analytical techniques have been implemented. The assessed physicochemical parameters include:

- Concentration
- Purity
- Correct structure formation
- Antigen recognition capacity
- Aggregate content
- Molecular weight and glycosylation
- Endotoxin content
- Stability

3.3.3.1. Concentration, purity and correct structure formation of the obtained product: SDS-PAGE

Concentration and purity of Trastuzumab in the different obtained samples was performed by means of densitometry analysis of the protein bands of a SDS-PAGE (Sodium Dodecyl Sulfate Polyacrylamide Gel Electrophoresis) gel using a molecular weight marker with a known amount of a reference protein (see 10.9.1. section for further detail). An example of a SDS-PAGE gel with Trastuzumab is depicted on Figure 3.7.

This gel was also used to assess the correct formation of the Trastuzumab antibody: when it is correctly formed, heavy and light chains are bridged through disulfide bonds, forming an antibody of ~150 kDa (145585.6 Da). The gel is depicted in Figure 3.7., where a band of ~150 kDa, corresponding to fully formed Trastuzumab, can be observed. When the Trastuzumab sample is reduced, two bands appear, corresponding to the antibody heavy and light chains of around 50 and 25 kDa, respectively.

Chapter 3. Results (I)

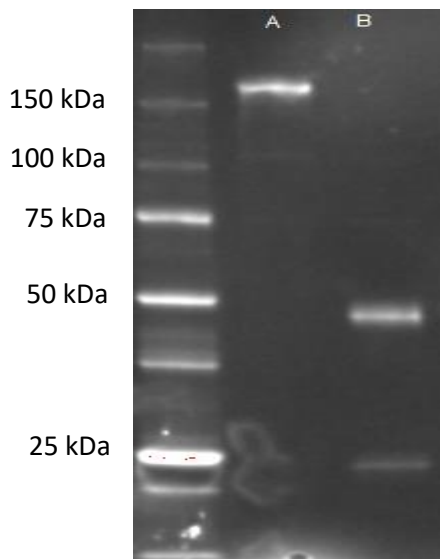


Figure 3.7. SDS-PAGE of a purified Trastuzumab sample (lane A) and the same sample reduced with β -mercaptoethanol (lane B), with the molecular weight marker at the left.

Purity of the Trastuzumab samples was also determined with the same SDS-PAGE analytics, in this case by measuring the intensity of the protein band of interest with respect to the total intensity of the total number of bands of the sample (see 10.9.1.). A band intensity profile of a purified Trastuzumab sample is shown on Figure 3.8, in this case, the whole Trastuzumab molecule accounts for 95.5% of the protein content of the sample.

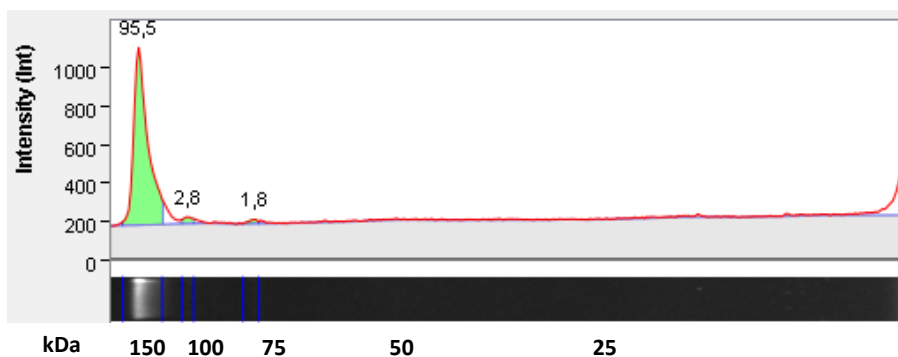


Figure 3.8. SDS-PAGE of a purified Trastuzumab sample, showing the relative intensities of the protein bands of the sample, where the band corresponding to Trastuzumab (150 kDa) represents 95.5% of the total protein.

3.3.3.2. Antigen recognition capacity: ELISA and flow cytometry

Once the correct formation of the product had been tested, its ability of recognizing the target antigen was assessed. Trastuzumab is an anti-HER2 antibody, therefore, HER2 was the antigen used for the antigen recognition assays. First, the antibody-antigen recognition was assessed through an ELISA (Enzyme Linked Immunosorbent Assay) assay, in which the antibody binds to an immobilized antigen. Then, a second assay has been implemented, in which the capacity of Trastuzumab to bind to its target antigen expressed in the surface of breast cancer model cells has been assessed by means of flow cytometry analysis.

The implemented ELISA assay disposition consists in the coating of a microplate well with HER2 protein, to which Trastuzumab selectively binds. Then, a secondary anti-human IgG1 antibody conjugated to alkaline peroxidase is added, binding to Trastuzumab and generating a colorimetric signal upon addition of the alkaline peroxidase substrate TMB (3,3',5,5'-Tetramethylbenzidine). The ELISA assay is depicted on Figure 3.9. and detailed on section 10.9.2.

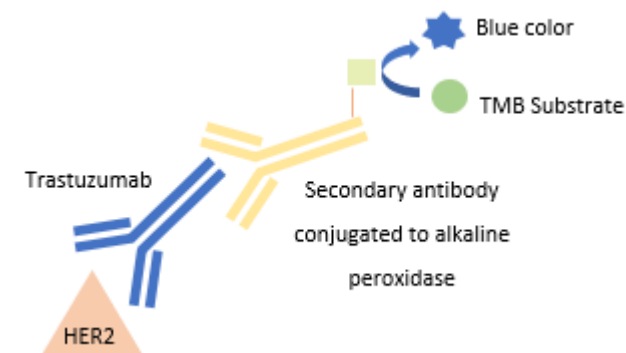


Figure 3.9. Depiction of the implemented ELISA assay.

With the implemented test, Trastuzumab was shown to efficiently bind to its target HER2 antigen (Figure 3.10.).



Figure 3.10. ELISA assay performed with produced Trastuzumab. Lane 1: produced Trastuzumab dilution in HER2 coated wells; Lane 2: negative control, produced Trastuzumab dilution in non-coated HER2 wells.

The next step consisted in the assessment of Trastuzumab's capacity to bind to the HER2 antigen expressed in the surface of breast cancer cells. The breast cancer model cell line SKBR3, which overexpresses the HER2 antigen (see introduction of the chapter), was used for this test. In this case, Trastuzumab binds to the HER2 antigen present on the cell membrane, and a secondary anti-IgG1 antibody conjugated to a phycoerythrin fluorochrome binds to Trastuzumab. Fluorimetry

values can then be checked by means of a flow cytometry analysis. A depiction of the assay can be observed on Figure 3.11.

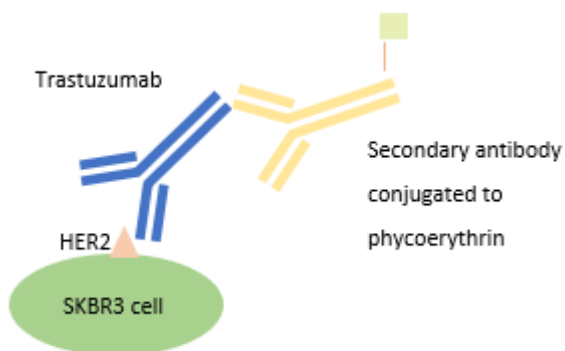


Figure 3.11. Depiction of the implemented assay for analyzing the Trastuzumab ability to bind to cell surface HER2.

This assay confirmed the ability of Trastuzumab to selectively bind to the HER2 antigen present on the surface of SKBR3 cells. As it can be observed on Figure 3.12., Trastuzumab binds to SKBR3 cells but not on Hybridoma cells, which do not overexpress HER2 antigen, or MCF7 cells, which present a mild overexpression of the HER2 antigen.

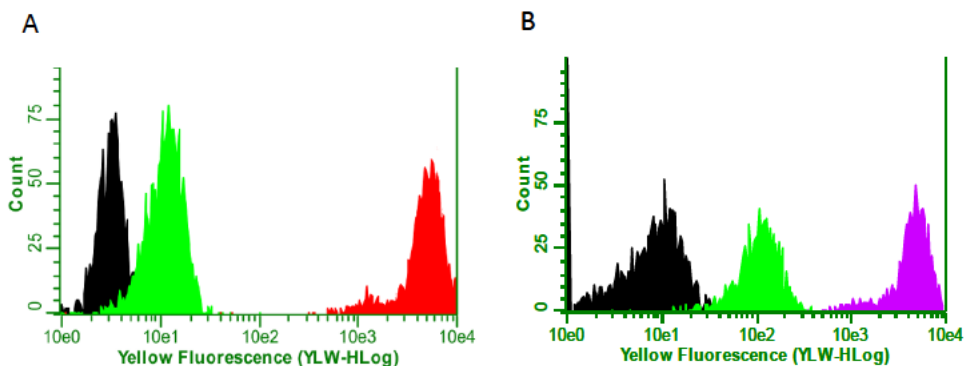


Figure 3.12. Trastuzumab selectively binding to SKBR3 cells. **A)** SKBR3 cells treated in different conditions. **Black:** negative control (cells not treated with Tzmb nor secondary antibody), **green:** cells treated with secondary antibody without previous addition of Trastuzumab; **red:** cells treated with Trastuzumab and secondary antibody. **B)** Different cell lines treated with Trastuzumab and secondary antibody: **black:** hybridoma cells; **green:** MCF7 cells; **violet:** SKBR3 cells.

3.3.3.3. Aggregate content: HPLC-SEC

Another quality parameter that was assessed was the aggregate content of the produced Trastuzumab antibody. This was achieved by means of a HPLC-SEC assay (High Performance Liquid Chromatography – Size-Exclusion Chromatography), in which the monomer fraction of the antibody (approximate weight of 150 kDa) can be quantified and differentiated from the aggregates, which have a higher weight and therefore are eluted before from the size exclusion column (Fig 3.13). See section 10.9.3. of materials and methods for more information of the procedure.

The produced Trastuzumab had a 98.3% of monomer content, as determined by this analysis, showing a low aggregate proportion, therefore validating its quality with regards to the aggregates parameter.

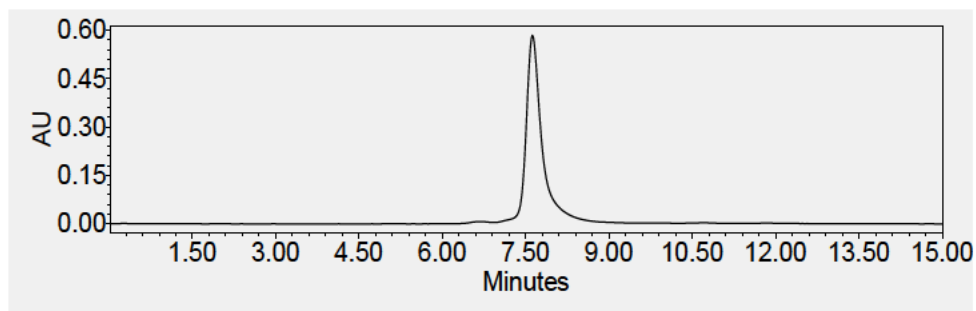


Fig 3.13. HPLC-SEC profile of a Trastuzumab sample. The peak corresponding to the Trastuzumab monomer can be observed at 7.56 min, whereas the aggregates peak can be observed at 6.51 min.

3.3.3.4. Molecular weight and glycosylation pattern: mass spectrometry assay

The obtained Trastuzumab product was then analyzed in terms of its mass through a mass spectrometry (MS) assay. The analysis was performed by the BioOrganic Mass Spectrometry Laboratory (LSMBO) at Université de Strasbourg. Trastuzumab samples were deglycosylated with IgGZero enzyme and analyzed by native MS analysis (see materials and methods section 10.9.4).

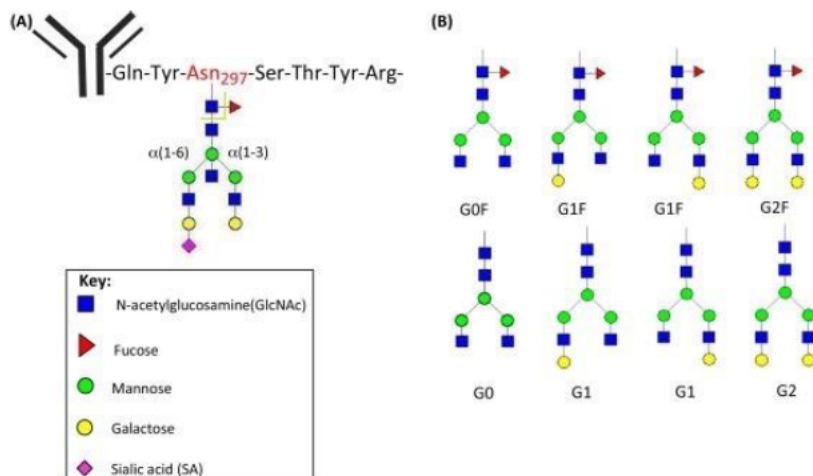


Fig 3.14. A) Schematic depiction of a glycosylated mAb, the two green lines indicating the cleavage of IgGZero enzyme, leaving the first GlcNAc residue attached to the asparagine 297 (Asn 297) of

Chapter 3. Results (I)

the mAb. B) Different glycans obtained in glycoproteins expressed in mammalian cell lines. Image modified from (Sha et al., 2016).

The deglycosylation with IgGZero hydrolyzes the β -1,4 linkage between the core N-Acetyl glucosamine (GlcNAc) residues in the mAb-glycan, leaving the innermost GlcNAc intact on the mAb (see Figure 3.14).

The analysis confirmed that the produced Trastuzumab had the expected molecular weight (Fig 3.15): a mass of 145999 Da was obtained. This mass corresponds to the Trastuzumab theoretical mass of 145586 Da to which the mass of two molecules of GlcNAc, of 203 Da each, have to be added, yielding the total mass of 145002 Da ($145586+203\cdot 2$), very close to the obtained 145999 Da. See the full mass spectrum in the Appendix III.

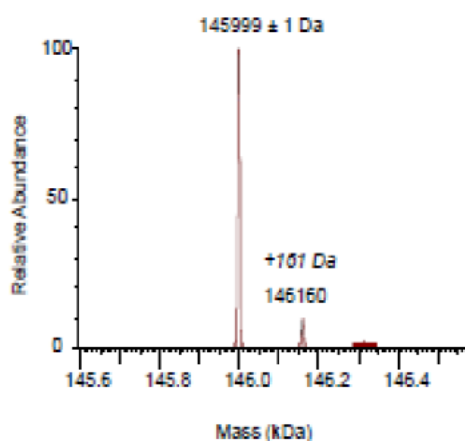


Fig 3.15. MS deconvoluted profile of the produced Trastuzumab, showing a mass of 145999 Da of deglycosylated Trastuzumab.

The glycosylation pattern of the obtained mAb has also been analyzed, it was performed in the same way than for the mass determination, but without performing the deglycosylation of the antibody. The obtained glycosylation pattern contained typical glycans found in mAbs produced in animal cell lines. Figure 3.16.

shows the glycosylation of the Trastuzumab antibody produced in this work compared to the pattern of commercial Trastuzumab.

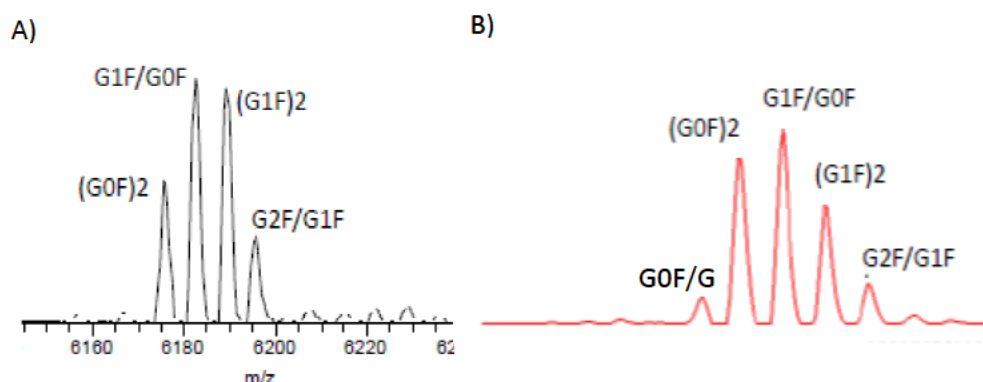


Fig 3.16. Glycoforms distribution of the produced Trastuzumab (A) compared to the commercial Trastuzumab (B), both being analyzed at LSMBO.

Glycoforms distribution slightly differs between commercial Trastuzumab and Trastuzumab produced in this work. This could be attributed to different factors, including differences in cell culture processes, downstream purification strategies and the used expression system (Zhang et al., 2016): commercial Trastuzumab is produced with Chinese Hamster Ovary (CHO) cell line (Li et al., 2010), whereas human cell line HEK293 has been used in this work, fact that corroborates the difference on the glycosylation pattern between the rodent cell line and the human cell line.

3.3.3.5. Endotoxin content test

Endotoxin content of the obtained product was also assessed, by means of a Limulus amoebocyte lysate (LAL) chromogenic test (see section 10.9.5 of materials and methods), which allows determining the concentration of endotoxin units (EU/ml or EU/mg) of the sample of interest. Applied to the obtained Trastuzumab product, an endotoxin level of 81.47 EU/mg was obtained. These levels would not ensure the

necessary quality of the product for clinical assays: as determined by the US Pharmacopeia, endotoxin limit levels for Trastuzumab should be at 0.63 EU/mg of product (Dawson, 2017) (considering a dose of 8 mg/kg body weight, which corresponds to the dose to be administered) (EMA, 2018).

3.3.3.6. Stability: HPLC-SEC

The stability of the produced Trastuzumab was assessed through a SEC-HPLC analysis: the monomer content of the product was determined at different times, while being stored at 4°C. The results are summarized in Table 3.1. The produced Trastuzumab presents very high monomer proportion (>98%) after 2 months of storage. After 5 months, monomer levels were still over 92%, which had slightly dropped 1 month later, after 6 months, when fragments also appeared.

**Table 3.1. Stability of
Trastuzumab**

Time (months)	Monomer (%)	Fragments (%)
1	98.29	0
2	98.25	0
5	92.76	0
6	91.1	0.9

3.4. Production in bioreactor platforms

3.4.1. Production in 5L single use wave bioreactor

After the small-scale characterization of the production process had been performed, a 5L batch production in a single use bag of 10Lwave bioreactor was performed (see section 10.4.1.1.3), in order to obtain more product for performing the subsequent conjugation assays (see chapter 5) and also as an intermediary production scale prior to the pilot scale of 50L (see next section, 3.4.2). The cell culture was performed without controlling the pH of the medium (pH-free), since it had previously been shown in our group that in these conditions, HEK293 cells present a more balance metabolism that can result in higher biomass densities and product titers (Liste-Calleja et al., 2015), (Martínez-Monge et al., 2019). The production was successfully carried out, reaching a MCD of $10.68 \cdot 10^6$ cell/ml and a final concentration of Trastuzumab of 6.6 mg/L, with a maximum exponential growth rate of 0.0228 h^{-1} corresponding to a doubling time of 30.4 h.

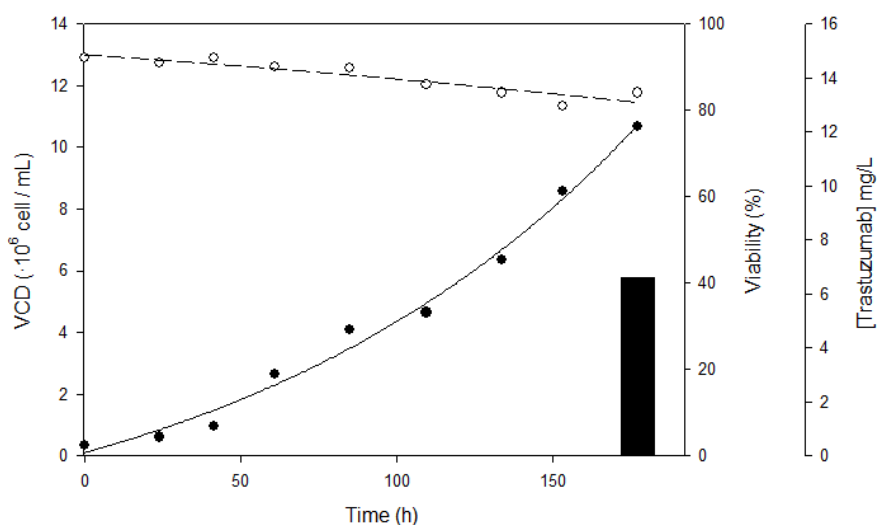


Figure 3.17. HEK293_Tzmb growth profile and Trastuzumab production titers in wave 5L culture.

Recovery of the produced Trastuzumab was performed following a downstream sequence slightly modified with respect to the sequence previously described in section 3.2.2 in order to adapt it to the higher culture volume. The applied sequence consisted in this case in a solid-liquid separation through depth filtration followed by a 0.22 μm microfiltration, a concentration performed by tangential flow filtration, an affinity chromatography with protein A and a dialysis to PBS (see 10.8 section). This purification process had a global yield of 85% and allowed the obtention of >99% of purity for the final product, therefore being confirmed as an efficient purification sequence.

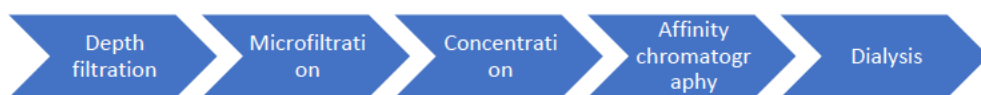


Figure 3.18. Scheme of the downstream process implemented for the wave culture purification of Trastuzumab.

3.4.2. Production in 50L single use STR bioreactor

Once the production and purification had been established for a 5L culture, a pilot scale production was attempted. A batch culture was performed with a single use cultibag stirred tank reactor (STR) bioreactor (see section 10.4.1.1.4) in order to obtain enough product for performing all the different conjugation assays with Trastuzumab (see chapter 5). The production was again successfully performed, reaching a MCD of $8.65 \cdot 10^6$ cell/ml and a final concentration product of 19.0 mg/ml was obtained, with a maximum growth rate of 0.019 h^{-1} , corresponding to a duplication time of 36.5 h. Lower biomass levels and growth rates than in previously described smaller scale processes were achieved, but product titers were higher.

This relation between slower culture growth and higher product titers had already been observed in our group (data not shown).

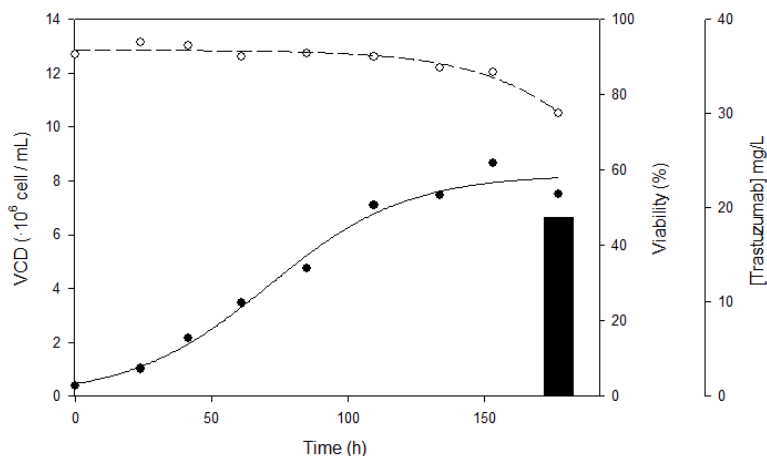


Figure 3.19. HEK293_Tzmb growth profile and Trastuzumab production titers in single use 50L STR culture.

The produced Trastuzumab was purified following the same sequence applied for the 5L culture. The devices, size of membranes and chromatography columns were scaled up in order to adapt them to the higher culture volume (see section 10.8). In this case, the recovery yield was lower than in the previous purifications: a yield of 60% was obtained, due to lower efficiency of microfiltration and concentration steps. However, the purity of the product remained high, at >99%.

3.5. Conclusions

In this chapter, Trastuzumab production has been successfully achieved, starting from the construction of the expression vector and generating the HEK293 productive cell line. The production and purification of the product has been performed at shake flask level and then scaled up at 5L and 50L using single use systems. The final scheme for the Trastuzumab production is presented in figure 3.20.

Chapter 3. Results (I)

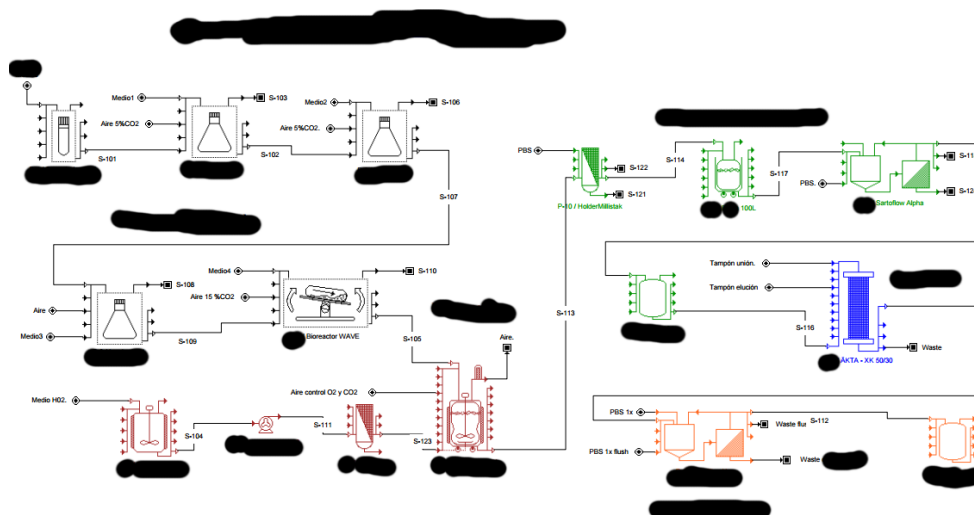


Figure 3.20. Flow diagram for Trastuzumab production and purification (made with SuperPro Designer).

Several tools for the physicochemical characterization of the produced Trastuzumab have been implemented, allowing the assessment of different parameters of the product: concentration, purity, antigen recognition, mass, aggregation, endotoxin content and stability. The production, purification and characterization sequences of Trastuzumab implemented in this chapter will be used as a model for Trastuzumab derived molecules later addressed (see chapters 4, 6 and 7), while some of the physicochemical characterization tools will also be applied to the conjugated ADC molecules (chapters 5-7). Finally, it can be stated that enough product of an appropriate quality for performing antibody conjugations, which will be described in chapter 5, has been obtained.

3.6. References

Butler, M., & Spearman, M. (2014). The choice of mammalian cell host and possibilities for glycosylation engineering. *Current Opinion in Biotechnology*,

30, 107–112. <https://doi.org/10.1016/j.copbio.2014.06.010>

Chin, J. X., Chung, B. K. S., & Lee, D. Y. (2014). Codon Optimization OnLine (COOL): A web-based multi-objective optimization platform for synthetic gene design. *Bioinformatics*, 30(15), 2210–2212. <https://doi.org/10.1093/bioinformatics/btu192>

Clontech. (2010). pIRESpuro3 Vector Map and Multiple Cloning Site (MCS). Retrieved March 13, 2019, from www.clontech.com

Dawson, M. (2017). *Endotoxin Limits For Parenteral Drug Products*. Retrieved from www.acciusa.com

Dumont, J., Eewart, D., Mei, B., Estes, S., & Kshirsagar, R. (2016). Human cell lines for biopharmaceutical manufacturing: history, status, and future perspectives. *Critical Reviews in Biotechnology*, 36(6), 1110–1122. <https://doi.org/10.3109/07388551.2015.1084266>

EMA. (2016). *Guideline on Development, Production, Characterization and Specifications for Monoclonal Antibodies and Related Products, EMEA/CHMP/BWP/157653/2007*. Retrieved from www.ema.europa.eu/contact

EMA. (2018). *Herceptin EPAR Product Information*. Retrieved from https://www.ema.europa.eu/en/documents/product-information/herceptin-epar-product-information_en.pdf

Franco, E., Garcia-Recio, V., Jiménez, P., Garrosa, M., Girbés, T., Cordoba-Diaz, M., & Cordoba-Diaz, D. (2018). Endotoxins from a Pharmacopoeial Point of View. *Toxins*, 10(8). <https://doi.org/10.3390/toxins10080331>

Haryadi, R., Ho, S., Kok, Y. J., Pu, H. X., Zheng, L., Pereira, N. A., ... Song, Z. (2015). Optimization of Heavy Chain and Light Chain Signal Peptides for High Level Expression of Therapeutic Antibodies in CHO Cells. *PLOS ONE*, 10(2), e0116878.

Chapter 3. Results (I)

<https://doi.org/10.1371/journal.pone.0116878>

- Ho, S. C. L., Koh, E. Y. C., van Beers, M., Mueller, M., Wan, C., Teo, G., ... Yang, Y. (2013). Control of IgG LC:HC ratio in stably transfected CHO cells and study of the impact on expression, aggregation, glycosylation and conformational stability. *Journal of Biotechnology*, 165(3–4), 157–166. <https://doi.org/10.1016/j.jbiotec.2013.03.019>
- Huang, M. T., & Gorman, C. M. (1990). Intervening sequences increase efficiency of RNA 3' processing and accumulation of cytoplasmic RNA. *Nucleic Acids Research*, 18(4), 937–947. Retrieved from <http://www.ncbi.nlm.nih.gov/pubmed/1690394>
- Jackson, R. J., Howell, M. T., & Kaminski, A. (1990). The novel mechanism of initiation of picornavirus RNA translation. *Trends in Biochemical Sciences*, 15(12), 477–483. Retrieved from <http://www.ncbi.nlm.nih.gov/pubmed/2077688>
- Kaiser, S. C., Kraume, M., Eibl, D., & Eibl, R. (2015). Single-Use Bioreactors for Animal and Human Cells (pp. 445–500). Springer, Cham. https://doi.org/10.1007/978-3-319-10320-4_14
- Khanal, O., Singh, N., Traylor, S. J., Xu, X., Ghose, S., Li, Z. J., & Lenhoff, A. M. (2018). Contributions of depth filter components to protein adsorption in bioprocessing. *Biotechnology and Bioengineering*, 115(8), 1938–1948. <https://doi.org/10.1002/bit.26707>
- Kim, J. Y., Kim, Y.-G., & Lee, G. M. (2012). CHO cells in biotechnology for production of recombinant proteins: current state and further potential. *Applied Microbiology and Biotechnology*, 93(3), 917–930. <https://doi.org/10.1007/s00253-011-3758-5>
- Komar, A. A. (2016). The Yin and Yang of codon usage. *Human Molecular Genetics*, 25(R2), R77–R85. <https://doi.org/10.1093/hmg/ddw207>

Chapter 3. Results (I)

- Li, F., Vijayasankaran, N., Shen, A. Y., Kiss, R., & Amanullah, A. (2010). Cell culture processes for monoclonal antibody production. *MABs*, 2(5), 466–479. <https://doi.org/10.4161/MABS.2.5.12720>
- Liste-Calleja, L., Lecina, M., & Cairó, J. J. (2014). HEK293 cell culture media study towards bioprocess optimization: Animal derived component free and animal derived component containing platforms. *Journal of Bioscience and Bioengineering*, 117(4), 471–477. <https://doi.org/10.1016/j.jbiosc.2013.09.014>
- Liste-Calleja, L., Lecina, M., Lopez-Repullo, J., Albiol, J., Solà, C., & Cairó, J. J. (2015). Lactate and glucose concomitant consumption as a self-regulated pH detoxification mechanism in HEK293 cell cultures. *Applied Microbiology and Biotechnology*, 99(23), 9951–9960. <https://doi.org/10.1007/s00253-015-6855-z>
- Löffelholz, C., Husemann, U., Greller, G., Meusel, W., Kauling, J., Ay, P., ... Eibl, D. (2013). Bioengineering Parameters for Single-Use Bioreactors: Overview and Evaluation of Suitable Methods. *Chemie Ingenieur Technik*, 85(1–2), 40–56. <https://doi.org/10.1002/cite.201200125>
- Mariati, Yeo, J. H. M., Koh, E. Y. C., Ho, S. C. L., & Yang, Y. (2014). Insertion of core CpG island element into human CMV promoter for enhancing recombinant protein expression stability in CHO cells. *Biotechnology Progress*, 30(3), 523–534. <https://doi.org/10.1002/btpr.1919>
- Marichal-Gallardo, P. A., & Lvarez, M. M. A. (2012). State-of-the-Art in Downstream Processing of Monoclonal Antibodies: Process Trends in Design and Validation. *American Institute of Chemical Engineers Bio-Technol. Prog*, 28, 899–916. <https://doi.org/10.1002/btpr.1567>
- Martínez-Monge, I., Albiol, J., Lecina, M., Liste-Calleja, L., Miret, J., Solà, C., & Cairó, J. J. (2019). Metabolic flux balance analysis during lactate and glucose concomitant consumption in HEK293 cell cultures. *Biotechnology and*

Chapter 3. Results (I)

Bioengineering, 116(2), 388–404. <https://doi.org/10.1002/bit.26858>

Martoglio, B., & Dobberstein, B. (1998). Signal sequences: more than just greasy peptides. *Trends in Cell Biology*, 8(10), 410–415. Retrieved from <http://www.ncbi.nlm.nih.gov/pubmed/9789330>

McAuley, A., Jacob, J., Kolvenbach, C. G., Westland, K., Lee, H. J., Brych, S. R., ... Matsumura, M. (2008). Contributions of a disulfide bond to the structure, stability, and dimerization of human IgG1 antibody CH3 domain. *Protein Science: A Publication of the Protein Society*, 17(1), 95–106. <https://doi.org/10.1110/ps.073134408>

Paik, S. Y., Sugiyama, M., & Nomi, R. (1985). Isolation and properties of a puromycin acetyltransferase from puromycin-producing *Streptomyces alboniger*. *The Journal of Antibiotics*, 38(12), 1761–1766. Retrieved from <http://www.ncbi.nlm.nih.gov/pubmed/4093336>

Rathore, A. S. (2009). Follow-on protein products: scientific issues, developments and challenges. *Trends in Biotechnology*, 27(12), 698–705. <https://doi.org/10.1016/j.tibtech.2009.09.004>

Román, R. (2018). *Desarrollo de procesos de producción de proteínas terapéuticas: aumento de la productividad específica en células HEK293*. Universitat Autònoma de Barcelona.

Sha, S., Agarabi, C., Brorson, K., Lee, D.-Y., & Yoon, S. (2016). N-Glycosylation Design and Control of Therapeutic Monoclonal Antibodies. *Trends in Biotechnology*, 34(10), 835–846. <https://doi.org/10.1016/j.tibtech.2016.02.013>

Shukla, A. A., & Gottschalk, U. (2013). Single-use disposable technologies for biopharmaceutical manufacturing. *Trends in Biotechnology*, 31(3), 147–154. <https://doi.org/10.1016/J.TIBTECH.2012.10.004>

Shukla, A. A., Hubbard, B., Tressel, T., Guhan, S., & Low, D. (2007). Downstream

Chapter 3. Results (I)

- processing of monoclonal antibodies—Application of platform approaches. *Journal of Chromatography B*, 848(1), 28–39. <https://doi.org/10.1016/J.JCHROMB.2006.09.026>
- Shukla, A. A., Wolfe, L. S., Mostafa, S. S., & Norman, C. (2017). Evolving trends in mAb production processes. *Bioengineering & Translational Medicine*, 2(1), 58–69. <https://doi.org/10.1002/btm2.10061>
- Thomas, P., & Smart, T. G. (2005). HEK293 cell line: A vehicle for the expression of recombinant proteins. *Journal of Pharmacological and Toxicological Methods*, 51(3), 187–200. <https://doi.org/10.1016/j.vascn.2004.08.014>
- Torkashvand, F., & Vaziri, B. (2017). Main Quality Attributes of Monoclonal Antibodies and Effect of Cell Culture Components. *Iranian Biomedical Journal*, 21(3), 131–141. <https://doi.org/10.18869/ACADPUB.IBJ.21.3.131>
- Wang, X., An, Z., Luo, W., Xia, N., & Zhao, Q. (2018). Molecular and functional analysis of monoclonal antibodies in support of biologics development. *Protein & Cell*, 9(1), 74–85. <https://doi.org/10.1007/s13238-017-0447-x>
- Wishart, D. S., Feunang, Y. D., Guo, A. C., Lo, E. J., Marcu, A., Grant, J. R., ... Wilson, M. (2017). DrugBank 5.0: a major update to the DrugBank database for 2018. *Nucleic Acids Research*. <https://doi.org/10.1093/nar/gkx1037>
- Xenopoulos, A. (2015). A new, integrated, continuous purification process template for monoclonal antibodies: Process modeling and cost of goods studies. *Journal of Biotechnology*, 213, 42–53. <https://doi.org/10.1016/J.JBIOTEC.2015.04.020>
- Zhang, P., Woen, S., Wang, T., Liao, B., Zhao, S., Chen, C., ... Rudd, P. M. (2016). Challenges of glycosylation analysis and control: an integrated approach to producing optimal and consistent therapeutic drugs. *Drug Discovery Today*, 21(5), 740–765. <https://doi.org/10.1016/J.DRUDIS.2016.01.006>

Chapter 4. Results (II): Development of an Immunocytokine fusion protein based on Trastuzumab and Interferon

4.1. Introduction

After having constructed and produced Trastuzumab, the next step of this work consisted in fusing it to a cytokine, in order to enhance its antiproliferative activity, generating an immunocytokine. Immunocytokines are fusion proteins based on an antibody fused to a cytokine, which have emerged as promising therapeutic tools for tackling cancer. Several immunocytokine formats have been explored, with different cytokines having been tested as therapeutic candidates (see section 1.2.6.). The cytokine that has been chosen in this work for fusion with Trastuzumab consists in interferon alpha 2b (IFN α 2), since it is a cytokine with antiproliferative activity and with the ability to activate the immune system, and it has been assessed for breast cancer therapy (Parker et al., 2016, Kontermann, 2012), and our research group had worked with it in a project related to recombinant proteins production.

IFN molecules are pleiotropic cytokines that are involved in innate and adaptive immunity that have been shown to promote antitumor immune responses (Dunn et al., 2005). There are three types of interferons, IFN I, II and III; interferons type I including 17 different types, 13 of which correspond to several IFN α subtypes in humans; IFN type I can be produced by most cell types in the body in response to several stimuli (Parker et al., 2016), including some cytokines such as colony-stimulating factor 1 in myeloid cells (Parker et al., 2016), or viral elements (Kato et al., 2005). IFN α 2 was the first IFN I subtype to be characterized, therefore, it was widely used in basic research to study its biological activities, and it was also the first IFN to be manufactured by the biopharmaceutical industry for its use as a drug (Antonelli et al., 2015). There exist several alleles for IFN α 2, the most described

being IFN α 2a and IFN α 2b, which differ in a neutral Lysine/Arginine substitution at position 23 (Paul et al., 2015). IFN α 2 variants have similar effects than the rest of IFN α subtypes (Paul et al., 2015). IFN α 2b is a protein of 165 amino acids of about 19 kDa, and has been approved for several antiviral and antitumoral indications, including chronic hepatitis B and C, hairy cell leukemia, follicular lymphoma, carcinoid tumor and malignant melanoma (Antonelli et al., 2015). The IFN α 2 can exert its function in two ways, by directly inducing an antiproliferative effect on its target cells; and by stimulating the immune system against the target cells:

- IFN α 2 interacts with the IFNAR receptor, which is composed of two subunits (IFNAR1 and IFNAR2), which are expressed in most cells. By binding to the receptor, it triggers signaling cascades that activate the transcription of genes involved in antiproliferative activities (Asmana Ningrum, 2014). These signaling pathways are depicted in Figure 4.1.

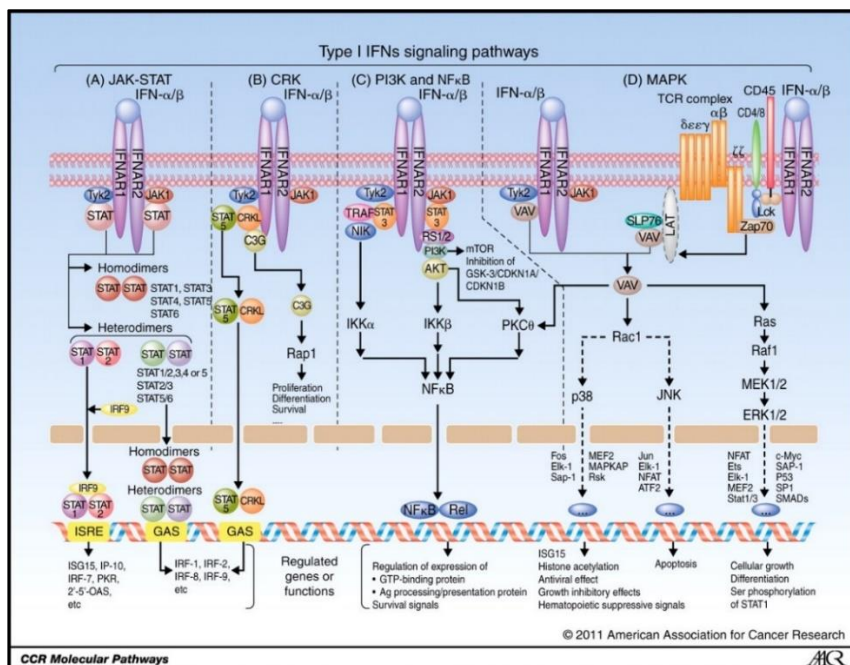


Figure 4.1: Molecular pathways of IFN α 2 interaction. Obtained from (Hervas-Stubbs et al., 2011).

- IFN α 2 is involved in immune system regulation through different mechanisms. The interaction with IFNAR receptor on some immune cells can trigger different effects, such as the induction of chemokines that allow the recruitment of immune cells to the site of infection; inducing the secretion of a second wave of cytokines, further regulating the number and activities of some immune cell types, such as lymphocytes, including T cells, natural killer (NK) cells and dendritic cells (Le Bon et al., 2001; Nguyen et al., 2002). Some of these pathways are again depicted on Figures 4.1 and 4.2. In this chapter, the immunomodulation activity of IFN α 2 will be analyzed by assessing its effect on the proliferation of lymphocytes.
 - Lymphocyte proliferation: a symptom of immune cell activity, for some cell types such as lymphocytes, consists in their proliferation. Lymphocyte proliferation can be triggered by different factors, including the presence of pro inflammatory cytokines, such as IL2 or IL15. Type I IFN have been described to induce the proliferation of different types of lymphocytes, including NK cells and CD8 lymphocyte T, mainly through the induction of IL15 production (Ortaldo et al., 1980; Sprent et al., 2000; Tough et al., 1996).
 - Lymphocyte degranulation: degranulation is a mechanism by which some immune cells, such as lymphocytes NK cells and CD8 cytotoxic T cells, release lytic granules against target cells, in order to kill them. There are reports of IFN α inducing the degranulation of NK cells (Benlahrech et al., 2009).

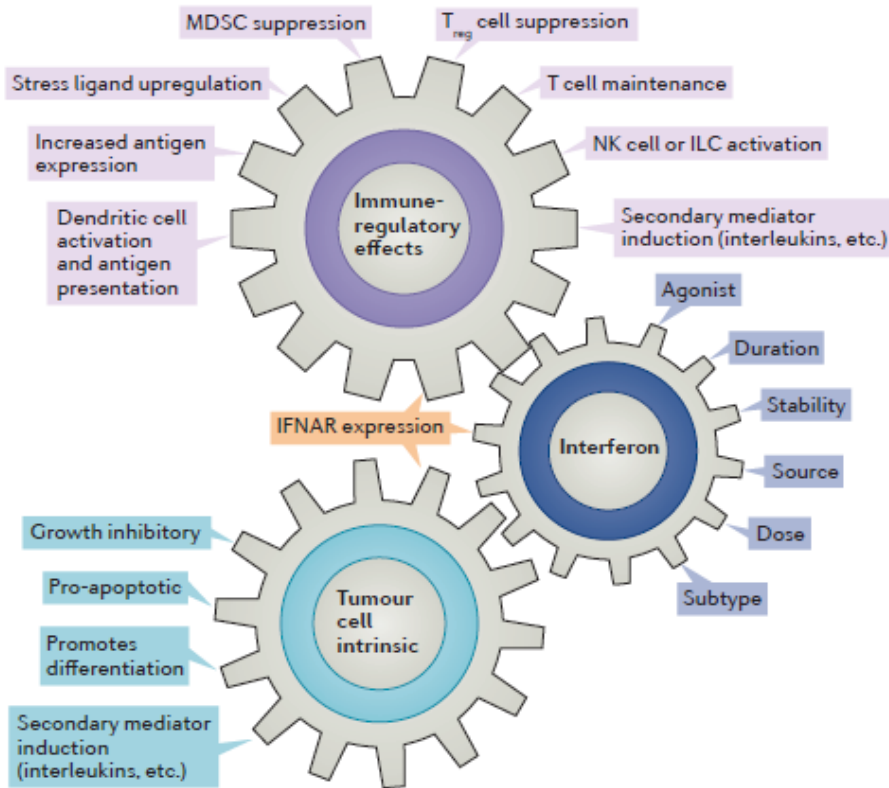


Figure 4.2. Representation of the interaction of type I IFN with the immune system cells and tumor cells in antitumor actions. Obtained from (Parker et al., 2016).

These different effects have rendered interesting the use of IFN α 2b for antitumor therapy, being approved as a therapy against several cancers, as previously stated. However, its use for treating breast cancer has not yet been approved, although several preclinical and clinical studies based on IFN α have been carried out, showing the interest of IFN α as a potential therapy. In *in vivo* preclinical assays:

- In some *in vivo* studies with mice, it has been observed that expression of transgenic IFN α , through the genetic modification of hematopoietic stem cells, affects the progress of breast cancer (Escobar, Moi et al., 2014). This same effect is observed when macrophages are engineered in order to generate IFN α (Escobar, Gentner et al., 2014).

Chapter 5. Results (III)

- It has been proven that inhibition of type I IFN signaling is a mechanism of immune escape of metastasis to the bone. Applying IFN α to these cells reduces the metastasis development and increases metastasis-free survival in mice models (Parker et al., 2016).

In clinical trials:

- The first pilot clinical trials with patients with advanced breast cancer treated with human leukocyte IFN (a mixture of IFN α subtypes) showed a promising effect (Borden et al., 1982). In subsequent Phase II clinical trials, using recombinant IFN α 2 in advanced metastatic breast cancers, the response was limited (Quesada et al., 1984). In all these cases, several toxic side effects were encountered.
- In light of these issues, it was attempted to use IFN α in combination with chemotherapeutics or other cytokines. Promising effects were obtained combining IFN α with chemotherapeutics in pilot studies, however, they were again associated to toxic side effects (Welander, 1987). The combination of IFN α with other cytokines, such as IL2 and TNF α , were ineffective or with very low response rates (Parker et al., 2016).

As a general comment observed for clinical trials with IFN α , they are limited by poor pharmacokinetics and by toxic secondary effects, which include fatigue, fever, nausea, dizziness, anorexia, depression and leucopenia (Parker et al., 2016). This fact limits the therapeutic potential of IFN, impeding applying high doses of the cytokine. A way to overcome this issue could consist in directing the cytokine to the tumor site, for example, by fusing it to an antibody, generating an immunocytokine.

This strategy had been previously tested in antibodies targeting CD20, an antigen present in lymphocyte B cells (Huang et al., 2007), (Xuan et al., 2010). In these cases, the immunocytokine was constructed by fusing the IFN α 2 to the C-terminal of the antibody, through a peptide linker consisting in 4 glycines and one serine (Gly₄Ser). These amino acids have a small side chain that allows the linker to be flexible and, therefore, ensures the correct folding of the different domains of the fusion protein (Van Rosmalen et al., 2017). This resulted in a molecule with a higher *in vivo* half life and with a higher antitumoral activity than individual IFN α 2, when applied against target lymphoma B cells (Kontermann, 2012).

In this chapter, the construction of an immunocytokine using the anti-HER2 antibody Trastuzumab fused to the cytokine IFN α 2b is assessed. The fusion is attempted in the same way as described above: the IFN α 2b molecule is fused to the C-terminal of the Trastuzumab antibody through a Gly₄Ser linker.

4.2. Assessment of antiproliferation and immunomodulation activity tests of IFN α 2

As a first step for the immunocytokine construction, the biological activity of the cytokine to be used in the immunocytokine (IFN α 2) was assessed. As it has been explained in the introduction of this chapter, the interferon- α 2 can have an antiproliferative activity on the tumor cells, while also having an immunomodulatory effect on the immune system. Therefore, its antiproliferative activity on the target breast cancer model SKBR3 cells was assessed, as well as its immunomodulation capacity, which was tested on lymphocytes.

4.2.1. Antiproliferation assay: MTS assay

The antiproliferative activity of IFN α 2 was tested on breast cancer model SKBR3 cells, by means of a MTS assay, which is based on the conversion of the MTS tetrazolium compound to a colored formazan product that can be detected and quantified (see section 10.12.1). Formazan is formed when MTS is reduced by the cells, therefore, the formazan amount can be related to cellular activity, and, thus, proliferation. With this test, a mild antiproliferative activity on SKBR3 cells was confirmed, as it can be observed in Figure 4.3. Therefore, the next step consisted in assessing the immunomodulation activity of IFN α 2.

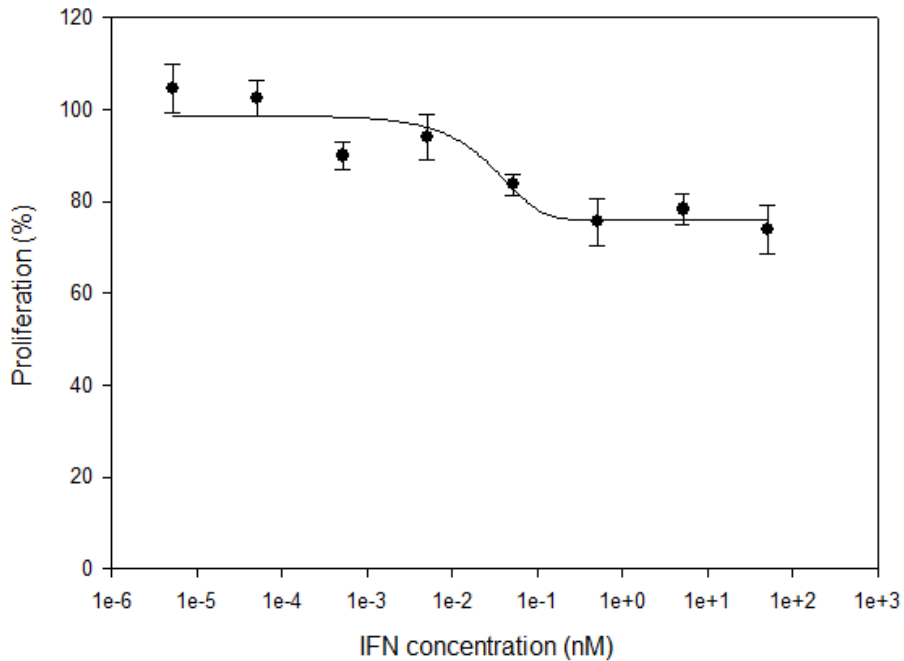


Figure 4.3. Antiproliferation activity of IFN α 2 assessed by MTS with SKBR3 cells.

4.2.2. Immunomodulation: Lymphocyte proliferation assay

The immunomodulation activity of IFN α 2 was assessed by a lymphocyte proliferation assay, which was carried out at the Advanced Therapies Group of the Blood and Tissues Bank (*Banc de Sang i Teixits* (BST), Barcelona).

Proliferation of lymphocytes is one of the main features of the adaptive immune response to pathogens (Heinzel et al., 2018), and plays an important role in tumor immunity (Datta et al., 2009). As it has been indicated in the introduction of this chapter, IFN α 2 could trigger lymphocyte proliferation through several mechanisms. The assessment was carried out by means of a test in which human peripheral blood mononuclear cells (PBMNC, they consist of mononuclear cells: lymphocytes and monocytes) are stained with a fluorescent compound (Carboxy-Fluorescein Diacetate Succinimidyl Ester, CFSE) that is incorporated into the cytoplasm of the cells, therefore allowing to detect the cells that have proliferated, since they have a diminished content of CFSE with respect to the cells that have not proliferated. The detection of the cells was performed by flow cytometry. This test had been previously developed by the Advanced Therapies group, aiming at measuring the impact of mesenchymal stromal cells (MSC) on the proliferation of lymphocytes (Oliver-Vila et al., 2018). In this case, it was adapted to the assessment of IFN α 2 activity, by replacing the PBMNC incubation with IFN α 2 instead of MSC (see 10.12.2).

The results of the test did not show a proliferating activity of the IFN α 2 molecule on lymphocyte population. As it can be observed on Fig 4.4., in row A, the PBMNC cells treated with IFN α 2 generally present a similar size and complexity profile (represented by the SSC (complexity) versus FSC (size) graph) than non-treated cells (basal medium), very different from the stimulated cells (stimulation medium). However, a small population of cells in the IFN α 2 treated cells condition, different to the untreated cells, appeared (circled in black). The histogram of CFSE fluorescence (detected through the FLI-H channel of the flow cytometer) shows the

same pattern of general distribution similitude between cells treated with IFN α 2 and untreated cells, while cells treated with stimulation medium confirm their proliferation.

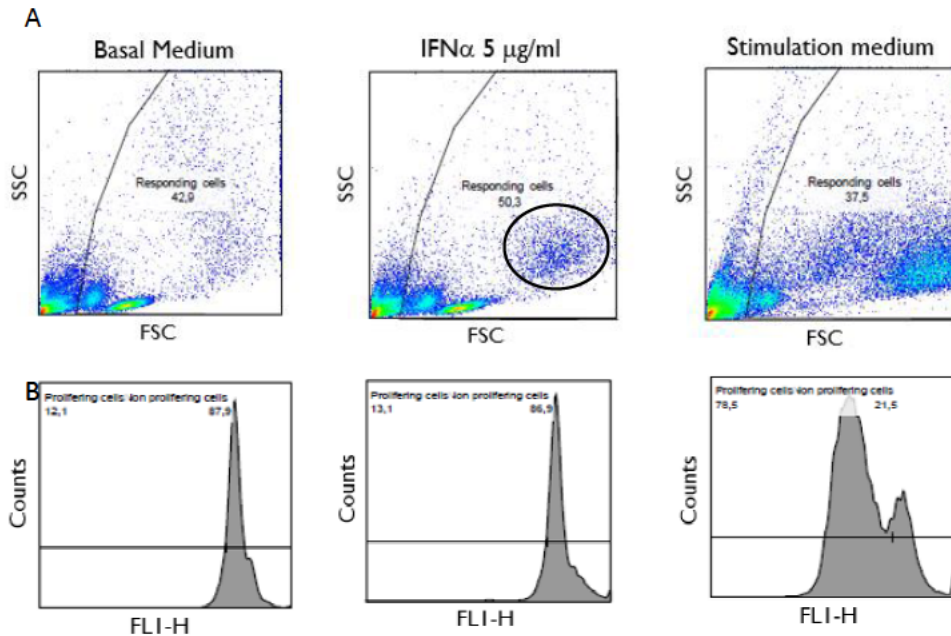


Figure 4.4. Row A) DotPlot graphs of PBMC treated with basal medium (negative control, C-), with IFN α 2 at a concentration of 5 μ g/ml, or with stimulation medium (positive control, C+). Row B) Histograms of the fluorescence (FLI-H) of PBMC treated with the same conditions as in row A.

Figure 4.4. show the profiles of PBMC treated with IFN α 2 at 5 μ g/ml, which corresponds to the highest IFN α 2 concentration applied. Lower concentrations of IFN α 2 were also applied to the PBMC, also yielding similar results, which can be observed in Figure 4.5. Therefore, it can be stated that IFN α 2 did not cause a proliferation effect on PBMC.

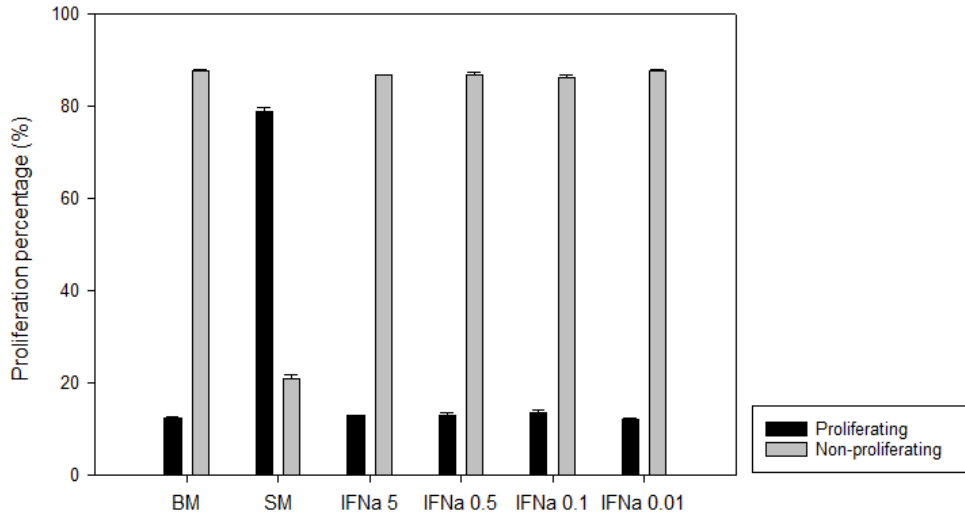


Figure 4.5. Lymphocyte proliferation of treated cells with basal medium (BM), stimulation medium (SM), and IFN α 2b at different concentrations (μ g/ml).

4.3. Trastuzumab-IFN α 2 sequence construction and production

Once the biologic activity of the cytokine had been analyzed, its fusion to the Trastuzumab antibody was attempted. As it has been explained in the introduction of this chapter, the IFN α 2 sequence was aimed to be fused to the C-terminal of the heavy chain of Trastuzumab. In order to obtain the Trastuzumab-IFN α 2 fusion protein, a genetic fusion of the DNA sequences of the heavy chain of Trastuzumab and IFN α 2 was attempted by means of a splicing overlap extension PCR (SOE-PCR) (see section 10.7.4.1). Through this strategy, a sequence codifying for a linker consisting in four glycines and one serine amino acids (GGGGS) was inserted between Trastuzumab and IFN α 2 sequences. These amino acids have a small side chain that allows the linker to be flexible, and therefore ensures the correct folding of the different domains of the fusion protein (Van Rosmalen et al., 2017).

The DNA sequence of the heavy chain of Trastuzumab was obtained as explained in Chapter 3, and the IFN α 2 sequence had been previously obtained in our group by

means of retrotranscriptase PCR (RT-PCR), using as a template the total mRNA extracted from blood cells of one of the members of our group, and cloning the resulting copy DNA (cDNA) into the pRESpuro3 plasmid.

For the fusion Trastuzumab-IFN α 2 DNA sequence construction, the oligonucleotides were designed so that the sequence of the mature IFN α 2 was fused to the antibody, avoiding the signal peptide sequence of the cytokine. The Trastuzumab and IFN α 2 DNA sequences are contained in Appendix I, while the oligonucleotides used for this SOE-PCR are listed in the Appendix II. In Figure 4.7 the obtained Trastuzumab-IFN α 2 DNA band is observed, having a molecular weight of around 2000 base pairs, corresponding to the addition of Trastuzumab heavy chain (1441 bp) and IFN α 2 (527 bp). The obtained fusion sequence was confirmed by sequencing (see 10.7.8), as depicted in Figure 4.6.

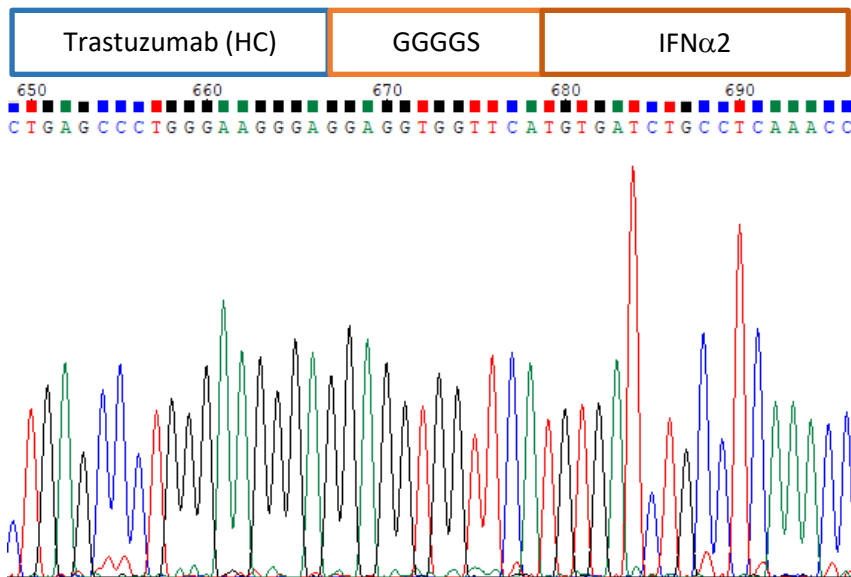


Figure 4.6. Sequencing chromatogram of the overlapping region of the Trastuzumab-IFN α 2 construction.

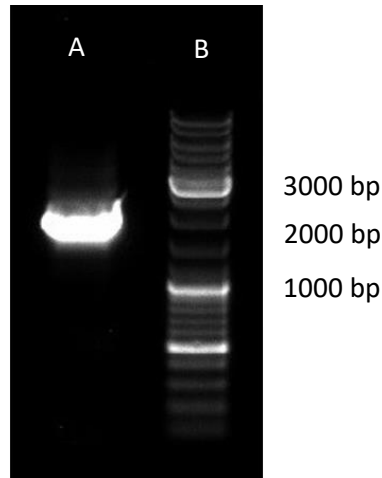


Figure 4.7. Electrophoresis gel of Tzmb-IFN α 2 PCR product. Lane A corresponds to the fused sequence while lane B corresponds to the molecular weight marker.

Once obtained the Trastuzumab-IFN α 2 DNA sequence, it was cloned into the previously described pTRIpuro3_Tzmb vector (Chapter 3) using the EcoRI and BamHI restriction sites, substituting the Trastuzumab heavy chain with the Trastuzumab-IFN α 2 fusion construct, resulting in pTRIpuro3_Tzmb-IFN α 2. The obtained expression vector was then transfected into HEK293 cells (see 10.7.7.2), and cell pools were selected with culture medium containing 10 mg/L of puromycin antibiotic (see 10.2.1.1). Once the cell pool had been selected, cells were transferred to 125 ml shake flasks and their growth profile and production titers were assessed, as depicted in Figure 4.8. Values of maximum cell density (MCD) of $8.72 \cdot 10^6$ cell/ml were reached, and a final concentration of 1.9 mg/L of Trastuzumab-IFN α 2 product was obtained, with a maximum exponential growth rate of 0.0219 h^{-1} corresponding to a doubling time of 31.67 h.

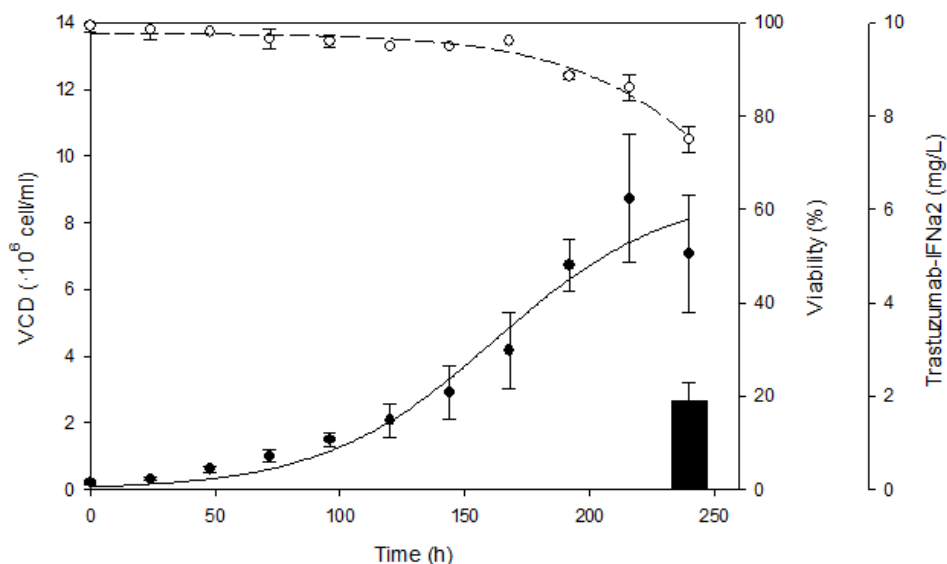


Figure 4.8. HEK293_Tzmb-IFN α 2 growth profile and Trastuzumab-IFN α 2 production titers in erlenmeyer culture. Error bars correspond to standard deviation of $n = 3$ replicates.

Once the cell line had been characterized, a 1L production was carried out in order to have enough product for the subsequent characterization steps. The product was purified following the purification sequence developed for Trastuzumab described in Chapter 3.

4.4. Product characterization:

4.4.1. Confirmation of the correct structure formation of the obtained product: SDS-PAGE

The purified product was analyzed by SDS-PAGE, which confirmed the structure and molecular weight of the obtained immunocytokine, as it can be observed in Figure 4.9. In this case, the light chain was the same as for Trastuzumab, while the heavy chain was larger due to its fusion with the interferon alfa 2 through the GGGGS linker. Therefore, a protein with a total weight of 184753.8 Daltons (Da) was expected, composed by the 23443.1 Da of the light chain, and the 68933.8 Da resulting of the

addition of heavy chain and linker-interferon sequence (both chains per duplicate). The fully formed fusion protein with its correctly formed disulfide bridges corresponded to approximately the 80% of the purified product, the rest of it being single heavy chain-IFN light chains.

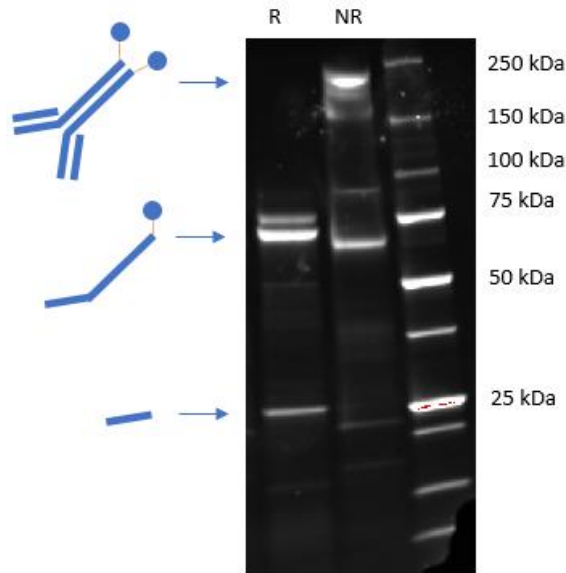


Figure 4.9. SDS-PAGE of the Trastuzumab-IFN α 2 produced protein. Lane R corresponds to a reduced sample, while lane NR corresponds to a non-reduced sample. Schematic structures of the fully formed fusion protein, a single heavy chain-IFN, and a single light chain are represented.

4.4.2. Antigen recognition capacity of both immobilized and cell surface antigen

The ability of the purified Trastuzumab-IFN α 2 to recognize its target HER2 antigen was assessed by means of the same ELISA developed for Trastuzumab in the previous chapter (section 3.3.3.2), as it can be observed in Figure 4.10. The Trastuzumab-IFN α 2 successfully bound to the immobilized HER2 antigen, the fused IFN α 2 molecule therefore was not impairing the ability of the antibody moiety of the immunocytokine to recognize its target antigen.

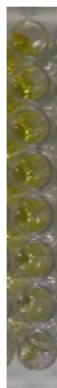


Figure 4.10. ELISA of Trastuzumab-IFN α 2.

Then, the ability of the immunocytokine to bind to the antigen present on the surface of HER2 overexpressing SKBR3 cells was assessed, in the same way as had been previously performed for Trastuzumab (see section 3.3.3.2). The ability of the immunocytokine to bind to the cell surface antigen in the same levels than Trastuzumab was confirmed, as it is shown on Figure 4.11.

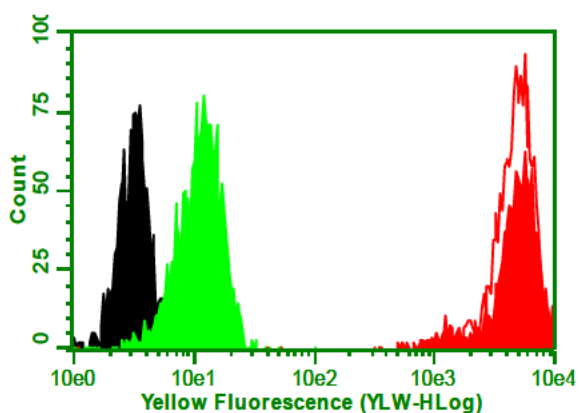


Figure 4.11. Trastuzumab selectively binds to SKBR3 cells treated in different conditions. Black: negative control (cells not treated with Tzmb nor secondary antibody), green: cells treated with secondary antibody without previous addition of Trastuzumab; red: cells treated with Trastuzumab and secondary antibody; white with red line: cells treated with Trastuzumab-IFN α 2.

4.4.3. Antiproliferative activity assessment of Trastuzumab-IFN α 2

The antiproliferative activity of the constructed Trastuzumab-IFN α 2 protein was then assessed by means of an MTS test with the target SKBR3 breast cancer model cells, as previously performed with the IFN α 2. This test revealed that the produced immunocytokine did not have an improved antiproliferative with respect to the antibody Trastuzumab.

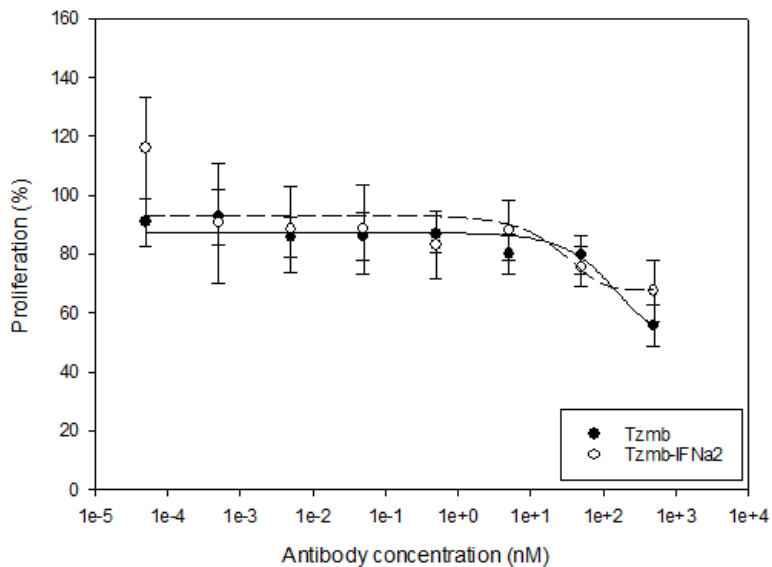


Figure 4.12. Antiproliferative activity of Trastuzumab and Trastuzumab-IFN α 2 molecules on SKBR3 cells measured by means of the MTS test.

4.5. Conclusions

In this chapter, the construction of a Trastuzumab-IFN α 2 immunocytokine has been attempted. First, the IFN α 2 immunomodulatory activity has been assessed, showing no stimulation of lymphocyte proliferation. However, it showed an antiproliferative activity against target HER2 positive SKBR3 cells, justifying its use as the cytokine moiety for the attempted immunocytokine. The Trastuzumab-IFN α 2 fusion protein

was successfully cloned, produced, and purified, and had its antiproliferative activity tested, resulting in no improved effect with respect to the Trastuzumab antibody. Therefore, alternative antibody-based molecules (Antibody-Drug Conjugates, ADCs) with higher therapeutic activities will be constructed and assessed in the following chapters.

4.6. References

- Antonelli, G., Scagnolari, C., Moschella, F., & Proietti, E. (2015). Twenty-five years of type I interferon-based treatment: A critical analysis of its therapeutic use. *Cytokine & Growth Factor Reviews*, 26(2), 121–131. <https://doi.org/10.1016/J.CYTOGFR.2014.12.006>
- Asmana Ningrum, R. (2014). Human interferon alpha-2b: a therapeutic protein for cancer treatment. *Scientifica*, 2014, 970315. <https://doi.org/10.1155/2014/970315>
- Benlahrech, A., Donaghy, H., Rozis, G., Goodier, M., Klavinskis, L., Gotch, F., & Patterson, S. (2009). Human NK Cell Up-regulation of CD69, HLA-DR, Interferon γ Secretion and Cytotoxic Activity by Plasmacytoid Dendritic Cells is Regulated through Overlapping but Different Pathways. *Sensors*, 9(1), 386–403. <https://doi.org/10.3390/s90100386>
- Borden, E., Holland, J. F., Dao, T. L., Gutterman, J. U., Wiener, L., Chang, Y., & Patel, J. (1982). Leukocyte-Derived Interferon (Alpha) in Human Breast Carcinoma. *Annals of Internal Medicine*, 97(1), 1. <https://doi.org/10.7326/0003-4819-97-1-1>
- Datta, S., & Sarvetnick, N. (2009). Lymphocyte proliferation in immune-mediated diseases. *Trends in Immunology*, 30(9), 430–438. <https://doi.org/10.1016/j.it.2009.06.002>
- Dunn, G. P., Bruce, A. T., Sheehan, K. C. F., Shankaran, V., Uppaluri, R., Bui, J. D., ...

Chapter 5. Results (III)

- Schreiber, R. D. (2005). A critical function for type I interferons in cancer immunoediting. *Nature Immunology*, 6(7), 722–729. <https://doi.org/10.1038/ni1213>
- Escobar, G., Gentner, B., Naldini, L., & Mazziari, R. (2014). Engineered tumor-infiltrating macrophages as gene delivery vehicles for interferon- α activates immunity and inhibits breast cancer progression. *Oncoimmunology*, 3, e28696. <https://doi.org/10.4161/onci.28696>
- Escobar, G., Moi, D., Ranghetti, A., Ozkal-Baydin, P., Squadrito, M. L., Kajaste-Rudnitski, A., ... Naldini, L. (2014). Genetic engineering of hematopoiesis for targeted IFN- α delivery inhibits breast cancer progression. *Science Translational Medicine*, 6(217), 217ra3. <https://doi.org/10.1126/scitranslmed.3006353>
- Heinzel, S., Marchingo, J. M., Horton, M. B., & Hodgkin, P. D. (2018). The regulation of lymphocyte activation and proliferation. *Current Opinion in Immunology*, 51, 32–38. <https://doi.org/10.1016/j.coi.2018.01.002>
- Hervas-Stubbs, S., Perez-Gracia, J. L., Rouzaut, A., Sanmamed, M. F., Le Bon, A., & Melero, I. (2011). Direct Effects of Type I Interferons on Cells of the Immune System. *Clinical Cancer Research*, 17(9), 2619–2627. <https://doi.org/10.1158/1078-0432.CCR-10-1114>
- Huang, T.-H., Chintalacharuvu, K. R., & Morrison, S. L. (2007). Targeting IFN- α to B Cell Lymphoma by a Tumor-Specific Antibody Elicits Potent Antitumor Activities. *The Journal of Immunology*, 179(10).
- Kato, H., Sato, S., Yoneyama, M., Yamamoto, M., Uematsu, S., Matsui, K., ... Akira, S. (2005). Cell type-specific involvement of RIG-I in antiviral response. *Immunity*, 23(1), 19–28. <https://doi.org/10.1016/j.immuni.2005.04.010>
- Kontermann, R. E. (2012). Antibody-cytokine fusion proteins. *Archives of Biochemistry and Biophysics*, 526(2), 194–205. <https://doi.org/10.1016/j.abb.2012.03.001>
- Le Bon, A., Schiavoni, G., D'Agostino, G., Gresser, I., Belardelli, F., & Tough, D. F.

- (2001). Type I Interferons Potently Enhance Humoral Immunity and Can Promote Isotype Switching by Stimulating Dendritic Cells In Vivo. *Immunity*, 14(4), 461–470. [https://doi.org/10.1016/S1074-7613\(01\)00126-1](https://doi.org/10.1016/S1074-7613(01)00126-1)
- Nguyen, K. B., Salazar-Mather, T. P., Dalod, M. Y., Van Deusen, J. B., Wei, X., Liew, F. Y., ... Biron, C. A. (2002). Coordinated and distinct roles for IFN-alpha beta, IL-12, and IL-15 regulation of NK cell responses to viral infection. *Journal of Immunology (Baltimore, Md. : 1950)*, 169(8), 4279–4287. Retrieved from <http://www.ncbi.nlm.nih.gov/pubmed/12370359>
- Oliver-Vila, I., Ramírez-Moncayo, C., Grau-Vorster, M., Marín-Gallén, S., Caminal, M., & Vives, J. (2018). Optimisation of a potency assay for the assessment of immunomodulative potential of clinical grade multipotent mesenchymal stromal cells. *Cytotechnology*, 70(1), 31–44. <https://doi.org/10.1007/s10616-017-0186-0>
- Ortaldo, J. R., Phillips, W., Wasserman, K., & Herberman, R. B. (1980). Effects of metabolic inhibitors on spontaneous and interferon-boosted human natural killer cell activity. *Journal of Immunology (Baltimore, Md. : 1950)*, 125(4), 1839–1844. Retrieved from <http://www.ncbi.nlm.nih.gov/pubmed/6157747>
- Parker, B. S., Rautela, J., & Hertzog, P. J. (2016). Antitumour actions of interferons: implications for cancer therapy. *Nature Reviews Cancer*, 16(3), 131–144. <https://doi.org/10.1038/nrc.2016.14>
- Paul, F., Pellegrini, S., & Uzé, G. (2015). IFNA2: The prototypic human alpha interferon. *Gene*, 567(2), 132–137. <https://doi.org/10.1016/j.gene.2015.04.087>
- Quesada, J. R., Hawkins, M., Horning, S., Alexanian, R., Borden, E., Merigan, T., ... Gutterman, J. U. (1984). Collaborative phase I-II study of recombinant DNA-produced leukocyte interferon (clone A) in metastatic breast cancer, malignant lymphoma, and multiple myeloma. *The American Journal of Medicine*, 77(3), 427–432. Retrieved from <http://www.ncbi.nlm.nih.gov/pubmed/6548079>
- Sprent, J., Zhang, X., Sun, S., & Tough, D. (2000). T-cell proliferation *in vivo* and the

- role of cytokines. *Philosophical Transactions of the Royal Society of London. Series B: Biological Sciences*, 355(1395), 317–322.
<https://doi.org/10.1098/rstb.2000.0568>
- Tough, D. F., Borrow, P., & Sprent, J. (1996). Induction of bystander T cell proliferation by viruses and type I interferon in vivo. *Science (New York, N.Y.)*, 272(5270), 1947–1950. Retrieved from <http://www.ncbi.nlm.nih.gov/pubmed/8658169>
- Van Rosmalen, M., Krom, M., & Merkx, M. (2017). Tuning the Flexibility of Glycine-Serine Linkers To Allow Rational Design of Multidomain Proteins, 56, 46. <https://doi.org/10.1021/acs.biochem.7b00902>
- Welander, C. (1987). Overview of preclinical and clinical studies of interferon alfa-2b in combination with cytotoxic drugs. *Investigational New Drugs*, 5(S4), S47–S59. <https://doi.org/10.1007/BF00207263>
- Xuan, C., Steward, K. K., Timmerman, J. M., & Morrison, S. L. (2010). Targeted delivery of interferon-alpha via fusion to anti-CD20 results in potent antitumor activity against B-cell lymphoma. *Blood*, 115(14), 2864–2871. <https://doi.org/10.1182/blood-2009-10-250555>

Chapter 5. Results (III): ADCs: Heterogeneous conjugation of Trastuzumab

5.1. Introduction

Antibody drug conjugates represent an emerging class of cancer treatment in which a cytotoxic payload is targeted to the tumor site. Their structure is based on an antibody covalently linked to a cytotoxic payload (Figure 5.1), having a mechanism of action consisting in recognizing an antigen and being internalized into the target cell (see introduction section 1.2.4).

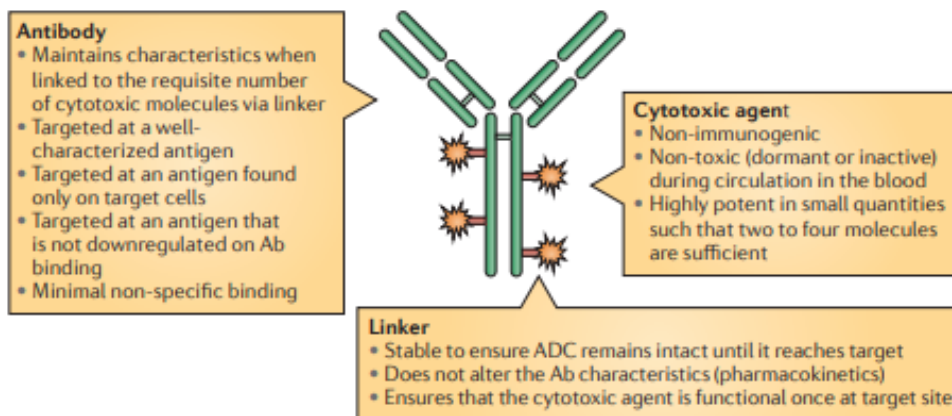


Fig. 5.1: Scheme of the structure of an ADC, with its three main parts (antibody, linker and cytotoxic drug) and features of each part. Obtained from (Zolot et al., 2013).

Several parameters influence the efficiency of an ADC, including the conjugation strategy by which the cytotoxic payload is linked to the antibody and the nature of the payload. Conjugation strategies can be classified in two types: heterogeneous and homogeneous (see section 1.2.6).

An heterogeneous conjugation yields an ADC that is a mixture of products that differ in the site and stoichiometry of conjugation (Behrens et al., 2015). This can be

observed in Figure 5.2, where conjugations through native lysine residues, or native interchain cysteine residues generate heterogeneous ADC products that are conjugated to 0-8 drugs per antibody.

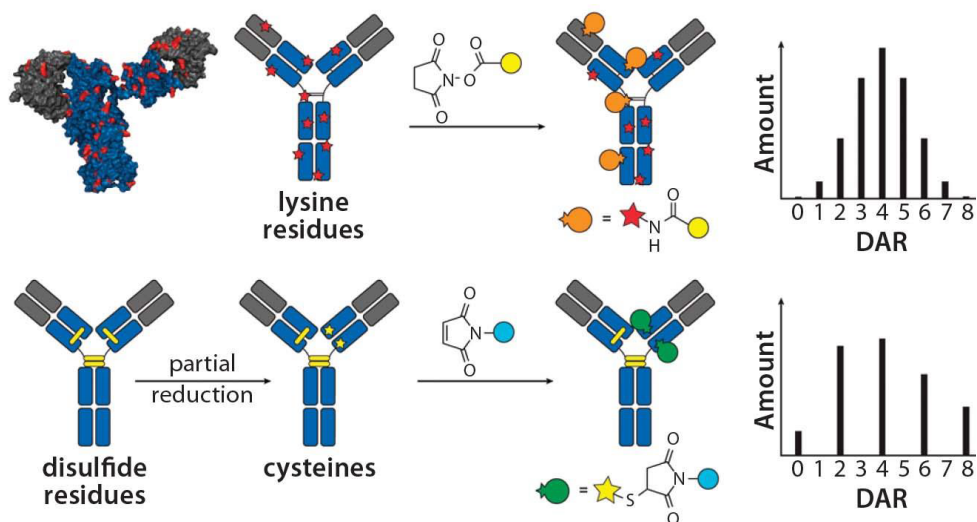


Fig. 5.2. Scheme of heterogeneous lysine and cysteine residues conjugation (Bhat et al., 2014).

The broad DAR (Drug Antibody Ratio) distribution obtained in heterogeneous products leads to reduced efficacy: high DAR species can increase potency and the risk of aggregation, clearance rate and premature release of the cytotoxic drug during circulation (Tsuchikama et al., 2018), while unconjugated antibodies, if present, will block potential binding sites on tumor surface and thus lower ADC efficacy (Merten et al., 2015). Therefore, alternative conjugation strategies, aiming at directing the drug at specific sites of the antibody in order to obtain homogeneous ADCs, thus, widening the therapeutic window, have been developed.

Several of these conjugation strategies, as well as the conventional heterogeneous strategies, are summarized in Figure 5.3. Despite this fact, conventional conjugation to native lysine and cysteine residues, which were the first developed conjugation

Chapter 5. Results (III)

strategies, still remain a benchmark in the field of ADCs, with most ADCs entering late clinical phases being conjugated in this way and with the 4 current commercially approved ADCs being heterogeneous.

The 4 approved ADCs consist in (in order of approval): gemtuzumab ozogamicin (Mylotarg), brentuximab vedotin (Adcetris, approved in 2011 (de Claro et al., 2012)), trastuzumab-emtansine (Kadcyla, approved in 2013 (Amiri-Kordestani et al., 2014)), and inotuzumab ozogamicin (Besponsa, approved in 2017 (Lamb, 2017)). Gemtuzumab ozogamicin was firstly approved in 2000 for the treatment of acute myeloid leukemia in an accelerated-approval process, then removed in 2010 due to bad results in a confirmatory trial (Jen et al., 2018), and later reapproved in 2017 after subsequent trials and data meta-analysis (Egan et al., 2018).

Reaction Chemistry	Reaction scheme	ReactionRate	Conjugation Site in Protein	Incorporation Method
<i>Amine-NHS</i>	<p>Primary amine + NHS-Ester $\xrightarrow{\text{pH 7-9}}$ Amide bond + NHS</p>	fast	Lysine, terminal amine	Natural
<i>Thiol-Maleimide Michael Addition</i>	<p>Reactive thiol + Maleimide $\xrightarrow[\text{Base}]{\text{pH 6.5-7.5}}$ Thioether bond</p>	fast	Cysteine	Natural
<i>Oxime Ligation</i>	<p><i>p</i>-Acetylphenylalanine + Aminoxy reagent $\xrightarrow{\text{pH 4.0}}$ Oxime bond</p>	slow	<i>p</i> -Acetylphenylalanine	Amber suppression
<i>Cycloaddition CuAAC</i>	<p>Azide Amino Acid + Terminal alkyne $\xrightarrow[\text{Cu(I)}]{\text{physiological pH}}$ Stable triazole</p>	slow	Azidohomoalanine	Methionine - auxotrophic <i>E. coli</i>
<i>Cycloaddition SPAAC</i>	<p>Azide Amino Acid + Dibenzocyclooctyne $\xrightarrow{\text{physiological pH}}$ Stable triazole</p>	slow	Azidohomoalanine	Methionine - auxotrophic <i>E. coli</i>
<i>Inverse-electron-demand Diels-Alder reaction</i>	<p>trans-Cyclooctene + Tetrazine reagent $\xrightarrow[\text{-N}_2]{\text{physiological pH}}$ Substituted cyclohexene</p>	very fast	trans-Cyclooctene-Lysine	Amber suppression

Fig. 5.3. Different conjugation chemistries for ADCs (Merten et al., 2015).

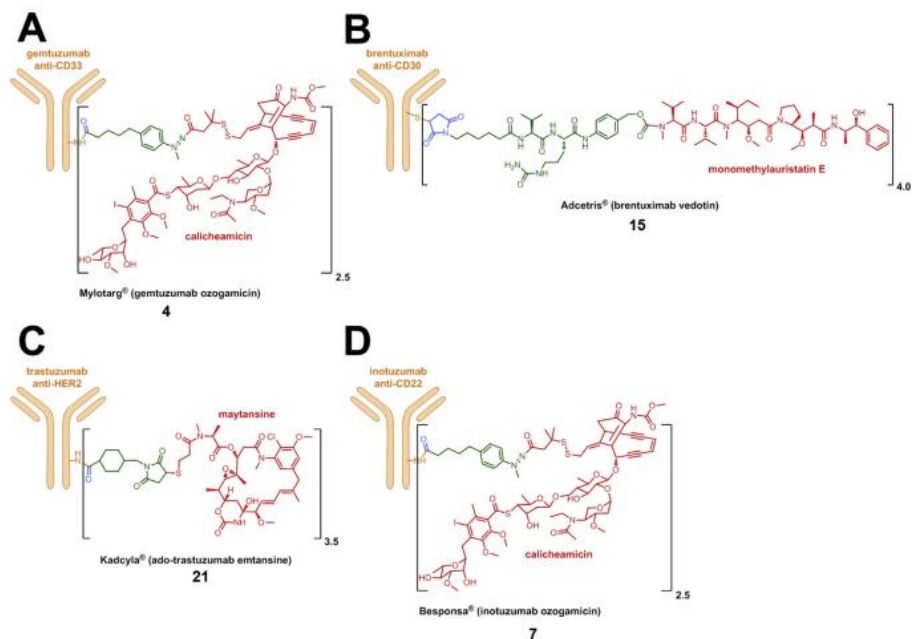


Figure 5.4.: representation of the 4 approved ADCs. A) Mylotarg; B) Adcetris; C) Kadcyia; D) Besponsa. Obtained from (Joubert et al., 2017).

In order to carry out the mentioned conjugations of cytotoxic drug to the antibody, a third element is critical: the linker. As it has been indicated in the introduction chapter (see 1.2.5), there are two main linker categories: cleavable and non-cleavable linkers (Panowski et al., 2014). Cleavable linkers allow the release of the drug in the tumor microenvironment (Lu et al., 2016) and can be divided into three main groups: acid labile, protease cleavable linkers and disulfide linkers.

- Acid labile linkers are stable in blood at neutral pH, but break at acidic pH found in lysosomes.
- Protease cleavable linkers are also stable in plasma, but are designed to be cleaved by specific proteases found in lysosomes of cancer cells.

- Disulfide linkers exploit the high level of intracellular reduced glutathione to release the free drug inside the cell (Panowski et al., 2014).

In the case of non-cleavable linkers, the mAb needs to be degraded into the lysosomes in order to release the cytotoxic drug. As an advantage with respect to the cleavable linkers, they present a higher stability in plasma, therefore reducing the drug leaking and potentially widening their therapeutic window (Lu et al., 2016). Both cleavable and non-cleavable linkers have been used in the approved ADCs.

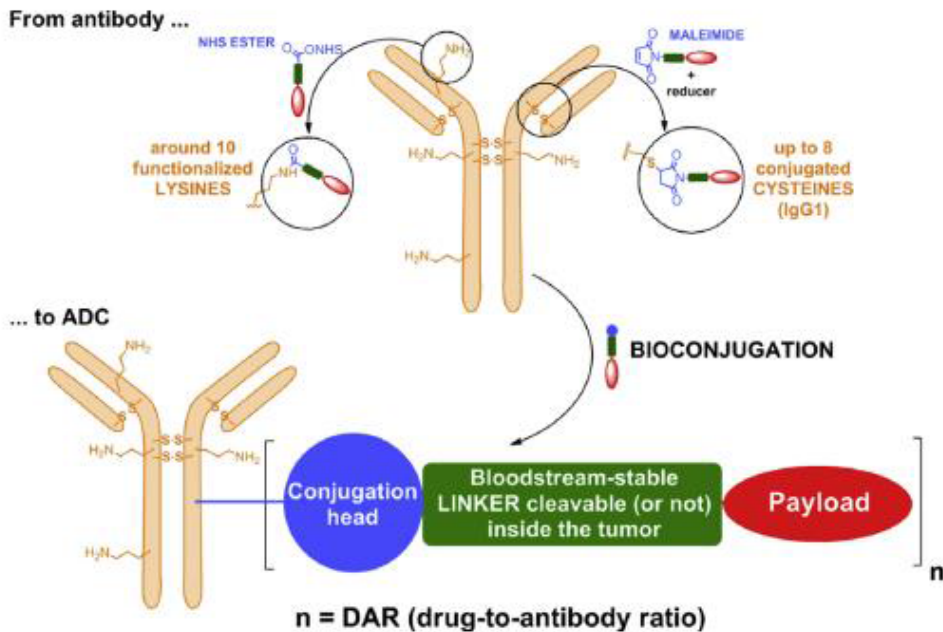


Figure 5.5. Conjugation of an antibody to ADC, using the example Lysine and cysteine conjugation strategies (Joubert et al., 2017).

In order to establish a platform for ADC production, a first step could consist in implementing the conjugation of the selected model antibody to the cytotoxic drugs used in the reference approved products. Therefore, in this chapter, the heterogeneous conjugation of the model antibody Trastuzumab will be attempted with the cytotoxic drugs DM1 (mertansine) and vcMMAE (monomethyl auristatin E).

They were the payloads of the approved ADCs in September 2015, the time when this thesis was started, and are still the most used payloads in ADCs that are in clinical phases: 2 thirds of these payloads are DM1 or vcMMAE (Hoffmann et al., 2018). will be attempted.

The selected model antibody Trastuzumab will be conjugated to the cytotoxic drug DM1 following the example of the approved ADC Trastuzumab-emtansine (commercial name: Kadcyla), developed by the company Immunogen in collaboration with Genentech (Ballantyne et al., 2013) (Genentech produced the antibody and the conjugation to the cytotoxic drug was developed by Immunogen). In this case, the lysine residues of the antibody are used as conjugation sites for the linker SMCC (Succinimidyl-4-(N-maleimidomethyl)cyclohexane-1-carboxylate), which is a heterobifunctional molecule with two reactive groups at each end: a N-hydroxysuccinimide (NHS) ester and a maleimide (Koniev et al., 2015). It is a non-cleavable linker and it might be one of the most popular crosslinkers ever designed for protein conjugation purposes (Hermanson, 2013). The N-hydroxysuccinimide group reacts with primary amines forming stable amide bonds, whereas the maleimide group reacts with sulfhydryl (thiol) groups (Fig 5.7). Applied to Trastuzumab-DM1 conjugation, the NHS group of the linker SMCC reacts with the amine of lysine residues and then the maleimide group reacts with the sulfhydryl group located in the DM1 cytotoxic drug. The cytotoxic drug DM1 (Fig 5.6), also called mertansine, is a maytansinoid, derivate from the molecule maytansine (a microtubule assembly inhibitor molecule isolated from the shrub *Maytenus ovatus* (Lopus et al., 2010)). The conjugation yields the Trastuzumab-SMCC-DM1 conjugate (Figure 5.8) with an aimed drug-antibody ratio (DAR) of 3.1, following the example described on the reference patent (WO/2005/037992, 2005).

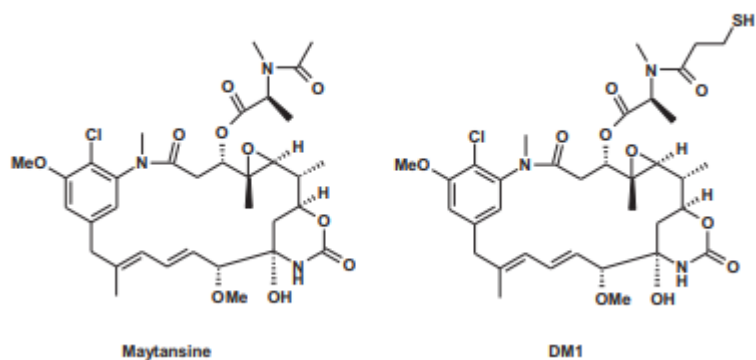


Figure 5.6: Structures of maytansine and DM1 (Bouchard et al., 2014).

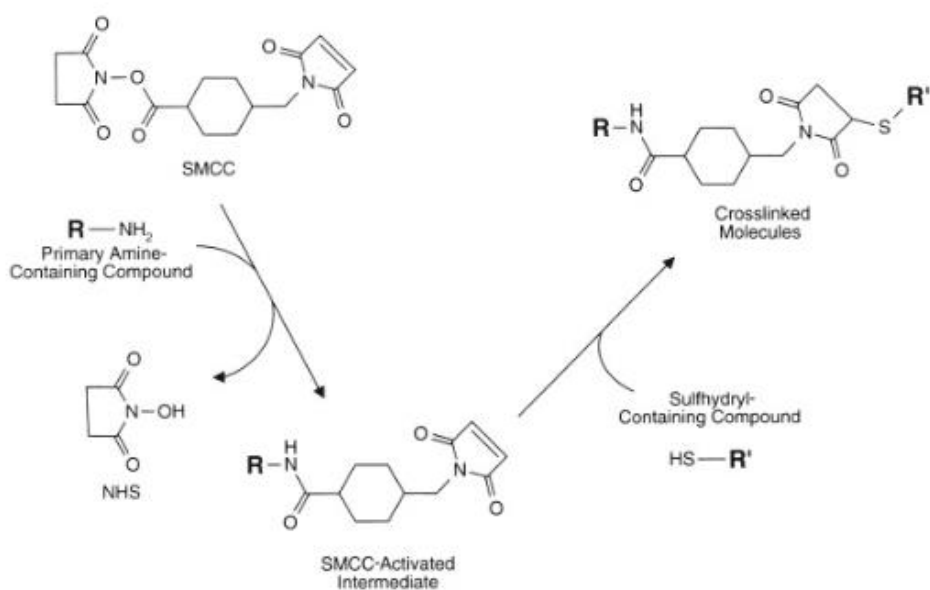


Figure 5.7: Reaction scheme of the SMCC linker with primary amines and sulfhydryl groups. Obtained from (Hermanson, 2013).

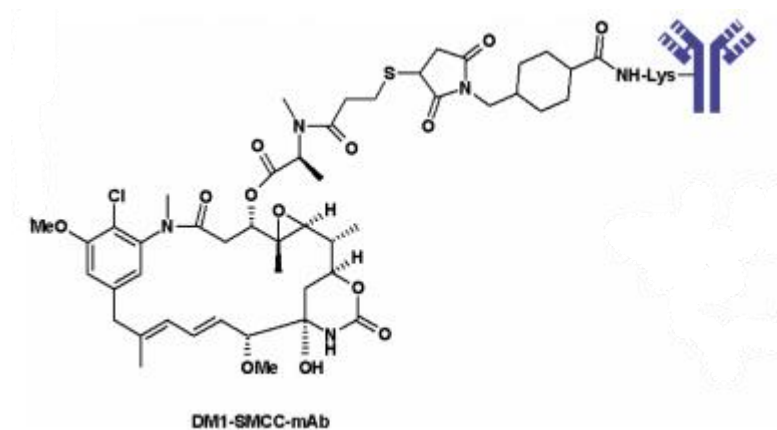


Figure 5.8: Depiction of DM1 linked through the SMCC linker to a lysine residue of an antibody (Bouchard et al., 2014).

The conjugation of Trastuzumab with vcMMAE will also be attempted. In this case, the conjugation process will be analogous to the procedure performed for the approved antibody brentuximab-vedotin (Adcetris), developed by Seattle Genetics (Van de Donk et al., 2012). The aimed product is an ADC with a DAR of 4, and the conjugation strategy followed is based on using the interchain cysteines as conjugation sites. In this process, the antibody undergoes a first step of partial reduction which allows breaking its interchain disulfide bonds, therefore rendering available for conjugation the thiol groups contained in the cysteine residues involved in the disulfide bonds. An antibody has 4 interchain disulfide bonds, with 2 cysteines per bond, therefore a maximum of 8 drug molecules can be linked per antibody. In order to obtain a DAR of 4, the antibody is partially reduced, generating an average of 4 free thiols per antibody, which are subsequently conjugated to the cytotoxic drug. The conjugation is performed using the cytotoxic drug vcMMAE, a derivative from MMAE (monomethyl auristatin E), which is an auristatin (which consist in antimitotic agents related in structure to the marine natural product dolastatin 10 (Francisco et al., 2003)), and acts by inhibiting the polymerization of tubulin in dividing cells (Doronina et al., 2003). The vcMMAE molecule consists in the cytotoxic

drug MMAE with the addition of an arm that serves as a linker. The conjugation chemistry of this molecule is the same than for the SMCC conjugation to DM1: in this case, the maleimide group present in the linker reacts with the thiol group from the antibody. The rest of the molecule consists of the spacer sequence PAB (*p*-aminobenzylcarbamate) and the two amino acids valine-citrulline (vc), which are a cleavage site for the protease cathepsine B, which is overexpressed in the lysosomes of some carcinomas. This renders the vcMMAE arm a cleavable linker, selectively freeing the cytotoxic drug in the tumor site (Figure 5.9).

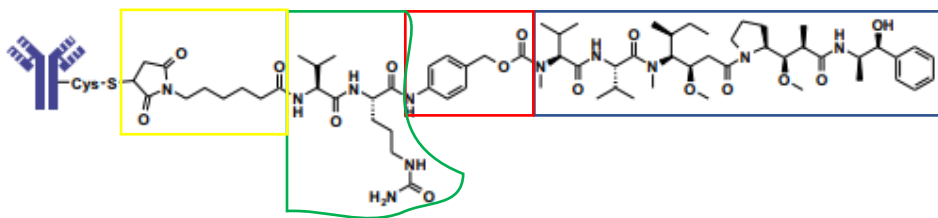


Figure 5.9: Depiction of vcMMAE linked to a cysteine residue of an antibody. Modified from (Bouchard et al., 2014). In blue, the MMAE molecule, in red, the PAB spacer, in green, the vc cathepsine cleavable sequence, and in yellow, the maleimido-craproyl sequence.

Once conjugated, the obtained products will be characterized in terms of the DAR and the content of aggregates and free drug, for which different analytic techniques will be implemented. In the case of the Trastuzumab-DM1 ADC, the DAR will be firstly assessed through spectroscopy analysis, by assessing the absorbance of ultraviolet/visible (UV/Vis) light, and will be confirmed with a more precise Mass Spectrometry (MS) analysis. In the case of the Trastuzumab-vcMMAE molecule, it will be performed with a hydrophobic chromatography HIC-HPLC analysis. This chromatographic analysis can be performed for cysteine conjugated products but not with lysine conjugated products, which are too heterogeneous and do not allow obtaining defined peak profiles.

The two attempted conjugations have been carried out using the previously produced Trastuzumab (Chapter 3).

5.2. Trastuzumab conjugation to DM1

5.2.1. Conjugation process definition

The conjugation process for Trastuzumab-DM1 was defined, as stated before, following a reference patent (WO/2005/037992, 2005) and literature related to lysine conjugation methodologies (Brun et al., 2013). The resulting conjugation process is depicted in Figure 5.10, consisting in a first step of SMCC linker addition to the antibody solution, incubation for 2h at room temperature, followed by a diafiltration in order to remove the excess of linker, then by the addition of DM1 and reaction step for 16.5h at room temperature and agitation at 300 rpm, followed by a final diafiltration in order to remove the excess of non-conjugated DM1 drug. In order to achieve the aimed DAR of 3.1, a SMCC molar proportion with respect to antibody of 7.5 was applied, and then 8.5 molecules of DM1 per antibody were added in the conjugation step.

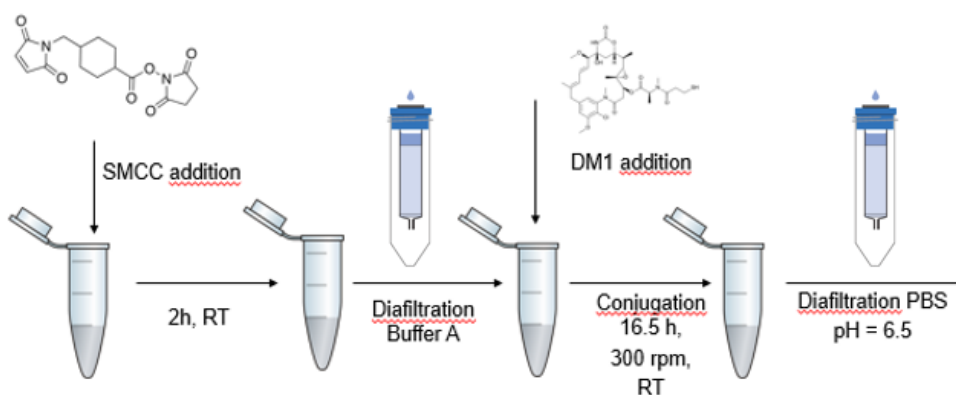


Figure 5.10: Scheme of the applied conjugation process for Trastuzumab-DM1 conjugation.

The process was implemented at a small scale: around 5 mg of antibody were conjugated, with a working volume of around 0.25 ml in the first step (linker addition) and around 0.5 ml in the DM1 conjugation step. The yield of the process, regarded as the percentage of antibody recovered after each step with respect to the initial antibody, was of 66 +/- 15.1% for the total process, being lower than for the reference process, which was 84% (WO/2005/037992, 2005). Four repetitions were performed of the conjugation process. Process data are summarized in Table 1. See section 10.10.1 of the Materials and methods chapter for more information of the performance of the conjugation process.

Table 5.1: Summary of Trastuzumab-DM1 conjugation process data

Amount of Trastuzumab antibody conjugated (mg)	Yield for SMCC addition + dialysis step	Yield for DM1 addition + dialysis step	Total process yield
~5	78.83 +/- 11.5	83.7 +/- 14.9	66 +/- 15.1

5.2.2. Physicochemical characterization of the conjugated product

Once the conjugation of the antibody had been performed, in order to analyze the quality and characterize the conjugated ADC, several analytical techniques were implemented. The analyzed parameters included most of the ones previously analyzed for Trastuzumab (see chapter 3), adding, in this case, the DAR and free drug levels:

- DAR
- Antigen recognition capacity

- Aggregate content and free drug levels
- Endotoxin content
- Stability

5.2.2.1. DAR: UV/Vis, MS

The number of DM1 molecules per antibody, referred to as drug antibody ratio or DAR, has been assessed by ultraviolet/visible (UV/Vis) spectroscopy and also by mass spectrometry (MS). The UV/Vis spectroscopy analysis represents a first fast analysis that allows determining the DAR of the ADC. Through the absorbance measure and using the molar extinction coefficient of both the cytotoxic drug and antibody of interest, the concentrations of both the cytotoxic drug and the antibody can be calculated (Wakankar et al., 2011) (see section 10.11.1. of the Materials and methods chapter).

Figure 5.11 shows the absorbance profile of a Trastuzumab-DM1 (T-DM1) ADC obtained, in which the absorbance maximum of the antibody can be observed at a wavelength of $\sim 280\text{nm}$, and the peak absorbance of DM1 can be observed at $\sim 252\text{nm}$. The average DAR obtained for the conjugated Trastuzumab-DM1 product has been of 3.13 ± 0.53 . This value corresponds to the average DAR obtained for the 4 conjugation processes attempted. It is very similar to the aimed 3.1 DAR value, however, it presents a high variability (standard deviation of 0.53), which could be attributed to the heterogeneity of the products derived from lysine conjugation, which have been reported to difficult the implementation of manufacturing processes ensuring a controlled DAR (Tsuchikama et al., 2018).

Chapter 5. Results (III)

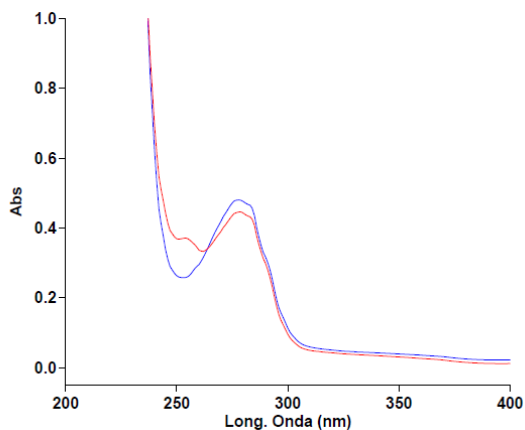


Figure 5.11: Absorbance profile of a Trastuzumab-DM1 ADC obtained in this work (red) and a Trastuzumab naked antibody (blue).

Regarding the MS analysis, of the 4 different T-DM1 batches performed, the product of only one of the batches could be analyzed by MS due to limitations in the available resources. The product was analyzed with an Orbitrap mass spectrometer at the *Laboratoire de Spectrométrie de Masse Bio-Organique* of the Université de Strasbourg (see section 10.11.3 of the Materials and Methods chapter). The obtained DAR for this analysis was 3.0, with the drug load distribution depicted in Figure 5.12.

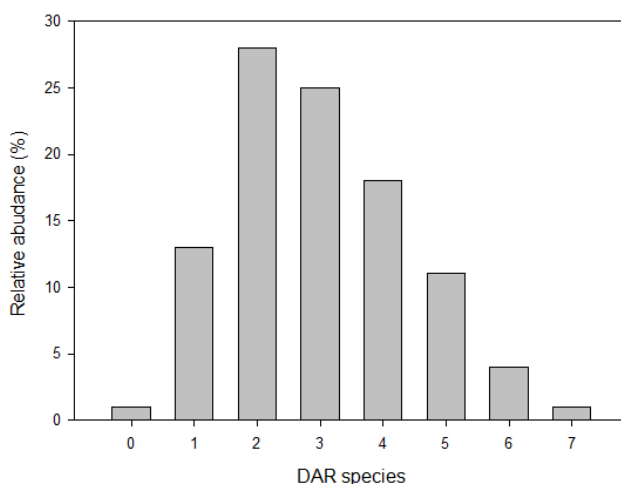


Figure 5.12: drug load distribution of the T-DM1 sample analyzed by MS (percentage of each ADC specie).

This value is coherent with the DAR value that had been obtained with UV/Vis analysis for the same batch process, which was 2.93. This result confirms the UV/Vis spectroscopy analysis as a reliable, fast and simple alternative for the DAR determination in lysine-conjugated ADCs. Reliability between UV/Vis and MS DAR values determination have been reported in the literature (Kim et al., 2014).

5.2.2.2. Antigen recognition capacity: ELISA and flow cytometry

In order to assess the recognition ability of the conjugated Trastuzumab-DM1 ADC, an ELISA assay was performed (see section 3.3.3.2 and 10.9.2), which showed that the ADC recognizes the HER2 antigen in a similar way than the naked Trastuzumab. This was later confirmed with the assay of recognition of the HER2 antigen expressed in the surface of breast cancer cells (Figure 5.13), showing that Trastuzumab-DM1 presented, with respect to naked Trastuzumab, a 102.3% average intensity level.

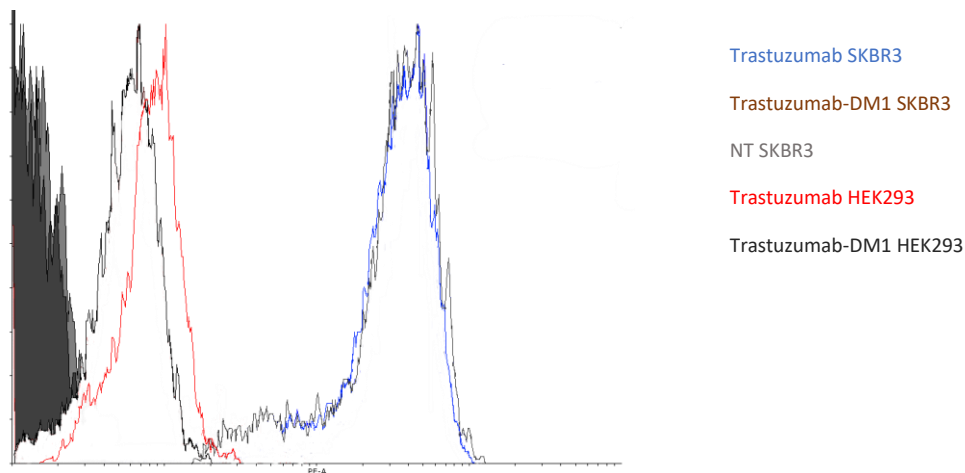


Figure 5.13. Trastuzumab and Trastuzumab-DM1 selectively binding to SKBR3 cells. HEK293 is used as a negative control. NT: non-treated (cells non-treated with Trastuzumab, Trastuzumab-DM1 nor secondary antibody).

5.2.2.3. Aggregates and free drug determination

The aggregates and free drug determination has been performed through a size exclusion (SEC)-HPLC analysis (see section 10.9.3 of the Materials and Methods section). As in the previous case of the MS analysis, only one of the 4 performed batches could be analyzed. The results obtained are summarized in Table 2 and the chromatography profile obtained is shown in Figure 5.14.

Table 5.2: summary of aggregates and free drug SEC-HPLC analysis

Retention time (min)	Area (%)	Aggregates (%)	Monomer (%)	Free drug (%)
6.77	7.13	7.13	92.87	n.d.
7.71	92.87			

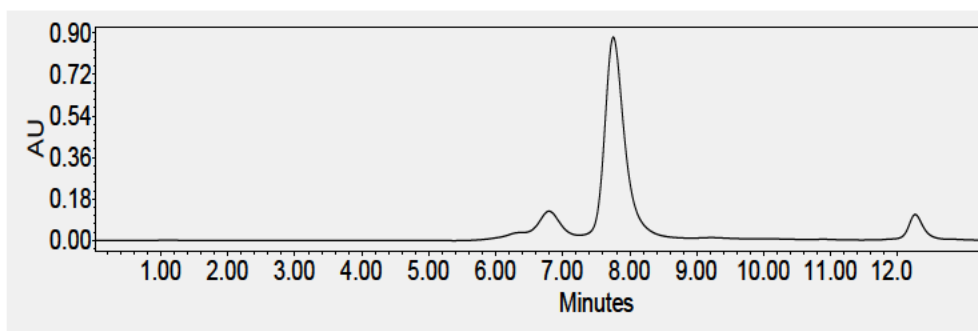


Figure 5.14: HPLC-SEC profile obtained from a T-DM1 sample. The aggregates peak (retention time: 6.77 min) and monomer peak (7.71 min) are depicted.

Aggregates (which elute first from the column, with a retention time of 6.77 min) consisted in the 7.13% of the conjugated product, which represents an increase from

the naked initial antibody, where the aggregates were at 1.75%. Increasing aggregate levels in the ADC with respect to the naked antibody could be attributed to the hydrophobicity of the drug. Free drug was not observed, therefore validating the clearance of the drug from the product during the post-conjugation dialysis step. The fact that no free drug is observed is coherent with the fact that the DAR value obtained with MS is similar to the value obtained with UV/Vis: a higher DAR value with UV/Vis than with MS could have meant that free drug was present in the ADC final product, since UV/Vis measures the absorbance of both attached and free drug, whereas MS only takes linked drug into account.

5.2.2.4. Stability

The stability of the conjugated ADC was assessed through a SEC-HPLC analysis: the monomer content of the product was determined at different times, while being stored at 4°C. The results are summarized in Table 5.3. The produced ADC presents a monomer proportion that diminishes over time, especially between 1 and 2 months of storage. This was mainly due to the increasing presence of aggregates and antibody fragments. Compared to naked (non-conjugated) Trastuzumab, the ADC presents a higher tendency to lower its monomer content where at 2 months it was still at 98.25%, compared to 79.69% for Trastuzumab-DM1 (see section 3.3.3.6), with monomer decrease due to the hydrophobicity of DM1. Free drug remained undetected along time, showing a high stability of the product in this regard.

Table 5.3. Stability of Trastuzumab-DM1

Time (months)	Monomer (%)	Free drug (%)
0 (fresh)	92.87	0

1	89.03	0
2	79.69	0
3	75.96	0

5.3. Trastuzumab conjugation to vcMMAE

5.3.1. Conjugation process definition

The conjugation process for Trastuzumab-vcMMAE was defined from several references, including research articles and patents (Doronina et al., 2003), (Francisco et al., 2003), (Klussman et al., 2004), (Sun et al., 2005), (US20050238649, 2004), (WO2006065533, 2006). The resulting conjugation process is depicted in Figure 5.15, consisting in a first step of partial reduction with TCEP addition and incubation for 1h at 37°C, followed by a dilution, addition of vcMMAE and reaction step for 1h at 4°C, then quenching with cysteines (in order to inactivate not-conjugated drug and to cap remaining free thiols) and finally followed by a final diafiltration in order to remove the excess of non-conjugated vcMMAE drug.

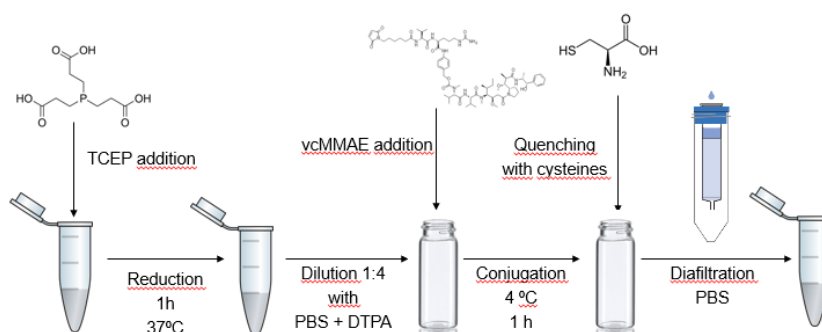


Figure 5.15: Scheme of the applied conjugation process for Trastuzumab-vcMMAE conjugation.

The process was implemented at the same scale as in the previous Trastuzumab-DM1 conjugation process: 5 mg of antibody were conjugated, with a working volume of around 0.5 ml in the first step (reduction) and around 2 ml in the vcMMAE conjugation step. In order to achieve the aimed DAR of 4, the partial reduction step was performed with a molar proportion of TCEP of 4 with respect to the antibody, and then 6 molecules of vcMMAE per antibody (1.5x free thiol group) were added in the conjugation step. The yield of the process, regarded as the percentage of antibody recovered after each step with respect to the initial antibody, was of 73.5+/- 13.5% for the total process. Four repetitions were also performed in this conjugation process. See section 10.10.2 of the Materials and methods chapter for more information of the performance of the conjugation process.

5.3.2. Characterization of the conjugated product

For the obtained Trastuzumab-vcMMAE ADC, the characterization of the conjugated product in terms of the DAR is performed with a hydrophobic interaction chromatography (HIC)-HPLC analysis. Mass spectrometry analysis could not be performed in this case, due to resource and timing limitations.

5.3.2.1. DAR: HIC-HPLC

A good way to obtain a DAR value for cysteine-conjugated ADCs consists in HIC-HPLC: differently loaded species of the ADC mixture have different hydrophobicity levels (higher loaded species are more hydrophobic, since the cytotoxic drug vcMMAE is hydrophobic) and thus have different retention times. Assigning a specific drug loaded specie to each peak of the chromatogram profile, a DAR value can be obtained. In this case, a reference profile from the column supplier (see 10.11.2) was used. In Figure 5.16, a chromatography profile from one of the Trastuzumab-

vcMMAE products obtained is shown. The DAR value resulting from this analysis for the obtained Trastuzumab-vcMMAE product is 3.98 ± 0.31 , which corresponds to the aimed value of 4.

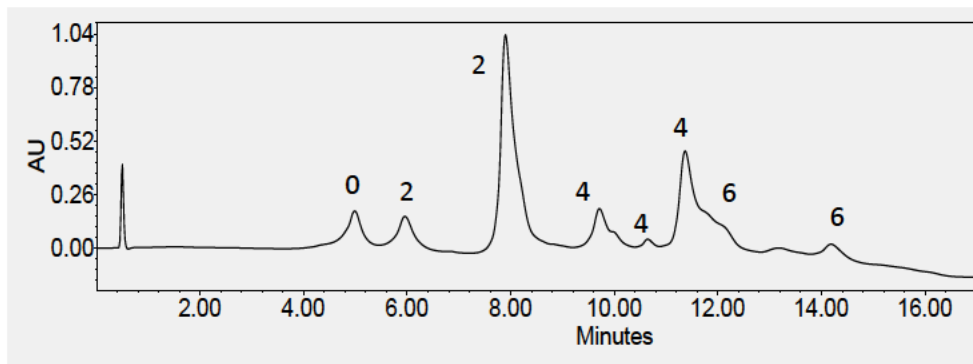


Figure 5.16: HIC-HPLC profile from Trastuzumab-vcMMAE product obtained. Retention times for each peak are indicated, as well as the DAR assigned to each peak.

5.3.2.2. Antigen recognition capacity: ELISA

The recognition ability of the target antigen of the conjugated Trastuzumab-vcMMAE ADC has been performed in the same way than the Trastuzumab-DM1 (see 5.2.2.2), showing again a recognition of the antibody to the HER2 target. Again, this was later confirmed with the assay of recognition of the HER2 antigen expressed in the surface of breast cancer cells (Figure 5.17), showing that Trastuzumab-vcMMAE presented, with respect to naked Trastuzumab, a 92% average intensity level.

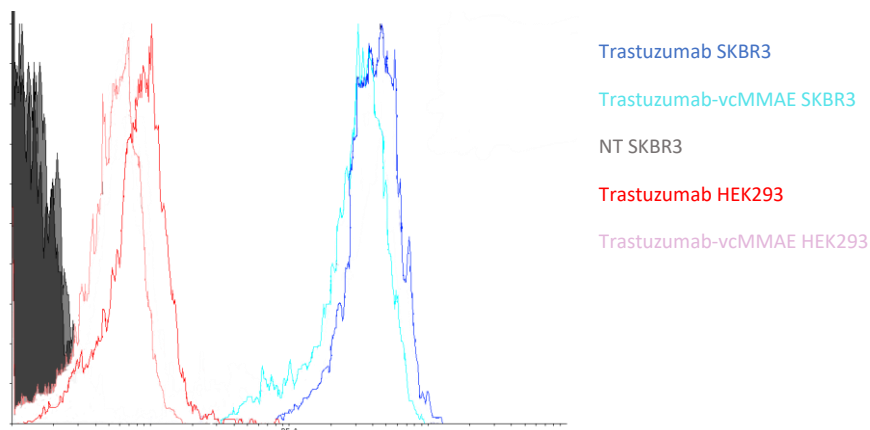


Figure 5.17. Trastuzumab and Trastuzumab-vcMMAE selectively binding to SKBR3 cells. HEK293 is used as a negative control. NT: non-treated (cells non-treated with Trastuzumab, Trastuzumab-vcMMAE nor secondary antibody).

5.3.2.3. Aggregates and free drug determination

As for the previous Trastuzumab-DM1 conjugation product, the aggregates and free drug determination has been performed through a SEC-HPLC analysis (see section 10.9.3 of the Materials and Methods section). Aggregates consisted in the 0.75% (+/- 0.49) of the conjugated product, representing a decrease from the naked initial antibody, where the aggregates were at 1.75%. The reduction step applied in this conjugation process could be a possible explanation for this fact.

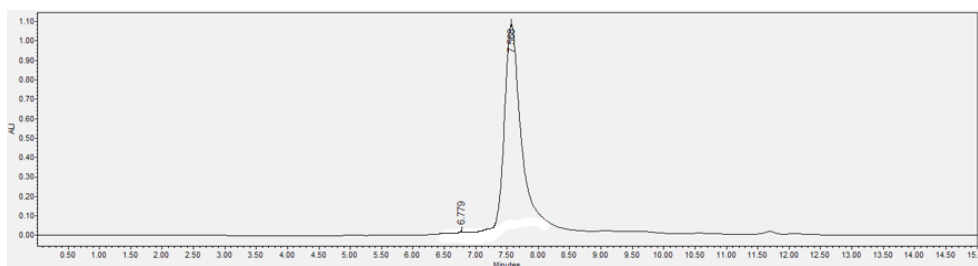


Figure 5.18. SEC-HPLC profile of Trastuzumab-vcMMAE.

Table 5.4: summary of aggregates and free drug SEC-HPLC analysis for Trastuzumab-vcMMAE

Retention time (min)	Area (%)	Aggregates (%)	Monomer (%)	Free drug (%)
6.78	0.75			
		0.75	99.25	n.d.
7.57	99.25			

Free drug, again, was not observed, therefore validating the clearance of the drug from the product during the post-conjugation dialysis step.

5.3.2.4. Endotoxin content

The endotoxin content was determined through the LAL assay (see sections 3.3.3.5 and 10.9.5), and showed that for the conjugation process of Trastuzumab with vcMMAE, an increasing of 36% in the endotoxin content occurred (EU (endotoxin units)/mg) with respect to the unconjugated Trastuzumab.

5.3.2.5. Stability

As for previously performed with Trastuzumab-DM1 (section 5.2.2.4), the stability of Trastuzumab-vcMMAE was assessed through a SEC-HPLC analysis. The results are summarized in Table 5.6. The produced ADC presents a monomer proportion that diminishes over time, especially between 2 and 3 months of storage at 4°C. This was mainly due to the increasing presence of aggregates and antibody fragments. Compared to naked (non-conjugated) Trastuzumab, the ADC presents a higher tendency to lower its monomer content, where at 6 months Trastuzumab was still at 91.1%, compared to 76.43% for Trastuzumab-vcMMAE at 3 months (see section

3.3.3.6), with monomer decrease due to the hydrophobicity of vcMMAE. Free drug remained undetected along time, showing a high stability of the product in this regard.

Table 5.6. Stability table of Trastuzumab-vcMMAE

Time (months)	Monomer (%)	Free drug (%)
0 (fresh)	98.33	0
1	97.53	0
2	89.6	0
3	76.43	0

5.4. Conclusions

In this chapter, Trastuzumab has been successfully conjugated to the cytotoxic drugs DM1 and vcMMAE in an heterogeneous way. The obtained products show a DAR value coherent with the aimed DARs for both conjugation strategies, with low aggregates percentage and no free drug observed. Therefore, it can be stated that a heterogeneous conjugation process platform based on the benchmark approved ADCs Kadcyla and Adcetris has been implemented.

Heterogeneous ADCs, however, present drawbacks in terms of therapeutic activity and also from a manufacturing point of view, as seen in this chapter, where variability in the DAR value has been observed, particularly in the case of Trastuzumab lysine conjugation to DM1. These issues can be overcome by using homogeneous ADCs, the production of which will be analyzed in the following

chapter. The antiproliferative activity of the generated heterogeneous ADCs will be assessed later and compared with the homogeneous ADCs.

5.5. References

- Amiri-Kordestani, L., Blumenthal, G. M., Casey Xu, Q., Zhang, L., Tang, S. W., Ha, L., ... Cortazar, P. (2014). FDA Approval: Ado-trastuzumab Emtansine for the Treatment of Patients with HER2-Positive Metastatic Breast Cancer. *American Association for Cancer Research*. <https://doi.org/10.1158/1078-0432.CCR-14-0012>
- Ballantyne, A., & Dhillon, S. (2013). Trastuzumab Emtansine: First Global Approval. *Drugs*, 73(7), 755–765. <https://doi.org/10.1007/s40265-013-0050-2>
- Behrens, C. R., Ha, E. H., Chinn, L. L., Bowers, S., Probst, G., Fitch-Bruhns, M., ... Jackson, D. Y. (2015). Antibody-Drug Conjugates (ADCs) Derived from Interchain Cysteine Cross-Linking Demonstrate Improved Homogeneity and Other Pharmacological Properties over Conventional Heterogeneous ADCs. *Molecular Pharmaceutics*, 12(11), 3986–3998. <https://doi.org/10.1021/acs.molpharmaceut.5b00432>
- Bhat, A. S., Rabuka, D., & Bleck, G. (2014). The next step in homogeneous bioconjugate development: optimizing payload placement and conjugate composition. *Bioprocess International*. Retrieved from <https://bioprocessintl.com/manufacturing/monoclonal-antibodies/next-step-homogenous-bioconjugate-development-optimizing-payload-placement-conjugate-composition/>
- Bouchard, H., Viskov, C., & Garcia-Echeverria, C. (2014). Antibody–drug conjugates—A new wave of cancer drugs. *Bioorganic & Medicinal Chemistry Letters*, 24(23), 5357–5363. <https://doi.org/10.1016/j.bmcl.2014.10.021>

Chapter 5. Results (III)

- Brun, M.-P., & Gauzy-Lazo, L. (2013). Protocols for Lysine Conjugation (pp. 173–187).
https://doi.org/10.1007/978-1-62703-541-5_10
- de Claro, R. A., McGinn, K., Kwitkowski, V., Bullock, J., Khandelwal, A., Habtemariam, B., ... Pazdur, R. (2012). U.S. Food and Drug Administration approval summary: brentuximab vedotin for the treatment of relapsed Hodgkin lymphoma or relapsed systemic anaplastic large-cell lymphoma. *Clinical Cancer Research : An Official Journal of the American Association for Cancer Research*, 18(21), 5845–5849. <https://doi.org/10.1158/1078-0432.CCR-12-1803>
- Doronina, S. O., Senter, P. D., & Toki Brian, E. (2004). US20050238649. Retrieved from
<https://patentscope.wipo.int/search/es/detail.jsf?docId=US40873540&tab=NATIONALBIBLIO&maxRec=1000>
- Doronina, S. O., Toki, B. E., Torgov, M. Y., Mendelsohn, B. A., Cervený, C. G., Chace, D. F., ... Senter, P. D. (2003). Development of potent monoclonal antibody auristatin conjugates for cancer therapy. *Nature Biotechnology*, 21(7), 778–784. <https://doi.org/10.1038/nbt832>
- Egan, P. C., & Reagan, J. L. (2018). The return of gemtuzumab ozogamicin: a humanized anti-CD33 monoclonal antibody-drug conjugate for the treatment of newly diagnosed acute myeloid leukemia. *OncoTargets and Therapy*, 11, 8265–8272. <https://doi.org/10.2147/OTT.S150807>
- Francisco, J. A., Cervený, C. G., Meyer, D. L., Mixan, B. J., Klussman, K., Chace, D. F., ... Wahl, A. F. (2003). cAC10-vcMMAE, an anti-CD30 – monomethyl auristatin E conjugate with potent and selective antitumor activity, 102(4), 1458–1465. <https://doi.org/10.1182/blood-2003-01-0039>.The
- Hermanson, G. T. (2013). *Bioconjugate techniques* (3rd ed.). Elsevier.
<https://doi.org/https://doi.org/10.1016/C2009-0-64240-9>

- Hoffmann, R. M., Coumbe, B. G. T., Josephs, D. H., Mele, S., Ilieva, K. M., Cheung, A., ... Karagiannis, S. N. (2018). Antibody structure and engineering considerations for the design and function of Antibody Drug Conjugates (ADCs). *Oncoimmunology*, 7(3), e1395127. <https://doi.org/10.1080/2162402X.2017.1395127>
- Jen, E. Y., Ko, C.-W., Lee, J. E., Del Valle, P. L., Aydanian, A., Jewell, C., ... Pazdur, R. (2018). FDA Approval: Gemtuzumab Ozogamicin for the Treatment of Adults with Newly Diagnosed CD33-Positive Acute Myeloid Leukemia. *Clinical Cancer Research : An Official Journal of the American Association for Cancer Research*, 24(14), 3242–3246. <https://doi.org/10.1158/1078-0432.CCR-17-3179>
- Joubert, N., Denevault-Sabourin, C., Bryden, F., & Viaud-Massuard, M.-C. (2017a). Towards antibody-drug conjugates and prodrug strategies with extracellular stimuli-responsive drug delivery in the tumor microenvironment for cancer therapy. *European Journal of Medicinal Chemistry*, 142, 393–415. <https://doi.org/10.1016/J.EJMECH.2017.08.049>
- Joubert, N., Denevault-Sabourin, C., Bryden, F., & Viaud-Massuard, M.-C. (2017b). Towards antibody-drug conjugates and prodrug strategies with extracellular stimuli-responsive drug delivery in the tumor microenvironment for cancer therapy. *European Journal of Medicinal Chemistry*, 142, 393–415. <https://doi.org/10.1016/j.ejmech.2017.08.049>
- Kim, M. T., Chen, Y., Marhoul, J., & Jacobson, F. (2014). Statistical Modeling of the Drug Load Distribution on Trastuzumab Emtansine (Kadcyla), a Lysine-Linked Antibody Drug Conjugate. *Bioconjugate Chemistry*, 25(7), 1223–1232. <https://doi.org/10.1021/bc5000109>
- Klussman, K., Mixan, B. J., Cervený, C. G., Meyer, D. L., Senter, P. D., & Wahl, A. F. (2004). Secondary mAb-vcMMAE conjugates are highly sensitive reporters of antibody internalization via the lysosome pathway. *Bioconjugate Chemistry*,

- 15(4), 765–773. <https://doi.org/10.1021/bc049969t>
- Koniev, O., & Wagner, A. (2015). Developments and recent advancements in the field of endogenous amino acid selective bond forming reactions for bioconjugation. *Chem. Soc. Rev.*, 44(15), 5495–5551. <https://doi.org/10.1039/C5CS00048C>
- Lamb, Y. N. (2017). Inotuzumab Ozogamicin: First Global Approval. *Drugs*, 77(14), 1603–1610. <https://doi.org/10.1007/s40265-017-0802-5>
- Lopus, M., Oroudjev, E., Wilson, L., Wilhelm, S., Widdison, W., Chari, R., & Jordan, M. A. (2010). Maytansine and Cellular Metabolites of Antibody-Maytansinoid Conjugates Strongly Suppress Microtubule Dynamics by Binding to Microtubules. *Molecular Cancer Therapeutics*, 9(10), 2689–2699. <https://doi.org/10.1158/1535-7163.MCT-10-0644>
- Lu, J., Jiang, F., Lu, A., & Zhang, G. (2016). Linkers Having a Crucial Role in Antibody-Drug Conjugates. *International Journal of Molecular Sciences*, 17(4), 561. <https://doi.org/10.3390/ijms17040561>
- MCDONAGH, C., & CARTER, P. (2006). WO2006065533. Retrieved from <https://patentscope.wipo.int/search/es/detail.jsf?docId=WO2006065533&tab=PCTBIBLIO&maxRec=1000>
- Panowski, S., Bhakta, S., Raab, H., Polakis, P., & Junutula, J. R. (2014). Site-specific antibody drug conjugates for cancer therapy. *MAbs*, 6(1), 34–45. <https://doi.org/10.4161/mabs.27022>
- Steeves, R., Lutz, R., Chari, R., Xie, H., & Kovtun, Y. (2005). WO/2005/037992. Retrieved from <https://patentscope.wipo.int/search/es/detail.jsf?docId=WO2005037992&tab=PCTBIBLIO&maxRec=1000>
- Sun, M. M. C., Beam, K. S., Cervený, C. G., Hamblett, K. J., Blackmore, R. S., Torgov, M. Y., ... Alley, S. C. (2005). Reduction–Alkylation Strategies for the Modification

Chapter 5. Results (III)

of Specific Monoclonal Antibody Disulfides. *Bioconjugate Chemistry*, 16(5), 1282–1290. <https://doi.org/10.1021/bc050201y>

Tsuchikama, K., & An, Z. (2018). Antibody-drug conjugates: recent advances in conjugation and linker chemistries. *Protein & Cell*, 9(1), 33–46. <https://doi.org/10.1007/s13238-016-0323-0>

van de Donk, N. W. C. J., & Dhimolea, E. (2012). Brentuximab vedotin. *MAbs*, 4(4), 458–465. <https://doi.org/10.4161/mabs.20230>

Wakankar, A., Chen, Y., Gokarn, Y., & Jacobson, F. S. (2011). Analytical methods for physicochemical characterization of antibody drug conjugates. *MAbs*, 3(2), 161–172. Retrieved from <http://www.ncbi.nlm.nih.gov/pubmed/21441786>

Zolot, R. S., Basu, S., & Million, R. P. (2013). Antibody–drug conjugates. *Nature Reviews Drug Discovery*, 12(4), 259–260. <https://doi.org/10.1038/nrd3980>

Chapter 6. Results (IV): ADCs: Homogeneous conjugation of Trastuzumab with vcMMAE

6.1. Introduction

Homogeneous ADCs contain a specific number of conjugated drugs at defined sites on the antibody (Jain et al., 2015). This leads to a uniform ADC product, limiting batch-to-batch variability, positively impacting their manufacturing process as well as their clinical potential (Sochaj et al., 2015).

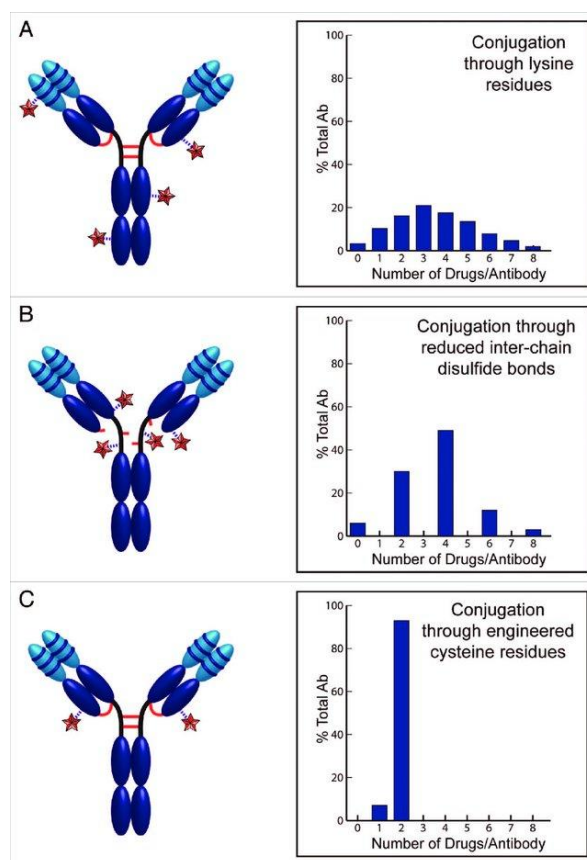


Fig 6.1. Scheme and DAR distribution of two heterogeneous ADCs (generated by conventional lysine and cysteine conjugations) and an homogeneous ADC generated through a site-directed conjugation to an added cysteine (obtained from (Panowski et al., 2014)).

Homogeneous ADCs have a wider therapeutic window with respect to heterogeneous ADCs (McDonagh et al., 2006), which contain a mixture of highly-conjugated (overloaded) and unconjugated (naked) antibodies. Naked antibodies compete with drug-loaded species for antigen binding, which can diminish the efficiency of the ADC therapeutic effect. Moreover, high-loaded species may result in antibody aggregation, increased toxicity, decreased stability and shorter half-life of ADCs in circulation (Sochaj et al., 2015). Several homogeneous ADCs have reached late clinical trial phases (Beck et al., 2017; Nejadmoghaddam et al., 2019).

Several protein site-directed conjugation chemistries have been developed, which can be applied for specifically labeling proteins for several applications including homogeneous ADC generating purposes (Krall et al., 2016). Most of these strategies rely on the genetic modification of the antibody or on complex chemistry linkers. Some of the most relevant strategies include:

- 1.- **Thiomabs:** The typical cysteine-based homogeneous conjugation process relies on a genetically modified antibody which normally contains a single point mutation where one of the amino acids of the antibody is substituted by a cysteine, to which the cytotoxic drug will be conjugated in a selective manner (Sochaj et al., 2015). The mutation introduced to the antibody should avoid altering the structure of the antibody and its function, and the selected location should also allow the reaction of the added cysteine with the cytotoxic drug of interest (Junutula et al., 2008), (Junutula et al., 2010). The location of the added cysteine in the antibody is critical, since it can affect the stability and pharmacokinetics of the ADC (Strop et al., 2013; Vollmar et al., 2017), for example by interacting with other cysteine residues of the same protein, and, hence, result in conformational issues that may lead to the inactivation of the protein or its improper folding. This problem has been overcome by the development of tools that allow detecting sites on the antibody that do not affect its activity, such as the PHESELECTOR

(Phage ELISA for Selection of Reactive Thiols). This method relies in the introduction of reactive cysteine residues at various sites, displaying the Fab on phage, and screening to identify reactive cysteines that do not interfere with antigen binding (Junutula et al., 2008).

2.- Antibodies with unnatural amino acids: These are antibodies which contain unnatural amino acids in concrete locations. They are homologous to Thiomabs, but contain unnatural amino acids instead of cysteines. These amino acids have specific side-chains that allow them to be conjugated in a site-directed way, since the applied conjugation chemistry will not react with the rest of the amino acids of the antibody. There are several unnatural amino acids applied in ADCs, the most common being p-acetylphenylalanine (pAcPhe) and selenocysteine (Sec) (Panowski et al., 2014).

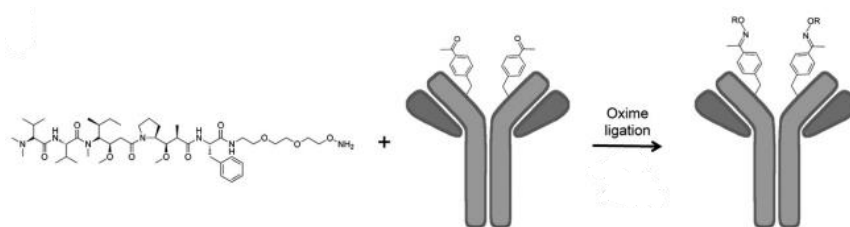


Figure 6.2. Conjugation of an antibody containing a pAcPhe with a an auristatin payload derivatized alkoxy amine. Modified from (Axup et al., 2012).

Both of these methods require genetically engineering the antibody producing cell line:

- P-acetylphenylalanine: it is added through introducing the amber stop codon (UAG) at the desired location of the antibody. The antibody cDNA is then coexpressed with an amber-suppressor tRNA and the properly paired mutant tRNA synthetase. The tRNA synthetase loads pAcPhe onto the amber tRNA and thus pAcPhe is incorporated into the antibody at the amber site UAG (Liu et al.,

2007; Wang et al., 2003). pAcPhe contains a keto group that can be selectively conjugated to a drug containing an alkoxy-amine through an oxime ligation (Axup et al., 2012).

- Selenocysteine: in this case, selenocysteine (Sec) can be added through the opal stop codon (UGA). Normally, UGA codes for transcriptional termination, however, in the presence of a Sec insertion sequence (SECIS) located in the 3' UTR (untranslated region) of Sec containing proteins, termination is prevented by the formation of an mRNA secondary structure and Sec is inserted at the UGA codon (Caban et al., 2006). Selenocysteine is very similar to the classical cysteine, but contains selenium instead of a sulfur atom. The selenolate group is more reactive than its thiol counterpart, rendering it easier to conjugate with electrophilic compounds in conditions in which selenocysteine is selectively activated (Hofer et al., 2009).
- Other unnatural amino acids are being investigated for their use in site-directed conjugation. One of them is *p-azidomethyl L-phenylalanine* (pAMF), introduced into the antibody with a cell free expression system (Cai et al., 2015), which allows its conjugation to alkyne linkers via strain-promoted azide-alkyne cycloaddition copper-free chemistry (Jackson, 2016) (Zimmerman et al., 2014).

3.- Enzymatic conjugations: Site-directed conjugations can be driven by enzymes that selectively modify antibodies with unique functional groups. Several enzymatic methodologies have been developed, depending on the enzyme. They include:

- Glycosyltransferases: glycosyltransferases are enzymes involved in the oligosaccharides synthesis and are responsible for the transfer of a sugar residue from an activated sugar nucleotide to a sugar

acceptor or glycoprotein/lipid. Mutant glycosyltransferases can be used to attach a chemically active sugar moiety to a specific glycosylation site on the antibody. Molecules of choice can then be conjugated to the chemical handle on the sugar moiety. This technique has been applied in mutant glycosyltransferases which are able to transfer the reactive sugar residue 2-keto-Gal (Ramakrishnan et al., 2002) to the conserved Asn-297 N-glycosylation site of the Fc fragment. 2-keto-Gal can then be coupled to biomolecules with an orthogonal reactive group (Boeggeman et al., 2009).

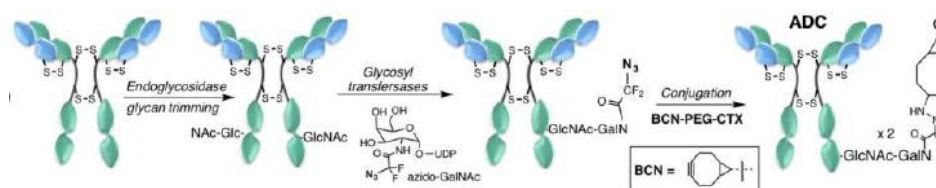


Figure 6.3. Scheme of the conjugation reaction using glycosyltransferases. Obtained from (Jackson, 2016).

- Transglutaminases: there are different transglutaminase enzymes. Microbial transglutaminase (mTG) recognizes a sequence tag (LLQGA), in which the glutamine serves as an acyl donor for enzymatic ligation to primary amines catalyzed by the transglutaminase (Farias et al., 2014). In the case of bacterial transglutaminase (BTG), it can be used without introducing a sequence tag: following deglycosylation of the antibody, a site-directed conjugation mediated by BTG takes place at the native glutamine Q295 (Dennler et al., 2014).

Chapter 6. Results (IV)

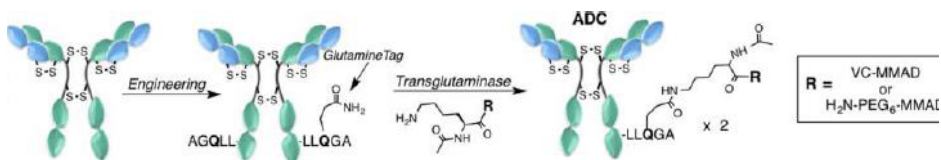


Figure 6.4. Scheme of the conjugation reaction using transglutaminases. Obtained from (Jackson, 2016).

- Formylglycine generating enzymes (FGE): they have been used to construct homogeneous ADCs through the insertion of its recognition tag (CXPXR), in which its cysteine is converted by FGE to formylglycine, which can then be conjugated to the corresponding payload (Rabuka et al., 2012).

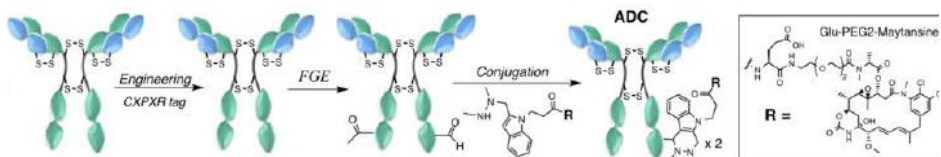


Figure 6.5. Scheme of the conjugation reaction using FGE. Obtained from (Jackson, 2016).

- Sortase A (Processes for constructing antibody drug conjugates). It is a transpeptidase which catalyzes the transfer of polyglycine substrates to the C-terminus of the sequence motif LPXTG, resulting in a stable linkage with the antibody (Beerli et al., 2015).

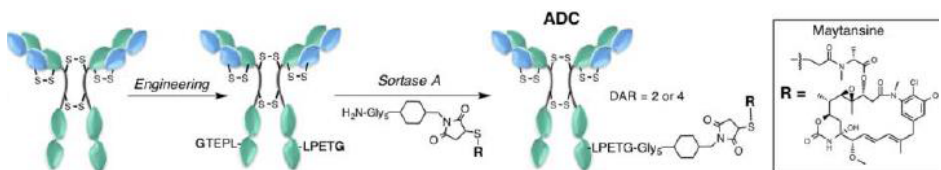


Figure 6.6. Scheme of the conjugation reaction using Sortase A. Obtained from (Jackson, 2016).

4.- **Linker-based approaches:** Site-directed conjugations can also be performed through linker-based processes. In this case, the processes are chemically driven and differ from previously described processes in that they are focused on linker modifications. The majority of this linker-based strategies use interchain cysteines for conjugation obtaining homogeneous ADCs with four or eight drug/antibody (Jackson, 2016a). These methodologies include bis-alkylating linkers (Badescu et al., 2014) and substituted maleimides (Castañeda et al., 2013), in which bifunctional linkers are used to cross-link interchain cysteines.

In this chapter, 3 different strategies for the generation of homogeneous ADC using site-directed cysteine conjugation will be applied:

- 1) Generation of a Trastuzumab ADC with an aimed DAR of 8.
 - 2) Generation of a Trastuzumab tiomab ADC with an aimed DAR of 2 by means of site-directed conjugation to an added cysteine at the 114 position.
 - 3) Generation of a Trastuzumab ADC with an aimed DAR of 2 without genetic modification: assembly and conjugation of independently produced heavy and light antibody chains.
-
1. **Trastuzumab-vcMMAE with a DAR of 8.** Trastuzumab will be conjugated to the cytotoxic drug vcMMAE using all the available cysteines of the antibody, thus, obtaining a DAR of 8. In this case, the product will not be a mixture of different ADC species as it is the case for Tzmb-vcMMAE with a DAR of 4 (see section 5.3): a product in which each antibody molecule is conjugated to 8 drug molecules will be aimed. Its conjugation strategy consists in a reduction step that reduces all the disulfide bridges of the antibody, followed by a dialyzing step in order to remove the reducing agent, and then by the

conjugation with vcMMAE and a final dialyzing step in order to remove the excess of cytotoxic drug. This conjugation will be used as a first simple way to generate an homogeneous ADC.

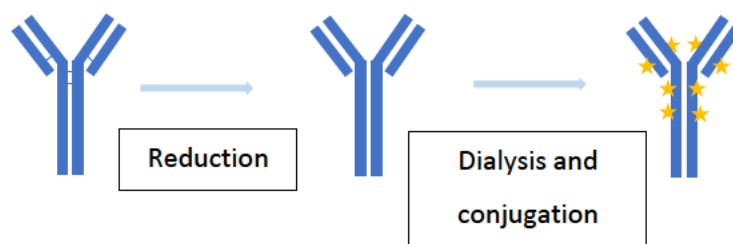


Fig 6.7. Scheme of the conjugation process for homogeneous Trastuzumab-vcMMAE with a DAR of 8.

2. **Trastuzumab thiomab with a DAR of 2.** In this strategy, the cytotoxic drug will be conjugated in a site-directed way to an added cysteine in the position 114 (Kabat numbering) of the heavy chain of the antibody. This location has been chosen since it had been reported to be an optimal conjugation site on an anti-MUC16 antibody (Junutula et al., 2008) and on Trastuzumab (Junutula et al., 2010). In this site-specific type of conjugation, a first reduction step is required in order to free the thiol group of the target cysteine from disulphide bonds formed with glutathione or other reactive thiol-containing molecules during the antibody production in cell culture (Junutula et al., 2008). This reduction step also breaks the endogen interchain disulphide bridges of the antibody. Next, a diafiltration step is needed in order to remove the mentioned glutathione and/or cysteine molecules and the excess of reducing agent, followed by a reoxidation step that rebuilds the previously broken interchain disulphide bridges of the antibody, hence allowing only the engineered cysteines as available conjugation sites (Fig 6.8).

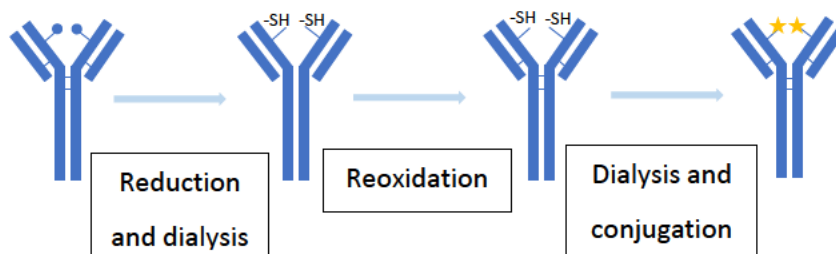


Fig 6.8. Scheme of the conjugation process for homogeneous Trastuzumab_cys114-vcMMAE with a DAR of 2.

In homogeneous cysteine-based conjugation processes, it is crucial to have a good understanding of each step of the conjugation sequence. Reduction conditions for obtaining a homogeneous thiomab conjugated ADC have been described in different cases (Bhakta et al., 2013; Junutula et al., 2008; Watkinson et al., 2017). However, there is a lack of in-depth studies of this reduction step. In this chapter, the reduction conditions that allow the obtention of a further homogeneous antibody will be analyzed. In this case, the antibody construction, production and conjugation will be carried out, with special insight being put into the reduction conditions that allow the success of the conjugation and obtention of a homogeneous ADC with a DAR of 2.

3. **Trastuzumab-vcMMAE with a DAR of 2 from independent chains.** As it has been stated, most of homogeneous generating ADC strategies rely in genetic modifications of the antibody (engineering of cysteines, addition of unnatural amino acids, tags, etc) or using complex chemistries (bis-alkylating linkers, etc). These approaches are time consuming and specific for each construct, since they often require extensive antibody engineering to identify the optimal conjugation sites (Shinmi et al., 2016; Sochaj et al.,

2015), where unique side chains can be introduced for conjugation, or they require complex linker and payload modifications that have not been clinically validated (Jain et al., 2015). As a result, they are not suitable for converting existing antibodies directly into ADCs (Jackson, 2016; Kline et al., 2015). Therefore, an alternative way to obtain homogeneous conjugates has been developed in this thesis, avoiding the genetic modification of the antibody sequence and using conventional simple linking chemistries. This has been achieved by independently producing the heavy and light chains of Trastuzumab and then selectively conjugating the interchain cysteine of the light chain to the vcMMAE cytotoxic drug (Figure 6.9), by means of a reduction step in order to free the capped cysteine of the light chain (in an analogous way to the previous Trastuzumab thiomab approach) followed by a diafiltration step in order to remove the reducing agent and by the addition of the vcMMAE cytotoxic drug. Reassembling conjugated light chains with heavy chains allowed the formation of the homogeneously conjugated ADC.

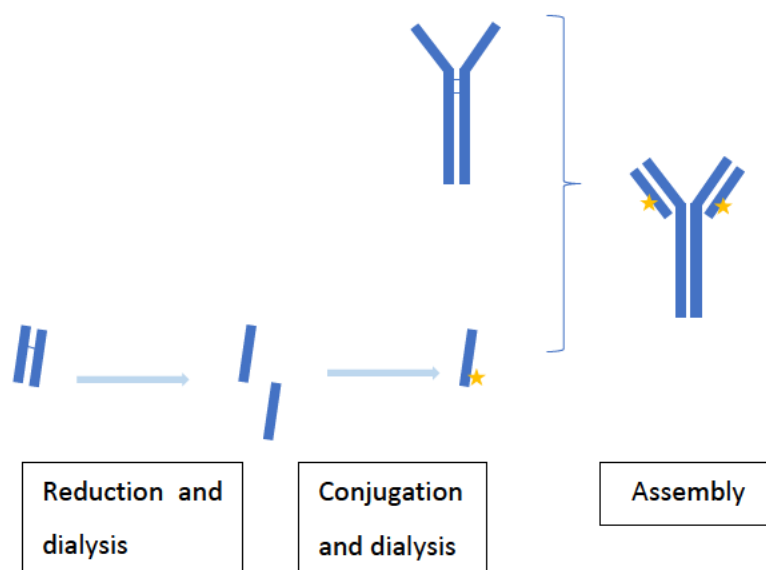


Fig 6.9. Scheme of the conjugation process for homogeneous Trastuzumab assembled from independent HC and LC with a DAR of 2.

6.2. Homogeneous conjugation of Trastuzumab with a DAR of 8:

6.2.1. Conjugation process definition

The first attempt of generating a homogeneous ADC consisted in conjugating Trastuzumab to vcMMAE with an aimed DAR of 8. The process was defined from several references, including (Doronina et al., 2003), (Francisco et al., 2003). This process consists in a first complete reduction step for 1h at 37°C in order to break all the interchain disulfide bridges of the antibody, followed by a dialysis in order to eliminate the excess reducing agent, and the conjugation with vcMMAE (1h at 4°C), quenching with cysteines and final dialysis steps. The resulting scheme can be observed at Fig. 6.10. With respect to the heterogeneous conjugation of Trastuzumab with vcMMAE with an aimed DAR of 4 (section 5.3), the main difference consists in the reduction conditions: in order to obtain a DAR of 8, all the interchain disulfide bridges need to be reduced in order to free their 8 thiols, therefore, reducing agent amount is increased. Furthermore, a dialysis step is added after the

reduction, in order to eliminate the excess reducing agent. This step is not necessary in heterogeneous conjugation, since the amount of added reducing agent (4 molar equivalents with respect to the antibody) is lower and does not interfere in the conjugation reaction.

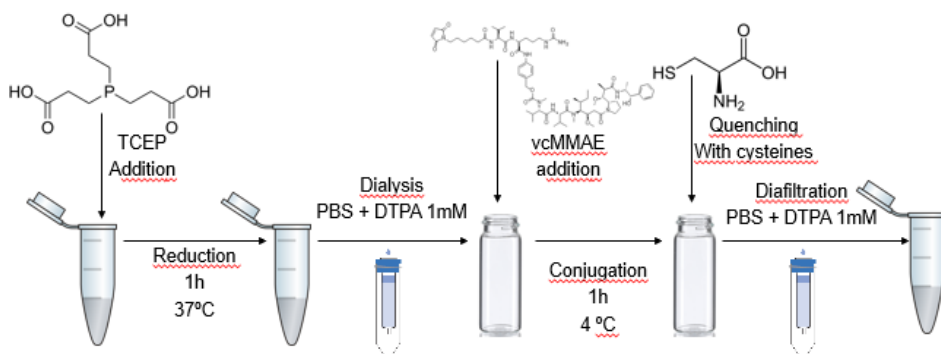


Figure 6.10: Scheme of the applied conjugation process for Trastuzumab-vcMMAE DAR 8 conjugation.

In this case, the reduction conditions were set applying the reducing agent (TCEP) at a molar proportion of 70 with respect to Trastuzumab, and after dialysis, applying vcMMAE at a 1.5 molar proportion with respect to each free thiol of the reduced Trastuzumab (same proportion than for obtaining DAR 4 Trastuzumab ADC (section 5.3.1)).

The yield of the process, regarded as the percentage of antibody recovered after each step with respect to the initial antibody, was of 47.82 +/- 6.71% for the total process. Four repetitions were also performed in this conjugation process. See section 10.10.3.1 of the Materials and methods chapter for more information of the performance of the conjugation process.

6.2.2. Physicochemical characterization of the conjugated product

Once conjugated, the product was characterized in terms of its DAR (through HIC-HPLC and MS) and its monomer content (HPLC-SEC).

The DAR obtained by HIC-HPLC corresponded to 7.3, close to the aimed DAR of 8. When analyzed by mass spectrometry (see materials and methods section 10.11.3), the obtained value was 7.7, close to the obtained value with HIC-HPLC (Figure 6.11).

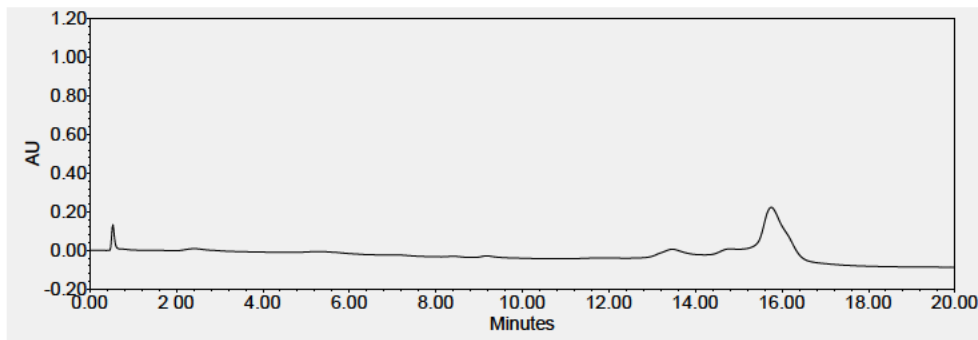


Figure 6.11: HIC-HPLC profile of obtained Trastuzumab-vcMMAE ADC.

Aggregates accounted for the 3% of the conjugated product, representing a decrease from the naked initial antibody, where the aggregates were at 5%. The reduction step applied in this conjugation process could be a possible explanation for this fact, as had already happened for Trastuzumab conjugation to vcMMAE with an aimed DAR of 4 (section 5.3.2.3). However, in this case, antibody fragments appeared in the conjugated product (5% vs 0% in the initial naked antibody), caused by the strong conditions of antibody reduction. Free drug, again, was not observed, therefore validating the clearance of the drug from the product during the post-conjugation dialysis step.

The described Trastuzumab ADC DAR 8 conjugation consists in a straightforward conjugation method, however, highly-loaded ADCs have been reported as unstable and limiting the therapeutic effect of the molecule (Hamblett et al., 2004). Therefore, the construction of alternative homogeneous ADCs, in the form of a site-directed conjugation aiming a DAR of 2 with genetically modified Trastuzumab_{cys114} is attempted in the next section.

6.3. Construction and site-directed conjugation of Trastuzumab_cys114 thiomab

One of the main strategies for site-directed conjugation consists in conjugation to added cysteines, in genetically modified antibodies (thiomabs). In this section, the construction of the thiomab Trastuzumab_cys114 and its conjugation to the cytotoxic drug vcMMAE to an aimed DAR of 2 are described.

6.3.1. Trastuzumab_cys114 construction

This section includes the construction of the Trastuzumab_cys114 antibody, going from the construction of the genetic sequences to the purification and characterization of the protein product, following the same sequence developed for Trastuzumab, explained in Chapter 3.

6.3.1.1. Genetic sequence construction and cloning

As explained in the introduction of this chapter, Trastuzumab_cys114 is a thiomab, containing an extra cysteine in the heavy chain of the antibody, in the position 114 (Kabat numbering), instead of an alanine residue (A114C mutation). Therefore, the heavy chain of the constructed Trastuzumab (see section 3.2) was modified accordingly by means of a single traditional PCR step: the reverse oligonucleotide contained the mutated codon and the KfII restriction site, which is located close to the 114 position and which was used to clone the modified sequence. The forward primer contained the BamHI restriction site. The amplified fragment, containing the mutated sequence, was cloned into a restricted pTRIpuro3_Trastuzumab vector also restricted with BamHI and KfII, generating the vector pTRIpuro3_Tcys114. The original GCC codon (Ala) was substituted by a TGC codon (Cys) (Figure 6.12). The resulting sequence is contained in Appendix I and was checked by sequencing, and the primers used, in Appendix II.

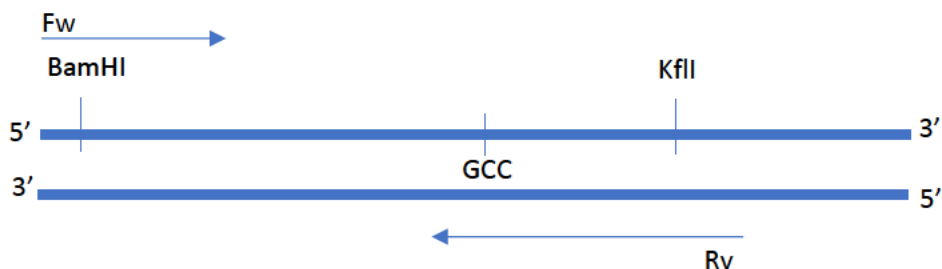


Fig. 6.12. Scheme of the modification performed for the A114C mutation on Trastuzumab heavy chain DNA sequence. Primers forward (Fw) and reverse (Rv) are indicated.

6.3.1.2. Growth curves and productions of transfected cell lines

Once constructed, pTRIpuro3_Tcys114 was transfected to HEK293 cells (see section 10.7.6), resulting in HEK293_Tcys114, and cell pools were selected with culture medium containing 10 mg/L of the eucaryotic antibiotic puromycin (see section 10.2.1.1.). Once the cell pool established, cells were transferred to 125 ml shake flasks and their growth profile and production titers were assessed, as depicted in Figure 6.14. Values of maximum cell density (MCD) of $5.96 \cdot 10^6$ cell/ml were reached, and a final concentration of 6.2 mg/L of Trastuzumab_cys114 product was obtained, with a maximum exponential growth rate of 0.0167 h^{-1} corresponding to a doubling time of 41.5 h.

The product was purified following the purification sequence developed for Trastuzumab described in Chapter 3 (Figure 6.13).



Figure 6.13. Scheme of the downstream process implemented for small scale purification of Trastuzumab_cys114.

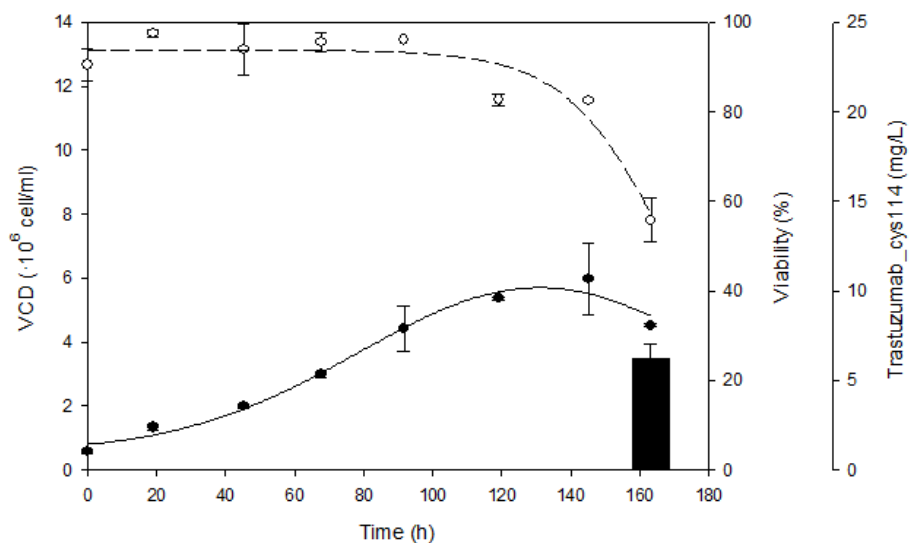


Figure 6.14. HEK293_Tcys114 growth profile and Trastuzumab_cys114 production titers in erlenmeyer culture. Error bars correspond to standard deviation of $n = 3$ replicates.

6.3.1.3. Product characterization

The obtained product was characterized in the same way as for Trastuzumab. A product with a purity higher than 99% was obtained, and it showed the same structure on a SDS-PAGE as Trastuzumab (Fig. 6.15). Its antigen recognition was also confirmed by means of an ELISA.

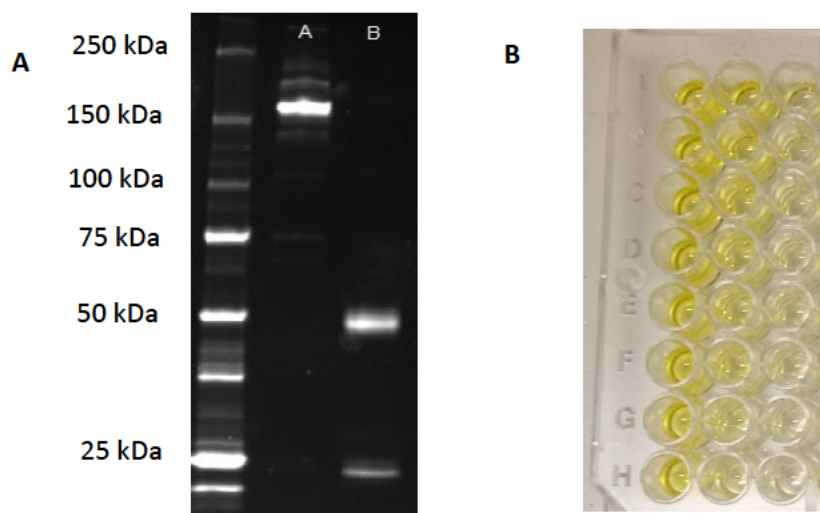


Fig. 6.15. A) SDS-PAGE of a purified Trastuzumab_cys114 sample (lane A) and the same sample reduced with β -mercaptoethanol (lane B), with the molecular weight marker at the left. B) ELISA of the produced Trastuzumab_cys114.

Bands with corresponding to a higher molecular weight than 150 kDa (weight of the antibody) appeared on the gel (lane A, Fig. 6.15). These bands could correspond to aggregates, possibly caused by some interaction of the added cysteine forming a disulfide bridge, since, in reducing conditions (lane B) these aggregates disappeared. The presence of aggregates was also observed in the SEC-HPLC profile, showing a slightly different profile than the one obtained with Trastuzumab (Fig 6.16), with monomer value of 91.7%, lower than the 98.3% obtained for Trastuzumab.

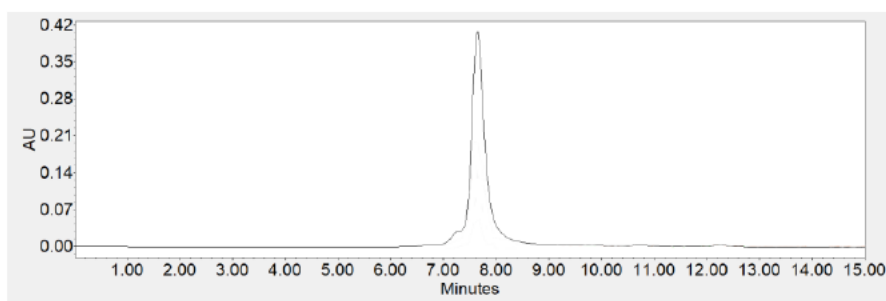


Fig 6.16. HPLC-SEC profile of a Trastuzumab_cys114 sample. The peak corresponding to the monomer can be observed at 7.6 min.

6.3.1.4. Higher scale production: wave and pilot scale bioreactor

Once characterized, a higher scale production was performed in order to have product enough for conjugation steps. As it had been the case with Trastuzumab, productions using single use devices were carried out: wave bioreactor (5L) and STR bioreactor (50L) (see material and methods: 10.4.1.1.2 and 10.4.1.1.3).

Regarding the wave bioreactor, the product was collected at 138 h, when viable cell density reached values of $5.1 \cdot 10^6$ cell/ml, close to the maximum cell density reached in the small-scale characterization culture. A product concentration of 5.6 mg/L was obtained (Fig 6.17), and Trastuzumab_cys114 was purified following the sequence implemented for the purification of the wave scale bioreactor for Trastuzumab (see section 3.4.1), obtaining a product with a purity of >99%.

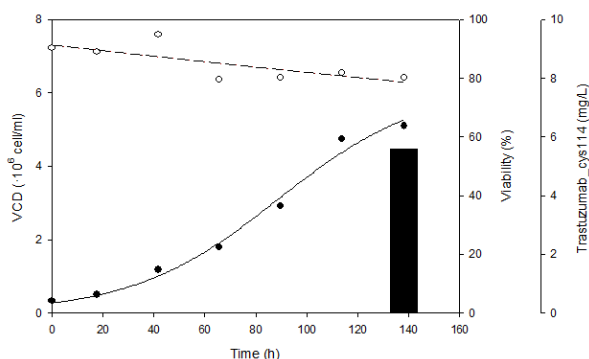


Figure 6.17. HEK293_Tcys114 growth profile and Trastuzumab_cys114 production titers in wave bioreactor culture.

A pilot scale production was also performed with the STR 50L reactor, in this case, the product was collected at 120 h, since the viable cell density had reached values of $6.9 \cdot 10^6$ cell/ml, higher than the reference cultures. In this case, 4 mg/L of Trastuzumab_cys114 were produced (Fig 6.18), a little lower than in the previous cultures, maybe associated to the faster growth of the culture. The product was purified applying the implemented sequence for Trastuzumab (see section 3.4.2),

with a recovery yield of 64% (loss of the product mainly in protein A chromatography and dialysis steps), and a purity of >99%.

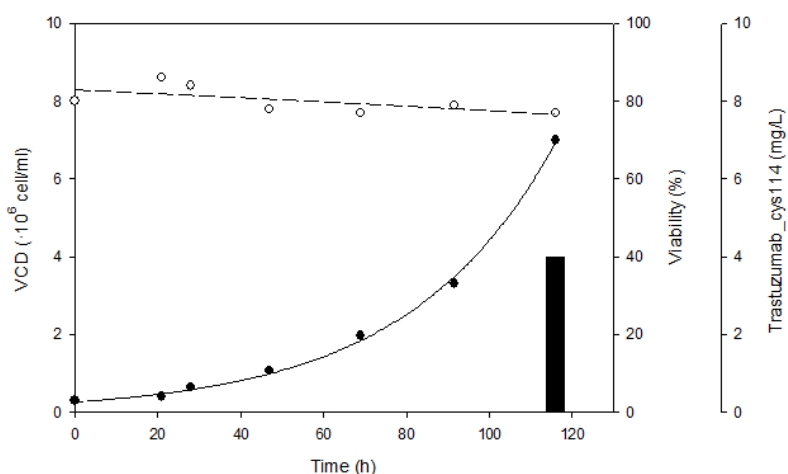


Figure 6.18. HEK293_Tcys114 growth profile and Trastuzumab_cys114 production titers in STR 50L bioreactor culture.

6.3.2. Conjugation of Trastuzumab_cys114: generation of an homogeneous thiomab ADC

Once the antibody produced, its homogeneous conjugation was attempted. As it has been stated in the introduction of this chapter, the site-directed conjugation of Trastuzumab_cys114 consists of several steps: an initial reduction in order to free the capped cys114; a dialysis step in order to eliminate the reducing agent; a reoxidation step, so interchain disulfide bridges can be rebuilt; a second dialysis in order to eliminate the reoxidating agent, and then the conjugation and final dialysis steps (Fig 6.19), based on a reference protocol developed by Junutula et al. (Junutula et al., 2008) for an anti-MUC16 antibody. In this protocol, the reduction step is set at a molar proportion of 10 with respect to the antibody and the reoxidation is carried out with dhAA (dehydroascorbic acid), added at a molar excess of 2 with respect to the previously added reducing agent.

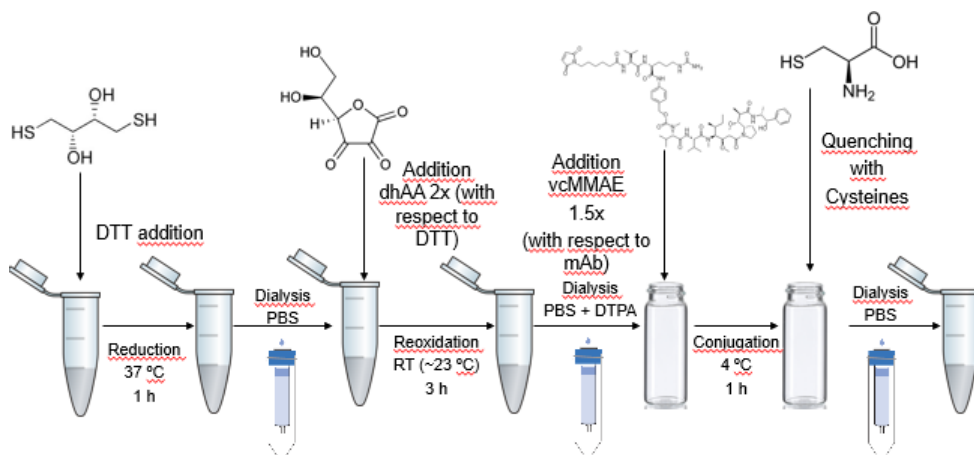


Figure 6.19: Scheme of the applied conjugation process for Trastuzumab_cys114 conjugation.

Applying this protocol, the obtained ADC product showed three different peaks when analyzed with hydrophobic chromatography (HIC-HPLC) (Figure 6.20 A). The first peak corresponds to unconjugated product (naked antibody). The two other peaks have a higher hydrophobicity and, therefore, they could correspond to conjugated fractions with a different drug load. They also could be antibody aggregates, which are more hydrophobic than the antibody monomer: in the HIC-HPLC profile (Figure 6.20 A), the peak corresponding to the aggregates of the unconjugated mAb displays the same retention time as the second peak of the ADC. However, these peaks of the ADC product were discarded to be aggregates through analysis with size-exclusion chromatography (HPLC-SEC). In a first analysis, the conjugated product presented the same profile as the non-conjugated antibody (Figure 6.20 B).

Chapter 6. Results (IV)

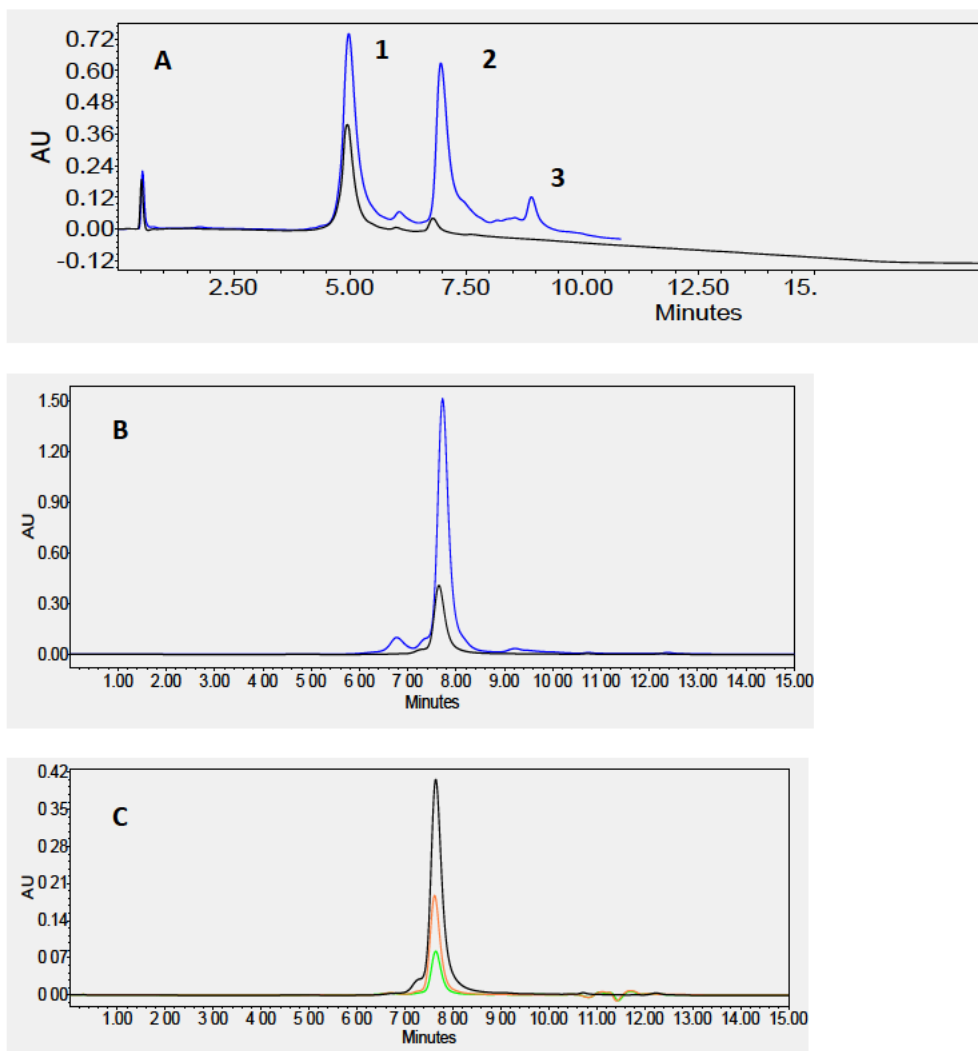


Figure 6.20: HIC profile (A) and SEC profile (B and C) of Trastuzumab_cys114 conjugated after a reduction step with 10 molar equivalents of DTT. In figures A and B, black profile corresponds to the non-conjugated mAb, whereas blue corresponds to conjugated ADC. In figure C, black corresponds to the non-conjugated mAb, orange profile corresponds to the second peak obtained in HIC-HPLC (peak 2, A) and green corresponds to the third peak obtained in HIC-HPLC (peak 3, A).

In a second analysis, the two peaks obtained in HIC-HPLC corresponding to conjugated species were collected and independently analyzed on SEC-HPLC, showing that they correspond to monomeric antibody (Figure 6.20 C). Comparing the absorbance of the conjugated fraction with the one of a control Trastuzumab-

vcMMAE with a DAR of 4, revealed that the conjugated product had a DAR lower than 4: 280/248nm absorbance proportion for Trastuzumab-vcMMAE DAR4 was 1.42, whereas for the conjugated product it was 1.87. This result supported the idea that the second peak of the conjugated T_cys114 product obtained by HIC contains one payload per antibody, whereas the third one is effectively conjugated to 2 payloads per antibody. This could be explained by an incomplete reduction of the antibody in the reduction step, meaning that some cys114 are not available for conjugation in further steps, yielding an ADC with a lower DAR than expected.

In order to increase the reduction rate of the antibody and obtaining an ADC product closer to the target DAR of 2, a screening of reduction conditions was performed, consisting in carrying out the reduction step at reducing agent/Trastuzumab_cys114 molar equivalents of 10, 15, 20, 50, 100, 150 and 200, each condition was then followed by reoxidation and conjugation to vcMMAE.

The results show that high reducing agent proportion in the reduction step, resulted in more reduced antibody (Fig 6.21).

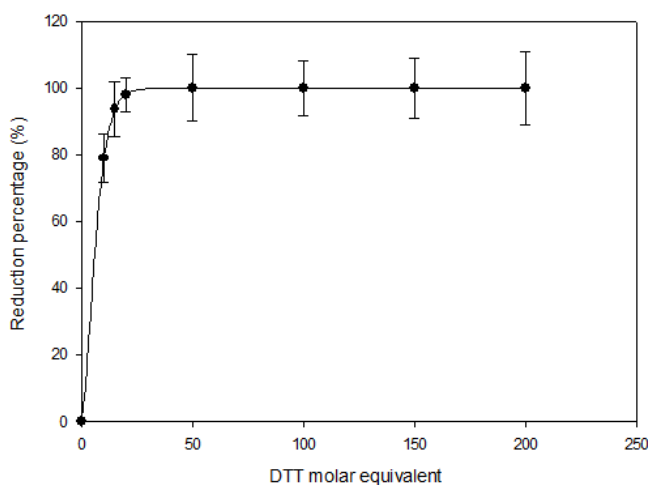


Figure 6.21: reduction percentage of Trastuzumab_cys114 reduced at different reducing agent molar proportions.

Chapter 6. Results (IV)

Consequently, the higher the reducing agent proportion in the reduction step, the lower the naked antibody and DAR 1 fraction in the product, and, thus, the proportion of the correctly conjugated fraction is higher, resulting in an almost homogeneous antibody from a molar equivalent DTT: Trastuzumab_cys114 of 50 (Figure 6.22, 6.23 and 6.24).

Interestingly, even when reduction is carried out with high reducing agent concentrations (up to 200 molar equivalents), no additional higher-loaded conjugated antibody species appear in the product (Figure 6.23), suggesting a good efficiency of the reoxidation step. The HPLC profiles show that the obtained product contains a DAR close to 2, reinforced again by comparing the 280/248nm absorbance proportion for Trastuzumab-vcMMAE DAR4 with the conjugated product, which were 1.42 and 1.69, respectively.

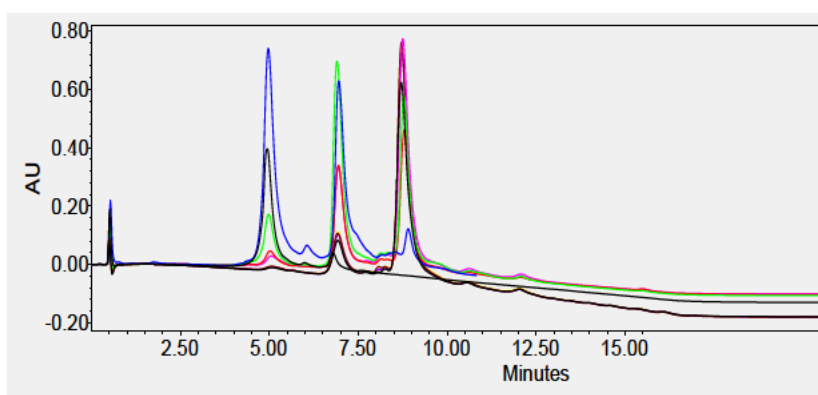


Figure 6.22: HIC profile of Trastuzumab_cys114 conjugated after reduction with different DTT concentrations. Black profile corresponds to unconjugated antibody, blue corresponds to a DTT molar equivalent with respect to the antibody of 10, green to an equivalent of 15, red to 20, pink to 50, brown to 100, violet to 150 and 200 to yellow.

Chapter 6. Results (IV)

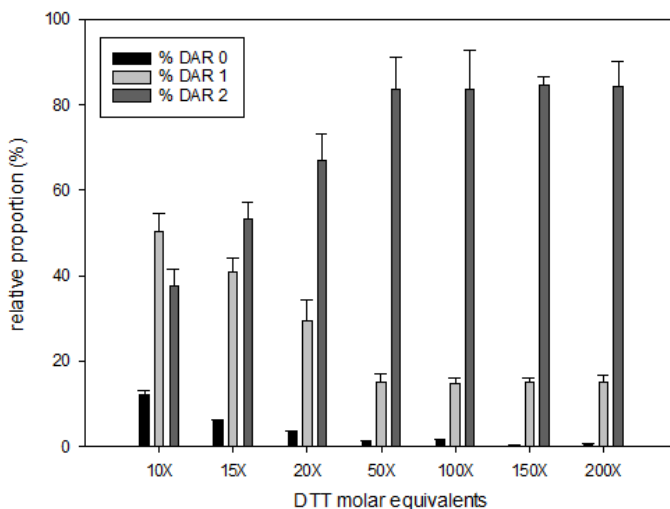


Figure 6.23: Relative proportion of each DAR species in the final conjugated T_{cys114} product after reduction with different DTT molar equivalents with respect to the antibody.

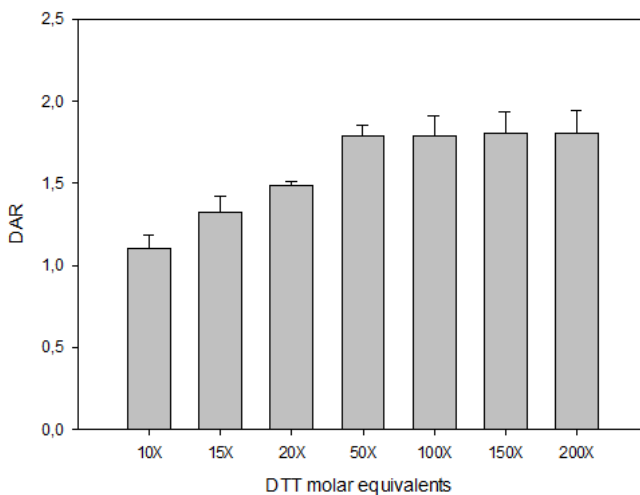


Figure 6.24: DAR obtained for each final conjugated T_{cys114} product after reduction with different DTT molar equivalents with respect to the antibody.

Therefore, from a reducing agent/mAb molar proportion of 50 or higher, a product with a DAR of 1.79-1.81 was obtained, consistent with the DAR obtained for similar thiomabs reported in the literature (Junutula et al., 2010).

Chapter 6. Results (IV)

The conjugation process described, allowing the obtention of an ADC product with a DAR close to 2, and using 5 mg of initial antibody, presented a recovery yield of 40.14 +/- 6.9%. Regarding the monomer content of the conjugated product, a monomer content of 83.48% was obtained, together with 3.25% of aggregates and 13.44% of antibody fragments. With respect to the initial antibody, it represents a lower monomer (83.48 vs 87.5%) and aggregate content (12.07 vs 3.25%), whereas fragments content increases (0.47 vs 13.44%). This behavior is very similar to the one observed for the conjugation of Trastuzumab with an aimed DAR of 8, where the aggregate content also decreases and fragments appear in the conjugated product. As in the DAR 8 case (section 6.2.2), in the Trastuzumab_cys114 conjugation, the strong reducing conditions (high reducing agent amount) applied could be an explanation for the high fragments amount appearance.

The site-directed conjugation of Trastuzumab_cys114 allowing the obtention of an ADC with a DAR close to the aimed DAR of 2 has been obtained. This method, however, relies on the genetic modification of the antibody, since a cysteine is added in the position 114 (Kabat numbering) of the heavy chain. This includes first identifying an appropriate conjugation site and then applying the genetic modification. This can result in a loss of process efficiency, therefore, a conjugation process resulting in an homogeneous ADC without needing the genetic modification of the antibody would be of great interest. A proposal of this process is described in the next section.

6.4. Construction and conjugation of an homogeneous Trastuzumab ADC without genetic modification: conjugation and assembly of independently produced heavy and light antibody chains

An alternative approach to obtaining a homogeneous ADC is described in this section, avoiding the genetic modification of the antibody sequence. This approach consists in taking advantage of the modular nature of immunoglobulins: the heavy chain and the light chain of the antibody are independently produced and purified, then the light chain is conjugated to the cytotoxic drug (vcMMAE) and heavy and light chains are reassembled in order to form the whole antibody, generating an homogeneous ADC with a DAR of 2 (Figure 6.9). The obtention of Trastuzumab antibody chains, assays of chain assembly, conjugation of the light chain and characterization of the conjugated ADC are addressed in this section.

6.4.1. Heavy and light chains sequence obtention

In order to obtain the heavy and light chains of Trastuzumab, in this section is explained from the construction of the expression vectors to the purification and characterization of the protein product, following the same sequence developed for Trastuzumab and Trastuzumab_cys114.

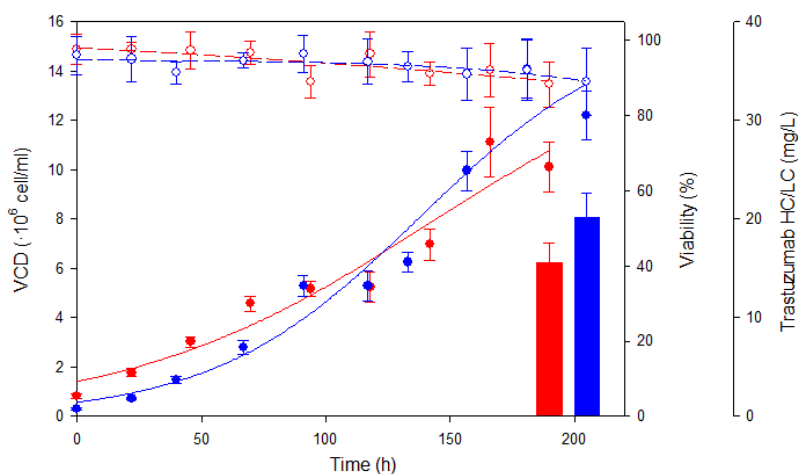
6.4.1.1. Genetic sequence construction and cloning

The DNA sequence codifying for the heavy and light chains of Trastuzumab were synthetically obtained, as explained in section 3.2. They were cloned from the original pUC57 plasmid to the bicistronic expression vectors pRESpuro3 (for HC) and pRESneo3 (LC). LC was cloned in pRESneo3 since in a previous work in our group, the simultaneous expression of HC and LC using two different plasmids had been attempted, therefore, in order to assure the selection of both plasmids, each one of them had to contain a different antibiotic resistance (cells transfected with

pIRESpuro3 are resistant to puromycin, while with pIRESneo3 are resistant to neomycin or G418 antibiotic). HC was cloned into pIRESpuro3 using the restriction sites BamHI-NotI and LC was cloned into pIRESneo3 using the sites NheI-AgeI. The cloned sequences were checked by sequencing (see section 10.7.8).

6.4.1.2. Growth curves and productions of transfected cell lines

Once constructed, pIRESpuro3_HC and pIRESneo3_LC were transfected to HEK293 cells (see section 10.7.6), resulting in HEK293_HC and HEK293_LC, respectively, and cell pools were selected with culture medium containing 10 mg/L of puromycin antibiotic or 20 mL/L of neomycin (see section 10.2.1.1.) these concentrations were selected based on previous works. Once the cell pool established, cells were transferred to 125 ml shake flasks and their growth profile and production titers were assessed, as depicted in Figure 6.25. Values of maximum cell density (MCD) of $11.12 \cdot 10^6$ cell/ml were reached for HEK293_HC, while HEK293_LC reached $14.08 \cdot 10^6$ cell/ml, and a final concentration of 15.5 mg/L of Trastuzumab_HC and 20.75 mg/L of Trastuzumab_LC products were obtained.



Chapter 6. Results (IV)

Figure 6.25. HEK293_HC (red) and HEK293_LC (blue) growth profiles and Trastuzumab HC and LC production titers in erlenmeyer culture. Error bars correspond to standard deviation of $n = 3$ replicates.

Trastuzumab's Heavy Chain was purified following the purification sequence developed for Trastuzumab described in Chapter 3, while for Light Chain, a different affinity column (Protein L column, which binds specifically to the light chain of immunoglobulins) was used (see Figure 6.26 and materials and methods section 10.8.5.1). In both cases, purities >99% were obtained.

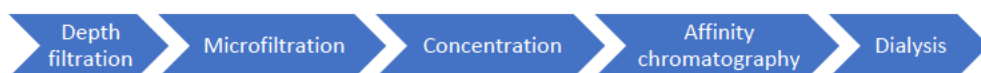


Figure 6.26. Scheme of the downstream process implemented for the wave culture purification of Trastuzumab's light and heavy chains.

However, in the case of Trastuzumab's heavy chain, precipitation was observed when the product was stored overnight at 4°C in PBS (the storage buffer that had been used for Trastuzumab). This was attributed to the fact that the isoelectric point of the heavy chain protein (7.39, calculated with Isoelectric Point Calculator software (Kozlowski, 2016)) was incompatible the pH of the PBS (7.4). Therefore, citrate buffer, at a lower pH (6) was applied in this case as storage buffer. It was also applied to light chain, in order to facilitate the subsequent assembling steps.

6.4.1.3. Product characterization

Once purified, the obtained products were characterized in terms of structure. Purified heavy chain adopted a conformation of covalently-linked dimers (referred to as double-chain heavy chain, or dcHC), as it can be seen on Figure 6.27, where a ~100 kDa band, corresponding to two linked heavy chains, appears in the SDS-PAGE gel. This structure is logical considering that in a whole IgG, the two heavy chains are linked through their interchain disulfide bridges, forming a structure on which the

Chapter 6. Results (IV)

light chains are coupled. It has also to be considered that the cysteines of the heavy chain that in a whole conventional IgG would be forming a disulfide bridge with the light chain, in this case will be capped by a thiol-containing small molecule (e.g. glutathione or cysteine), as in the case of the added cysteine of Trastuzumab_cys114 thiomab.

In the case of the light chain, unexpectedly, it appeared in the gel in the form of two bands (Figure 6.20): one of ~23 kDa, corresponding to a single light chain (representing the ~45% of the total LC product), and another of ~46 kDa, corresponding to a dimer (double chain light chain, dcLC, representing the ~55% of the total LC product).

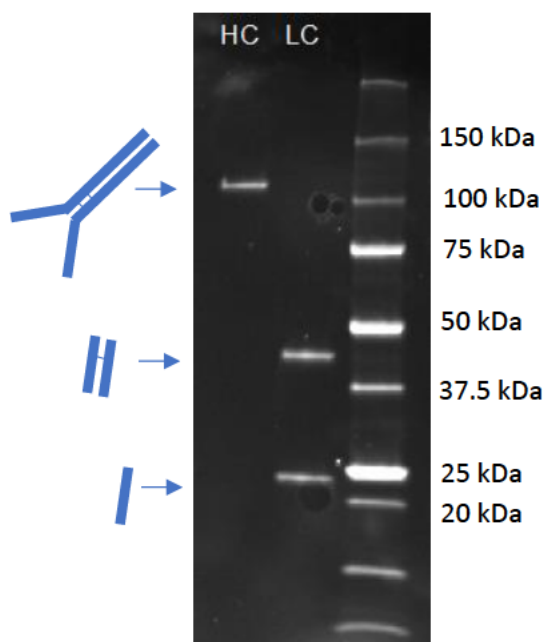


Figure 6.27. SDS-PAGE gel of HC and LC purified samples.

In a further analysis with SEC chromatography (Figure 6.28), a single main peak was obtained from the LC product, meaning that the whole LC product holds a dimer conformation, but that 45% of it (the ~23 kDa band observed in the gel) corresponds

to non-covalently linker dimers, being separated as single light chains in the denaturing conditions of the SDS-PAGE gel. The light chain presented, moreover, a 3% of aggregate proportion, which was not observed on the heavy chain.

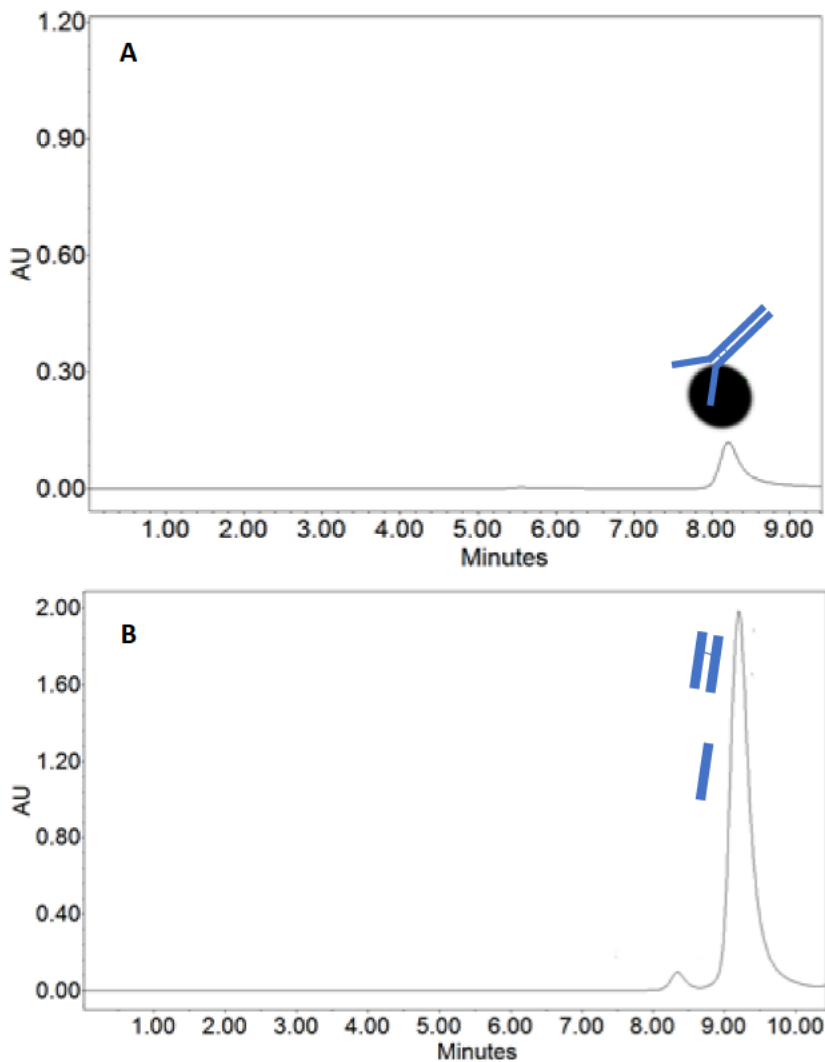


Fig 6.28. SEC chromatography profile of produced Trastuzumab heavy (A) and light chains (B).

Regarding the antigen recognition capacity of the heavy and light chains, they were unable to recognize the HER2 antigen (no signal was detected in the ELISA test), being at the same concentration range in which Trastuzumab binds to it.

6.4.2. Chains assembly assessment

In order to generate the whole Trastuzumab from the independently produced heavy and light chains, two different assembly strategies were attempted.

6.4.2.1. Reduction-oxidation assembly approach

In this approach, HC and LC were mixed at an equivalent molar proportion and were reduced in order to break the disulfide bonds of the dimers and to free the capped cysteines of HC and LC. This was followed by a dialysis step in order to remove the reducing agent (and the small thiol-containing molecules capping the cysteines residues of HC and LC), and followed by a reoxidation step allowing the reformation of the disulfide bonds, this time between both HC-HC and HC-LC, enabling the obtention of a whole reassembled IgG (see section 10.10.3.3.1.1. of materials and methods) (Fig 6.29).

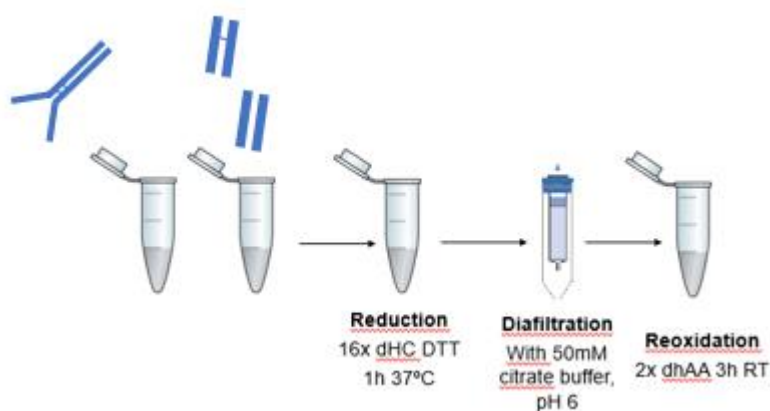


Fig 6.29. Scheme of reduction-oxidation chain assembly approach.

With this approach, a 73% of reassembled IgG could be obtained (see Table 6.1 on next section), which was able to recognize the HER2 antigen, unlike isolated HC or LC (Table 6.1).

6.4.2.2. Spontaneous approach chain assembly

In parallel to the reduction-oxidation approach, a simpler strategy was tested, based on mixing HC and LC in a molar equivalent proportion and maintaining them for 3h at room temperature. Applying this method, no disulfide bonds were generated, but the IgG structure was formed by non-covalent interactions, since SEC-HPLC confirmed the presence of 85,3% of monomer (Table 6.1); moreover, removing disulfide bonds from an antibody has been reported not to affect its functions ((Andersen et al., 2004). This higher monomer proportion with respect to the previous reduction-oxidation method was due to the lower proportion of non-assembled HC and LC present in the final product: only residual dcHC was detected (Table 6.1).

Table 6.1 Molecules detected under native conditions on HPLC-SEC

Isolation method	Aggregates (% area)	Monomer mAb (% area)	dcHC (% area)	dcLC (% area)
Reduction-oxidation	2.1	73.0	14.5	10.4
Spontaneous assembly	8.0	85.3	6.7	n.d.

Table 6.2 Isolated antigen HER2 recognition in ELISA test

	dcLC	dcHC	<i>In vitro</i> reassembled Trastuzumab	<i>In vitro</i> reassembled Trastuzumab	Control Trastuzumab

			(red-ox approach)	(spontaneous approach)	
Isolated					
HER2 antigen recognition	-	-	+	+	+

The resulting product recognized isolated HER2 antigen in an ELISA assay in the same efficiency as produced Trastuzumab (Table 6.2). Since this method was simpler and more efficient than the previous reduction-oxidation approach, it was selected as the preferred antibody chains assembly strategy.

6.4.3. Conjugation of the light chain and assembly of the ADC

6.4.3.1. Conjugation process definition on the light chain

Once a strategy for the assembly of the chains had been successfully achieved, the conjugation of the light chain was attempted as a first step for the generation of the homogeneous ADC. The conjugation process consisted in a complete reduction of the antibody (using TCEP) in order to free and render available for conjugation the thiol group of the light chain, which was occupied either forming a disulfide bridge in covalently bonded dcLC, or being capped with thiol-containing small molecules in non-covalently bonded dcLC (in the same way than for Trastuzumab_cys114 thiomab). The reduction agent was then removed by dialyzing, then vcMMAE was added and then a second dialyzing step to eliminate the unconjugated drug was carried out (see Figure 6.30, and materials and methods section 10.10.3.3.1).

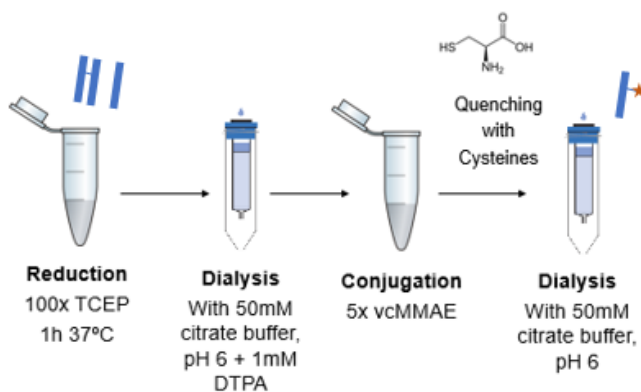


Fig 6.30. Scheme of the conjugation process of LC-vcMMAE.

In order to ensure the complete reduction of the light chain in the first step of the process, several reducing agent concentrations were tested, with a molar equivalent TCEP:LC of 100 resulting in the TCEP amount that ensured this reduction levels (Fig 6.31).

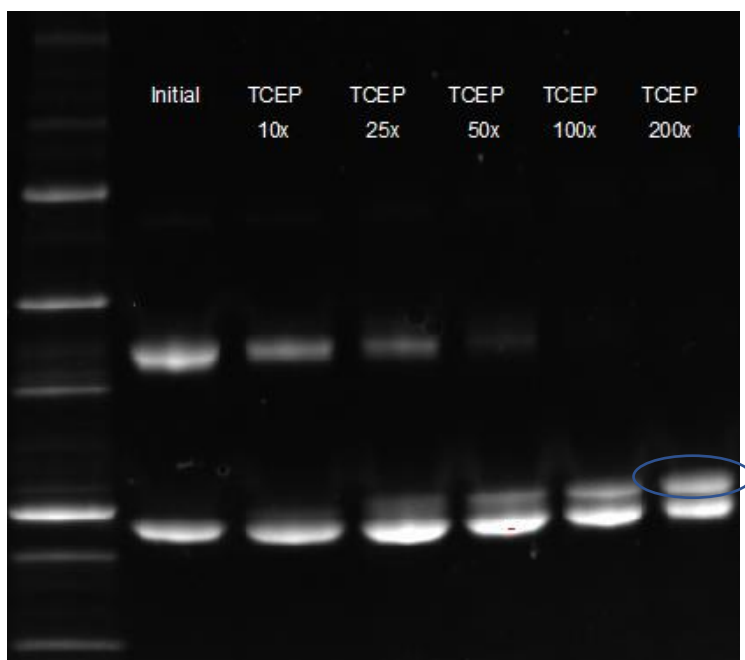


Figure 6.31: SDS-PAGE of LC reduced at 0, 10, 25, 50, 50, 100, 150 and 200 TCEP:LC molar proportion. The band that appears above scLC band at higher reducing agent concentrations

(circled in blue in the figure) corresponds to LC with internal disulfide bridges reduced. The reduction of the internal disulfide bridge, despite not interfering with the conjugation process nor the activity of the LC, causes a shift in the band migration in SDS-PAGE gels (Gaciarz et al., 2016).

6.4.3.2. Characterization of the conjugated LC-vcMMAE

The LC conjugation was assessed by HIC-HPLC, showing that a single peak with higher hydrophobicity levels was obtained, corresponding to the conjugated LC (Figure 6.32), revealing a successful conjugation of LC to vcMMAE with an efficiency close to 100%.

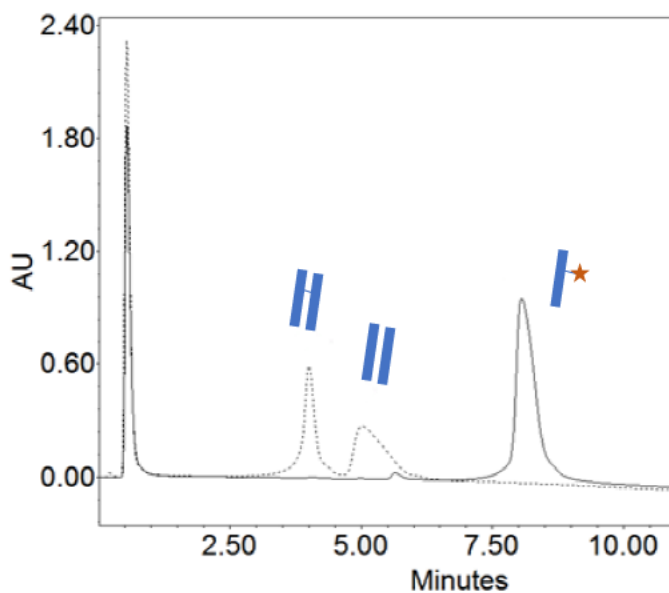


Fig 6.32. HIC-HPLC profile of naked (unconjugated) LC with its two double chain forms (discontinuous line) and LC-vcMMAE (continuous line).

The conjugation of the LC was also analyzed by mass spectrometry (by LSMBO, *Université de Strasbourg*), which confirmed the proper conjugation of each LC to 1 molecule of vcMMAE (Fig 6.33), mostly forming dimers.

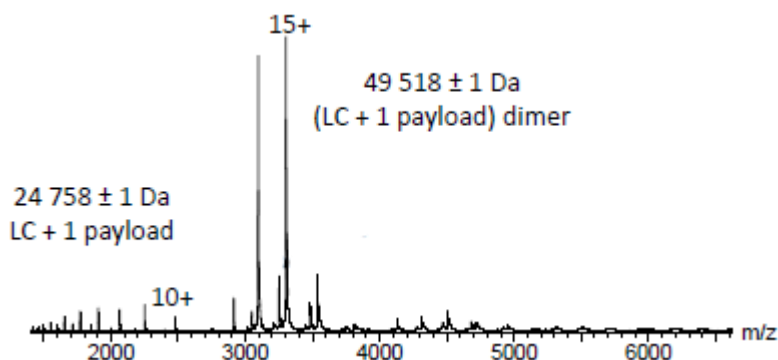


Fig 6.33. Deconvoluted MS spectrum of conjugated LC-vcMMAE.

The conjugated LC-vcMMAE did not present aggregates (Fig 6.34), following the trend of lowering aggregates amount observed for Trastuzumab-vcMMAE conjugations at different DARs (sections 5.3.2.3. and 6.2.2.).

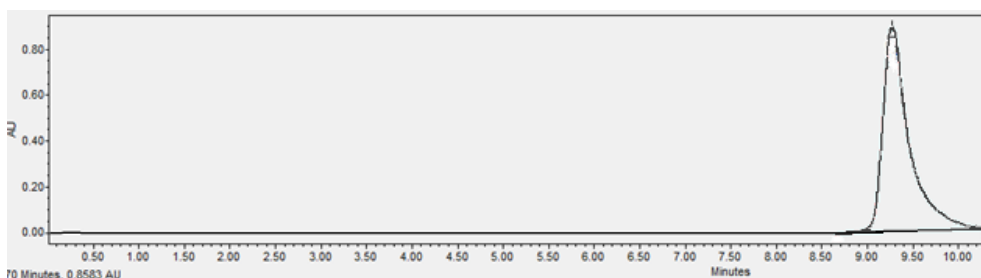


Fig 6.34. SEC-HPLC profile of LC-vcMMAE, in which a single peak is obtained.

6.4.3.3. ADC reassembly and characterization

The next step consisted in the reassembly of the conjugated LC-vcMMAE with dcHC in order to construct the whole ADC. The previously developed spontaneous assembly strategy was applied, and the obtained ADC was characterized in terms of aggregate content and DAR. In terms of aggregate content, the obtained ADC presented a 4.75% of aggregates, slightly higher than the initial 3.3% observed for the reassembled mAb using dcLC (non-conjugated). Since in this case the dcHC,

which contain the initial aggregates, have not been reduced, aggregates of the whole reassembled ADC are not lowered with respect to the unconjugated reassembled non-conjugated antibody.

DAR was then assessed first through a HIC-HPLC analysis, which showed a single peak for the reassembled conjugated ADC (Fig 6.35), implying the obtention of a DAR of 2 and consistent with the previous assessment of the conjugation of LC-vcMMAE.

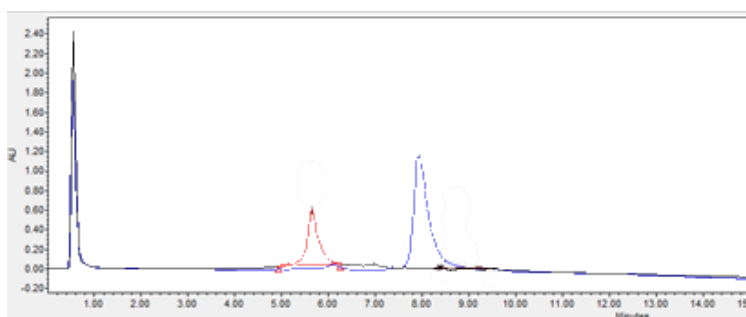


Fig 6.35. HIC-HPLC profile of the reassembled Trastuzumab-vcMMAE ADC (blue) overlapped with the reassembled non-conjugated Trastuzumab (red)

In order to confirm the DAR of the generated ADC more precisely, an analysis with mass spectrometry was performed (again at LSMBO, *Université de Strasbourg*, as in the previous case (see section 5.2.2.1)). The MS assay confirmed again the DAR of the obtained product (Fig 6.36), which contained only the DAR 2 specie, being completely homogeneous. Traces of 100 kDa molecules, corresponding to dcHC, were also found in the product, consistent with the fact that no previous purification of the assembled ADC with protein L affinity chromatography had been performed.

Chapter 6. Results (IV)

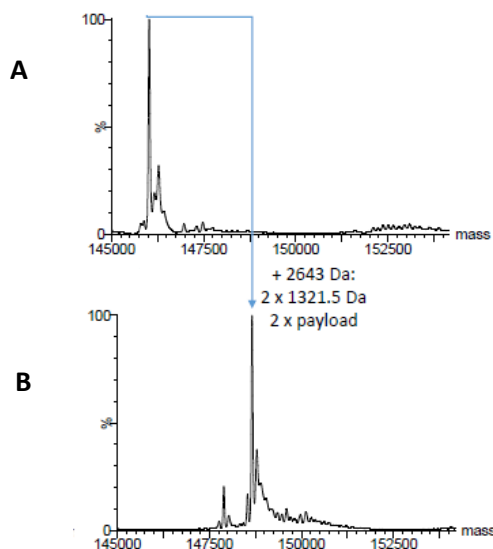


Fig 6.36. Deconvoluted MS spectrum of reassembled non-conjugated Trastuzumab (A) and reassembled conjugated Trastuzumab ADC (B).

The mass spectrometry analysis confirmed the obtention of a homogeneous ADC with a DAR of 2.0, completely avoiding antibody species of DAR 0 or 1, which are found in many other homogeneous ADCs aiming at a DAR of 2 and obtained through conventional strategies, as already seen in thiomab conjugation.

In this conjugation strategy, a DAR of 2 has been aimed and successfully obtained. Alternatively, other DARs could be achieved through a different conjugation approach: in order to obtain a DAR of 6, instead of conjugating the light chain, all the thiol groups of the heavy chain could be conjugated. A DAR of 4 could be achieved by reducing all the disulfide bridges of the heavy chains and then reoxidating them: this would result in only one thiol group of the heavy chains, the one linking the heavy chain with light chain in a conventional antibody, available for conjugation. Assembling this single heavy chain conjugated to one cytotoxic drug with a light chain conjugated to one cytotoxic drug would result in a DAR of 4. Moreover, applying this strategy, different drugs could be conjugated, combined in a controlled way, for example, 2 vcMMAE molecules could be conjugated to the light chain, and 2 molecules of another cytotoxic drug could be conjugated to the heavy chains.

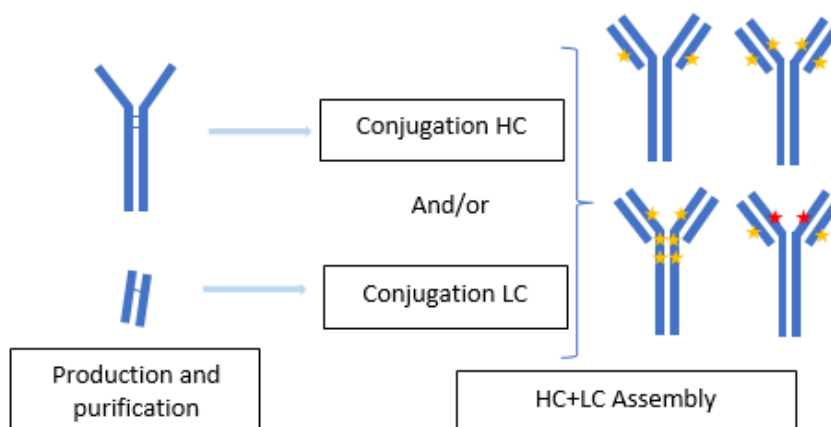


Fig 6.37. Scheme of the conjugation process for homogeneous Trastuzumab assembled from independent HC and LC with DARs of 2, 4 and 6.

6.5. Conclusions

In this chapter, different strategies for an homogeneous conjugation of Trastuzumab have been attempted and successfully achieved. In a first approach, Trastuzumab has been conjugated to vcMMAE with a DAR of 8: the cytotoxic drug has been conjugated to all available reactive thiol groups of the antibody. This has been achieved through a first reduction step with high reducing agent concentration, obtaining a product with a DAR of 7.7 (analyzed by mass spectrometry), and containing fragments.

Another homogeneous ADC was generated through engineered cysteines based on the thiomab approach, with an aimed DAR of 2. In this case, mild reduction conditions resulted in a non-homogeneous product, due to an incomplete reduction of the antibody. Complete conjugation was achieved when the molar equivalent of the reducing agent with respect to the antibody was increased to 50. A product with a DAR of 1.79 was obtained, consistent with the DAR obtained for similar thiomabs reported in the literature (Junutula et al., 2010). Here we have shown that the antibody reduction step is critical and the reducing agent molar equivalent with

respect to the antibody must be correctly adjusted in order to obtain the desired ADC product.

Finally, an alternative homogeneous strategy was developed, which avoided genetically modifying the amino acids sequence of the antibody. This was achieved by independently producing heavy and light chains, then conjugating the light chain of the antibody and finally assembling heavy and light chains, forming a whole antibody, with an aimed DAR of 2. A straightforward reassembly approach consisting in mixing heavy and light chains in a citrate buffer allowed obtaining a whole reassembled antibody. The conjugation of the light chain required a reduction step with high reducing agent concentrations. The resulting ADC displayed a DAR of 2.0, consistent with the aimed DAR, and therefore obtaining a more homogeneous product than the reference thiomab system. This method for generating homogeneous ADCs could be applied to other existing antibodies.

The *in vitro* antiproliferative activity of the different homogeneous ADCs described in this chapter will be assessed and compared later in this work, and in the case of the homogeneous ADC obtained through reassembly method, its *in vivo* activity will also be analyzed (see Chapter 8).

6.6. References

- Andersen, D. C., & Reilly, D. E. (2004). Production technologies for monoclonal antibodies and their fragments. *Current Opinion in Biotechnology*, *15*(5), 456–462. <https://doi.org/10.1016/j.copbio.2004.08.002>
- Axup, J. Y., Bajjuri, K. M., Ritland, M., Hutchins, B. M., Kim, C. H., Kazane, S. A., ... Schultz, P. G. (2012). Synthesis of site-specific antibody-drug conjugates using unnatural amino acids. *Proceedings of the National Academy of Sciences*, *109*(40), 16101–16106. <https://doi.org/10.1073/pnas.1211023109>

Chapter 6. Results (IV)

- Badescu, G., Bryant, P., Swierkosz, J., Khayrzad, F., Pawlisz, E., Farys, M., ... Godwin, A. (2014). A New Reagent for Stable Thiol-Specific Conjugation. *Bioconjugate Chemistry*, *25*(3), 460–469. <https://doi.org/10.1021/bc400245v>
- Beck, A., Goetsch, L., Dumontet, C., & Corvaia, N. (2017). Strategies and challenges for the next generation of antibody–drug conjugates. *Nature Reviews Drug Discovery*, *16*(5), 315–337. <https://doi.org/10.1038/nrd.2016.268>
- Beerli, R. R., Hell, T., Merkel, A. S., & Grawunder, U. (2015). Sortase Enzyme-Mediated Generation of Site-Specifically Conjugated Antibody Drug Conjugates with High In Vitro and In Vivo Potency. *PLOS ONE*, *10*(7), e0131177. <https://doi.org/10.1371/journal.pone.0131177>
- Bhakta, S., Raab, H., & Junutula, J. R. (2013). Engineering THIOMABs for Site-Specific Conjugation of Thiol-Reactive Linkers. In *Methods in molecular biology (Clifton, N.J.)* (Vol. 1045, pp. 189–203). https://doi.org/10.1007/978-1-62703-541-5_11
- Boeggeman, E., Ramakrishnan, B., Pasek, M., Manzoni, M., Puri, A., Loomis, K. H., ... Qasba, P. K. (2009). Site Specific Conjugation of Fluoroprobes to the Remodeled Fc N-Glycans of Monoclonal Antibodies Using Mutant Glycosyltransferases: Application for Cell Surface Antigen Detection. *Bioconjugate Chemistry*, *20*(6), 1228–1236. <https://doi.org/10.1021/bc900103p>
- Caban, K., & Copeland, P. R. (2006). Size matters: a view of selenocysteine incorporation from the ribosome. *Cellular and Molecular Life Sciences*, *63*(1), 73–81. <https://doi.org/10.1007/s00018-005-5402-y>
- Cai, Q., Hanson, J. A., Steiner, A. R., Tran, C., Masikat, M. R., Chen, R., ... Yin, G. (2015). A Simplified and Robust Protocol for Immunoglobulin Expression in Escherichia coli Cell-Free Protein Synthesis Systems. <https://doi.org/10.1002/btpr.2082>
- Castañeda, L., Maruani, A., Schumacher, F. F., Miranda, E., Chudasama, V., Chester, K. A., ... Caddick, S. (2013). Acid-cleavable thiomaleamic acid linker for

homogeneous antibody-drug conjugation. *Chemical Communications (Cambridge, England)*, 49(74), 8187–8189.
<https://doi.org/10.1039/c3cc45220d>

Dennler, P., Chiotellis, A., Fischer, E., Brégeon, D., Belmant, C., Gauthier, L., ... Schibli, R. (2014). Transglutaminase-Based Chemo-Enzymatic Conjugation Approach Yields Homogeneous Antibody–Drug Conjugates. *Bioconjugate Chemistry*, 25(3), 569–578. <https://doi.org/10.1021/bc400574z>

Doronina, S. O., Toki, B. E., Torgov, M. Y., Mendelsohn, B. A., Cerveny, C. G., Chace, D. F., ... Senter, P. D. (2003). Development of potent monoclonal antibody auristatin conjugates for cancer therapy. *Nature Biotechnology*, 21(7), 778–784. <https://doi.org/10.1038/nbt832>

Farias, S. E., Strop, P., Delaria, K., Galindo Casas, M., Dorywalska, M., Shelton, D. L., ... Rajpal, A. (2014). Mass Spectrometric Characterization of Transglutaminase Based Site-Specific Antibody–Drug Conjugates. *Bioconjugate Chemistry*, 25(2), 240–250. <https://doi.org/10.1021/bc4003794>

Francisco, J. A., Cerveny, C. G., Meyer, D. L., Mixan, B. J., Klussman, K., Chace, D. F., ... Wahl, A. F. (2003). cAC10-vcMMAE , an anti-CD30 – monomethyl auristatin E conjugate with potent and selective antitumor activity, 102(4), 1458–1465. <https://doi.org/10.1182/blood-2003-01-0039>.The

Gaciarz, A., Veijola, J., Uchida, Y., Saaranen, M. J., Wang, C., Hörkö, S., & Ruddock, L. W. (2016). Systematic screening of soluble expression of antibody fragments in the cytoplasm of *E. coli*. *Microbial Cell Factories*, 15(1), 22. <https://doi.org/10.1186/s12934-016-0419-5>

Hamblett, K. J., Senter, P. D., Chace, D. F., Sun, M. M. C., Lenox, J., Cerveny, C. G., ... Francisco, J. A. (2004). Effects of Drug Loading on the Antitumor Activity of a Monoclonal Antibody Drug Conjugate. *Clinical Cancer Research*, 10(20), 7063–7070. <https://doi.org/10.1158/1078-0432.CCR-04-0789>

Chapter 6. Results (IV)

- Hofer, T., Skeffington, L. R., Chapman, C. M., & Rader, C. (2009). Molecularly Defined Antibody Conjugation through a Selenocysteine Interface. *Biochemistry*, 48(50), 12047–12057. <https://doi.org/10.1021/bi901744t>
- Jackson, D. Y. (2016). Processes for Constructing Homogeneous Antibody Drug Conjugates. *Organic Process Research & Development*, 20(5), 852–866. <https://doi.org/10.1021/acs.oprd.6b00067>
- Jain, N., Smith, S. W., Ghone, S., & Tomczuk, B. (2015). Current ADC Linker Chemistry. *Pharmaceutical Research*, 32(11), 3526–3540. <https://doi.org/10.1007/s11095-015-1657-7>
- Junutula, J. R., Bhakta, S., Raab, H., Ervin, K. E., Eigenbrot, C., Vandlen, R., ... Lowman, H. B. (2008). Rapid identification of reactive cysteine residues for site-specific labeling of antibody-Fabs. *Journal of Immunological Methods*, 332(1–2), 41–52. <https://doi.org/10.1016/J.JIM.2007.12.011>
- Junutula, J. R., Flagella, K. M., Graham, R. A., Parsons, K. L., Ha, E., Raab, H., ... Sliwkowski, M. X. (2010). Engineered Thio-Trastuzumab-DM1 Conjugate with an Improved Therapeutic Index to Target Human Epidermal Growth Factor Receptor 2-Positive Breast Cancer. *Clinical Cancer Research*, 16(19), 4769–4778. <https://doi.org/10.1158/1078-0432.CCR-10-0987>
- Junutula, J. R., Raab, H., Clark, S., Bhakta, S., Leipold, D. D., Weir, S., ... Mallet, W. (2008). Site-specific conjugation of a cytotoxic drug to an antibody improves the therapeutic index. *Nature Biotechnology*, 26(8), 925–932. <https://doi.org/10.1038/nbt.1480>
- Junutula, J. R., Raab, H., Clark, S., Bhakta, S., Leipold, D. D., Weir, S., ... Mallet, W. (2008). Site-specific conjugation of a cytotoxic drug to an antibody improves the therapeutic index. *Nature Biotechnology*, 26(8), 925–932. <https://doi.org/10.1038/nbt.1480>

Chapter 6. Results (IV)

- Kline, T., Steiner, A. R., Penta, K., Sato, A. K., Hallam, T. J., & Yin, G. (2015). Methods to Make Homogenous Antibody Drug Conjugates. *Pharmaceutical Research*, 32(11), 3480–3493. <https://doi.org/10.1007/s11095-014-1596-8>
- Kozlowski, L. P. (2016). IPC-Isoelectric Point Calculator. *Biology Direct*. <https://doi.org/10.1186/s13062-016-0159-9>
- Krall, N., da Cruz, F. P., Boutureira, O., & Bernardes, G. J. L. (2016). Site-selective protein-modification chemistry for basic biology and drug development. *Nature Chemistry*, 8(2), 103–113. <https://doi.org/10.1038/nchem.2393>
- Liu, W., Brock, A., Chen, S., Chen, S., & Schultz, P. G. (2007). Genetic incorporation of unnatural amino acids into proteins in mammalian cells. *Nature Methods*, 4(3), 239–244. <https://doi.org/10.1038/nmeth1016>
- McDonagh, C. F., Turcott, E., Westendorf, L., Webster, J. B., Alley, S. C., Kim, K., ... Carter, P. (2006). Engineered antibody-drug conjugates with defined sites and stoichiometries of drug attachment. *Protein Engineering Design and Selection*, 19(7), 299–307. <https://doi.org/10.1093/protein/gzl013>
- Nejadmoghaddam, M.-R., Minai-Tehrani, A., Ghahremanzadeh, R., Mahmoudi, M., Dinarvand, R., & Zarnani, A.-H. (2019). Antibody-Drug Conjugates: Possibilities and Challenges. *Avicenna Journal of Medical Biotechnology*, 11(1), 3–23. Retrieved from <http://www.ncbi.nlm.nih.gov/pubmed/30800238>
- Panowski, S., Bhakta, S., Raab, H., Polakis, P., & Junutula, J. R. (2014). Site-specific antibody drug conjugates for cancer therapy. *MAbs*, 6(1), 34–45. <https://doi.org/10.4161/mabs.27022>
- Rabuka, D., Rush, J. S., deHart, G. W., Wu, P., & Bertozzi, C. R. (2012). Site-specific chemical protein conjugation using genetically encoded aldehyde tags. *Nature Protocols*, 7(6), 1052–1067. <https://doi.org/10.1038/nprot.2012.045>
- Ramakrishnan, B., & Qasba, P. K. (2002). Structure-based design of beta 1,4-

- galactosyltransferase I (beta 4Gal-T1) with equally efficient N-acetylgalactosaminyltransferase activity: point mutation broadens beta 4Gal-T1 donor specificity. *The Journal of Biological Chemistry*, 277(23), 20833–20839. <https://doi.org/10.1074/jbc.M111183200>
- Shinmi, D., Taguchi, E., Iwano, J., Yamaguchi, T., Masuda, K., Enokizono, J., & Shiraishi, Y. (2016). One-Step Conjugation Method for Site-Specific Antibody–Drug Conjugates through Reactive Cysteine-Engineered Antibodies. *Bioconjugate Chemistry*, 27(5), 1324–1331. <https://doi.org/10.1021/acs.bioconjchem.6b00133>
- Sochaj, A. M., Świdarska, K. W., & Otlewski, J. (2015a). Current methods for the synthesis of homogeneous antibody-drug conjugates. *Biotechnology Advances*, 33(6), 775–784. <https://doi.org/10.1016/j.biotechadv.2015.05.001>
- Sochaj, A. M., Świdarska, K. W., & Otlewski, J. (2015b). Current methods for the synthesis of homogeneous antibody–drug conjugates. *Biotechnology Advances*, 33(6), 775–784. <https://doi.org/10.1016/j.biotechadv.2015.05.001>
- Strop, P., Liu, S.-H., Dorywalska, M., Delaria, K., Dushin, R. G., Tran, T.-T., ... Rajpal, A. (2013). Location Matters: Site of Conjugation Modulates Stability and Pharmacokinetics of Antibody Drug Conjugates. *Chemistry & Biology*, 20(2), 161–167. <https://doi.org/10.1016/j.chembiol.2013.01.010>
- Vollmar, B. S., Wei, B., Ohri, R., Zhou, J., He, J., Yu, S.-F., ... Erickson, H. K. (2017). Attachment Site Cysteine Thiol pK_a Is a Key Driver for Site-Dependent Stability of THIOMAB Antibody–Drug Conjugates. *Bioconjugate Chemistry*, 28(10), 2538–2548. <https://doi.org/10.1021/acs.bioconjchem.7b00365>
- Wang, L., Zhang, Z., Brock, A., & Schultz, P. G. (2003). Addition of the keto functional group to the genetic code of Escherichia coli. *Proceedings of the National Academy of Sciences*, 100(1), 56–61. <https://doi.org/10.1073/pnas.0234824100>

Chapter 6. Results (IV)

- Watkinson, A., Trapp, A., Koehn, J., Mckee, C., & Stimpson, W. (2017). Antibody-Drug Conjugates Fast-Track Development from Gene to Product. *Bioprocess International*, *15*(10), 24–33. Retrieved from <https://bioprocessintl.com/wp-content/uploads/2017/11/15-10-Watkinson.pdf>
- Zimmerman, E. S., Heibeck, T. H., Gill, A., Li, X., Murray, C. J., Madlansacay, M. R., ... Sato, A. K. (2014). Production of Site-Specific Antibody–Drug Conjugates Using Optimized Non-Natural Amino Acids in a Cell-Free Expression System. *Bioconjugate Chemistry*, *25*(2), 351–361. <https://doi.org/10.1021/bc400490z>

Chapter 7. Results (V): Generation and conjugation of antibody fragments based on Trastuzumab

7.1. Introduction

In this work, several ADCs have been generated through heterogeneous and homogeneous approaches, using different variants of a whole Trastuzumab antibody (chapters 5 and 6).

To date, all ADCs that are in clinical trial are based on whole antibodies, which display an elevated half-life in circulation (1-2 weeks), due to the interaction of their constant fraction (Fc) with the FcRn receptors (Hess et al., 2014). This constant fraction is also able to activate the antibody-derived immune response antibody-dependent cellular cytotoxicity (ADCC) and complement-dependent cytotoxicity (CDC) (Stern et al., 2005) (see section 1.2.1.). However, differently to other antibody-based therapies, these activities are not considered essential for the therapeutic effect of ADCs. However, the Fc fraction can also cause other interactions with Fc receptors expressed by some immune cells (Hess et al., 2014), leading to potential harmful effects. Moreover, the whole IgG format can also impair the extravasation and tumor penetration rates of ADCs (Yokota et al., 1992).

Therefore, antibody fragments lacking the Fc fraction are being considered for therapeutic use, since they could extravasate with more efficiency and display a faster blood clearance from non-disease organs, reducing systemic toxicities (Hess et al., 2014) and resulting in improved biodistribution profiles (Schmidt et al., 2009). Several formats of fragments for antibody conjugation can be used, including from Fab (Fragment antigen binding), to single chain fragments including scFv (single chain fragment variable) and other derivatives such as domain antibodies or scFv dimers (Figure 7.1).

Approved fragments in the market include Lucentis[®] (Ranibizumab), which consists in a Fab derived from an humanized IgG1, targeting the vascular endothelial growth factor; Cimzia[®] (Certolizumab pegol), which also consists in a Fab from humanized IgG, targeting tumor necrosis factor alpha; and Praxbind[®] (Idarucizumab), consisting in a human Fab that targets dabigatran, an anticoagulating agent; and Blicynto[®] (Bevacizumab) a bivalent scFv dimer that targets both the antigen CD19 present in lymphoblastic leukaemia-lymphoma and the CD3 antigen present in T lymphocytes (Animal Cell Technology Industrial Platform, 2017). However, there are no therapeutic fragment conjugates currently approved.

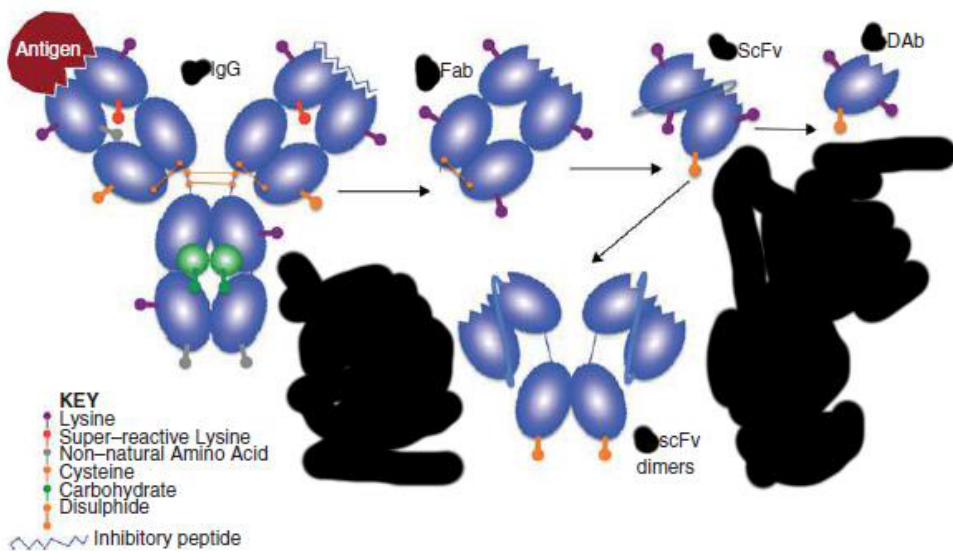


Fig 7.1. Whole IgG and several fragment formats. DAb: domain antibody. Adapted from (Deonarain et al., 2015).

One of the most employed fragments in clinical trials and used in other studies are scFv, which consist in a fusion protein in which the variable region of the light chain (V_L) and the variable region of the heavy chain (V_H) are connected through a peptide linker (Figure 7.2.). Single-chain fragment variables have been engineered in both V_L -linker- V_H or V_H -linker- V_L orientations (Dimasi et al., 2019). They are significantly

smaller than a whole antibody, they have molecular weights around 25 kDa, while an IgG typically has a MW around 150 kDa. They are also simpler in terms of structure: they do not have interchain disulfide bridges, since they are a single chain. However, the disulfide bridges from intrachain V_L and V_H domains are still present (Fig 7.2) in the scFv. These disulfide bonds are typical of immunoglobulin domains, and are necessary for the stability of the antibody molecule (Guglielmi et al., 2009). Another difference with a whole IgG reveals in the lack of a sugar moiety: scFv are not glycosylated, since the glycosylation of a mAb is located on the Asn₂₉₇ residue of the constant fraction. This absence of complex post-translational modifications allows the expression of antibody fragments such as scFv in bacterial systems, the most typical of them being *Escherichia coli* (Guglielmi et al., 2009).

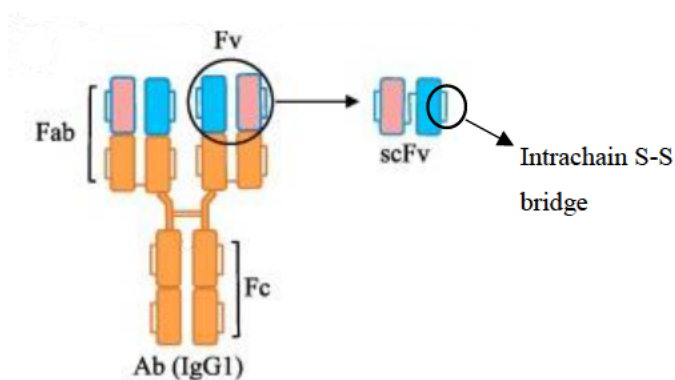


Fig 7.2. Scheme of a full-length mAb and derived scFv fragment. Adapted from (Dimasi et al., 2019).

Regarding their conjugation, scFv can be conjugated to cytotoxic drugs applying similar conjugation strategies than the ones applied to whole mAbs. These include heterogeneous conjugation using lysines (Zhang et al., 2017) (see section 5.1), and also different approaches to homogeneous conjugations, including conjugation to engineered cysteines in an analog strategy to the one applied in this work for Trastuzumab_{cys114} (see section 6.3), addition of unnatural amino acids or strategies combining engineered cysteines with several chemistries (second

generation maleimides) that allow the obtention of conjugates with improved stability (Schumacher et al., 2013), (Hervé-Aubert et al., 2018).

In this chapter, the production, purification and heterogeneous conjugation of a scFv and the homogeneous conjugation of a cysteine-engineered scFv (scFv_cys) will be attempted. Both scFv and scFv_cys will be derived from Trastuzumab, therefore targeting the HER2 antigen.

7.2. scFv production in *Escherichia coli*

scFv production was first attempted in *E. coli*, since it represents an easier, faster and less expensive production strategy with respect to alternatives such as animal cell culture. In this section, the obtention of the genetic sequence of scFv is described, as well as the production in a small-scale bioreactor and the purification and characterization of the product.

7.2.1. Sequence construction and cloning

As it has been explained in the introduction, the scFv sequence consists in the fusion of the variable regions of the light and heavy chains of the antibody, linked through a spacer sequence. In this case, the sequence of the aimed Trastuzumab-derived scFv consisted, from N-terminal to C-terminal of the protein, in the variable region of the light chain (V_{LC}) followed by the linker and the variable region of the heavy chain (V_{HC}). This disposition was based on reports from literature (Zhao et al., 2009). The linker sequence used for fusing the two variable regions consisted in the 218 linker, a 18-amino acid peptide linker designed for scFv proteins aimed to enhancing their stability and reducing aggregation (Whitlow et al., 1993). This linker sequence has a high glutamine-serine (GS) content, conferring flexibility to it, therefore helping the correct folding of the different domains of the fusion protein. Similar linkers have

Chapter 11. Appendix

been used for generating other anti-HER2 scFvs (Olafsen et al., 2004). The DNA and protein sequence of the generated scFv can be found in the Appendix I section.

The DNA sequences of the scFv molecule was obtained from the previously described pTRI_Tzmb plasmid (see chapter 3). By means of a splicing overlap extension PCR (see section 10.7.4.1.), the fusion of the light and heavy chains variable regions was achieved, generating the scFv sequence of 762 base pairs. The used oligonucleotides are listed in Appendix II. The obtained fusion DNA sequence can be observed at Figure 7.3, and it was confirmed by sequencing (see section 10.7.8.).

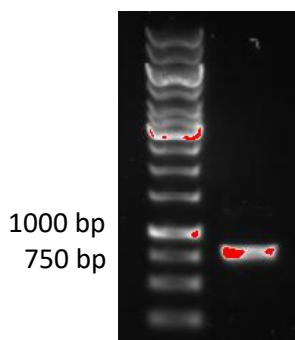


Figure 7.3. DNA sequence of scFv.

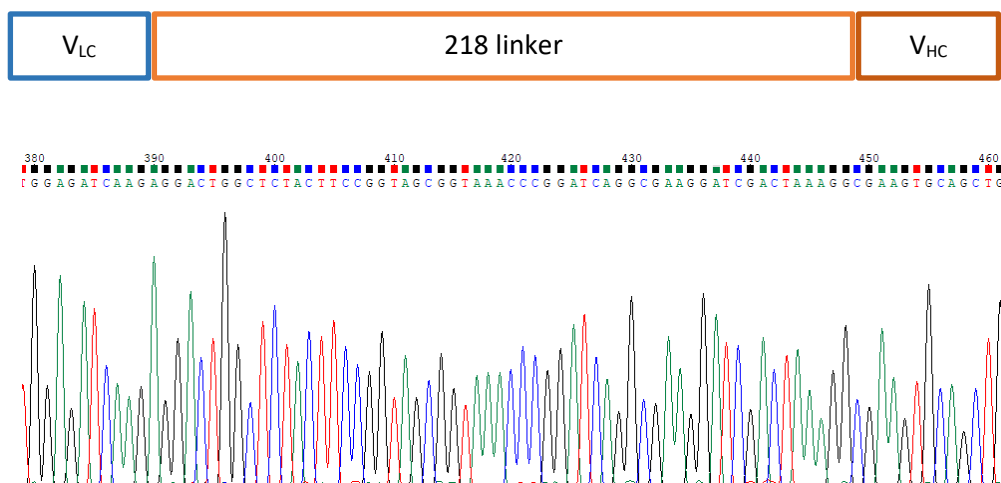


Fig 7.4. Sequencing chromatogram of the overlapping region of the light chain variable region, 218 linker and heavy chain variable region for the scFv construct.

Once constructed, the scFv DNA sequence was cloned (between NheI and EcoRI sites) into the expression vector pET21d (see section 10.6.1.3), an expression vector in which the expression of the gene of interest is driven by the strong T7 promoter and the *lac* operator, therefore only being allowed in the presence of the IPTG inductor.

7.2.2. Production, purification and characterization

7.2.2.1. Selection of the production host and reactor production

The expression plasmid was transformed into the *E. coli* expression hosts BL21(DE3) and Rosetta. BL21 was used since it is one of the most used *E. coli* strains for recombinant protein production due to the high yield of produced protein (Robichon et al., 2011), while the Rosetta strain contains tRNAs that allow the optimal expression of genes with eukaryotic codon usages (Fathi-Roudsari et al., 2016): since the scFv sequences were generated from DNA sequences with a codon usage adapted for HEK293 (see section 3.2), it was expected that the Rosetta strain could overcome possible inefficiencies in the protein expression derived from this codon usage.

For scFv production, 5 clones of each strain were selected and tested, and then the highest productor clones of each strain were compared side by side in small scale Erlenmeyer culture (Fig 7.5.) in a defined medium (see section 10.2.2.2.1) and induced with 500 μ M of IPTG for 3h from a $DO_{550} = 1$.

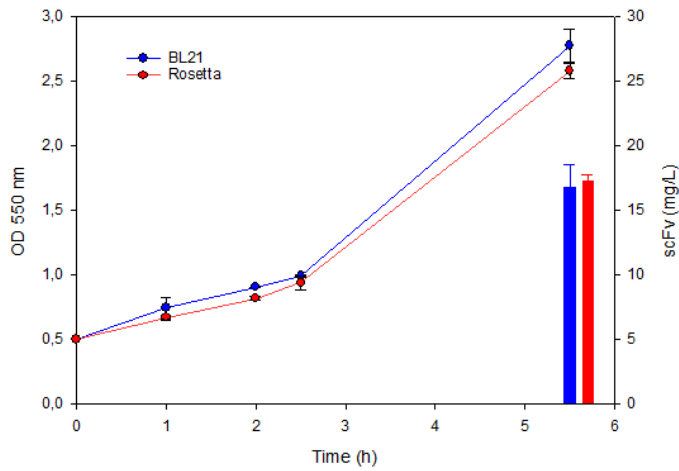


Fig 7.5. Comparison of scFv production (mg/L) and growth of BL21(DE3) and Rosetta *E. coli* clones in Erlenmeyer culture, with 3 independent replicates.

Since no significant difference could be observed between strains, BL21(DE3) was selected as the expression host, as our research group had more experience working with this strain. At this point, the size of the product was assessed with SDS-PAGE gels and was obtained directly from pellets of the *E. coli* cultures, without being purified. The obtained scFv had the expected size of 26.686 kDa (Fig 7.6.).

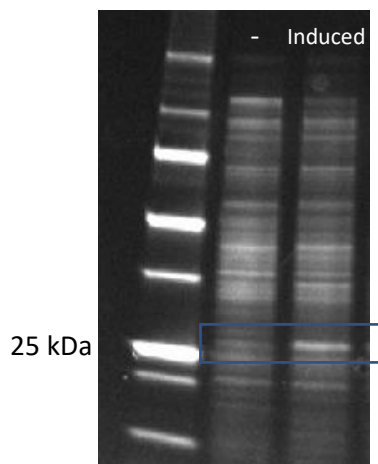


Fig 7.6. SDS-PAGE of the pellet of *E. coli* BL21(DE3) scFv producer, with and without IPTG induction. In the IPTG-induced culture, a band of the scFv expected weight (around 25 kDa) can be observed.

In order to obtain more product for the conjugation and characterization steps, a new production was performed in a 2L bioreactor (see section 10.4.2.3.). When the culture reached a DO_{550} of 3, it was induced with 500 μ M IPTG for 3h, since a final DO_{550} of 10.3. The culture displayed a specific growth rate of 0.47 h^{-1} , and a final concentration of 51.6 mg/L of scFv was obtained. The growth profile and final product titer is depicted in Figure 7.7.

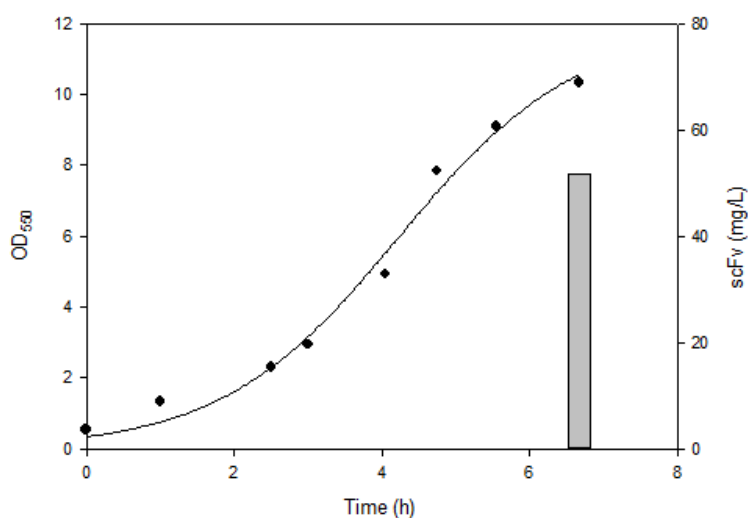


Figure 7.7. Growth profile of scFv producer *E. coli* BL21(DE3).

7.2.2.2. Purification and characterization of the product

The product obtained from the bioreactor was purified following a purification sequence similar to the one described for whole Trastuzumab antibody (see chapter 3, section 3.3.2), but implementing several changes due to the nature of the bacterial expression host (Figure 7.8).

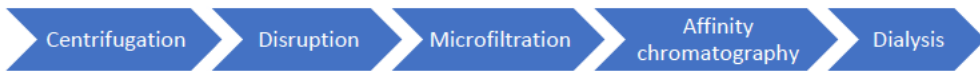


Figure 7.8.. Scheme of the downstream process implemented for the scFv produced in *E. coli*.

The first step of the recovery process consisted in a solid-liquid separation mediating centrifugation (see 10.8.1.1.2.), followed by a disruption step (see 10.8.2.), a microfiltration step (see 10.8.3.1.), an affinity chromatography using a column containing Protein L resin (see 10.8.5.1.), which selectively binds to the light chain of antibodies and antibody fragments, and, finally, a dialysis with sodium citrate buffer (pH = 6). The production of protein by this method resulted in a product with a purity of around 95%, and with its 26.868 kDa weight confirmed, as it can be observed in Figure 7.9.

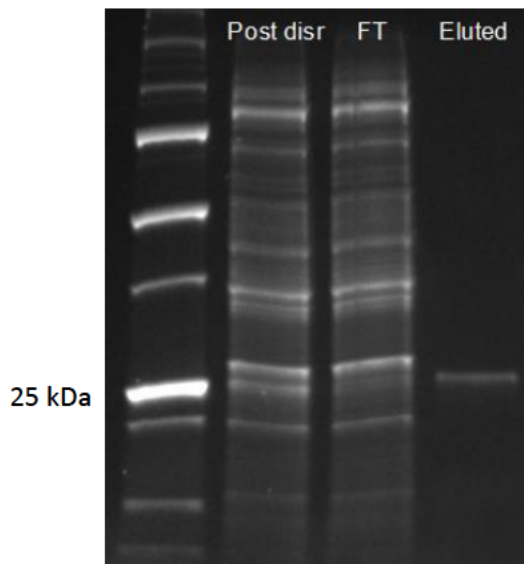


Fig. 7.9. scFv purified with Protein L affinity chromatography: post disruption, flow-through (FT) and eluted product are observed.

However, the product recovered by this method precipitated after the dialysis step, resulting in the loss of more than 95% of the product. Since the elution of the product

is performed at an acid pH (2.3), several buffer conditions were tested: eluted aliquots of scFv were diluted with phosphate-citrate buffer at different pH. However, from a pH of 4, the levels of precipitated product were not reduced (Figure 7.10), therefore rendering the obtained product not suitable for its further conjugation with DM1 or vcMMAE, since in both cases the product needs to be closer to a neutral pH (see section 10.10).

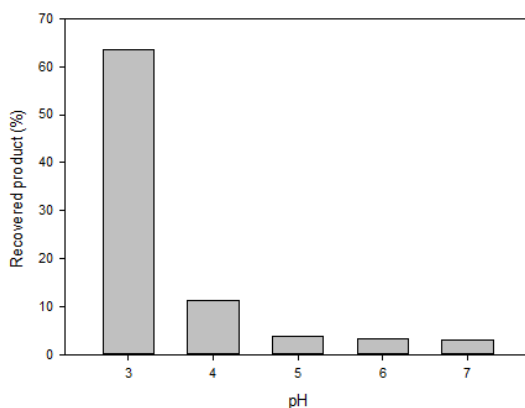


Fig. 7.10. Percentage of recovered scFv after dilution into phosphate-citrate buffer at different pH.

It was hypothesized that the product was not being properly folded by the *E. coli* BL21 host. In this regard, it was observed by testing the integrity of the disulfide bridge of the product in reduced and non reduced conditions in a SDS.PAGE gel that the intrachain disulfide bridge of the produced scFv, necessary for its stability (Guglielmi et al., 2009), was not correctly formed (Figure 7.11).

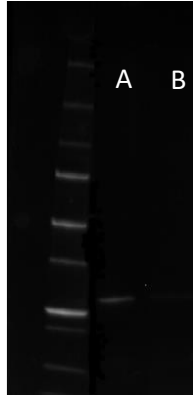


Fig 7.11. SDS-PAGE gel of purified scFv: the protein presents the same migration pattern when reduced (A) than non-reduced (B). When the intrachain disulfide bridge is correctly formed, proteins present a different migration pattern when reduced with respect to the non-reduced form (Gaciarz et al., 2016).

Therefore, an alternative production strategy was attempted in the form of using the human HEK293 cell line for the producing the scFv, since animal cell lines are able to produce proteins involving complex processing and post-translational modifications than bacterial hosts.

7.3. scFv production in HEK293 and heterogeneous conjugation

7.3.1. Sequence construction and cloning

The same previously scFv sequence described for expression with *E. coli* was used for its expression in HEK293. In this case, however, a signal peptide had to be added in order to assure the secretion of the product to the media by the cell, in the same way than had been done for Trastuzumab and the antibody chains. Therefore, the same signal peptide employed for the secretion of the light chain of the antibody was added to the scFv sequence. This was performed by repeating the overlap-extension PCR using a different forward light chain oligonucleotide (see Appendix II) that allowed the incorporation of the signal peptide sequence of the light chain of

the antibody to the final scFv sequence. The obtained DNA sequence (Figure 7.12) was then cloned to the expression vector pIREpuro3 (see section 3.2), suited for recombinant protein expression in animal cells, resulting in the pRESpuro3_scFv vector.

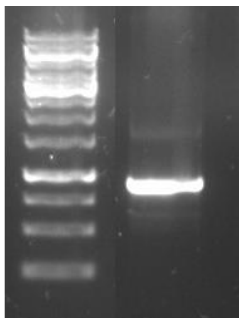


Fig 7.12. scFv sequence for HEK293 expression obtained from overlapping PCR.

7.3.2. Production, purification and characterization

The pRESpuro3_scFv vector was transfected to HEK293 cells, cell pools (HEK293_scFv) were selected and characterized as previously described (see section 3.3.1). When the recombinant strain where grown in an erlenmeyer, a maximum cell density of $13.05 \cdot 10^6$ cell/ml was obtained, with a doubling time of 26.2 h, obtaining a product concentration of 7.2 mg/L (Figure 7.13).

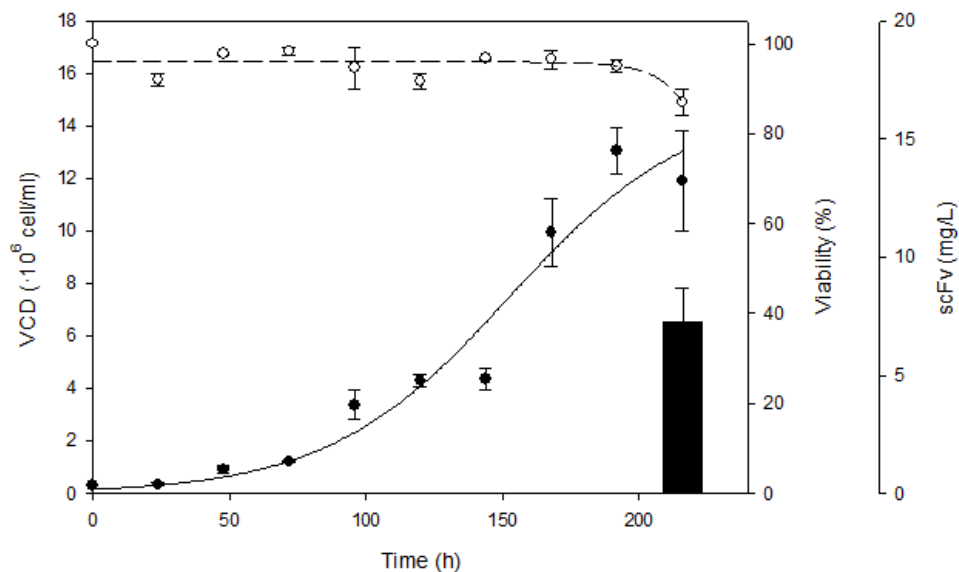


Figure 7.13. HEK293_scFv growth profile and scFv production titers in erlenmeyer culture. Error bars correspond to standard deviation of $n = 3$ replicates.

The purification sequence followed consisted in the same sequence performed for light chain purification (see section 6.4.1.2), allowing the obtention of a product with a purity higher than 99% (Figure 7.14). In this case, unlike for the *E. coli*-produced scFv, a precipitation of the product after the dialysis of the eluted product was not observed. However, after incubation at 4°C for 24h, some precipitated appeared, consisting in around 25% of the product. Therefore, in this case, since the major fraction of the product remained soluble in a compatible buffer for the subsequent conjugation steps, these product and purification process were considered acceptable.

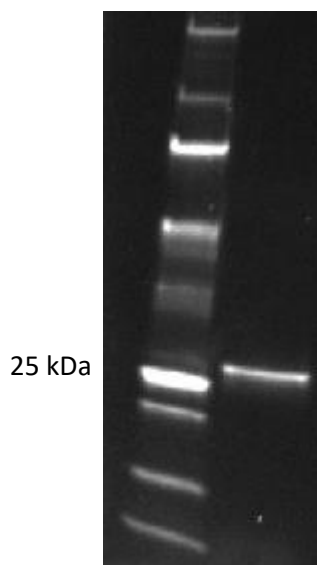


Fig. 7.14. scFv produced with HEK293 and purified with Protein L affinity chromatography.

The antigen-binding capacity of the purified product was also checked (Figure 7.15).



Fig 7.15. ELISA assay performed with produced scFv. Lane 1: produced scFv dilution in HER2 coated wells; Lane 2: negative control, produced scFv dilution in non-coated HER2 wells.

In order to have enough product for the subsequent conjugation, more scFv was produced using single use devices in the same way than for previously described

Trastuzumab molecules: a 5L wave bioreactor production (Figure 7.16) was carried out (see section 10.4.1.1.2). In this case, the product was recovered when the culture reached a cell density of $9.8 \cdot 10^6$ cell/ml, obtaining a product concentration of 7.5 mg/L, which was purified applying the same downstream processing described for previous wave bioreactor cultures (see section 10.8), obtaining a purity >99%.

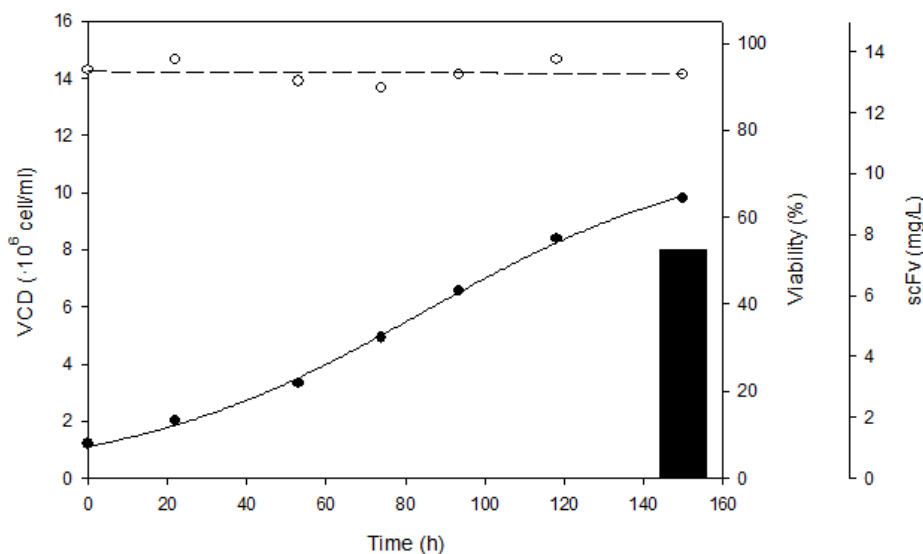


Figure 7.16. HEK293_scFv growth profile and scFv production titers in wave bioreactor culture.

7.3.3. Conjugation and characterization

Once enough product was obtained, a conjugation procedure was defined for the heterogeneous conjugation of the scFv protein to the cytotoxic drug DM1.

In a first attempt, the same protocol defined for the whole Trastuzumab antibody conjugation (see section 5.2.1 and Figure 7.17) was applied. This conjugation sequence consisted in SMCC linker addition to the scFv fragment solution, incubation for 2h at room temperature, followed by a diafiltration in order to remove the excess

of linker, then by the addition of DM1 and reaction step for 16.5h at room temperature and agitation at 300 rpm, followed by a final diafiltration in order to remove the excess of non-conjugated DM1 drug. The same DAR of 3.1 was aimed, therefore applying a SMCC molar proportion with respect to scFv of 7.5, and then 8.5 molecules of DM1 per scFv were added in the conjugation.

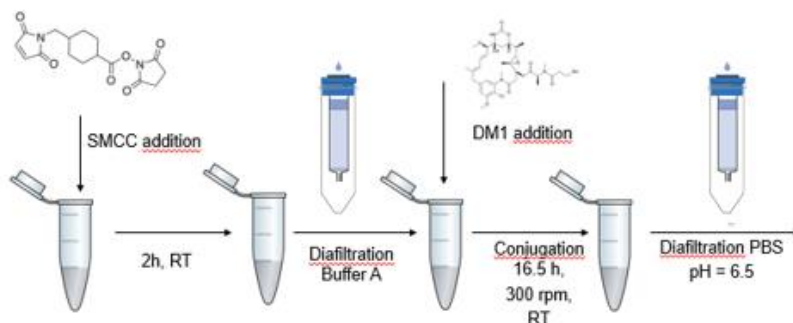


Figure 7.17: Scheme of the applied conjugation process for scFv-DM1.

When these conjugation conditions were applied, a strong precipitation of the product was observed, both after the SMCC linker addition and the DM1 cytotoxic drug addition, resulting in a very low recovery yield (Table 7.1), close to 10%. Moreover, the DAR of the conjugated product did not correspond to the aimed DAR of 3.1, instead, a DAR of 0.9 was obtained (measured by UV/Vis (Figure 7.16)).

It was hypothesized that, since the scFv molecule is smaller than the whole Trastuzumab antibody, a DAR of 3.1 for the scFv results in a too high hydrophobic load for this molecule: since Trastuzumab has a molecular weight of around 6 times higher than the scFv (145.531 vs 26.686 kDa), the same cytotoxic drug load per molecule results in 6 times more drug load per amount of protein in the case of the scFv. Therefore, the precipitates observed for the conjugated scFv were expected to correspond to the higher-loaded scFv species.

Chapter 11. Appendix

In order to lower the precipitation levels, conjugation attempts lowering the amount of SMCC linker and DM1 to add to the scFv were carried out, since both SMCC linker and DM1 are hydrophobic molecules. However, adding lower amounts of linker and cytotoxic drug results in a lower DAR: in these alternative conjugation conditions, the aimed DARs were of 1.5 and 0.5 (using the same reference of the previous aimed DAR of 3.1). Applying these conditions, precipitate levels were lowered and the recovery yield improved: they were of 36.4 and 46.2%, respectively. However, the obtained DARs were still lower than before: they corresponded to 0.5 and 0.2 (Table 7.2 and Figure 7.18).

Table 7.1: Summary of scFv-DM1 conjugation process data

Amount of scFv conjugated (mg)	Yield for SMCC addition + dialysis step	Yield for DM1 addition + dialysis step	Total process yield	Aimed DAR	Obtained DAR
1	28.5	27.5	7.8	3.1	0.9
1	72	50.6	36.4	1.5	0.5
1	61.2	75.5	46.2	0.5	0.2

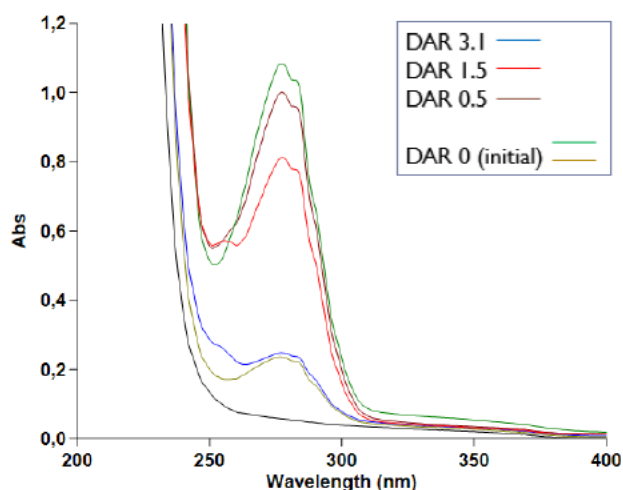


Fig. 7.18. Absorbance profile of the different scFv-DM1 ADC obtained in this work, with different initial aimed DARs.

In order to overcome this issue, an alternative approach consisting in conjugating a cytotoxic drug in a site-directed manner to the scFv was envisaged, being detailed in the next section.

7.4. scFv_cys111: production in HEK293 and homogeneous conjugation

An homogeneously conjugated scFv was aimed by genetically modifying the antibody fragment, generating a cysteine-engineered scFv by inserting a cysteine residue into the fragment sequence, to which vcMMAE cytotoxic drug could be selectively conjugated, in an analog way to the conjugation strategy described in section 6.3.2. This section includes the scFv DNA sequence definition, the scFv production and its purification and conjugation.

7.4.1. Sequence definition, construction and cloning

The same sequence that has been defined before in the 7.2.1 section was employed for the generation of the cysteine-engineered scFv, in which a cysteine was added to the reference sequence. The cysteine was added into the linker, in order to avoid disturbing the variable light or heavy sequences of the scFv, and therefore not impairing the binding ability of the antibody fragment. The concrete location for insertion in the linker was finally set at the position 111 of the scFv sequence (resulting in the scFv_cys111), based on a simulation of the 3D structure of the scFv, using the Phyre2 software (Kelley et al., 2015). This simulation showed that this position was sterically accessible, therefore being suitable for the conjugation of the cysteine (Figure 7.21).

Then, the DNA sequence codifying for the scFv_cys111 protein was obtained by means of an overlap extension PCR, as previously performed for the scFv, and using this same scFv as a template for the PCR.

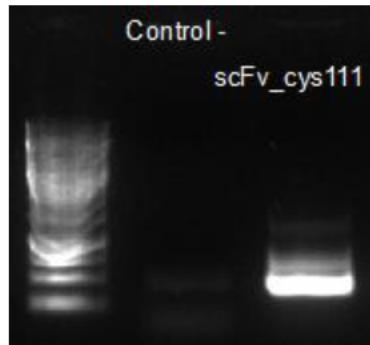


Fig 7.19. scFv sequence for HEK293 expression obtained from overlapping PCR.

In this case, a TGT codon codifying for the added cysteine at position 111 (cys111) was added in the overlap-enabling oligonucleotides (Appendix II). Finally, the sequence was cloned in the same pIRESpuro3 vector, using the same restriction sites (NheI and EcoRI), generating the plasmid pIRESpuro3_scFv_cys111.

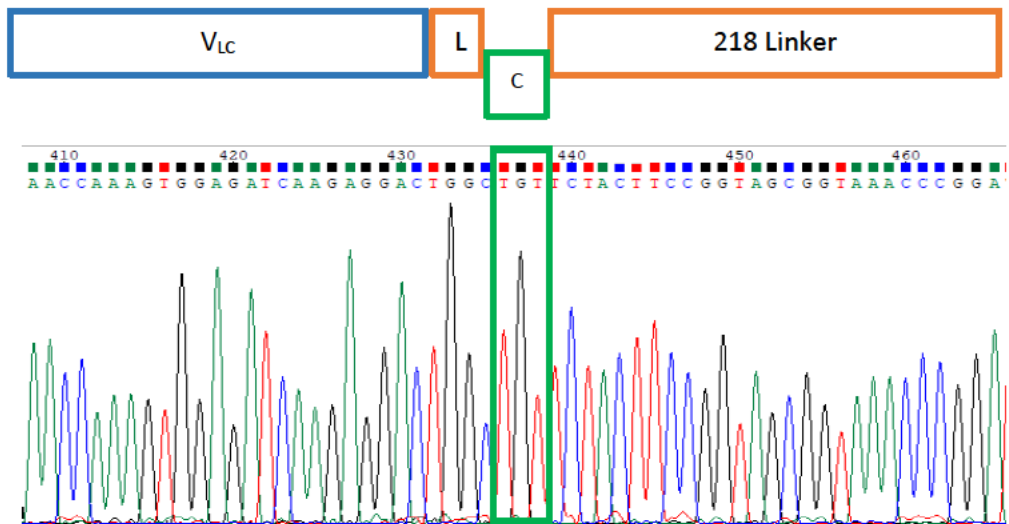


Fig 7.20. Sequencing chromatogram of the V_L (blue) - linker (orange) region of the scFv_{cys111}, comprising the added cysteine in the 111 position (green).

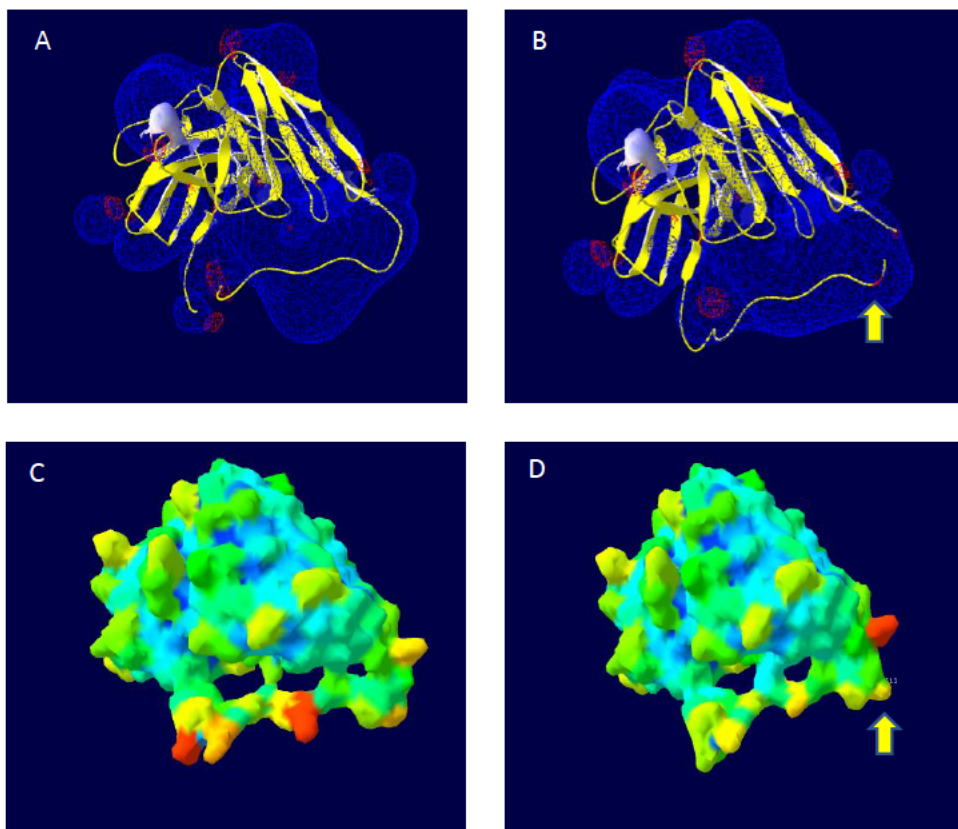


Fig 7.21. A and B: 3D structure of the scFv (A) and scFv_{cys111} (B), observed with PDB Viewer. The electrostatic potential is displayed in blue (negative) and red (positive), with white region corresponding to a hydrophobic patch. C and D: 3D structure of scFv (C) and scFv_{cys111} (B) observed with PDB Viewer (Guex et al., 1997). The color pattern corresponds to the solvent accessibility of the molecule, red being the maximum accessible and blue the minimum accessible. In B and D, the yellow arrow indicates the location of the inserted cysteine.

7.4.2. Production, purification and characterization

The pIRESpuro3_scFv_cys111 vector was transfected to HEK293 cells, cell pools (HEK293_scFv_cys111) were selected and characterized as previously described (see section 3.3.1).

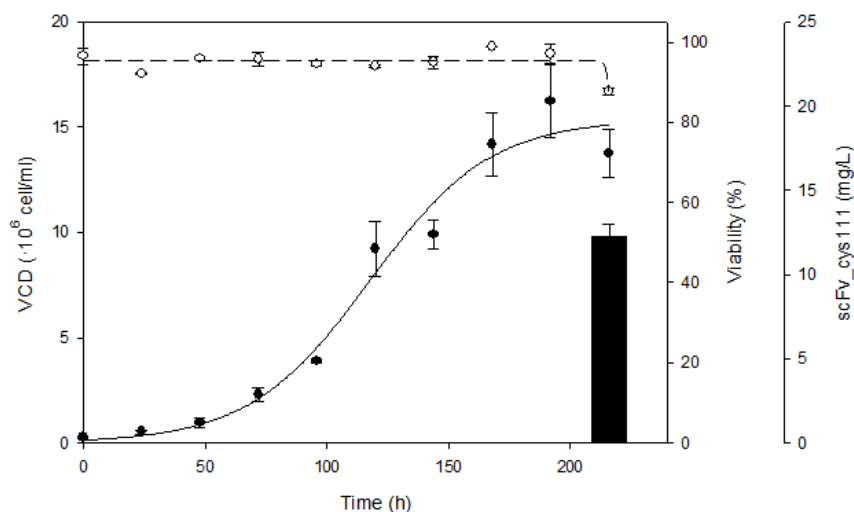


Figure 7.22. HEK293_scFv_cys111 growth profile and scFv production titers in erlenmeyer culture. Error bars correspond to standard deviation of $n = 3$ replicates.

When the recombinant strain was grown in an erlenmeyer a MCD of $16.2 \cdot 10^6$ cell/ml was obtained, with a doubling time of 24.6 h, obtaining a product concentration of 12.2 mg/L (Figure 7.22).

The purification sequence followed consisted in the same sequence performed for the scFv, allowing the obtention of a product with a purity higher than 97% (Figure 7.23). Similarly, after incubation at 4°C for 24h, some precipitated appeared, consisting in around 20% of the product. Therefore, in this case, since the major fraction of the product remained soluble in a compatible buffer for the subsequent conjugation steps, this product and purification process was considered suitable. It is also worth pointing out that, despite having a cysteine added to its sequence,

which can lead to dimers formation through disulfide bridges (Schumacher et al., 2013), no covalently linked dimers were observed in the SDS-PAGE gel (Figure 7.23).

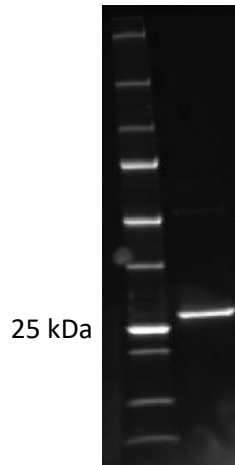


Fig. 7.23. scFv_cys111 produced with HEK293 and purified with Protein L affinity chromatography.

The antigen-binding capacity of the purified product was also checked (Figure 7.24).

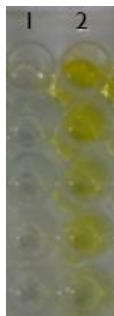


Fig 7.24. ELISA assay performed with produced scFv_cys111. Lane 1: negative control, produced scFv dilution in non-coated HER2 wells; Lane 2: produced scFv dilution in HER2 coated wells.

In order to have enough product for the subsequent conjugation, a 1L Erlenmeyer production was carried out. In this case, the product was recovered when the culture reached a cell density of $13.7 \cdot 10^6$ cell/ml, obtaining a product concentration of 9.6

mg/L, which was purified applying the same downstream processing described for scFv, obtaining a purity >97%.

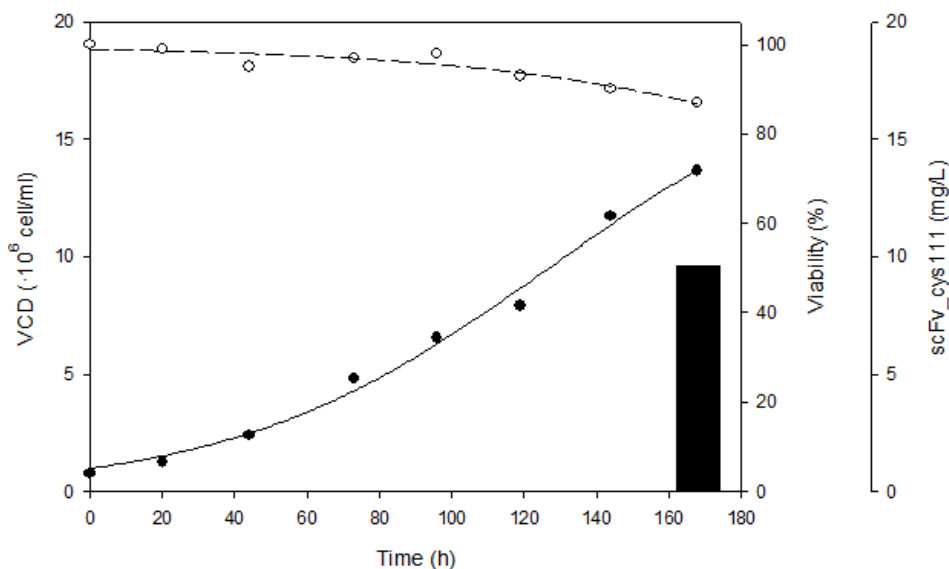


Figure 7.25. HEK293_scFv growth profile and scFv production titers in 1L erlenmeyer culture.

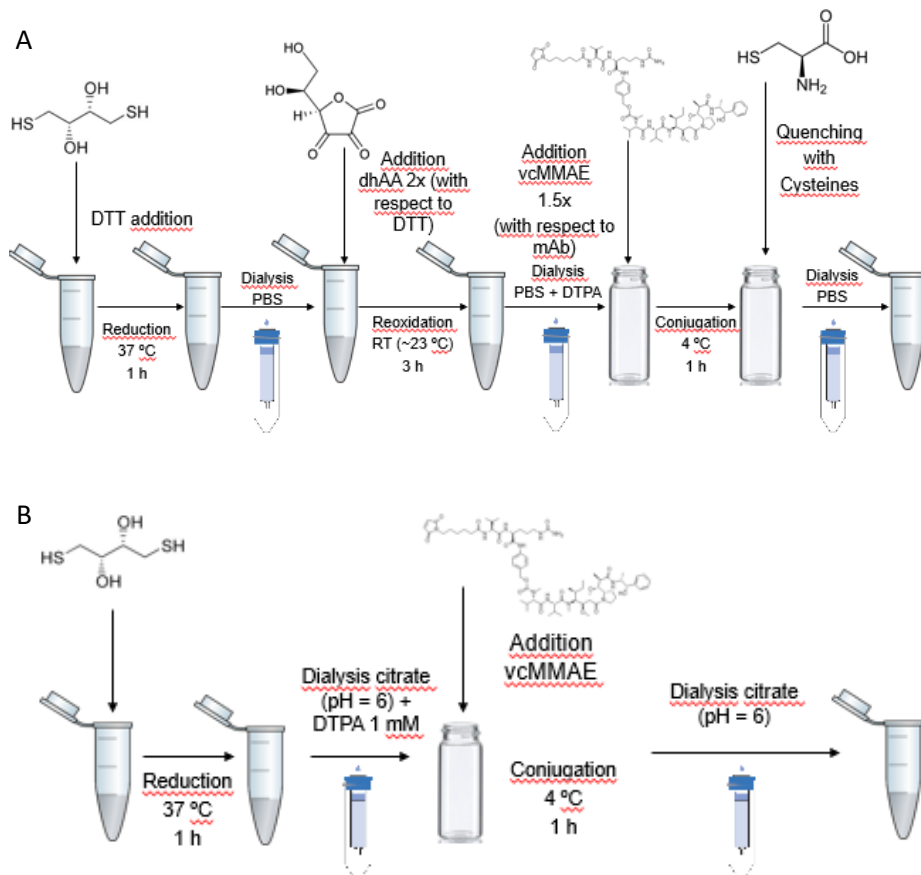
7.4.3. Conjugation and characterization

Once enough scFv_cys111 product was obtained, its site-directed conjugation with vcMMAE cytotoxic drug was attempted. The conjugation principle was the same than the one applied for the conjugation of Trastuzumab_cys114 (see sections 6.3.2, and 10.10.3.3.2).

The conjugation process applied for the whole Trastuzumab_cys114 consists of several steps: an initial reduction in order to free the capped cys114; a dialysis step in order to eliminate the reducing agent; a reoxidation step, so interchain disulfide bridges can be rebuilt; a second dialysis in order to eliminate the reoxidating agent, and then the conjugation and final dialysis steps (Figure 7.26, A). In the case of the scFv_cys111 fragment, the applied protocol is shorter, since the reoxidation step

does not need to be carried out: after the reduction step, the only available cysteine for conjugation is the added cys111 (Fig 7.26, B), since the cysteines from the intrachain disulfide bridges are not sterically available for conjugation.

The reducing agent molar proportion to apply in the reduction step of the whole antibody Trastuzumab_cys114 was found to be of 50 times (50x) with respect to the antibody, in order to ensure the complete reduction of the antibody and thus obtain an homogeneous ADC (same section 6.3.2). In the case of the scFv_cys111 molecule, the molar proportion of applied reducing agent was set at 20x. It was expected that this molar proportion would be enough to completely reduce the added cys111, since the relation reducing agent vs available cysteines is even higher in this case (20) than the 50x reducing agent proportion for the whole mAb (5).



Chapter 11. Appendix

Figure 7.26: Scheme of the applied conjugation process for Trastuzumab_cys114 conjugation (A) and for scFv_cys111 conjugation (B).

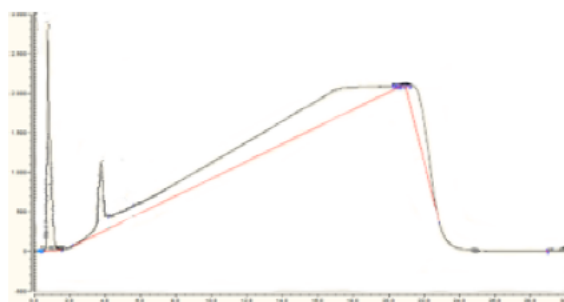
This conjugation process resulted in a conjugated scFv_cys111-vcMMAE molecule with a DAR of 1 measured by HIC-HPLC (Figure 7.24), with a global recovery yield of 27.6% (Table 7.2). Therefore, with this conjugation strategy, an homogeneous conjugated scFv was obtained.

Compared to the previously generated heterogeneous scFv-DM1, in the condition in which the scFv-DM1 has a similar DAR than the site-directed scFv-vcMMAE (0.9 vs 1) the homogeneous conjugation process displays a higher recover yield (27.6 vs 7.8%).

Table 7.2: Summary of scFv_cys111-vcMMAE conjugation process data

Amount of scFv conjugated (mg)	Yield for reduction + dialysis step	Yield for vcMMAE addition + dialysis step	Total process yield	Aimed DAR	Obtained DAR
1	77.7	35.5	27.6	1	1

A



B

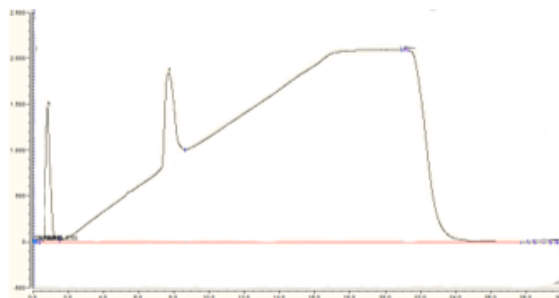


Fig 7.27. HIC-HPLC profile of unconjugated scFv_cys111 (A) and scFv_cys111-vcMMAE (B).

7.5. Conclusions

In this chapter, the previously implemented strategies for antibody conjugation have been applied to antibody fragments (scFv). First, the scFv antibody fragment based on Trastuzumab has been designed and its production attempted in *E. coli*. The scFv produced in this expression system presented high precipitate levels in the dialysis step after the elution from the affinity chromatography, impairing its subsequent conjugation. It was hypothesized that *E. coli* was not able to properly fold the scFv, therefore, its expression with the animal system HEK293 was attempted. In this case, despite the precipitation of a fraction of the product (25%), the scFv could be recovered and conjugated. A heterogeneous conjugation to the cytotoxic drug DM1 was attempted, obtaining a conjugated product with a DAR of 0.9 but recovering only around a 10% of the product due to precipitation issues. This issue was attempted to be overcome through the site-directed conjugation of the fragment, by genetically inserting a cysteine on the scFv, to which the vcMMAE cytotoxic drug would be conjugated. This strategy yielded a conjugated scFv with a DAR of 1, recovering around 27% of the product, thus improving the yield of the heterogeneous conjugation process. In the next chapter, the antiproliferation assessment of the scFv conjugates generated in this chapter will be performed.

7.6. References

- Animal Cell Technology Industrial Platform. (n.d.). Monoclonal Antibodies Approved by the EMA and FDA for Therapeutic Use – ACTIP. Retrieved December 17, 2018, from <https://xpv.uab.cat/products/monoclonal-antibodies-approved-by-the-ema-and-fda-for-therapeutic-use/>,DanaInfo=.awxyCehzpxly2s+
- Deonarain, M. P., Yahioğlu, G., Stamati, I., & Marklew, J. (2015). Emerging formats for next-generation antibody drug conjugates. *Expert Opinion on Drug Discovery*, *10*(5), 463–481. <https://doi.org/10.1517/17460441.2015.1025049>
- Dimasi, N., Fleming, R., Wu, H., & Gao, C. (2019). Molecular engineering strategies and methods for the expression and purification of IgG1-based bispecific bivalent antibodies. *Methods*, *154*, 77–86. <https://doi.org/10.1016/J.YMETH.2018.08.004>
- Fathi-Roudsari, M., Akhavian-Tehrani, A., & Maghsoudi, N. (2016). Comparison of Three Escherichia coli Strains in Recombinant Production of Reteplase. *Avicenna Journal of Medical Biotechnology*, *8*(1), 16–22. Retrieved from <http://www.ncbi.nlm.nih.gov/pubmed/26855731>
- Gaciarz, A., Veijola, J., Uchida, Y., Saaranen, M. J., Wang, C., Hörkö, S., & Ruddock, L. W. (2016). Systematic screening of soluble expression of antibody fragments in the cytoplasm of E. coli. *Microbial Cell Factories*, *15*(1), 22. <https://doi.org/10.1186/s12934-016-0419-5>
- Guex, N., & Peitsch, M. C. (1997). SWISS-MODEL and the Swiss-Pdb Viewer: An environment for comparative protein modeling. *Electrophoresis*, *18*(15), 2714–2723. <https://doi.org/10.1002/elps.1150181505>
- Guglielmi, L., & Martineau, P. (2009). Expression of single-chain Fv fragments in E. coli cytoplasm. *Methods in Molecular Biology (Clifton, N.J.)*, *562*, 215–224. https://doi.org/10.1007/978-1-60327-302-2_17

- Hervé-Aubert, K., Allard-Vannier, E., Joubert, N., Lakhri, Z., Alric, C., Martin, C., ... Chourpa, I. (2018). Impact of Site-Specific Conjugation of ScFv to Multifunctional Nanomedicines Using Second Generation Maleimide. *Bioconjugate Chemistry*, 29(5), 1553–1559. <https://doi.org/10.1021/acs.bioconjchem.8b00091>
- Hess, C., Venetz, D., Neri, D., Carter, P. J., Walsh, G., Coiffier, B., ... Braisted, A. C. (2014). Emerging classes of armed antibody therapeutics against cancer. *MedChemComm*, 5(4), 408. <https://doi.org/10.1039/c3md00360d>
- Kelley, L. A., Mezulis, S., Yates, C. M., Wass, M. N., & Sternberg, M. J. E. (2015). The Phyre2 web portal for protein modeling, prediction and analysis. *Nature Protocols*, 10(6), 845–858. <https://doi.org/10.1038/nprot.2015.053>
- Olafsen, T., Tan, G. J., Cheung, C. -w., Yazaki, P. J., Park, J. M., Shively, J. E., ... Wu, A. M. (2004). Characterization of engineered anti-p185HER-2 (scFv-CH3)2 antibody fragments (minibodies) for tumor targeting. *Protein Engineering Design and Selection*, 17(4), 315–323. <https://doi.org/10.1093/protein/gzh040>
- Robichon, C., Luo, J., Causey, T. B., Benner, J. S., & Samuelson, J. C. (2011). Engineering Escherichia coli BL21(DE3) Derivative Strains To Minimize E. coli Protein Contamination after Purification by Immobilized Metal Affinity Chromatography. *Applied and Environmental Microbiology*, 77(13), 4634–4646. <https://doi.org/10.1128/AEM.00119-11>
- Schmidt, M. M., & Wittrup, K. D. (2009). A modeling analysis of the effects of molecular size and binding affinity on tumor targeting. *Molecular Cancer Therapeutics*, 8(10), 2861–2871. <https://doi.org/10.1158/1535-7163.MCT-09-0195>
- Schumacher, F. F., Sanchania, V. A., Tolner, B., Wright, Z. V. F., Ryan, C. P., Smith, M. E. B., ... Baker, J. R. (2013). Homogeneous antibody fragment conjugation by disulfide bridging introduces ‘spinostics.’ *Scientific Reports*, 3(1), 1525.

<https://doi.org/10.1038/srep01525>

- Stern, M., & Herrmann, R. (2005). Overview of monoclonal antibodies in cancer therapy: present and promise. *Critical Reviews in Oncology/Hematology*, *54*(1), 11–29. <https://doi.org/10.1016/j.critrevonc.2004.10.011>
- Whitlow, M., Bell, B. A., Feng, S. L., Filpula, D., Hardman, K. D., Hubert, S. L., ... Milenic, D. E. (1993). An improved linker for single-chain Fv with reduced aggregation and enhanced proteolytic stability. *Protein Engineering*, *6*(8), 989–995. Retrieved from <http://www.ncbi.nlm.nih.gov/pubmed/8309948>
- Yokota, T., Milenic, D. E., Whitlow, M., & Schlom, J. (1992). Rapid tumor penetration of a single-chain Fv and comparison with other immunoglobulin forms. *Cancer Research*, *52*(12), 3402–3408. Retrieved from <http://www.ncbi.nlm.nih.gov/pubmed/1596900>
- Zhang, H., Wang, Y., Wu, Y., Jiang, X., Tao, Y., Yao, Y., ... Yang, J. (2017). Therapeutic potential of an anti-HER2 single chain antibody–DM1 conjugates for the treatment of HER2-positive cancer. *Signal Transduction and Targeted Therapy*, *2*(1), 17015. <https://doi.org/10.1038/sigtrans.2017.15>
- Zhao, Y., Wang, Q. J., Yang, S., Kochenderfer, J. N., Zheng, Z., Zhong, X., ... Morgan, R. A. (2009). A Herceptin-Based Chimeric Antigen Receptor with Modified Signaling Domains Leads to Enhanced Survival of Transduced T Lymphocytes and Antitumor Activity. *The Journal of Immunology*, *183*(9), 5563–5574. <https://doi.org/10.4049/jimmunol.0900447>

Chapter 8. Results (VI): biological activity assessment of the generated ADCs

8.1. Introduction

Once produced, purified and after the physicochemical characterization, the drugs developed in this work will have their therapeutic activity tested. In the case of an antitumoral drug, such as the ADCs that have been developed in this work, the antiproliferative activity is one of the main parameters to be assessed. This will be performed using different assays that validate a drug in its preclinical development: *in vitro* assays (2D and 3D) as well as an *in vivo* assay.

In vitro 2D assays have been traditionally used for drug discovery and preclinical development, with human cell lines providing a defined platform for investigating cell and tissue physiology. Bidimensional assays present advantages including high reproducibility, relatively low costs, short time to set up and high throughput (Stock et al., 2016). In 2D cell culture, cells are grown on flat surfaces optimized for attachment and growth (Saji et al., 2019), and model cell lines or primary cell lines from patients can be used for testing the drug of interest.

In the case of HER2+ breast cancer, several cell lines are used as representative models of the disease, including, among others, SKBR3 and BT474 (Jernström et al., 2017), two of the most used HER2 positive breast cancer cell lines in *in vitro* assays. SKBR3 cell line is sensitive to Trastuzumab, grows in grape-like appearance with poor cell-cell contact (Kenny et al., 2007) and presents a poor tumorigenic potential when incorporated in animal models (Holliday et al., 2011). BT474 cell line has a better tumor formation ability than SKBR3. Both cell lines have been used for Trastuzumab ADCs *in vitro* testing (Phillips et al., 2008).

In order to assess the effect of the drug of interest on the breast cancer target cells in an *in vitro* assay, the antiproliferation rate of the cells represents a critical

parameter. This can be assessed through different methodologies, including nucleoside-analog incorporation, cell cycle-associated protein detection, use of cytoplasmic proliferation dyes, cell counting and viability and metabolic activity assays (Romar et al., 2016). One of the most typical methods, based on metabolic activity, relies on tetrazolium salts, which can be reduced by dehydrogenases or reductases from the cell, therefore generating formazan, a colored product that can be monitored by measuring its absorbance (Riss et al., 2004). Thus, the generation of formazan is directly proportional to the metabolic activity of the cells. In this chapter, the MTS tetrazolium salt will be used as the key reagent for the 2D *in vitro* antiproliferative assay.

2D culture is generally accepted and has been useful to increase the understanding of drug mechanisms of action, however, there are limitations associated with it, mainly the fact that cells grow on a monolayer on flat plates or flasks, being rigid platforms that do not reproduce the microenvironment of the tumor (Saji Joseph et al., 2019).

3D culture models have several parameters more similar to the *in vivo* tumor microenvironment than 2D cultures, including: morphology of the cells; differentiation, being better characterized and evidenced in 3D cultures; viability, since cells in 3D culture are more viable and less prone to apoptosis than 2D cells, due to the stronger interactions between cells; drug metabolism; gene expression and protein synthesis. All of this makes 3D systems more *in vivo* relevant than 2D (Gupta et al., 2016). 3D culture models comprise different displays, which can be divided in two main groups: the 3D structures which are cultured using anchorage-independent approaches (without the use of a substrate that promotes cellular attachment) or those that use anchorage-dependent conditions (utilizing a substrate which promotes cellular attachment) (Lovitt et al., 2014). Some of these 3D strategies include: the formation of spheroids (which can be of one cell type or multicellular) by different methods such as hanging drop; forced floating; agitation

in devices such as spinner flask bioreactors; using hydrogel matrices and scaffolds such as Matrigel, which is composed of tumor-derived basement membrane proteins; bioprinting approaches, in which biocompatible materials, constituent cells and supporting structures can form functional living organs; and microfluidic related methods such as the Lab-on-a-chip approach, which provides microenvironments compatible with those found *in vivo* (Gupta et al., 2016).

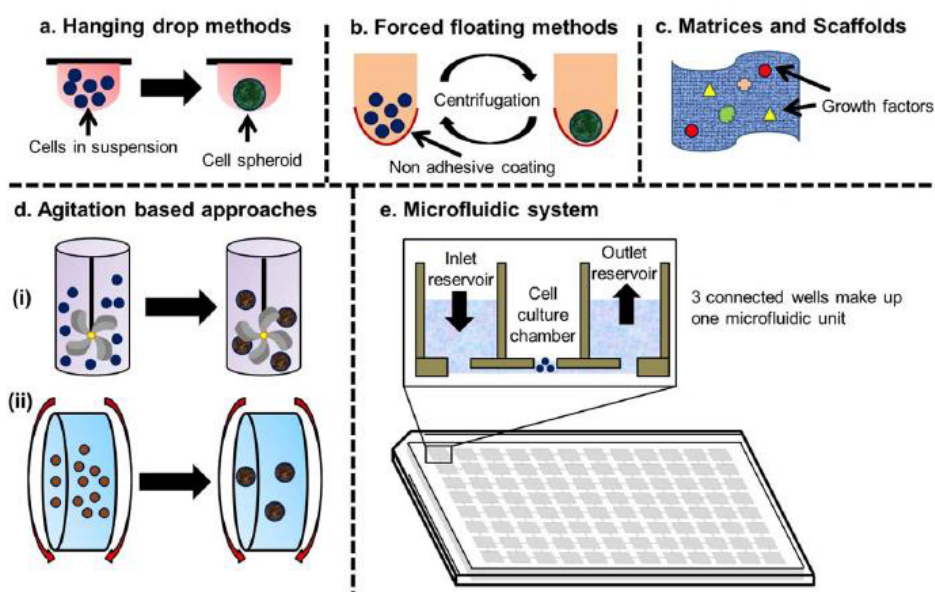


Figure 8.1. Methods for 3D culture. Obtained from (Gupta et al., 2016).

In vitro tests with cancer model human cell lines has led to increased understanding of the molecular events that lead to malignancy as well as assessing the therapeutic activity of potential drugs. However, many of the mechanisms responsible for tumorigenicity are modified during cell culture, and drugs that show efficacy *in vitro* against human tumor cell lines can be ineffective when translated to tumors in patients. This can be caused by different factors, including genetic alterations that appear through multiple passages of the cell line, and issues associated with

vascularization and the three-dimensional structure of the tumor *in vivo* as compared to a two-dimensional cell layer *in vitro*. In order to overcome these issues, human tumor cell lines and solid human tumors can be engrafted into immunosuppressed animal models allowing a more accurate reproduction of the tumor *in vivo* environment (L. D. Shultz et al., 2014). Rodent models, particularly mice (*mus musculus*), are the most used animal model in oncology due to the convenience of using a small, rapidly breeding animal which bears relatively close resemblance to humans (Sausville et al., 2006).

Immunosuppression of these animal models is necessary in order to allow the engraftment of human tumor cells, otherwise, they would be rejected by the action of the immune system of the host.

Several immunodeficient mouse models have been developed, their immunodeficiency degree depending on the mutation presented by the mouse. The most relevant immunocompromised mice strains, based on implemented mutations, include:

- **Nude:** nude mice were discovered in the 1960s, and have a mutation consisting in the disruption of the gene *FOXP1*, which is involved in the thymus development (Vaidya et al., 2016). Therefore, homozygous nude mice are deficient for T cell activity, and provided an early model for tumor engraftment of human cell lines derived from solid tumors (Shultz et al., 2014). The nude mutation (*Foxn1^{nu}*) also affects the mouse hair growth (Wettersten et al., 2014), giving way to its naming as “nude”.
- **SCID:** while nude mice lack only T cells, mice homozygous for the severe combined immunodeficiency (SCID) mutation are deficient for both T and B cells and are thus characterized by an absence of both innate and adaptative immune response (Bosma et al., 1983), providing a better environment for xenografting with respect to nude mice (Wettersten et al., 2014). SCID phenotype was first described in C.B17 mice containing a mutation of the

protein kinase DNA activated catalytic polypeptide gene (*Pkrdc^{SCID}*) (Bosma et al., 1983), which is involved in the rearrangement of the genetic components of antibodies and T cell receptors during B and T cell development. Currently, the term “SCID” has been adapted to refer to all severely immunodeficient strains of mice, including those expressing the *Rag1^{null}* or *Rag2^{null}* mutations (Bosma et al., 1983), (Shinkai et al., 1992). The *RAG1* and *RAG2* genes are also involved in the rearrangement of the genetic components of antibodies and T cell receptors. Rag mice present the advantage of not generating any T and B cell, whereas SCID mice with the *Pkrdc^{SCID}* mutation are “leaky”, meaning that they can generate low amounts of T and B cells (Kotloff et al., 1993). Therefore, Rag mice can present higher tolerance to engraftment.

- **NOD-SCID:** Further predisposition to engraftment was achieved by backcrossing the *scid* mutation into a Non-Obese Diabetic (NOD) strain. The NOD strain background provides intrinsic defects in innate immunity, including lowered NK cell activity, reduced levels of macrophage activation, abnormal dendritic cell development and function, and an absence of hemolytic complement. Combining these innate immune defects with the *scid* mutations led to a murine host more receptive for human tumors: when compared with C.B17-*scid* mice, NOD-*scid* mice were more prone to engraftment with solid human tumors that failed to grow or grew poorly in C.B17-*scid* mice (L. D. Shultz et al., 2014).
- **NSG:** NOD-SCID mice, despite being highly immunosuppressed, still present some residual innate immune function, mostly due to Natural Killer (NK) cell activity (L. D. Shultz et al., 2014). Stricter immunodeficiency can be achieved via the mutation in the IL2-receptor common gamma chain (*IL2rg^{null}*) (Ito et al., 2012). The *IL2rg* gene is responsible for high affinity signaling for different interleukin (IL) receptors (IL2, IL4, IL7, IL9, IL15 and IL21). Absence of signaling through these receptors hinders both the adaptive and immune

system. Combination of the *IL2rg^{null}* mutation with the SCID background results in mice completely deficient in adaptive immunity and severely deficient in innate immunity that are highly receptive to engraftment of human cells, tissues and primary tumors (Shultz et al., 2012).

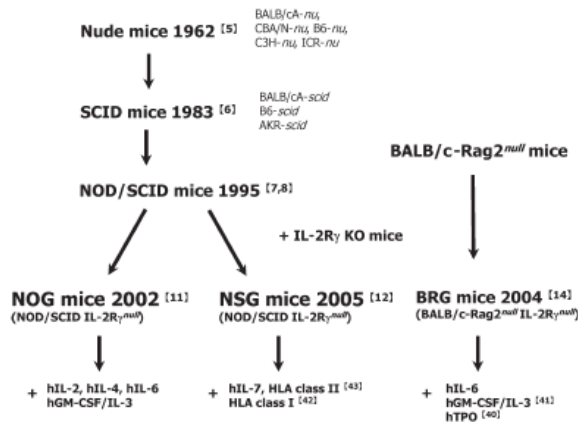


Figure 8.2. Scheme of model mice strains development. Obtained from (Ito et al., 2012).

The several described mutations can be implemented into different mice strain backgrounds. Several mice strains are used in biomedical research, the most used being C57BL/6 and BALB/c strains (Johnson, 2012). C57BL/6 is the most used mouse strain for research, it was the earliest implanted strain given its strain stability and easy breeding. C57BL/6 mice are employed as physiological or pathological models for *in vivo* studies, and they are also used as a background strain for generating congenics with both spontaneous and induced mutations (Johnson, 2012). BALB/c mice is an albino strain, which is used extensively for hybridoma and antibody production, and are especially useful for cancer therapy research and immunology. Similarly to the C57BL/6 strain, BALB/c strain is also used as a background strain for various gene deficiency/knockout studies (Johnson, 2012). In this work, BALB/c nude, NOD-SCID and Rag strains will be used.

In this chapter, the assessment of the antiproliferative activity of the developed antibody-conjugate molecules will be attempted in 2D and 3D *in vitro* models, and one of the candidates, the homogeneous Trastuzumab-vcMMAE with a DAR of 2 generated from the *in vitro* assembly of its chains, being the most innovative of the proposed molecules, will also be analyzed in an *in vivo* animal model.

8.2. 2D *in vitro* assays with SKBR3 cell line:

8.2.1. MTS antiproliferation activity assay development and ADCs assessment

The first assay developed for the assessment of the antiproliferation activity of the constructed ADCs consisted in a two dimensional antiproliferative assay based on the reagent MTS. The test is based on the conversion of the MTS tetrazolium compound to a colored formazan product that can be detected and quantified (see section 10.12.1). Formazan is formed when MTS is reduced by the cells, therefore, the formazan amount can be related to cellular activity, and, thus, proliferation. This test has been applied to the different ADC molecules developed in this work. In a first assay, the cytotoxic drugs that have been used in this work, DM1 and vcMMAE, had their antitumoral activity assessed (Figure 8.3).

Chapter 11. Appendix

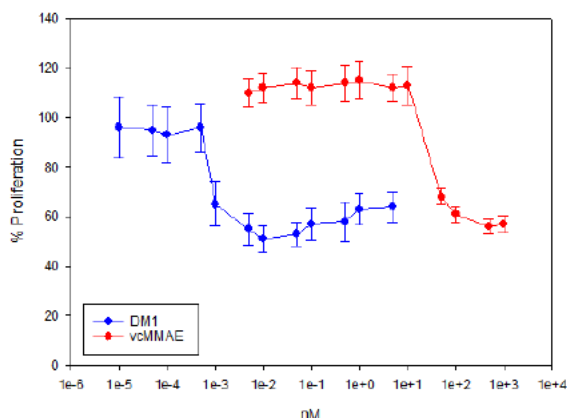


Figure 8.3. Antiproliferative activity of DM1 and vcMMAE cytotoxic drugs tested on SKBR3 cells and measured with MTS test.

The DM1 cytotoxic drug presented a stronger effect on the SKBR3 cells, with its IC_{50} value close to the 0.001 nM, while vcMMAE was around 50 nM (Table 8.1). The IC_{50} factor corresponds to the index of cytotoxicity 50, which indicates the concentration of the drug at which it exerts an effect corresponding to the 50% of its maximum effect. For both drugs, these values were similar than bibliographic values (Abdollahpour-Alitappeh et al., 2017), (Lambert et al., 2014), therefore validating the activity assessment methods and the cytotoxic drugs.

Table 8.1. IC_{50} of DM1 and vcMMAE cytotoxic drugs

DM1	0.001 nM
vcMMAE	50 nM

In the case of the generated antibody-drug conjugate products, the heterogeneous ADCs Trastuzumab-DM1 (DAR 3) and Trastuzumab-vcMMAE (DAR 3.9) (see sections 5.2 and 5.3) were first evaluated, and their activity was compared to unconjugated Trastuzumab (Figure 8.4).

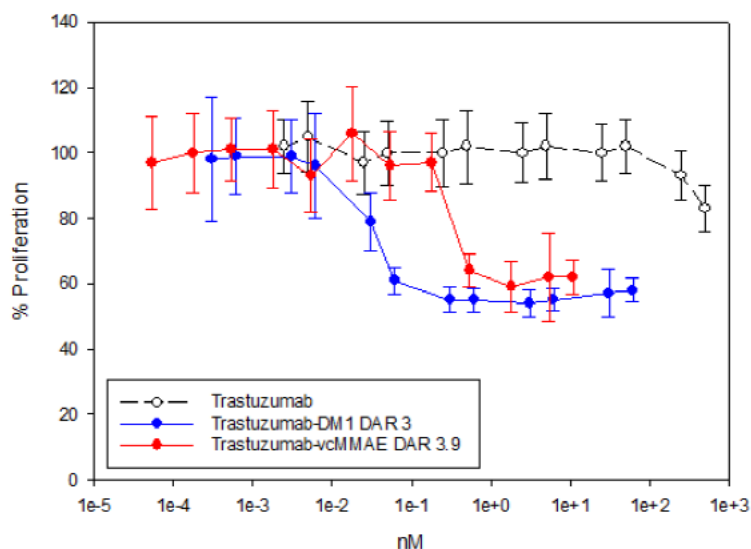


Figure 8.4. Antiproliferative activity of Trastuzumab, Trastuzumab-DM1 (DAR 3) and Trastuzumab-vcMMAE (DAR 3.9) tested on SKBR3 cells and measured with MTS test.

Trastuzumab, when unconjugated, presented almost no antiproliferation activity on target SKBR3 cells: only at very high concentrations, close to 500 nM, a lightly effect was observed. However, when conjugated, the potency of the molecule increased, reaching IC₅₀ values of around 0.03 nM for Trastuzumab-DM1 and 0.3 nM for Trastuzumab-vcMMAE (Table 8.2). Trastuzumab-DM1 IC₅₀ values are similar to reported bibliographic values (Phillips et al., 2008). The higher potency of DM1 was also observed in the conjugated products, where for similar DARs, or even with a slightly higher DAR for the vcMMAE conjugated ADC, the Trastuzumab-DM1 product displayed a higher antiproliferation activity.

Table 8.2. IC₅₀ of Trastuzumab heterogeneous conjugates

Trastuzumab	>100 nM
Trastuzumab-DM1 (DAR 3)	0.034 nM
Trastuzumab-vcMMAE (DAR 3.9)	0.32 nM

The generated homogeneous ADCs were also analyzed, and their antiproliferative activity profiles can be observed on Figure 8.5. The ADCs consisting in Trastuzumab conjugated to vcMMAE with a DAR of 7.3 (close to being completely homogeneous, with a targeted DAR of 8 (see section 6.2)), and a DAR of 3.9 (heterogeneous Trastuzumab-vcMMAE with a targeted DAR of 4) and Trastuzumab_cys114 conjugated to vcMMAE with a DAR of 1.79 (close to being homogeneous, aimed DAR of 2 (see section 6.3)) were evaluated. The ADCs displayed an efficacy proportional to their DAR value: the more loaded the antibody, the more antitumoral activity it has (Table 8.3). This is in concordance with some reports from literature, in which a similar trend is observed when the *in vitro* antiproliferative activity for ADCs with different DARs is assessed.

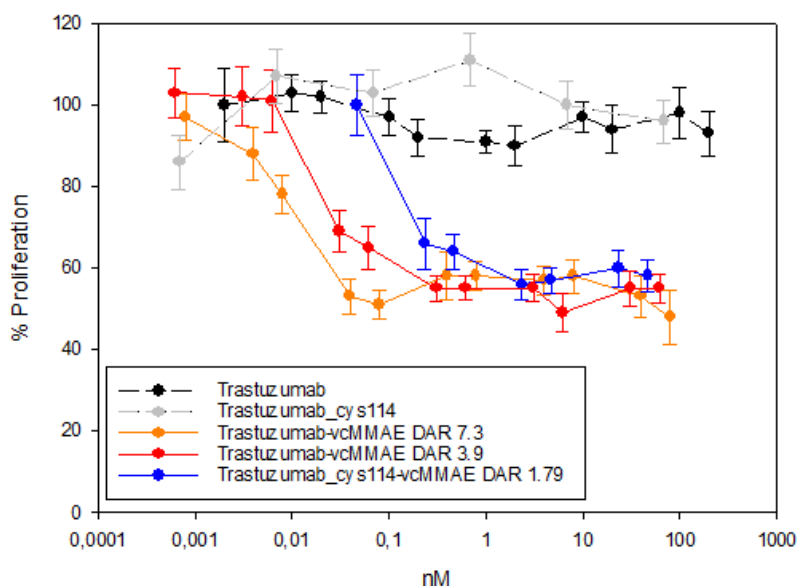


Figure 8.5. Antiproliferative activity of Trastuzumab conjugated to vcMMAE to DARs of 3.9 and 7.3; of Trastuzumab_cys114 conjugated to vcMMAE with a DAR of 1.79, and of the respective naked Trastuzumab and Trastuzumab_cys114 antibodies. Assays performed on SKBR3 cells and measured with MTS test.

Table 8.3. IC₅₀ of Trastuzumab and Trastuzumab_cys114-vcMMAE conjugates

Trastuzumab_cys114-vcMMAE (DAR 1.79)	0.14 nM
Trastuzumab-vcMMAE (DAR 3.9)	0.046 nM
Trastuzumab-vcMMAE (DAR 7.3)	0.008 nM

In the case of the homogeneous ADC with a DAR of 2 generated from the conjugation of light chains and their subsequent *in vitro* assembly with independently produced heavy chains (see section 6.4), its antiproliferative activity was also coherent with the load of the ADC, being lower than an heterogeneous Trastuzumab-vcMMAE with a DAR of 3.9 (Figure 8.6).

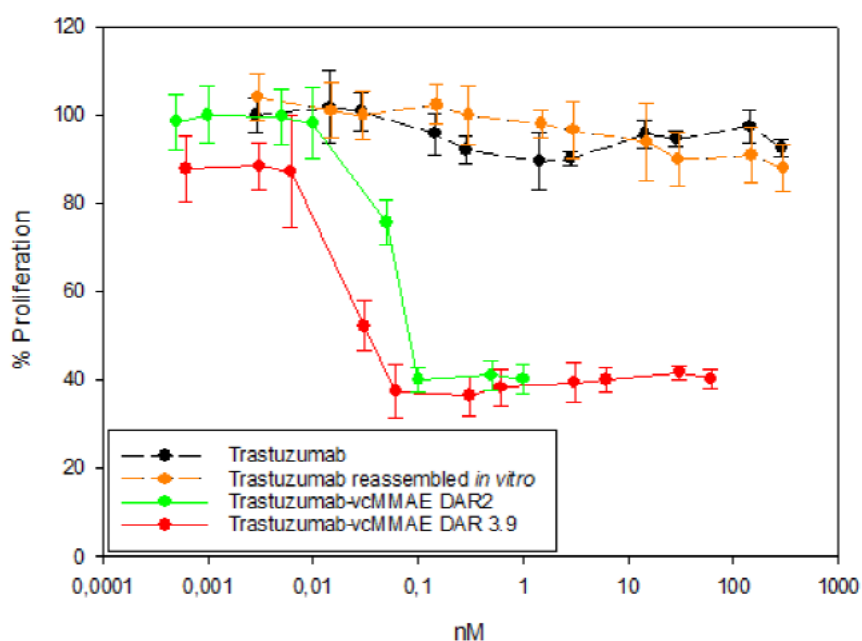


Figure 8.6. Antiproliferative activity of Trastuzumab conjugated to vcMMAE to a DARs of 3.9 and of Trastuzumab *in vitro* reassembled conjugated to vcMMAE with a DAR of 2, and of the respective naked Trastuzumab and Trastuzumab *in vitro* reassembled antibodies. Assays performed on SKBR3 cells and measured with MTS test

Chapter 11. Appendix

Table 8.4. IC₅₀ of Trastuzumab and Trastuzumab *in vitro* reassembled conjugates

Trastuzumab-vcMMAE (DAR 2)	0.050 nM
Trastuzumab-vcMMAE (DAR 3.9)	0.023 nM

The conjugated scFv fragments (see chapter 7) also showed an antitumoral effect on SKBR3 cells (Figure 8.7). The heterogeneous scFv-DM1 (DAR of 0.9) and the homogeneous scFv_cys111 (DAR of 1) had very similar antiproliferative profiles, with almost identical IC₅₀ values (Table 8.5). However, they have a lower efficacy than the ADCs generated from the whole Trastuzumab antibody. This could be due to the fact that whole ADCs are loaded with higher drug content (2-8 drug molecules per antibody, in contrast to around 1 for the conjugated scFv fragments). Another explanation could rely on a possible lower binding affinity of the fragments with respect to the whole antibodies for the target HER2 antigen: an scFv fragment has only one binding domain to the target antigen, compared to two domains for a whole IgG, resulting in a loss of avidity (accumulated strength of multiple affinities of non-covalent interactions (Kitov et al., 2003)) for the scFv (Hess et al., 2014).

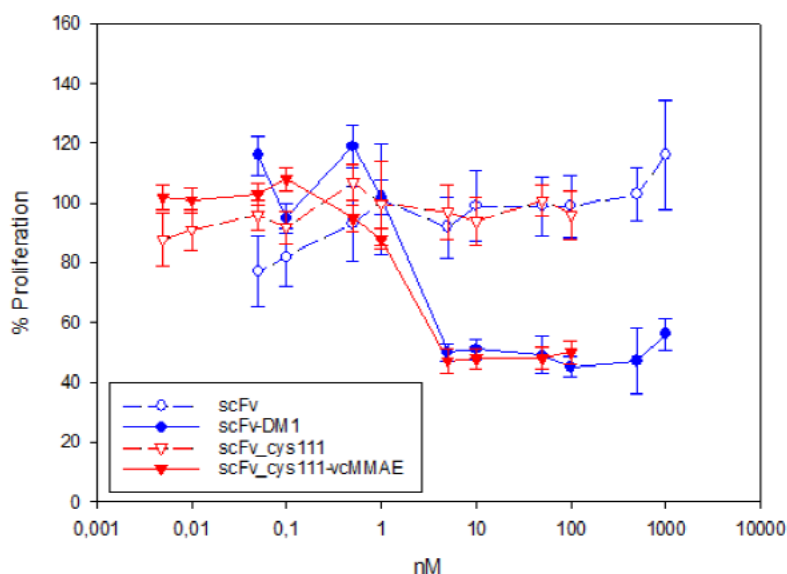


Fig. 8.7. MTS activity of scFv and scFv_cys111 conjugates.

Table 8.5. IC₅₀ of scFv and scFv_cys111 conjugates

scFv-DM1 (DAR 0.9)	3 nM
scFv_cys111-vcMMAE	3 nM

Once the antitumoral capacity of the generated ADCs had been tested on a classical 2D *in vitro* platform, a different approach was attempted, consisting in developing a 3D model.

8.3. 3D *in vitro* assays with SKBR3 cell line:

A 3D *in vitro* assay for an improved assessment of the antiproliferative activity of the developed ADC molecules was attempted. Several methodologies for generating 3D cell culture models were employed, and then the suitability of the generated model for the assessment of the efficacy of the generated drugs was analyzed.

8.3.1. 3D culture with SKBR3: assessed methodologies

Different culture strategies were tested in order to generate a 3D model for the SKBR3 model cell line, in the form of cell spheroids. Some scaffold-free methods (hanging drop and culture in ultra-low attachment plates) were employed, as well as methodologies taking advantage of organic scaffolds (Matrigel and collagen). The applied approaches are summarized in Table 8.6. and consist in the following (see section 10.12.4 of Material and Methods section for more information):

- Hanging drop: a culture medium drop containing the cells of interest is left hanging from the inside part of the lid of a culture plate. The cells end by forming a spheroid by gravity (Montanez-Sauri et al., 2013).

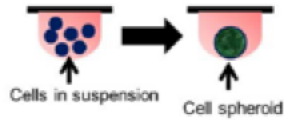


Figure 8.8. Schematic depiction of hanging drop method. Obtained from (Gupta et al., 2016).

- Culture in ultra-low attachment (ULA) plate: cells are cultured in plates with an hydrophilic neutrally charged hydrogel coating, therefore impairing the attachment of the cells and forcing them to grow forming aggregates or spheroids.

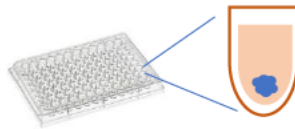


Figure 8.9. Schematic depiction of ULA culture.

- Embedded seeding with Matrigel/collagen: Matrigel is the commercial name of an extracellular matrix mixture extracted from Englebreth-Holm-Swarm tumors in mice, primarily consisting of the proteins collagen IV, laminin and enactin, which are typical structural proteins from extracellular matrices (Hughes et al., 2010). It also contains growth factors that can influence the growth of the cells in a 3D conformation. Directly using collagen hydrogels as a scaffold for cell culture also allows the growth of cell cultures in 3D, resulting in a more controlled approach than using Matrigel, but with a lower amount of proteins and factors that can be critical for the cell growth. In embedded cultures, the hydrogel is mixed with the culture medium and the cells, which grow inside the matrix (scaffold) formed when the hydrogel solidifies (Lee et al., 2010).

- On top seeding with Matrigel/collagen: in this case, the hydrogel and the culture medium are mixed, the hydrogel solidifies and the cells are seeded on top of the mixture (Weigelt et al., 2010).

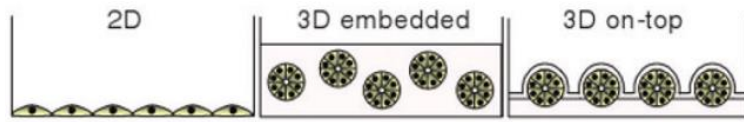


Figure 8.10. Schematic depiction of 3D embedded and on top cultures. Obtained from (Lee et al., 2010).

- Culture in ULA plate with Matrigel and centrifugation: this strategy combines the use of ULA plates with the addition of the Matrigel polymer. The cells are mixed with the culture medium and Matrigel (2.5% v/v), and before the polymerization of Matrigel takes place, a centrifugation step is applied, maintaining the cells in the center of the well, forming a spheroid (Ivascu et al., 2007).



Figure 8.11. Schematic depiction of ULA+centrifugation method for 3D culture generation. Obtained from (Gupta et al., 2016).

Chapter 11. Appendix

Table 8.6. Culture strategies tested for the obtention of 3D models with SKBR3

3D Methodology attempted	Resulting culture
Hanging drop	Loose aggregate
Culture in ultra low attachment plate	Loose aggregate
Embedded seeding with Matrigel	Individual cells
Embedded seeding with collagen	Individual cells
On top seeding with matrigel	Individual cells
On top seeding with collagen	Individual cells
Culture in ULA plate with Matrigel and centrifugation	Spheroid

From all the different culture strategies applied, only when SKBR3 cells were cultured in an ULA plate with Matrigel and centrifugated, they were able to grow forming a spheroid-like structure (Figure 8.12.). In the case of the other methodologies, cells grew individually, or were only able to form loose aggregates (Figure 8.12. A), which were not compact and resistant enough, their morphology not corresponding to a spheroid.

SKBR3 cells have been described as a difficult cell line for 3D culture, since they lack the E-cadherin protein that allows the intercellular cell-cell interaction, which is present in cell lines that spontaneously generate tight spheroids (Ivascu et al., 2007). Therefore, only in the very specific cell culture conditions described, they were able to grow in a spheroid conformation.



Figure 8.12. Pictures of SKBR3 cells: A) without matrigel nor centrifugation, B) with 2.5% matrigel, C) with 5% matrigel. Pictures obtained from a phase inverted microscope (Nikon, TMS) and a Nikon Coolpix 5400 camera.

Once the SKBR3 spheroid generation was achieved, they were used to evaluate the antiproliferative activity of the developed ADCs.

8.3.3. ADC antiproliferative activity assessment with SKBR3 spheroids

The developed spheroids were then used for assessing the antiproliferative activity of the generated ADCs. In a first assay, Trastuzumab and Trastuzumab-vcMMAE (DAR 7.3) antiproliferative activity was analyzed on SKBR3 spheroids and SKBR3 2D cultures side by side. In the 2D culture, the typical antiproliferation profile was observed, however, in the assay carried out with spheroids, an effect of the tested molecules could not be observed (Figure 8.13), the spheroid being much more resistant than the 2D culture.

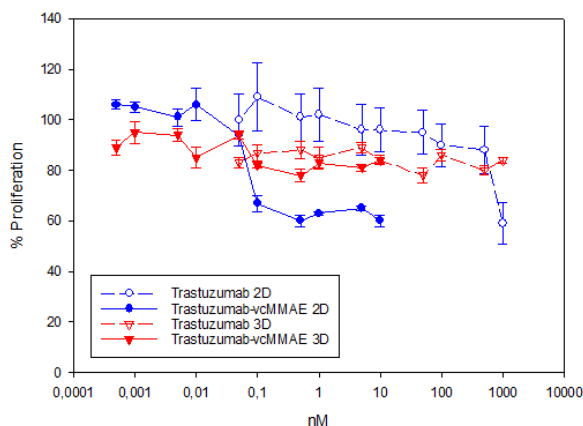


Figure 8.13. Antiproliferative profile of Trastuzumab and Trastuzumab-vcMMAE (DAR 7.3) in 2D and 3D SKBR3 cell cultures. MTS assay.

This effect can be attributed to the spheroid conformation, in which the involved cells are more resistant to drug treatment than in a bidimensional display.

In order to determine if the lack of effect on the SKBR3 spheroids was related to the size of the ADC, being too big and thus unable to penetrate into the spheroid,

spheroids were treated with vcMMAE (1316 Da vs >145000 Da for the ADC) (Figure 8.14). The assay resulted in a similar profile than the obtained for the ADC, therefore confirming the increased resistance of the 3D versus the 2D configuration, even for small molecules. This behavior has been reported in the literature (Imamura et al., 2015).

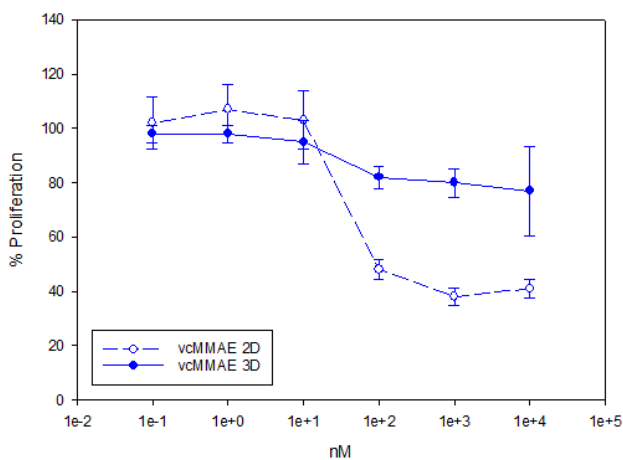


Figure 8.14. Antiproliferative profile of vcMMAE in 2D and 3D SKBR3 cell cultures. MTS assay.

An alternative methodology to quantify the antitumoral effect of the developed ADCs on the SKBR3 cells was also implemented, in order to discard a possible non-functionality of the MTS assay in the 3D cultures. In this case, the cells, after their incubation with the cytotoxic drug, were stained with propidium iodide and observed with confocal microscopy (Figures 8.15, 8.16 and 8.17) (see section 10.12.6). Propidium iodide is an intercalating agent that stains the DNA and RNA and is not membrane-permeable, therefore only staining the dead cells (both apoptotic and necrotic). This assay revealed, again, that the 3D cultures were more resistant than their 2D counterparts: when treated with vcMMAE, the viability was lower in the 2D than the 3D culture (Figure 8.18).

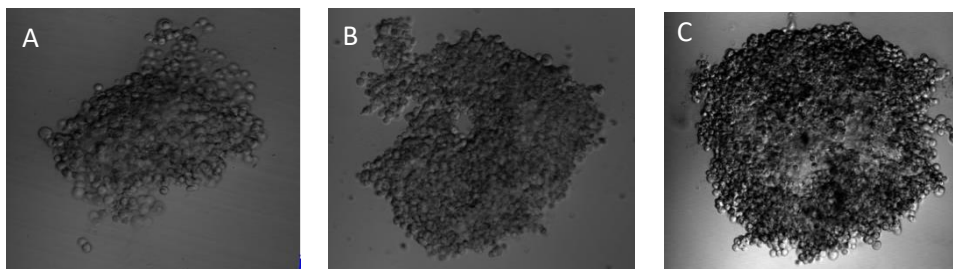


Figure 8.15. Pictures of SKBR3 cells 3D spheroids obtained with confocal microscopy (Leica TCS SP.5): A) Treated with vcMMAE 10 μM , B) Treated with vcMMAE 0.025 μM C) untreated (positive control). Pictures correspond to the brightfield channel.

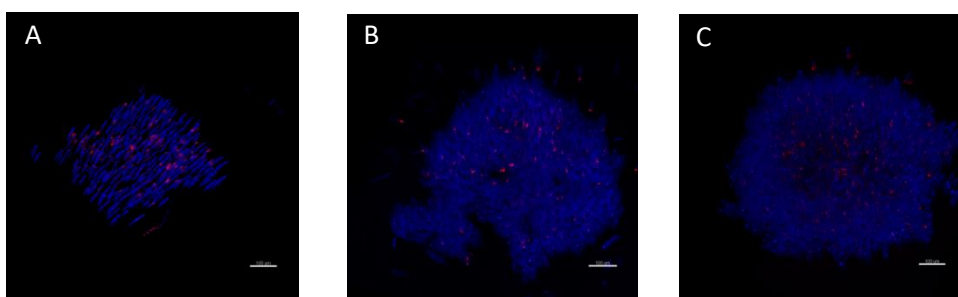


Figure 8.16. Pictures of SKBR3 cells 3D spheroids obtained with confocal microscopy (Leica TCS SP.5): A) Treated with vcMMAE 10 μM , B) Treated with vcMMAE 0.025 μM C) untreated (positive control). Blue staining (Hoetsch) corresponds to total nuclei number, while red staining (propidium iodide) corresponds to nuclei of dead cells.

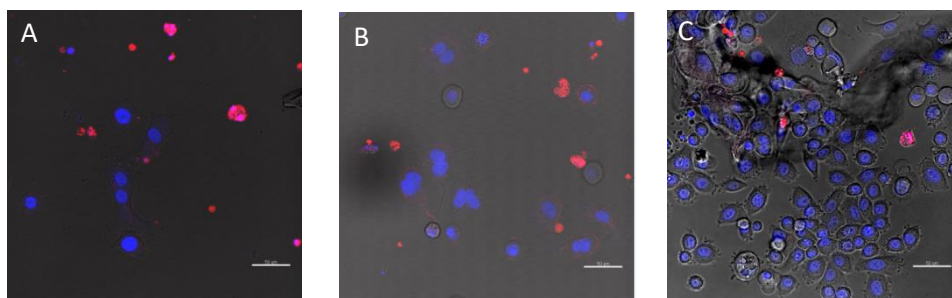


Figure 8.17. Pictures of SKBR3 cells in 2D 96 well plates obtained with confocal microscopy (Leica TCS SP.5): A) Treated with vcMMAE 10 μM , B) Treated with vcMMAE 0.025 μM C) untreated (positive control). Blue staining (Hoetsch) corresponds to total nuclei number, while red staining (propidium iodide) corresponds to nuclei of dead cells.

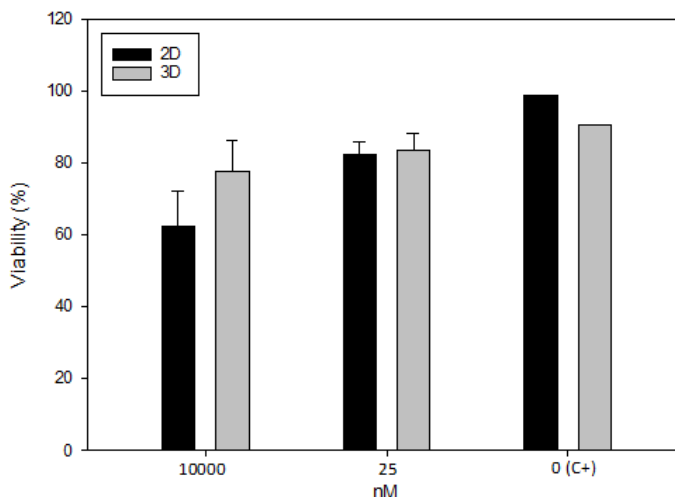


Figure 8.18. Viability of 2D and 3D (spheroid) SKBR3 cell cultures treated with vcMMAE at different concentrations and assessed with propidium iodide staining. Error bars represent the standard deviation from independent replicates.

In a further step to validate the antitumor activity of the generated ADCs, an *in vivo* assay was developed and applied.

8.4. *In vivo* assay: tumor model with SKBR3 cell line

8.4.1. Model mice generation

Once the antitumor effect of the developed ADCs had been proven *in vitro*, in order to definitively validate the activity of the developed cytotoxic drug, an *in vivo* assay was developed and applied. This assay was developed by the Functional Validation and Preclinical Research service of the Vall d'Hebron Institute of Research (Barcelona). The first step of the process consisted in the engraftment of the tumor in immunosuppressed mice. Since it was the cell line that had been used to develop the *in vitro* assays, SKBR3 cell line was first used to generate the mice model for performing the *in vivo* assay. In a first attempt, SKBR3 cells cultured at UAB were used for an orthotopic inoculation: a mixture of $10 \cdot 10^6$ cells with the gelatinous

protein mixture Matrigel were inoculated in the adipose panicle of the breast gland of the nude Balb/c mice that were used for the assay. This inoculation was deemed to be more potentially successful than a subcutaneous one, since it is reported to yield better growth of the implanted tumors (Kerbel et al., 1991; Manzotti et al., 1993). After 7 days, an initial tumor of around 50 mm³ seemed to be established, however, after 4-7 days the volume decreased to around 25 mm³ and remained stable at this value for the rest of the experiment (see Figure 8.19).

In a second attempt, nude NOD-SCID mice were inoculated with SKBR3 cells. Since NOD-SCID mice are more immunosuppressed than nude mice, it was expected that the tumor engraftment could be improved in this strain. The tumor evolution presented a similar trend to that observed in the nude mice: after 11 days a tumor of around 30 mm³ seemed to appear, but it did not grow any further (Figure 8.19).

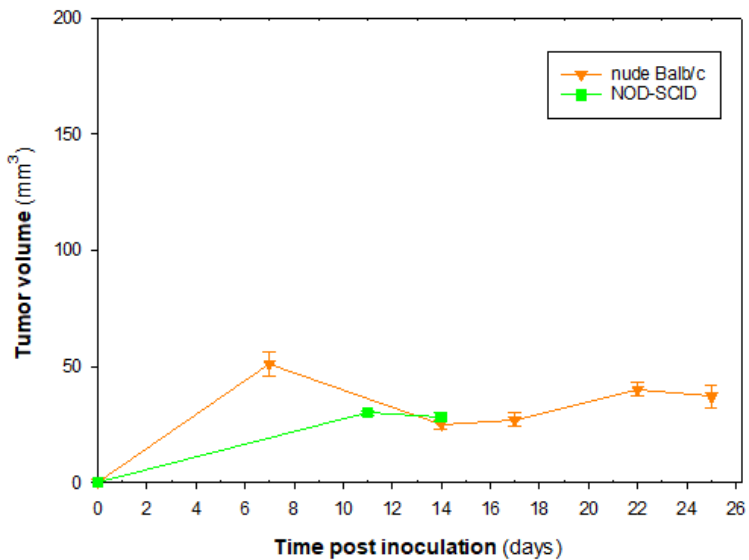


Figure 8.19: evolution of tumor volume of SKBR3 cells inoculated on NOD-SCID and nude Balb/c mice.

A third attempt was performed again, in this case, Rag mice were used. Since these mice are more immunosuppressed than previously used nude Balb/c and NOD-SCID mice, it was expected that the implementation of the tumor could be facilitated.

However, successful growth of the tumor was not observed in these conditions neither.

As previously stated in the introduction of this chapter, SKBR3 cell line has been reported to have successfully been used as a breast cancer model cell line for tumor generation in mice. However, other reports describe it as a cell line that forms poorly differentiated tumors in immunocompromised mice (ATCC, 2016), or that does not form tumors at all (van Slooten et al., 1995). This, added to the poor ability of 3D culture of this cell line in the form of spheroid generation, led to trying an alternative cell line for the *in vivo* model generation: BT474. This cell line has been reported to develop into tumors when inoculated in mice (Bryant et al., 2015), (G. D. Phillips et al., 2008). It has been specifically described as a better cell line than SKBR3 for mouse xenograft development (van Slooten et al., 1995).

8.5. 2D *in vitro* assays with BT474 cell line:

BT474 cell line was first assessed in the bidimensional MTS assay previously performed for SKBR3. Its response to the treatment with vcMMAE, heterogeneous Trastuzumab-vcMMAE (DAR 3.9) and homogeneous Trastuzumab-vcMMAE (DAR 2) generated from *in vitro* reassembled chains, was similar than for SKBR3 (Figure 8.20), thus validating the BT474 cell line for assessing the ADCs efficacy.

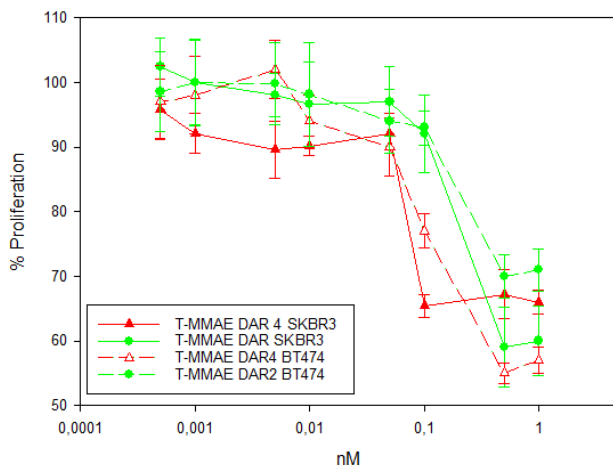


Figure 8.20. Proliferation profiles of SKBR3 and BT474 cells treated with Trastuzumab-vcMMAE (DAR 3.9) and Trastuzumab-vcMMAE (DAR 2).

Since BT474 has been described as a cell line more suitable for spheroid generation than SKBR3 (Ivascu et al., 2007), it was tested for 3D culture.

8.6. 3D *in vitro* assays with BT474 cell line:

BT474 cells displayed a spheroid formation when cultured in ultra-low attachment plates, without needing to add Matrigel nor centrifugate the plate (Figure 8.21), confirming the reports from literature (Ivascu et al., 2007).

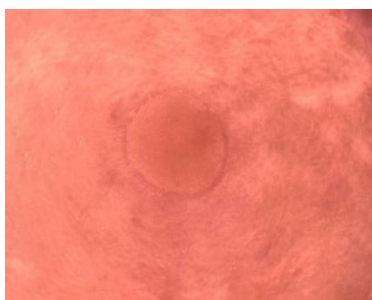


Figure 8.21. BT474 cells forming a spheroid when cultured in ULA plates.

The BT474 spheroids were more resistant to the effect of the vcMMAE drug than the 2D cultures, similarly than SKBR3 (Figure 8.22).

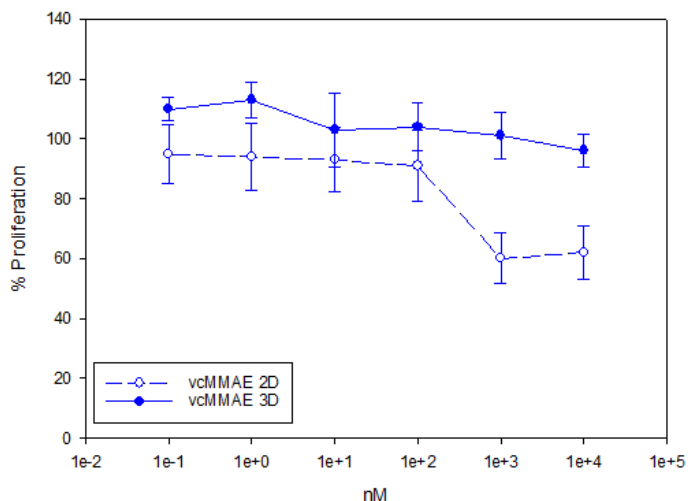


Figure 8.22.
Proliferation profiles
of BT474 spheroids
and 2D cultures
treated with
vcMMAE.

As it had been performed for SKBR3 cells, the spheroids were stained with propidium iodide and observed using a confocal microscope and pictures of the spheroids were taken (Figures 8.23, 8.24 and 8.25) and their viability assessed (Figure 8.26).

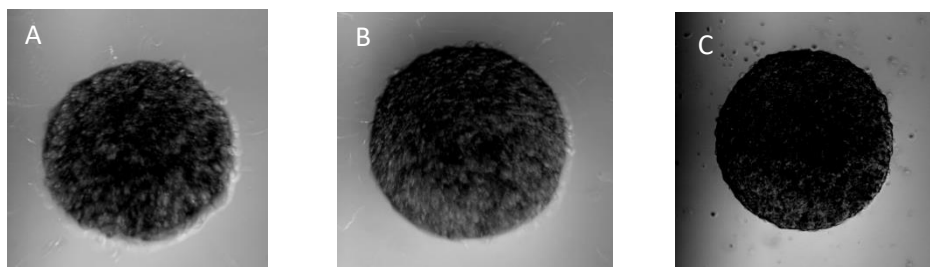


Figure 8.23. Pictures of BT474 cells 3D spheroids obtained with confocal microscopy (Leica TCS SP.5): A) Treated with vcMMAE 10 μ M, B) Treated with vcMMAE 0.025 μ M C) untreated (positive control). Pictures correspond to the brightfield channel.

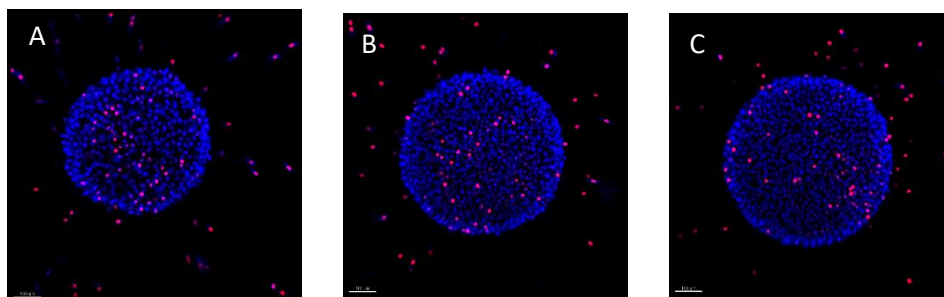


Figure 8.24. Pictures of BT474 cells 3D spheroids obtained with confocal microscopy (Leica TCS SP.5): A) Treated with vcMMAE 10 μ M, B) Treated with vcMMAE 0.025 μ M C) untreated (positive control). Blue staining (Hoetsch) corresponds to total nuclei number, while red staining (propidium iodide) corresponds to nuclei of dead cells.

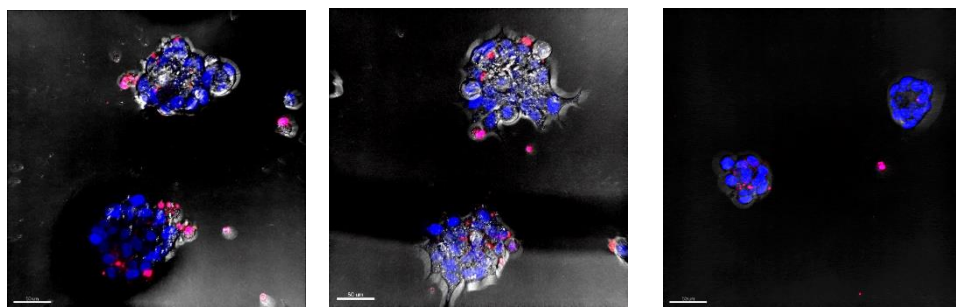


Figure 8.25. Pictures of BT474 cells in 2D 96 well plates obtained with confocal microscopy (Leica TCS SP.5): A) Treated with vcMMAE 10 μ M, B) Treated with vcMMAE 0.025 μ M C) untreated (positive control). Blue staining (Hoetsch) corresponds to total nuclei number, while red staining (propidium iodide) corresponds to nuclei of dead cells.

Similarly to SKBR3 spheroids, they were more resistant to vcMMAE than the 2D cultures. The pictures obtained from confocal microscopy reveal spheroid morphology much more round-shaped than the one obtained from SKBR3, again indicating the ability of BT474 cells to form spheroids.

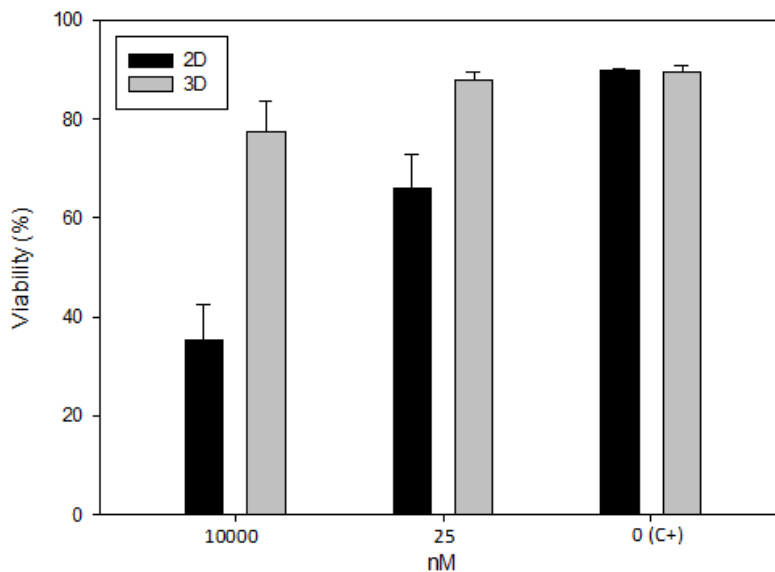


Figure 8.26. Viability of 2D and 3D (spheroid) BT474 cell cultures treated with vcMMAE at different concentrations and assessed with propidium iodide staining. Error bars represent the standard deviation from independent replicates.

Finally, once their response to the ADC products having been validated *in vitro*, BT474 cells were used to generate an *in vivo* model.

8.7. *In vivo* assay: tumor model with BT474 cell line

8.7.1. Model mice generation

In order to develop the *in vivo* model, BT474 cells were inoculated in athymic nude mice. The mice were orthotopically inoculated: a mixture of $10 \cdot 10^6$ cells with the gelatinous protein mixture Matrigel were inoculated in the adipose panicle of the breast gland of each mouse. Estrogen supplements pellets 17 β -Estradiol and enrofloxacin were fed to the mice. Since BT474 cell line expresses the estrogen receptor (ER), the estrogen supplementation contributes to induce the growth of the

cells into forming a tumor (Liang et al., 2010). In this case, the mice successfully developed a tumor, reaching between 75 and 125 mm³, therefore enabling starting with the ADC validation assay.

8.7.2. *In vivo* ADC validation

Using the successfully developed BT474 xenograft mouse model, the Trastuzumab-vcMMAE ADC with a DAR = 2 generated from the *in vitro* assembly of its chains had its antitumor activity assessed. The ADC was contained in a 50 mM sodium citrate solution, pH = 6, which was the solution used for the chains assembly (see section 6.4). This buffer has a similar osmolarity than other typical physiological buffers: 50 mM citrate buffer has a concentration of 13.5 g/l versus the approximate 9 g/l of phosphate buffered saline medium (PBS) or ringer buffer (NaCl 0.9%). Prior to the administration of the ADC, some mice were administrated with the buffer in order to assess that it did not have a negative impact over the mice wellbeing. After 24h, the mice did not show any unhealthy symptom.

The dose of administration was set at 15 mg/kg, based on literature review from other ADC *in vivo* assays (G. D. Phillips et al., 2008), (Lambert & Chari, 2014), (Barok et al., 2011), (Menderes et al., 2017), (Li et al., 2018). The dose was based on total mAb content. This dose aimed to be high enough to allow tumor regression while, at the same time, not resulting in toxicities derived from the drug. For the same reasons, administration pattern was set at once per week.

The administration of the ADC drug resulted in a regression of the tumor volume from the beginning of the treatment. After 8 days of treatment and the first administration had been performed, the treated mice showed a clear regression of the tumor volume (Figure 8.27). After the second administration, decrease in the body weight of the mice was observed (see Figure 8.23). Since the difference of body weight from the start of the experiment was close to 10%, and 2 of the mice were lower than 10%, it was decided to stop the administration of the ADC in order to see

if the weight was recovered. From this point on, the body weight of the mice remained stable, while the tumor volume continued to decrease, and at endpoint, after 23 days of treatment, 7 out of the 10 mice presented a complete regression of the tumor (Fig 8.27). At this point, 5 out of the 10 mice presented a 10% loss of weight from the beginning of the assay, and some toxicity effects were observed in some of the mice 4 mice, which had lost between 16 and 22% of the weight, presented signs of cachexia (loss of appetite), hunched (antalgic) position, apathy (reduced motility) and dermatitis.

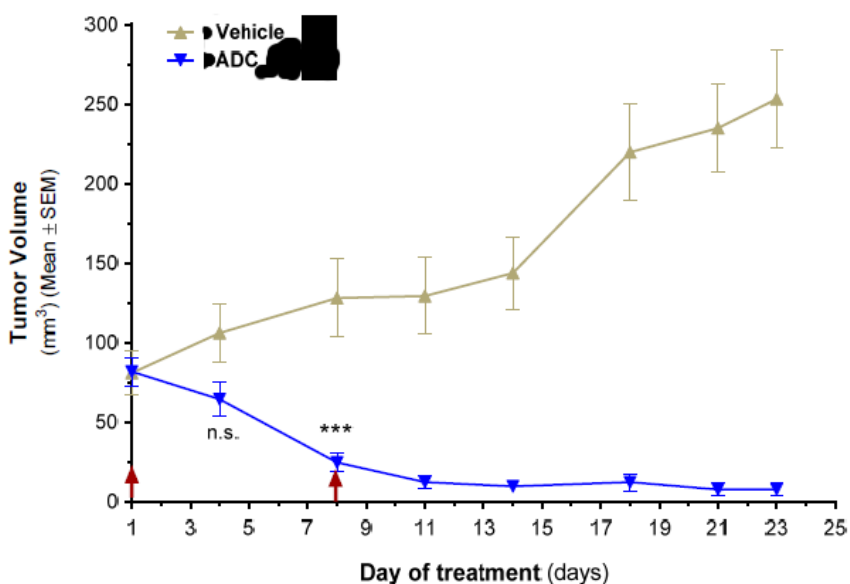


Figure 8.27: Comparative analysis of the primary orthotopic tumor growth of BT474 cells treated with the vehicle or the Trastuzumab-vcMMAE DAR2 ADC. Red arrows indicate when treatment was administered to both groups. The tumors no measurable are included with value 0. On day 8, ADC treated group presented much smaller tumor volumes ($p = 0.0003$, t-test).

It is worth pointing out that treatment with 17 β -Estradiol by itself might cause some weight loss. In this regard, in the control group (treated with the vehicle), no net gain of weight occurred (moreover, 3/8 mice showed losses above 5%), differently to what would be expected for young mice (6-10 week old) (Figure 8.28). Therefore,

the combination of 17β -Estradiol with the tested ADC might have increased the inherent toxicity of the tested ADC in this specific animal model. This observed pattern in weight loss is quite similar to other weight loss profiles reported in the literature for ADC-treated mice (Bryant et al., 2015). The toxicity effects of the ADC on the mice could be mitigated applying lower doses and a dosage pattern with a lower frequency, finding the compromise between tumor regression and avoidance of secondary effects.

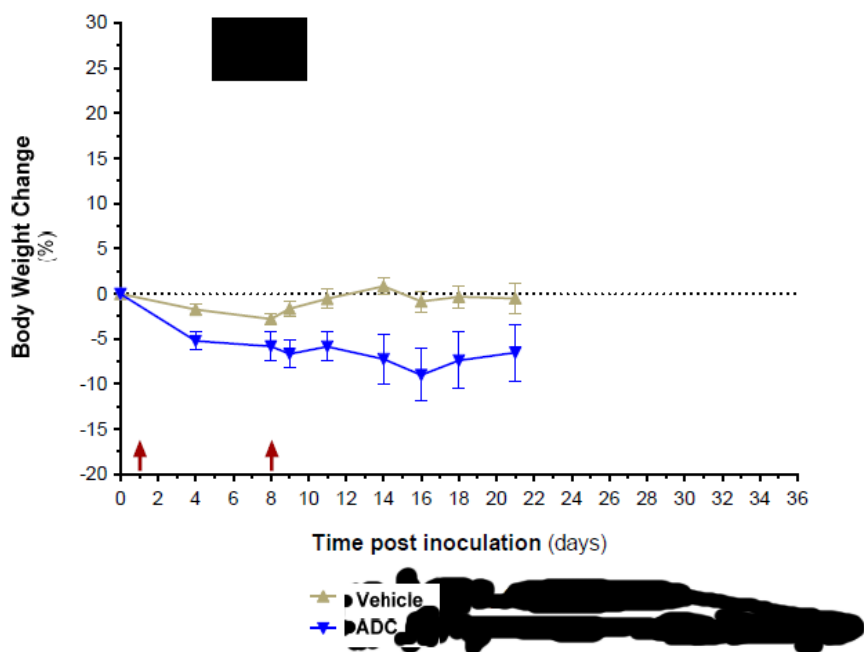


Figure 8.28: evolution of the mice weight loss measured in percentage of body weight change from the beginning of the assay. Red arrows indicate administration point.

It can be stated that the assessed ADC was successfully validated in terms of antitumoral activity: on day 8, mean tumor volumes in vehicle-treated group was 128.1 ± 24.59 and in ADC treated group it was 24.72 ± 5.67 mm³. This difference is already statistically significant (student t test, $p = 0.0003$). After the second administration on day 8, tumors continued to reduce their size along time, and on

day 23, at endpoint, only 3 animals showed palpable and measurable tumors, with mean tumor volumes of 253.2 ± 30.96 for vehicle-treated group and 7.853 ± 4.178 for ADC treated animals. Accordingly, tumor weight at end point was significantly smaller in the group treated with the ADC: 185.8 ± 23.3 mg for the vehicle-treated vs 17.01 ± 6.4 for the ADC treated.

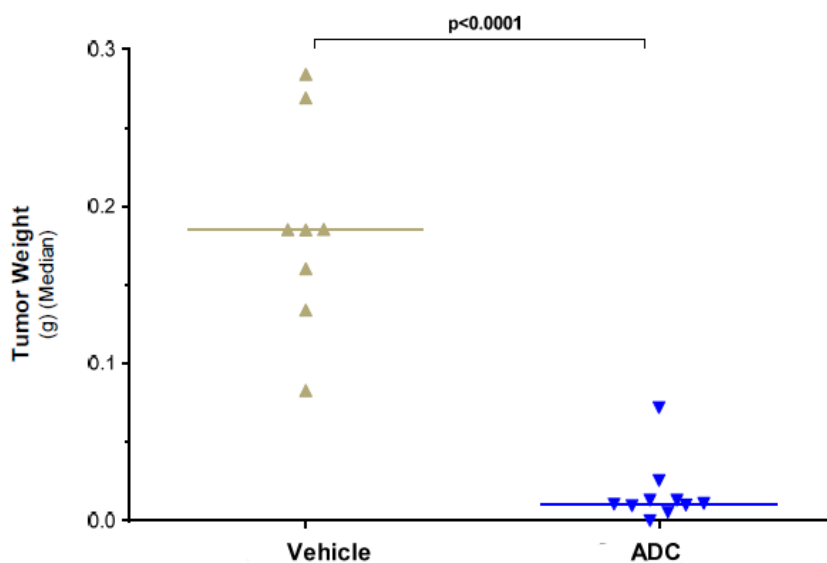


Figure 8.29. Ex vivo tumor weight at end point. Ex vivo weight was statistically different between both groups ($p < 0.0001$, t-test).

8.5. Conclusions

In this chapter, *in vitro* 2D and 3D models have been developed for the assessment of the antitumor activity of the antibody and fragment conjugates generated along this work. Moreover, one of the candidates, the ADC Trastuzumab-vcMMAE generated from the *in vitro* reassembly of its chains, has been *in vivo* assessed in an animal model.

In the 2D *in vitro* model based on the metabolic MTS assay, the developed molecules showed their antiproliferation activity, with all the ADCs having an IC_{50} in the pM (<1 nM) range. Regarding the heterogeneous ADCs, Trastuzumab-DM1 (DAR 3) showed a higher antiproliferative activity than the Trastuzumab-vcMMAE (DAR 4). In the Trastuzumab-vcMMAE conjugates at different DARs, the *in vitro* potency was directly proportional to their drug load. Regarding the scFv conjugates, heterogeneous scFv-DM1 (DAR 0.9) presented similar potency values than homogeneous scFv-vcMMAE (DAR 1), and they were less effective than their whole antibody counterparts.

A 3D model was attempted with SKBR3 cells applying several methodologies including scaffold-free methods such as culture in ultra-low attachment plates and methods using hydrogel scaffolds (Matrigel and collagen). However, the only approach resulting in the formation of spheroids consisted in the combination of the addition of Matrigel to the culture and centrifugation of the plate. These spheroids were much more resistant than their 2D counterparts to the developed ADCs, and also to the unconjugated cytotoxic drug vcMMAE.

Finally, in order to validate the most innovative generated ADC of this work, (Trastuzumab-vcMMAE obtained from *in vitro* assembly of its chains) an *in vivo* model was developed and used. The first attempt using SKBR3 cells did not result in the engraftment of tumors in the inoculated mice. This was solved by using an alternative cell line, BT474, which is more prone to its growth in 3D and tumor-like morphologies. In the animal model generated with BT474 cell line, the tested ADC caused a complete tumor regression in 7 of the 10 treated mice in three weeks, showing a potent antitumoral activity and thus validating the constructed molecule as a candidate for breast cancer therapy.

8.6. References

Abdollahpour-Alitappeh, M., Razavi-vakhshourpour, S., Lotfinia, M., Jahandideh, S., Najminejad, H., Balalaie, S., ... Abolhassani, M. (2017). Monomethyl auristatin

- E Exhibits Potent Cytotoxic Activity against Human Cancer Cell Lines SKBR3 and HEK293. *Novelty in Biomedicine*, 4(5), 145–151. Retrieved from <https://pdfs.semanticscholar.org/1aa5/4d204961938a4a05d0b01b1eabfbc1c2ba55.pdf>
- Barok, M., Tanner, M., Köninki, K., & Isola, J. (2011). Trastuzumab-DM1 causes tumour growth inhibition by mitotic catastrophe in trastuzumab-resistant breast cancer cells in vivo. *Breast Cancer Research*, 13(2), R46. <https://doi.org/10.1186/bcr2868>
- Bosma, G. C., Custer, R. P., & Bosma, M. J. (1983). A severe combined immunodeficiency mutation in the mouse. *Nature*, 301(5900), 527–530. Retrieved from <http://www.ncbi.nlm.nih.gov/pubmed/6823332>
- Bryant, P., Pabst, M., Badescu, G., Bird, M., McDowell, W., Jamieson, E., ... Godwin, A. (2015). In vitro and in vivo evaluation of cysteine rebridged trastuzumab-MMAE antibody drug conjugates with defined drug-to-antibody ratios. *Molecular Pharmaceutics*, 12(6), 1872–1879. <https://doi.org/10.1021/acs.molpharmaceut.5b00116>
- Gupta, N., Liu, J. R., Patel, B., Solomon, D. E., Vaidya, B., & Gupta, V. (2016a). Microfluidics-based 3D cell culture models: Utility in novel drug discovery and delivery research. *Bioengineering & Translational Medicine*, 1(1), 63–81. <https://doi.org/10.1002/btm2.10013>
- Gupta, N., Liu, R., Patel, B., Solomon, D. E., Vaidya, B., & Gupta, V. (2016b). Microfluidics-based 3D cell culture models : Utility in novel drug discovery and delivery research. *Bioengineering and Translational Medicine*, (March), 63–81. <https://doi.org/10.1002/btm2.10013>
- Hess, C., Venetz, D., Neri, D., Carter, P. J., Walsh, G., Coiffier, B., ... Braisted, A. C. (2014). Emerging classes of armed antibody therapeutics against cancer. *MedChemComm*, 5(4), 408. <https://doi.org/10.1039/c3md00360d>
- Holliday, D. L., & Speirs, V. (2011). Choosing the right cell line for breast cancer research. *Breast Cancer Research : BCR*, 13(4), 215.

<https://doi.org/10.1186/bcr2889>

- Hughes, C. S., Postovit, L. M., & Lajoie, G. A. (2010). Matrigel: A complex protein mixture required for optimal growth of cell culture. *PROTEOMICS*, *10*(9), 1886–1890. <https://doi.org/10.1002/pmic.200900758>
- Imamura, Y., Mukohara, T., Shimono, Y., Funakoshi, Y., Chayahara, N., Toyoda, M., ... Minami, H. (2015). Comparison of 2D- and 3D-culture models as drug-testing platforms in breast cancer. *Oncology Reports*, *33*(4), 1837–1843. <https://doi.org/10.3892/or.2015.3767>
- Ito, R., Takahashi, T., Katano, I., & Ito, M. (2012). Current advances in humanized mouse models. *Cellular & Molecular Immunology*, *9*(3), 208–214. <https://doi.org/10.1038/cmi.2012.2>
- Ivascu, A., & Kubbies, M. (2007). Diversity of cell-mediated adhesions in breast cancer spheroids. *International Journal of Oncology*, *31*(6), 1403–1413. <https://doi.org/10.3892/ijo.31.6.1403>
- Jernström, S., Hongisto, V., Leivonen, S.-K., Due, E. U., Tadele, D. S., Edgren, H., ... Sahlberg, K. K. (2017). Drug-screening and genomic analyses of HER2-positive breast cancer cell lines reveal predictors for treatment response. *Breast Cancer (Dove Medical Press)*, *9*, 185–198. <https://doi.org/10.2147/BCTT.S115600>
- Johnson, M. (2012). Laboratory Mice and Rats. *Materials and Methods*, *2*. <https://doi.org/10.13070/mm.en.2.113>
- Kenny, P. A., Lee, G. Y., Myers, C. A., Neve, R. M., Semeiks, J. R., Spellman, P. T., ... Bissell, M. J. (2007). The morphologies of breast cancer cell lines in three-dimensional assays correlate with their profiles of gene expression. *Molecular Oncology*, *1*(1), 84–96. <https://doi.org/10.1016/J.MOLONC.2007.02.004>
- Kerbel, R. S., Cornil, I., & Theodorescu, D. (1991). Importance of orthotopic transplantation procedures in assessing the effects of transfected genes on human tumor growth and metastasis. *Cancer Metastasis Reviews*, *10*(3), 201–215. Retrieved from <http://www.ncbi.nlm.nih.gov/pubmed/1764765>
- Kitov, P. I., & Bundle, D. R. (2003). On the Nature of the Multivalency Effect: A

Chapter 11. Appendix

- Thermodynamic Model. *J. Am. Chem. Soc.*, 125(52), 16271–16284.
<https://doi.org/10.1021/JA038223N>
- Kotloff, D. B., Bosma, M. J., & Ruetsch, N. R. (1993). V(D)J recombination in peritoneal B cells of leaky scid mice. *The Journal of Experimental Medicine*, 178(6), 1981–1994. Retrieved from <http://www.ncbi.nlm.nih.gov/pubmed/8245777>
- Lambert, J. M., & Chari, R. V. J. (2014). Ado-trastuzumab Emtansine (T-DM1): An Antibody–Drug Conjugate (ADC) for HER2-Positive Breast Cancer. *Journal of Medicinal Chemistry*, 57(16), 6949–6964. <https://doi.org/10.1021/jm500766w>
- Lee, G. Y., Kenny, P. a, Lee, E. H., & Bissell, M. J. (2010). Three-dimensional culture models of normal and malignant breast epithelial cells. *Nature Methods*, 4(4), 359–365. <https://doi.org/10.1038/nmeth1015>.Three-dimensional
- Lewis Phillips, G. D., Li, G., Dugger, D. L., Crocker, L. M., Parsons, K. L., Mai, E., ... Sliwkowski, M. X. (2008). Targeting HER2-Positive Breast Cancer with Trastuzumab-DM1, an Antibody-Cytotoxic Drug Conjugate. *Cancer Research*, 68(22), 9280–9290. <https://doi.org/10.1158/0008-5472.CAN-08-1776>
- Li, G., Guo, J., Shen, B.-Q., Yadav, D. B., Sliwkowski, M. X., Crocker, L. M., ... Phillips, G. D. L. (2018). Mechanisms of Acquired Resistance to Trastuzumab Emtansine in Breast Cancer Cells. *Mol Cancer Ther*, 17(7). <https://doi.org/10.1158/1535-7163.MCT-17-0296>
- Liang, Y., Benakanakere, I., Besch-Williford, C., Hyder, R. S., Ellersieck, M. R., & Hyder, S. M. (2010). Synthetic progestins induce growth and metastasis of BT-474 human breast cancer xenografts in nude mice. *Menopause (New York, N.Y.)*, 17(5), 1040–1047. <https://doi.org/10.1097/gme.0b013e3181d3dd0c>
- Lovitt, C., Shelper, T., & Avery, V. (2014). Advanced Cell Culture Techniques for Cancer Drug Discovery. *Biology*, 3(2), 345–367. <https://doi.org/10.3390/biology3020345>
- Manzotti, C., Audisio, R. A., & Pratesi, G. (1993). Importance of orthotopic implantation for human tumors as model systems: relevance to metastasis and invasion. *Clinical & Experimental Metastasis*, 11(1), 5–14.

<https://doi.org/10.1007/BF00880061>

- Menderes, G., Bonazzoli, E., Bellone, S., Altwerger, G., Black, J. D., Dugan, K., ... Santin, A. D. (2017). Superior in vitro and in vivo activity of trastuzumab-emtansine (T-DM1) in comparison to trastuzumab, pertuzumab and their combination in epithelial ovarian carcinoma with high HER2/neu expression. *Gynecologic Oncology*, *147*(1), 145–152. <https://doi.org/10.1016/j.ygyno.2017.07.009>
- Montanez-Sauri, S. I., Sung, K. E., Berthier, E., & Beebe, D. J. (2013). Enabling screening in 3D microenvironments: probing matrix and stromal effects on the morphology and proliferation of T47D breast carcinoma cells. *Integrative Biology*, *5*(3), 631. <https://doi.org/10.1039/c3ib20225a>
- Phillips, G. D. L., Li, G., Dugger, D. L., Crocker, L. M., Parsons, K. L., Mai, E., ... Sliwkowski, M. X. (2008). Targeting HER2-Positive Breast Cancer with Trastuzumab-DM1, an Antibody–Cytotoxic Drug Conjugate. *Cancer Res*, *68*(22), 9280–9290. <https://doi.org/10.1158/0008-5472.CAN-08-1776>
- Phillips, G. D., Li, G., Dugger, D. L., Crocker, L. M., Parsons, K. L., Mai, E., ... Sliwkowski, M. X. (2008). Targeting HER2-positive breast cancer with trastuzumab-DM1, an antibody-cytotoxic drug conjugate. *Cancer Research*, *68*(22), 9280–9290. <https://doi.org/10.1158/0008-5472.CAN-08-1776>
- Riss, T. L., Moravec, R. A., Niles, A. L., Duellman, S., Benink, H. A., Worzella, T. J., & Minor, L. (2004). *Cell Viability Assays. Assay Guidance Manual*. Eli Lilly & Company and the National Center for Advancing Translational Sciences. Retrieved from <http://www.ncbi.nlm.nih.gov/pubmed/23805433>
- Romar, G. A., Kupper, T. S., & Divito, S. J. (2016). Research Techniques Made Simple: Techniques to Assess Cell Proliferation. *Journal of Investigative Dermatology*, *136*(1), e1–e7. <https://doi.org/10.1016/J.JID.2015.11.020>
- Saji Joseph, J., Tebogo Malindisa, S., & Ntwasa, M. (2019). Two-Dimensional (2D) and Three-Dimensional (3D) Cell Culturing in Drug Discovery. In *Cell Culture*. IntechOpen. <https://doi.org/10.5772/intechopen.81552>

Chapter 11. Appendix

- Sausville, E. A., & Burger, A. M. (2006). Contributions of Human Tumor Xenografts to Anticancer Drug Development. *Cancer Research*, *66*(7), 3351–3354. <https://doi.org/10.1158/0008-5472.CAN-05-3627>
- Shinkai, Y., Rathbun, G., Lam, K. P., Oltz, E. M., Stewart, V., Mendelsohn, M., ... Stall, A. M. (1992). RAG-2-deficient mice lack mature lymphocytes owing to inability to initiate V(D)J rearrangement. *Cell*, *68*(5), 855–867. Retrieved from <http://www.ncbi.nlm.nih.gov/pubmed/1547487>
- Shultz, L. D., Brehm, M. A., Garcia-Martinez, J. V., & Greiner, D. L. (2012). Humanized mice for immune system investigation: progress, promise and challenges. *Nature Reviews. Immunology*, *12*(11), 786–798. <https://doi.org/10.1038/nri3311>
- Shultz, L. D., Goodwin, N., Ishikawa, F., Hosur, V., Lyons, B. L., & Greiner, D. L. (2014). Human Cancer Growth and Therapy in Immunodeficient Mouse Models. *Cold Spring Harbor Protocols*, *2014*(7), pdb.top073585-pdb.top073585. <https://doi.org/10.1101/pdb.top073585>
- SK-BR-3 [SKBR3] (ATCC ® HTB-30™). (2016). Retrieved February 6, 2019, from http://www.lgcstandards-atcc.org/products/all/HTB-30.aspx?geo_country=es#characteristics
- Stock, K., Estrada, M. F., Vidic, S., Gjerde, K., Rudisch, A., Santo, V. E., ... Graeser, R. (2016). Capturing tumor complexity in vitro: Comparative analysis of 2D and 3D tumor models for drug discovery. *Scientific Reports*, *6*(1), 28951. <https://doi.org/10.1038/srep28951>
- Vaidya, H. J., Briones Leon, A., & Blackburn, C. C. (2016). FOXP1 in thymus organogenesis and development. *European Journal of Immunology*, *46*(8), 1826–1837. <https://doi.org/10.1002/eji.201545814>
- van Slooten, H. J., Bonsing, B. A., Hiller, A. J., Colbern, G. T., van Dierendonck, J. H., Cornelisse, C. J., & Smith, H. S. (1995). Outgrowth of BT-474 human breast cancer cells in immune-deficient mice: a new in vivo model for hormone-dependent breast cancer. *British Journal of Cancer*, *72*(1), 22–30. Retrieved

Chapter 11. Appendix

from <http://www.ncbi.nlm.nih.gov/pubmed/7599056>

Weigelt, B., Lo, A. T., Park, C. C., Gray, J. W., & Bissell, M. J. (2010). HER2 signaling pathway activation and response of breast cancer cells to HER2-targeting agents is dependent strongly on the 3D microenvironment. *Breast Cancer Research and Treatment*, *122*(1), 35–43. <https://doi.org/10.1007/s10549-009-0502-2>

Wettersten, H. I., Ganti, S., & Weiss, R. H. (2014). Metabolomic Profiling of Tumor-Bearing Mice. *Methods in Enzymology*, *543*, 275–296. <https://doi.org/10.1016/B978-0-12-801329-8.00014-3>

Chapter 9. Concluding remarks and future work

In this work the production and characterization of several therapeutic antibody-derived molecules based on the anti-HER2 monoclonal antibody Trastuzumab has been attempted. These molecules consist on an immunocytokine formed by the fusion of Trastuzumab and interferon- $\alpha 2$, and different formats of antibody-drug conjugates (DM1 and MMAE as cytotoxic drugs), exploring heterogeneous and different homogeneous conjugation strategies on whole antibody and antibody scFv fragment. The production process for each molecule includes its cloning into an expression vector, the production of the protein using the human HEK293 cell line, its purification and the conjugation to a cytotoxic drug. The physicochemical and biological activity characterization has also been performed, for which several tools have been implemented, including 2D and 3D *in vitro* models and also an *in vivo* model using a tumoral human cell as target.

From the developed work and the obtained results it can be concluded that:

- The production of the Trastuzumab antibody and the derived antibodies and fragments (Trastuzumab_cys114, Trastuzumab light and heavy chain, and scFv fragments) has been achieved through HEK293 cultures in single use devices, including 50L productions for Trastuzumab and Trastuzumab_cys114. The implemented recovery and purification sequences, based on Protein A or Protein L affinity chromatography as the key step, have allowed to obtain products with >97% purity and recovery yields around between 65 and 80%. For Trastuzumab, several physicochemical characterization tools have been implemented, which have proved the obtention of antibody products available for conjugation.
- The constructed immunocytokine consisting in the fusion of Trastuzumab and IFN $\alpha 2$ has not shown an improved antiproliferative activity against target SKBR3 breast cancer model cells with respect to Trastuzumab.

Regarding the IFN α 2 cytokine, a mild antiproliferative activity was detected in *in vitro* test assays. However, its fusion to Trastuzumab did not result in an increase of its antitumor effect. Besides, the impact of the interferon on the activation of the immune system was not found to be significant: no lymphocyte proliferation was induced by the interferon. As a future work, alternative approaches could consist on generating a fusion construct based on an antibody fragment instead of a whole IgG: fusing the interferon to a lower molecular weight molecule such as the fragment, might help avoiding steric impediments allowing a better folding of the protein, preserving the native structure of the interferon and increasing its activity. Another strategy to obtain a more potent immunocytokine could rely on fusing a different cytokine to the antibody. Apoptosis activators such as TNF α (tumor necrosis factor α) (Krippner-Heidenreich et al., 2008) or FasL (Fas receptor ligand) hold a powerful cytotoxic activity, while cytokines such as interleukins 2, 6, 7 or 12 have a strong capacity to activate the immune system against the target tumor (Kontermann, 2012).

- The heterogeneous conjugation of Trastuzumab to the cytotoxic drugs DM1 and vcMMAE has been successfully achieved, generating ADCs with the expected DARs of 3.1 and 4, respectively. The heterogeneous conjugation methodologies based on conjugation to Lysine residues (in the case of DM1) and to interchain Cysteine residues (in the case of vcMMAE) have been successfully implemented, as well as the tools for characterizing the DAR of the obtained conjugates (UV spectroscopy (with its precision confirmed by mass spectrometry) and hydrophobic interaction chromatography). Similar recovery yields were obtained for both conjugation processes, around 70% (66% for Trastuzumab-DM1 vs 73.5% for Trastuzumab-vcMMAE). Trastuzumab-vcMMAE displayed a lower aggregates amount than T-DM1, due to the partial reduction step involved in the Trastuzumab-vcMMAE conjugation, which partially eliminated the initial aggregates present in the

Trastuzumab antibody. Both ADCs recognized their target HER2 antigen on the SKBR3 cell surface, in a similar proportion than naked Trastuzumab, therefore not showing any significant loss of effect due to the conjugation process. Regarding their antiproliferative activities, Trastuzumab-DM1 had a more potent antitumor effect than Trastuzumab-vcMMAE, in good accord with the free drug potencies, since DM1 is stronger than vcMMAE.

- Three different site-directed conjugation strategies of Trastuzumab with the cytotoxic drug vcMMAE have been implemented. In the first strategy, Trastuzumab was fully reduced and conjugated to vcMMAE with an aimed DAR of 8, obtaining an ADC with a DAR of 7.3. This method is simple and straightforward, avoiding genetically modifying the antibody or using complex chemistries, which are typical features of many site-directed conjugation strategies. However, the DAR of the product is high, which may affect the stability of the ADC and could impair its *in vivo* therapeutic efficacy (Hamblett et al., 2004). *In vivo* studies must be performed in order to confirm this possibility.
- In a second strategy of site-directed conjugation, the cytotoxic drug vcMMAE has been conjugated to an added cysteine of the cysteine-engineered Trastuzumab_cys114, in an analogous approach to the one described by Junutula et al (Junutula et al., 2008), based on the reduction of the antibody, in order to free the capped cys114. followed by a reoxidation step, that rebridges the interchain disulfide bonds collaterally broken by the reduction step. The reduction conditions that allow the full reduction of the antibody, therefore ensuring the obtention of an ADC with the aimed DAR of 2, were analyzed, obtaining an optimal excess of 50 molecules of reducing agent per Trastuzumab_cys114 antibody. This condition allowed the obtention of a DAR of 1.79 (measured by HIC-HPLC), close to the aimed DAR of 2. Reduction with higher reducing agent amounts did not result in an increase of the DAR, suggesting a good reoxidation efficiency. The

antiproliferation activity of the generated ADCs Trastuzumab_cys114-vcMMAE (DAR 1.79), the heterogeneous Trastuzumab-vcMMAE (DAR 3.9) and the homogeneous Trastuzumab-vcMMAE (DAR 7.3) were proportional to their drug load, when analyzed with a 2D *in vitro* cell viability assay.

- An new alternative approach, not described previously, into generating an homogeneous ADC conjugate with a DAR of 2 has been developed. In this strategy, no genetic modification of the antibody, nor complex conjugation chemistries are needed. The strategy relies in the independent production of the chains of the antibody, which can then be conjugated and reassembled forming an homogeneous ADC with a DAR lower than 8. In the developed strategy, the light chain was conjugated to vcMMAE, therefore yielding an ADC with a DAR of 2 after the reassembly of the chains. Independently produced light chain adopted a dimer structure, with approximately the 50% having the two light chain subunits covalently bond through interchain cysteines. All independently produced heavy chains formed covalently bond dimers. The assembly of the chains was achieved by simply incubating an equimolar amount of LC and HC for 3h at room temperature. The conjugation of the light chain with vcMMAE included a reduction step in order to break the interchain disulfide bridges of the dimers and free the capped cysteine of the non-covalently bond dimers. A complete conjugation of the light chain was ensured with this method, and its assembly with the heavy chain generated an ADC with a DAR of 2. It displayed an *in vitro* antiproliferation activity lower than Trastuzumab-vcMMAE (DAR 4), coherently therefore with its drug load. Most importantly, its therapeutic efficacy was confirmed in an *in vivo* assay, for which an animal model was developed.
- Three different mouse strains (BALB/c nude, NOD-SCID and Rag) were inoculated with SKBR3 cells, which did not engraft properly and did not result in the formation of a tumor. A proper engraftment of the breast

cancer tumor cells was achieved using the cell line BT474. The developed ADC was tested with this animal model, causing a complete regression of the tumor in 7 of the 10 treated animals and therefore showing a strong therapeutic effect, while also causing some toxicity effects in some of the mice. As a proposal for future work, studies with lower doses or different administration patterns could be tested, in order to find the therapeutic window that maximizes the therapeutic effect while minimizing the toxic side effects. Performing assays for obtaining the pharmacokinetic and pharmacodynamic profiles of the developed ADC could also be interesting, as well as comparing its therapeutic potential *in vivo* with other ADCs such as the Trastuzumab_cys114-vcMMAE DAR2 ADC. Generating an homogeneous ADC applying the developed chains assembly method with a different DAR, of 4 (by reducing and reoxidating all the disulfide bridges of the heavy chains and then conjugating the remaining cysteine and assembling them with conjugated light chains) or 6 (by conjugating all the available thiol groups of the heavy chains), and assessing its potential therapeutic could also be relevant. A last proposal could consist in attempting the implementation of this conjugation strategy to other therapeutic monoclonal antibodies, in order to test the robustness and reproducibility of the method.

- The heterogeneous and homogeneous conjugation strategies implemented in this work for Trastuzumab were also implemented in Trastuzumab-derived antibody fragments. The produced scFv fragment was heterogeneously conjugated to DM1 with an aimed DAR of 3.1, resulting, however, in a conjugated molecule with a DAR of 0.9 and a low recovery yield (approximately 10%), mostly due to precipitation issues. An alternative scFv_cys111 fragment, with a cysteine incorporated in the position 111, was also produced and used for site-directed conjugation to vcMMAE in a strategy analogous to the one employed for the conjugation of

Trastuzumab_cys114, obtaining a conjugated product with a DAR of 1, corresponding to the aimed DAR, and with a higher recovery yield, of close to 30%. The antiproliferative activity of the two scFv conjugates, analyzed with a 2D *in vitro* assay, showed similar potency values. Since the proportion of payload with respect to protein is higher in a conjugated fragment than a conjugated whole IgG for the same DAR, this can increase the instability and precipitation possibilities of the conjugated fragment. This could be solved by using more hydrophilic payloads. Another approach could consist in incrementing the protein mass of the fragment, for example by fusing it to a cytokine, therefore generating a conjugated immunocytokine.

- The generation of a 3D model for the antiproliferation activity assessment of the generated antibody-conjugated molecules has been attempted using SKBR3 cells. Several strategies have been attempted, including scaffold-free approaches such as culture in ultra-low attachment plates and methods using hydrogel scaffolds (Matrigel and collagen). However, spheroids were only formed when combining the addition of Matrigel to the culture and the centrifugation of the plate. These spheroids were much more resistant than the 2D cultures to the developed ADCs, and also to the unconjugated cytotoxic drug vcMMAE. 3D cultures with the BT474 cell line resulted in a much easier formation of spheroids, since they appeared with a simple culture with ultra-low attachment plates. They also displayed an increased resistance to the tested drugs.
- Taking altogether the obtained results, it can be stated that the main objectives defined at the beginning of the project have been achieved, generating several ADCs based on Trastuzumab, including the development of a new strategy for site-directed conjugation that could be applied to other antibodies and have a potential impact as an anticancer therapy.

References:

- Hamblett, K. J., Senter, P. D., Chace, D. F., Sun, M. M. C., Lenox, J., Cervený, C. G., ... Francisco, J. A. (2004). Effects of Drug Loading on the Antitumor Activity of a Monoclonal Antibody Drug Conjugate. *Clinical Cancer Research*, 10(20), 7063–7070. <https://doi.org/10.1158/1078-0432.CCR-04-0789>
- Junutula, J. R., Raab, H., Clark, S., Bhakta, S., Leipold, D. D., Weir, S., ... Mallet, W. (2008). Site-specific conjugation of a cytotoxic drug to an antibody improves the therapeutic index. *Nature Biotechnology*, 26(8), 925–932. <https://doi.org/10.1038/nbt.1480>
- Kontermann, R. E. (2012). Antibody-cytokine fusion proteins. *Archives of Biochemistry and Biophysics*, 526(2), 194–205. <https://doi.org/10.1016/j.abb.2012.03.001>
- Krippner-Heidenreich, A., Grunwald, I., Zimmermann, G., Kühnle, M., Gerspach, J., Sterns, T., ... Scheurich, P. (2008). Single-chain TNF, a TNF derivative with enhanced stability and antitumoral activity. *Journal of Immunology*, 180(12), 8176–8183. <https://doi.org/10.4049/jimmunol.180.12.8176>

Chapter 10. Materials and methods

10.1. Biologic material

10.1.1. Mammalian cell lines

10.1.1.1 HEK293 production cell line

For antibody and antibody-derived molecules production, HEK293SF-3F6 cell line (ATCC CRL-12585) has been used. This cell line derives from the parental HEK293, which was obtained from a human embryo kidney in 1973 and later immortalized by means of its transformation with human adenovirus 5 (Thomas et al., 2005). HEK293SF-3F6 cell line variant is adapted to suspension culture in culture medium without bovine serum (SFM, Serum-free medium) and was gently provided by Dr. A. Kamen from NRCC (National Research Council of Canada). In this thesis work, several HEK293 cell lines producing different antibody products have been generated, summarized in Table 10.1.

Table 10.1. Summary of generated HEK293 cell lines for protein production

HEK293 cell line	Plasmid	Protein product
HEK293_Tzmb	pTRIpuro3_Tzmb	Trastuzumab
HEK293_Tzmb-IFN α 2	pTRIpuro3_Tzmb-IFN α 2	Trastuzumab-IFN α 2
HEK293_Tcys114	pTRIpuro3_Tcys114	Trastuzumab_cys114
HEK293_scFv	pRESpuro3_scFv	scFv (Tzmb)
HEK293_scFv_cys111	pRESpuro3_scFv_cys111	scFv_cys111 (Tzmb)
HEK293_HC	pRESpuro3_HC	Trastuzumab heavy chain
HEK293_LC	pRESneo3_LC	Trastuzumab light chain

10.1.1.2. Cell lines used for Trastuzumab binding and antitumoral activity assessment: SKBR3, MCF7, Hybridoma KB26.5, BT474

SKBR3 is a HER2+ breast cancer model cell line widely used in breast cancer research, and in particular for *in vitro* testing the biological activity of HER2 targeting molecules such as Trastuzumab. It was originally isolated by the Memorial Sloan Kettering Cancer Center in 1970 from a 43-year-old caucasian female (Memorial Sloan Kettering Center, 2018). In this work, the SKBR3 cell line (ATCC-HTB30) has been gently given by Dr. Eduard Escrich, from the GMECM group (*Universitat Autònoma de Barcelona*).

MCF7 (ATCC-HTB22) is another breast cancer cell line used in breast cancer research, which was described for the first time in 1973 (Soule et al., 1973). It expresses the HER2 receptor, albeit at much lower levels than SKBR3 (Subik et al., 2010). This cell line was also obtained from Dr. Escrich.

Hybridoma KB26.5. Hybridoma KB26.5 was obtained by fusing a myeloma NS1 cell with a B lymphocyte from a Balb C mouse. It produces an IgG3 antibody directed against A1 antigen from human erythrocytes. Hybridoma KB26.5 was developed by Laboratoris Knickerbocker (Barcelona) and donated for research purposes to Universitat Autònoma de Barcelona.

BT474 is also a HER2+ breast cancer model cell line used in cancer research. It was originally obtained from a 60 years old Caucasian woman (ATCC, 2016). In this thesis it has been used to develop the 3D and *in vivo* assays. The cell line (ATCC HTB-20) has been gently provided by Dr. Ibane Abasolo of the Functional Validation Preclinical Research group of the Vall d'Hebron Institute of Research (Barcelona).

10.1.2. Bacterial strains

10.1.2.1. Strain for molecular biology: *Escherichia coli* DH5 α

E. coli strain DH5 α (ThermoFisher, ref. 18265017) has been used for the obtention and amplification of the plasmids constructed in this work. It has the following genotype: F⁻ Φ 80*lacZ* Δ M15 Δ (*lacZYA-argF*) U169 *recA1 endA1 hsdR17* (rK⁻, mK⁺) *phoA supE44* λ ⁻ *thi-1 gyrA96 relA1*.

10.1.2.2. Strain for antibody fragment production: BL21

E. coli BL21(DE3) is one of the most used bacterial strains for recombinant protein production. In this work, *E. coli* BL21(DE3) (ThermoFisher, ref C6000-03) has been used for the production of scFv(Tzmb). It has the following genotype: F⁻ *ompT gal dcm lon hsdS_B(r_B⁻ m_B⁻)* λ (DE3 [*lacI lacUV5-T7p07 ind1 sam7 nin5*]) [*malB*⁺]_{K-12}(λ ^S).

10.2. Culture media

10.2.1. Culture media for mammalian cell lines

10.2.1.1. Culture media for HEK293 cell line

The base medium that has been used for HEK293 cell line culture is the commercial medium SFM4Transfx (SH3086002, Hyclone). This is a serum-free medium, with an undisclosed composition. The performed analysis has shown that it has a glucose concentration of 4 g/l. For the production of antibody or antibody-derived molecules, the medium has been supplemented with the additional supplements indicated below. The following components have been added on 900 ml of SFM4Transfx, preserving the sterility in a laminar flow hood (Telstar AV-100):

- GlutaMAX (35050061, Gibco) at a final concentration of 4 mM: add 20 ml of GlutaMAX 200 mM.

- Cell Boost 5 (SH30865, Hyclone), at a final 6% (w/v): add 100 ml of a 60 g/l solution, sterilized by means of a 0.22 μm filtration with Sterivex filters (10411741, Millipore).
- Puromycin (540511, Merck), at final 10 $\mu\text{g/ml}$: add 10 ml of a 1 mg/ml stock, sterilized by means of a 0.22 μm filtration with Sterivex filters (10411741, Millipore).
 - For the culture of HEK293_LC, instead of puromycin, the selective antibiotic consists in G418 solution (Roche), at 20 ml/L.
- Antifoam C (Sigma, A8011), at final 50 mg/L: add 5 ml of a 10 g/L stock (previously sterilized by autoclave).
- Kolliphor P188 (Sigma, K4894), at 2 g/L: add 20 ml/L of a 100 g/L stock solution (previously sterilized by autoclave).

10.2.1.2. Medium for SKBR3, BT474, MFC7 and Hybridoma KB26.5 cells culture

SKBR3 and BT474 cells were cultured in base DMEM (Dulbecco's Modified Eagle's Medium, D5671, Sigma) medium, which was supplemented with faetal bovine serum (FBS) and GlutaMAX. The following components have been added on 900 ml of DMEM, preserving the sterility in a laminar flow hood (Telstar AV-100):

- GlutaMAX (35050061, Gibco) at a final concentration of 4 mM: add 20 ml of GlutaMAX 200 mM.
- FBS (Sigma), at 10% volume: add 100 ml of DMEM

10.2.2. Culture media for bacterial strains

10.2.2.1. Culture media for *E. coli* DH5 α

10.2.2.1.1. Luria Broth (LB) liquid medium

Luria Broth is a well-established rich medium for bacterial culture. Its composition and preparation are described below:

Chapter 11. Appendix

- Triptone / Peptone (Oxoid): 10 g/l
- Yeast Extract (Oxoid): 5 g/l
- NaCl (Panreac): 10 g/l

The medium is prepared by dissolving the previous components into deionized water and adjusting the pH at 7 with NaOH 30%. Then, it is autoclaved at 121°C for 20 minutes.

10.2.2.1.2. Luria Broth (LB) solid medium:

LB agar plates composition and preparation are described below:

- Triptone / Peptone (Oxoid): 10 g/l
- Yeast Extract (Oxoid): 5 g/l
- NaCl (Panreac): 10 g/l
- Agar (Oxoid): 15 g/l

The medium is prepared by dissolving the previous components into deionized water and adjusting the pH at 7 with NaOH 30%. Then, it is autoclaved at 121°C for 20 minutes. The medium is cooled in a bath at 50°C and then 20 ml are dispensed in each sterile Petri plate (Sterilin) and left to solidify. The plates are then conserved at 4°C.

10.2.2.1.3. Super Optimal Broth with Catabolite repression (SOC) medium:

For transformation of the *E. coli* DH5 α cells (see 10.7.6.), SOC medium has been used, which has the following composition:

- Yeast Extract (Oxoid): 5 g/l
- Triptone (Oxoid): 20 g/l
- NaCl (Panreac): 10 mM
- KCl (Panreac): 2.5 mM
- MgSO₄ (Sigma): 10 mM

- MgCl₂ (Sigma): 10 mM
- Glucose (Panreac): 20 mM

For preparing 100 ml of SOC medium, yeast extract (0.5 g), Triptone (20 g), NaCl (1 g) and KCl (0.019 g) are diluted in 95 ml of H₂O, and the pH is adjusted to 7.5 with NaOH 30%. Then the solution is autoclaved at 121°C for 20 minutes, and concentrated sterile solutions of MgSO₄ (1 M, 1 ml), MgCl₂ (0.4 M, 2.5 ml) and glucose (2 M, 1 ml) are added to it.

10.2.2.1.4. Selective LB medium

In order to amplify the plasmids used in this work, which contain a selection marker of resistance to the antibiotic ampicillin, the culture medium has to be selective for this antibiotic. Therefore, the above mentioned LB media have to be supplemented with ampicillin (A0166, Sigma) at a final concentration of 100 µg/ml. This is done by adding 1 ml/L of a 10% (w/v) ampicillin solution to the media, sterilized by filtration at 0.22 µm with a syringe filter (Millex, Millipore). For ampicillin addition, it is necessary to wait for the medium to reach a temperature below 50°C due to the antibiotic being termolabile.

10.2.2.2. Medium for *E. coli* BL21(DE3)

10.2.2.2.1. Liquid defined medium for antibody fragment production

Chemically defined media present several advantages with respect to rich media, including being cheaper and yielding more reproducible results. Therefore, a defined medium was used for scFv production with *E. coli* BL21. The composition of the medium is as presented in Table 10.2, and it was obtained from a previous work in the department (Pinsach, 2009). The reagents were obtained from Sigma Aldrich, unless otherwise indicated.

Table 10.2: defined medium composition and stock solutions for preparing 1L of medium

Chapter 11. Appendix

	Amount (g)	Volume preparation (ml)	Concentration of stock solutions (g/L)	Sterilization (Filtration or Autoclave)
Glucose·H ₂ O (Panreac)	22	100	-	Autoclave
K ₂ HPO ₄	11.9	890	-	Autoclave
KH ₂ PO ₄	2.4			
NaCl	1.8			
Mg ₂ SO ₄ ·7H ₂ O	0.11	0.28	400	Autoclave
FeCl ₃ ·6H ₂ O	0.01	0.1	100	Filtration
(NH ₄) ₂ SO ₄	3.0	10	300	Autoclave
Trace elements	0.72	0.72	-	Filtration
	ml			
Ampicillin	0.1	0.1	1	Filtration
Thiamine	0.03	2.5	12	Filtration

Table 10.3 Trace elements solution composition

Compound	g/L
AlCl ₃ ·6H ₂ O	0.041
ZnSO ₄ ·7H ₂ O	0.87
CoCl ₂ ·6H ₂ O	0.16
CuSO ₄ ·5H ₂ O	1.6
H ₃ BO ₃	0.01
MnCl ₂ ·4H ₂ O	1.42
NiCl ₂ ·6H ₂ O	0.01
NaMoO ₄ ·2H ₂ O	0.02

Chapter 11. Appendix

Trace elements solution is prepared by dissolving the trace elements into H₂O and sterilization by 0.22 µm with a syringe filter (Millex, Millipore).

The medium was prepared by adding the rest of the components on the K₂HPO₄, KH₂PO₄ and NaCl solution, once this solution has reached a temperature below 50°C, due to the termolability of the ampicillin and thiamine solutions.

10.2.2.2.2. Solid defined medium for antibody fragment production

Solid defined medium for antibody fragment production was prepared using the same protocol than for the liquid medium, and adding Agar (Oxoid) at a final concentration of 15 g/L. The agar was autoclaved together with the K₂HPO₄, KH₂PO₄ and NaCl solution, and the rest of solutions were again added once the temperature had dropped below 50°C. Then, 20 ml are dispensed in each sterile Petri plate (Sterilin) and left to solidify. The plates are then conserved at 4°C. Composition and preparation solutions are described in Table 10.4.

Table 10.4: defined medium composition and stock solutions for preparing 1L of solid medium

Amount (g)	Volume preparation (ml)	Concentration of stock solutions (g/L)	Sterilization (Filtration or Autoclave)	
Glucose·H ₂ O	22	100	-	Autoclave
K ₂ HPO ₄	11.9	890	-	Autoclave
KH ₂ PO ₄	2.4			
NaCl	1.8			
Agar	15			
Mg ₂ SO ₄ ·7H ₂ O	0.11	0.28	400	Autoclave

Chapter 11. Appendix

FeCl ₃ ·6H ₂ O	0.01	0.1	100	Filtration
(NH ₄) ₂ SO ₄	3.0	10	300	Autoclave
Trace elements	0.72	0.72	-	Filtration
	ml			
Ampicillin	0.1	0.1	1	Filtration
Thiamine	0.03	2.5	12	Filtration

10.3. Maintaining and assessment of the biologic material

10.3.1. Mammalian cell line maintenance

10.3.1.1. Thawing

All cell lines described in section 9.1.1. were maintained frozen in sterile cryovials (Nunc 377267) inside a N₂ container at -196°C (Forma Scientific, CMR 8031, Cryomed). Ensuring an optimal recovery of the cells after thawing (i.e. low aggregation, short or none lag phase) can be obtained by performing the following protocol. All the cell-manipulating steps are performed in a laminar flow cabinet:

- Dispense 9 and 10 ml of cell medium in one and two 15 ml centrifuge tube, respectively, and warm them up to 37°C in a water bath.
- Take out the cryovial from the liquid N₂ container and put it into the previously warmed water bath at 37°C, avoiding contact between the water and the cap of the vial.
- Pipette the content of the cryovial into the previously mentioned 15 ml centrifuge tube with 9 ml of cell medium. Swirl it gently.
- Centrifuge the tube at 500g for 5 minutes, and discard the supernatant inside the laminar flow cabinet in order to eliminate the dimethyl sulfoxide (DMSO, Sigma D2438) of the freezing medium, which acts as cryoprotecting agent but it is toxic to the cells. Resuspend the pellet in 10 ml of the

previously warmed cell medium and repeat the centrifugation and discarding the supernatant step in order to ensure the complete removal of DMSO.

- Resuspend the pellet in 10 ml of the previously warmed cell medium and pipette the cells into the appropriate culture platform (25 cm² T-flask (Corning) or 125 ml shake flask (Corning)).

10.3.1.2. Freezing

Cells to be frozen have to be in the middle of their exponential growth phase, and with viability levels higher than 90%. The following protocol was applied for cell freezing. All the cell-manipulating steps are performed in a laminar flow cabinet:

- Pipette the cells into a centrifuge tube and centrifuge it at 500g for 5 minutes. Centrifuge the volume of cell culture that allows having the following cell number in each cryovial to be generated:
 - HEK293 and KB26.5: $8 \cdot 10^6$ cells
 - SKBR3, BT474 and MCF7: $1 \cdot 10^6$ cells
- In a laminar flow cabinet, discard the supernatant and resuspend the cells with their specific culture medium. In the case of HEK293 and CHO, the FBS content of this medium is increased to 10% (v/v).
- Repeat the centrifugation and discarding the supernatant step.
- Resuspend the cells with their specific culture medium. Use a medium volume of 0.5 ml per each cryovial to be generated (i.e. 2 ml for the preparation of 4 cryovials).
- Add 0.5 ml of freezing medium per each cryovial to be generated into the cell suspension. The freezing medium consists of the cell culture medium with a 20% (v/v) of DMSO. Add then gently 1 ml of the cell suspension to each cryovial.

- Gently swirl the cryovials and put them into a Mr Frosty™ container, (ThermoScientific, Ref. 5001-0001) and store in -80°C freezer (Nuair, 6512-E).
- After 24h take the cryovials out of the Mr Frosty™ and transfer them to the N₂ container.

10.3.1.3. Subculture of suspension cells

Suspension cells (HEK293 and CHO-S) were cultured in 125 ml shake flasks (Corning) agitated at 110 rpm on an orbital shaker (SSL1, Stuart) at 37°C in a humidified atmosphere with 5% CO₂ incubator (Steri-cult 2000 Incubator, Forma Scientific). Two to three times a week, cell passaging was routinely performed, seeding 12 ml of culture at a density of 0.3·10⁶ cell/ml.

It is crucial to ensure the sterility of the different cell culture processes, therefore, it is important to maintain medium aliquots incubated at 37°C as controls. The different media and cell cultures have to be routinely observed in order to detect possible contaminations by bacteria, yeasts or fungi. Cells were maintained for up to 30 passages, if this passage number was reached, the culture was discarded and a new cryovial was used.

10.3.1.4. Subculture of adherent cells

Adherent cell lines (SKBR3 and BT474) were subcultured in 25 cm² T-flasks (NUNC, Ref.156367) at 37°C in a humidified atmosphere with 5% CO₂ incubator (Steri-cult 2000 Incubator, Forma Scientific). Passaging was routinely performed two to three times a week, ensuring that cells did not reach >80% confluence. The subculture was performed through trypsinization of the cells, applying the following protocol (all the cell and medium manipulating steps performed in a laminar flow cabinet in order to preserve the sterility:

- Remove cell media from the T-flask.

- Rinse the T-flask with 1 ml of sterile PBS. This allows removing any trace of FBS, which inhibits the activity of trypsin.
- Add 1 ml of Trypsin-EDTA 0.5% (ThermoScientific, 10779413) to the culture and incubate it at 37°C for 1 minute.
- Remove the Trypsin solution and incubate again at 37°C for 5 minutes. Visually check with a contrast phase inverted microscope (Nikon, TMS) that the cells are adopting a rounded-shape and that they begin to detach from the T-flask surface when tapping is applied.
- Add culture 1 ml of culture medium and gently tap the T-flask and pipette up and down in order to homogenize the cell suspension. Count the cell and reseed them at the following concentrations:
 - SKBR3: 10.000 cell/cm²
 - BT474: 5.000 cell/cm²
 - MCF7: 5.000 cell/cm²

Sterilization and number of maximum number of passages criteria applied are the same as for suspension cultures (see section 10.3.1.3.).

10.3.2. Mycoplasma contamination assessment of mammalian cell lines

Mycoplasma spp. is a bacterium parasite of animal cells. *Mycoplasma* can generate cellular changes, such as metabolic and growth changes, and can infect a cell line causing the invalidation of the performed experiments with this cell line. Therefore, it is crucial to make sure that the used cell lines are *Mycoplasma*-free (Uphoff & Drexler, 2014). In this work, this has been performed by means of a polymerase chain reaction (PCR), as described in the section 10.7.4., using a commercial kit validated for this use (EZ-PCR Mycoplasma Test kit (20-700-20), Biological Industries). All the original and constructed cell lines of this work have been analyzed and shown to be Mycoplasma free. In Figure 10.1, the results of the test can be seen for SKBR3 cell line.

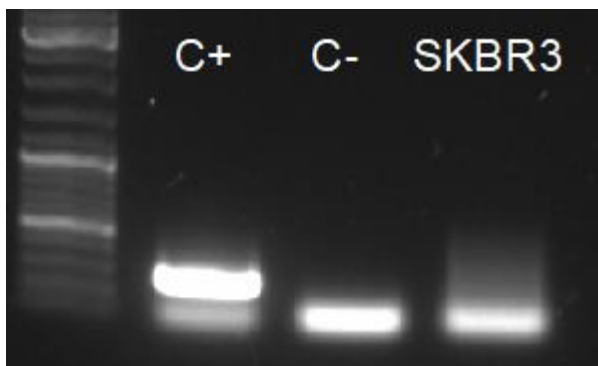


Figure 10.1. Mycoplasma test of SKBR3 cell line. A band corresponding to the amplified Mycoplasma DNA region appears in the positive control lane (C+), which is absent in the negative control (C-) and SKBR3 lanes.

10.3.3. Bacterial strains maintaining

10.3.3.1. Thawing

E. coli strains were stored frozen at -80°C in cryovials (Nunc, 377267). When required, the vials are thawed using the following protocol. All the cell-manipulating steps are performed in a laminar flow cabinet:

- Put the chosen vial in a box filled with ice. Allow it to thaw (achieved in around 5-10 minutes).
- Add 0.05 ml of the cryovial into 10 ml of the appropriate medium in a 100 ml Erlenmeyer and incubate it at 37°C , 135 rpm. Alternatively, seed it into an agar plate and incubate it at 37°C .

10.3.3.2. Freezing

As in the case of mammalian cell lines, at the moment of freezing bacterial cultures have to be in the middle of their exponential growth phase and volume of cell culture has to allow obtaining n vials of 1 ml at an $\text{OD}_{600} = 2.5$. Glycerinated stocks were

generated using the following protocol. All the cell-manipulating steps are performed in a laminar flow cabinet:

- Grow *E. coli* until it reaches middle log phase ($OD_{600} = 0.4-0.6$).
- Add the culture volume in a centrifuge tube and centrifuge it at 5000g for 10 minutes at 4°C.
- Discard the supernatant and resuspend the pellet in a culture medium volume equivalent to 0.5 ml for each vial to be generated (i.e. 2 ml for 4 vials).
- Add the same volume of a 30% (w/v) solution of sterile glycerol and dispense 1 ml to each cryovial.
- Store the cryovials in a freezer at -80°C (Nuaire, 6512-E).

10.3.3.3. Bacterial cultures maintenance

Bacterial cultures were maintained in agar plates at 4°C due to their fast growth. Cultures must be reseeded in new plates twice per month. In the case of transformed bacterial cultures, it is crucial to ensure that the specific antibiotic has been correctly added to the agar plate medium in order to maintain the plasmid in the cells.

10.4. Culture systems

10.4.1. Culture systems for mammalian cell lines

10.4.1.1. Suspension cell lines

10.4.1.1.1. Shake flasks

Polycarbonate shake culture flasks (Corning, 431143) were used in this work for suspension cell culture. These flasks have filtered vent caps that allow continuous gas exchange while ensuring stability and preventing leakage. For cell maintenance (12 ml of medium volume) and cell line characterization experiments (25 ml of

medium volume), 125 ml shake flasks were used. For antibody/ICK production or for scaling up the culture prior to a bioreactor inoculation, 1L shake flasks (Corning, 431147) were used, with 250 ml of medium volume. Shake flasks were generally inoculated at $0.3 \cdot 10^6$ cell/ml and incubated at 37°C in an incubator (Steri-cult 2000 Incubator, Forma Scientific) with an humidified atmosphere (95%) to avoid excessive media evaporation and CO₂ was set at 5% in order to control the pH of buffered cell media. Cells were agitated at 110 rpm, using the orbital SSL1 shaker (Stuart).

10.4.1.1.2. Single use bioreactor culture: wave bioreactor

A wave bioreactor is a device that allows cell culture using single use bags in controlled culture conditions of temperature, pH and pO₂, in which the homogenization of the culture is ensured through a rocking mixing technology. The wave bioreactor comprises a rock base (20/50 EHT, GE), to which the culture bag (DFB010L, Sartorius or CB0010L10-11, GE) is installed, and a wavepod that integrates monitoring and control of process variables: dissolved oxygen and pH. Setpoints of the variables and how they are monitored and controlled are briefly explained below:

- Temperature (37°C): temperature is controlled through an electric heater located in the rock base.
- pH (7.0): monitoring of this parameter can be performed using a pH probe embedded into the culture bag. It can be controlled using as acid correctors an HCl solution (0.5M) added by a peristaltic pump connected to the wavepod, or by incrementing the CO₂ content of the gas mix that enters into the culture. A solution of NaOH (1M) can be used as basic corrector, being added using a peristaltic pump connected to the wavepod. In the cultures performed in this thesis, however, pH was monitored off-line by measuring the pH of samples to an external pH-meter (Crison), and a 10% of CO₂ in the gas mixing was maintained along the culture.

Chapter 11. Appendix

- pO_2 : it can be monitored by using an optochemical probe connected to the culture bag. The control of this parameter can be performed by incrementing the rocking frequency or by incrementing the O_2 content of the gas mixing that enters into the culture. A current of 0.3 L/min of air was applied in the performed cultures.

The bioreactor is prepared following the sequence:

- Inside a laminar flow hood, a 1L bottle and a 10L bottle are connected in a sterile way to the culture bag through Luer-lock connectors.
- The bag is installed on the rock base.
- The culture medium is added to the 10L bottle inside the biosafety cabinet. Then, it is introduced inside the culture bag by air pressure.
- Temperature is set to 37°C, rocking frequency to 21 rpm and rocking angle to 8°. An air flow of 0.3 L/min is also defined. The medium at the setpoint conditions is incubated a minimum of 12 hours before inoculation, in order to check possible contaminations.
- Inside the flow cabinet, open the sterile 1L bottle that has been previously connected to the bag and trasvase the necessary volume for the inoculation from the shakes used for the scaling-up to the sterile bottle. Calculate the inoculation volume for an initial concentration of $0.3 \cdot 10^6$ cell/ml using the following equation (eq. 10.1):

$$V_i = \frac{V_r \cdot C_{r,0}}{C_i}$$

Eq 10.1. V_i corresponds to the inoculation volume (ml), V_r corresponds to the culture volume of the bioreactor (ml), C_i corresponds to the concentration of the inoculum ($\cdot 10^6$ cell/ml) and $C_{r,0}$ corresponds to the initial concentration desired into the bioreactor ($\cdot 10^6$ cell/ml).

10.4.1.1.3. Pilot scale single use bioreactor culture: Stirred Tank Reactor 50L

Pilot scale bioreactors allow cell culture at pilot scale (from 12L to 50L) allowing to define a process reproducible from the lab scale culture to a large scale production. In this work, a bioreactor Biostat STR50 (Sartorius), which is based on single-use technology, has been used. In this bioreactor, the fermentation vessel is substituted by a plastic bag that is used for a single process, therefore reducing risks of contamination from resistant microorganisms, and eliminating crossover contamination between different products and cell lines used.

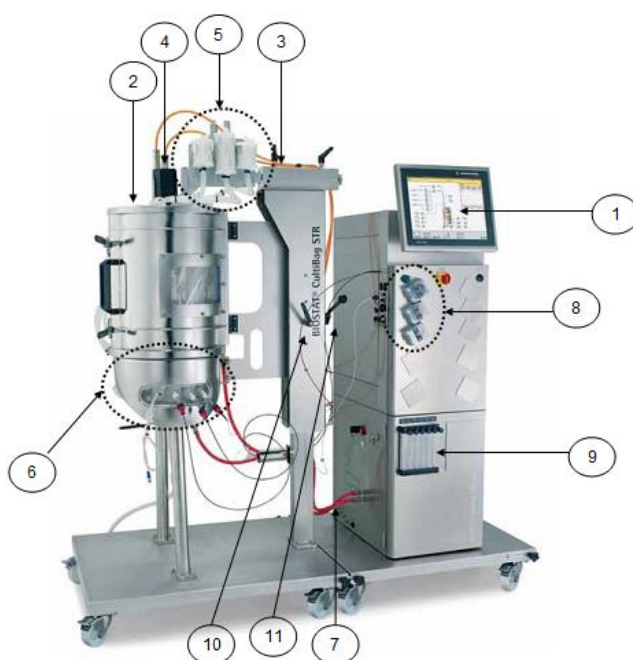


Figure 10.2. Parts of the STR50 SU bioreactor. 1. Screen of the digital control unit (DCU), 2. Support for the culture bag (Bag Holder); 3. Motor arm, 4. Stirring motor, 5. Filter suport, 6. Heating jacket, 7. Entry/Exit water tubes to the heating jacket, 8. DCU pmps, 9. Gas rotameter, 10. Support fixing handle, 11. Support position adjusting arm.

The bioreactor has been prepared following this protocol:

1. Installing the bag on the Bag Holder.
2. Connecting gas connections to the bag.

3. Preparation of the culture medium in a clean container, preferably a bag for the preparation of sterile medium. Once the medium is dissolved it is introduced into the bag of the biorreactor by means of a peristaltic pump and a sterilizing filter of 0.22 μm (Sartopore 2, Sartorius).
4. Introduction of the optical pH and pO₂ probes into the corresponding ports.
5. Once the medium has been introduced into the reactor, the setpoint values for the culture can be introduced through the MFCSWin software.
6. The medium at the setpoint conditions is incubated a minimum of 12 hours before inoculation, in order to check possible contaminations.
7. If the pH, pO₂ and stirring values are stable and no contamination is observed, inoculation is performed.
8. The inoculation biorreactor (a 5L wave biorreactor) is sterily connected to the 50L culture bag using the corresponding port in the biosafety cabinet.
9. Slightly pressurize the inoculation biorreactor with air in order to impulse the inoculum to the 50L reactor. Calculate the inoculum volume for an initial concentration of $0.3 \cdot 10^6$ cell/ml (see equation 10.1. from 10.4.1.1.2).

10.4.2. Bacterial strains

10.4.2.1. Solid culture: Petri dishes

Petri dishes with 20 ml of solid medium incubated at 37°C were used for the culture and isolation of individual colonies of *E. coli*.

10.4.2.2. Erlenmeyer culture

E. coli DH5 α cultures for molecular biology purposes and *E. coli* BL21 cultures for small scale or inocula cultures have been performed in erlenmeyers of different volumes (25, 50, 100 and 250 ml) at 37°C and 130 rpm.

10.4.2.3. Bioreactor culture

The laboratory bioreactor is a device that has been designed to culture microorganisms and animal cells in controlled conditions of temperature, pH and dissolved oxygen concentration (pO_2). It is compounded by two main elements: the monitoring and controlling digital unit (DCU), which gathers information from the different probes and acts over the culture in order to maintain the established parameters; and the fermentation vessel, in which the culture is performed. A Biostat B (B. Braun Biotech) was used in this thesis.

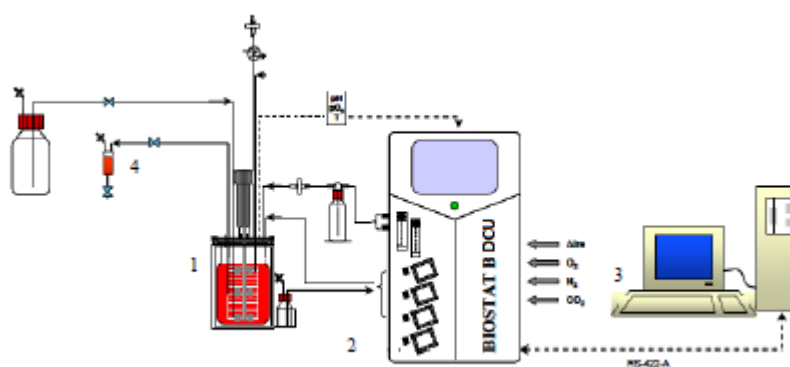


Figure 10.3. Scheme of a stirred tank bioreactor operating in batch mode. 1) 2L stirred glass vessel. 2) DCU: pH, temperature and pO_2 control sensors. 3) computer for data acquisition and parameter control. 4) Sample acquisition. Figure obtained from (Liste-Calleja, 2015).

The DCU performs the data acquisition and possesses the functions for sensor calibration and control loop management of basic variables. These variables are temperature, pH and dissolved oxygen (pO_2). It can also be integrated into a hierarchical automatization system in order to modify the pre-defined control parameters. The software used in the present work for monitoring and controlling was MFCS/win 3.0 (Sartorius Stedim Biotech). Setpoints of the variables and how they are monitored and controlled are briefly explained below:

Chapter 11. Appendix

- Temperature (37-30°C): the double-wall (jacketed) vessel enables water to flow around the bioreactor in order to maintain the set temperature. The heating element consists of an internal heating resistance and cooling is performed by water coming from the general pipeline. After the induction of the culture, the temperature was lowered from 37°C to 30°C.
- pH (7.0): monitoring of this parameter was performed using a pH electrode (Hamilton, Easyfer, Plus). The acid correctors were H₂SO₄ (2M) which was added by a peristaltic pump. A solution of NH₄OH (15%) was used as basic corrector and it was also added by a peristaltic pump.
- pO₂ (30% of saturation): it was monitored through a polarographic electrode (Hamilton, Oxyferm FDA). The DCU has four independent gas inlet channels (air, N₂, O₂ and CO₂), a gas mix chamber and two independent gas outlet channels each one of them provided with a mass flowmeter. By the proper mixture of the gases, pO₂ is controlled.

The fermentation vessel is made from borosilicate glass and the ratio height/diameter is 2:1. It has a total capacity of 2.5L but the working volume is 2L.

The bioreactor was used mediating the following protocol:

- Prepare the medium, add it to the fermentation vessel and sterilize it by autoclave at 121°C, 30 minutes (with filters and tubes but without acid and base correctors bottles).
- Once sterile, the setpoint values for the culture parameters can be established through the MFCS/win software.
- Let the medium at the setpoint conditions a minimum of 12 hours before inoculation, in order to check possible contaminations.
- Check that the values of pO₂, temperature, pH and stirring are stable, and that no contamination has appeared. Connect the acid and base correctors tubes to the bioreactor.

- Inside the flow cabinet, open the sterile bottle connected to the fermentation vessel and trasvase the necessary volume for the inoculation from the shakes used for the scaling-up to the sterile bottle. Calculate the inoculum volume for an initial OD₆₀₀ of 0.3.

10.5. Cell culture analysis

10.5.1. Cell counting and viability assessment

Cell counting is performed from a culture sample obtained in a sterile way. Viable cell number, dead cells, total cells and viability percentage of the culture are calculated from a counting performed using an hemocytometer, specifically a Neubauer chamber (Neubauer Improved, Brand), using a contrast phase inverted microscope (Nikon, TMS), at 10x magnification. The hemocytometer is a slide with four square-shaped fields where microscopic 4x4 quadrants are depicted. Each field contains a known volume, allowing the cell counting of each field.

In order to differentiate viable cells from dead cells, the aliquot of interest is dyed in a 1:1 proportion with a Trypan blue solution (Sigma, T8154) diluted at 0.2% (v/v) in PBS 0.1 M, pH = 7. The dye only penetrates into the dead cells, rendering them blue, while viable cells remain bright. A small volume is pipetted into the chamber, and the cell counting of each field is performed, and the highest and the lowest cell number values are not considered, while the other two taken into account, using the following equation for the viable cell density determination:

$$\text{Cell concentration} \left(\frac{\text{cells}}{\text{mL}} \right) = \frac{n_1 + n_2}{d * V}$$

Equation 10.2. n_1 and n_2 correspond to the cell number counted in each field, m corresponds to the field number (2), d corresponds to the dilution applied with the trypan blue (0.5), and V to the field volume (10^{-4} mL).

This equation can be applied to the counting of both alive and dead cells. Viability can be calculated through the following equation (eq. 10.3):

$$Viability (\%) = \frac{[Viable\ cells]}{[Total\ cells]} \cdot 100$$

10.6. Plasmid vectors

For the construction of recombinant expression vectors in this work, pIRESpuro3 (Clontech) and pIRESneo3 (Clontech) vectors have been used. Vector pUC57 has been used with the synthetically obtained genes.

10.6.1. Initial (base) vectors

10.6.1.1. pIRESpuro3 and pIRESneo3

Vectors pIRESpuro3 and pIRESneo3 (Fig. 10.4) are bicistronic expression vectors of around 5.2 kb. These plasmids contain an IRES sequence (Internal Ribosome Entry Site) of encefalomyocarditis virus (ECMV) which allows the translation of two open reading frames (ORFs) from a single mRNA: the gene of interest and the eukaryote selection marker, which confers resistance to puromycin (*pac*, pIRESpuro3) and to neomycin G418 (*nptIII*, pIRESneo3). The plasmids have a cytomegalovirus promoter, which is a strong constitutive promoter in animal cells, and a multiple cloning site (MCS), where the sequence of interest is inserted. Polyadenylation signal of the SV40 virus stops the mRNA transcription. These plasmids can be replicated in *E. coli* thanks to the replication origin ColE1, making them high-copy number plasmids, allowing the obtention of significant amounts of plasmid. The selection of the *E. coli* colonies that have incorporated the plasmid is realized by means of a selection marker that confers resistance to ampicillin (β -lactamase, *bla*). In this thesis, pIRESpuro3 has been used for the expression of antibody fragments and the heavy chain of

Trastuzumab while pIRESneo3 has been used for the expression of the light chain of Trastuzumab (see Table 10.5).

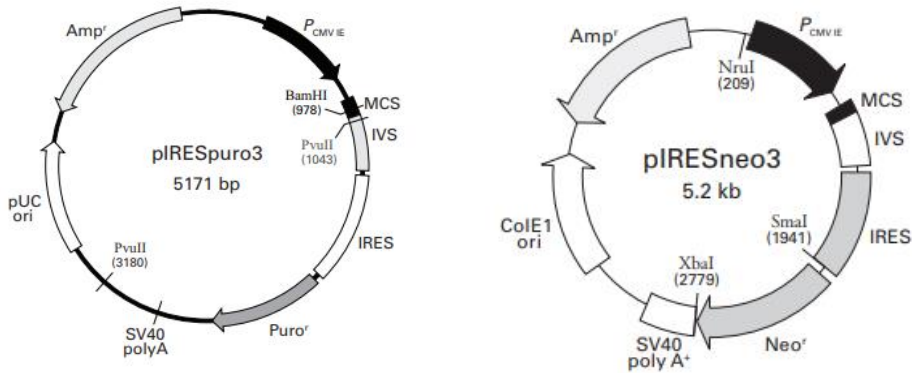


Figure 10.4. Map of pIRESpuro3 (Clontech, 2010) and pIRESneo3 (Clontech, 2008) vectors.

10.6.1.2. pUC57

It is an *E. coli* standard cloning vector, which comprises a replication origin (pMB1), the *bla* gen for ampicillin selection and a MCS integrated inside the gene *lacZ*. This fact allows the selection of bacteria, that have incorporated the insert of interest, by means of the blue/white screening. The insertion of a sequence in the MCS produces a disruption of the *lacZ* gene, impairing the expression of the codified β -galactosidase enzyme, allowing the differentiation of transformed colonies in plates containing IPTG and X-gal substrate (insert-containing colonies will be white, while *lacZ* expressing colonies will be blue). This vector has been used in this thesis work with the synthetically obtained genes from Genscript, the synthetic genes provider, cloned the synthetic genes of interest in the pUC57 vector.

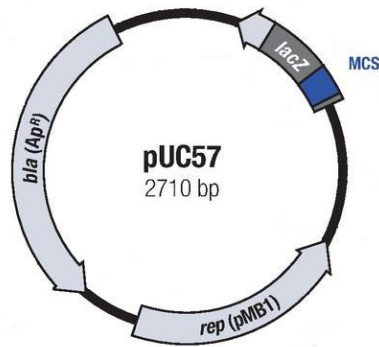


Figure 10.5. Map of pUC57 plasmid, adapted from (Thermo Scientific, 2010).

10.6.1.3. pET21d

pET21d is an expression vector in which the expression of the gene of interest is driven by the strong T7 promoter and the *lac* operator, therefore only being allowed in the presence of the IPTG inducer (*pET System Manual Novagen 1*, 1992). It is used to express proteins in the *E. coli* strain BL21(DE3). In this work, it has been employed to express a scFv fragment.

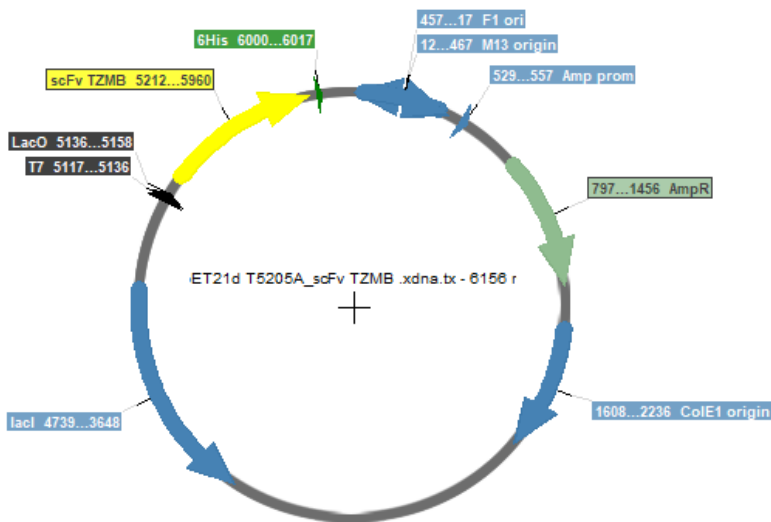


Figure 10.6 Map of pET21 vector containing the scFv, obtained with Serial Cloner.

10.6.2. Vector derived from pRESpuro3: pTRIpuro3

pTRIpuro3 is a tricistronic vector derived from pRESpuro3 which allows cloning and simultaneously expressing three genes: two genes of interest and the selection marker. In this work it has been used for the expression of the two chains of Trastuzumab and Trastuzumab-derived molecules (Table 10.X). The pTRIpuro3 plasmid had been previously constructed in our group. This was done, first, by designing a synthetic sequence called IRES1PS, which comprises a synthetic spacer equivalent to the IVS intron and another IRES sequence, this whole spacer and IRES sequence being flanked by the two restriction sites located on the center of the MCS of pRESpuro3. Once cloned, pTRIpuro3 vector is obtained, with two MCS allowing cloning two genes of interest coupled to the selection marker.

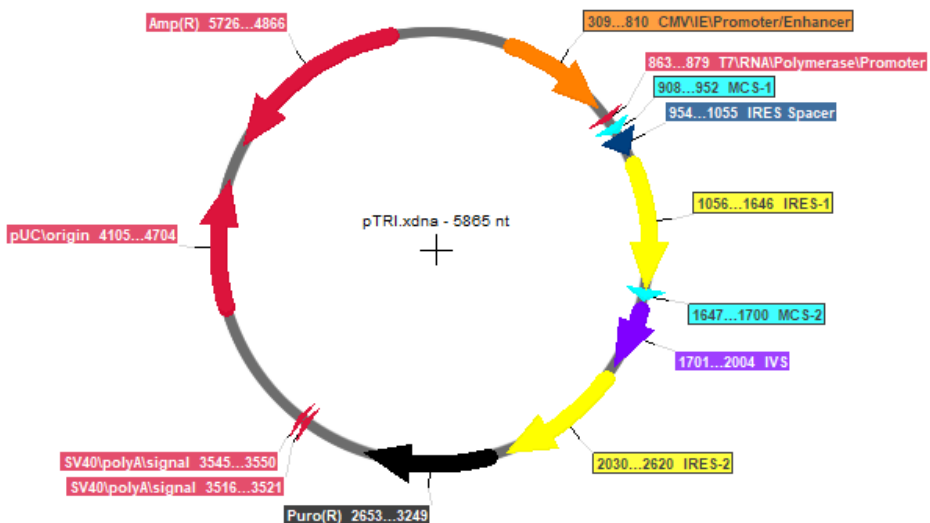


Figure 10.7 Map of pTRIpuro3 vector, obtained with Serial Cloner.

10.6.3. Expression vectors constructed in this thesis

Table 10.5. Expression vectors constructed

Plasmid	Protein product
pTRIpuro3_Tzmb	Trastuzumab
pTRIpuro3_Tzmb-IFN α 2	Trastuzumab-IFN α 2
pTRIpuro3_Tcys114	Trastuzumab_cys114
pRESpuro3_scFv	scFv (Tzmb)
pRESpuro3_scFv_cys111	scFv_cys111 (Tzmb)
pRESpuro3_HC	Trastuzumab heavy chain
pRESneo3_LC	Trastuzumab light chain

10.7. Molecular biology techniques

10.7.1. Extraction and obtaining of plasmid DNA

For the preparation of plasmid DNA of the mentioned expression vectors, the kit GeneJET Plasmid Miniprep Kit (K0503, ThermoFisher Scientific) has been used, following the manufacturer's instructions:

1. Inoculate a 5 ml culture of LB with ampicillin from a colony, in a 50 ml Erlenmeyer.
2. Incubate it at 37°C for 16h. It is important that the temperature remains at 37°C, since plasmid with replication origins pUC or derived (such as ColE1, found in pRESpuro3) will see their replication impaired at lower temperatures.
3. Transfer 1.5 ml of culture in a 1.5 ml eppendorf tube and centrifuge it at 6800 g for 2 minutes. Discard the supernatant.
4. Resuspend the pellet in 250 μ l of resuspension solution. Resuspend it completely mediating pipetting or vortex.

Chapter 11. Appendix

5. Add 250 μl of lysis solution and mix it by gently inverting the tube 4-6 times, until the solution becomes viscous and slightly clear. This causes an alkaline lysis: DNA is liberated from the cells and denaturalized.
6. Add 350 μl of neutralization solution and mix immediately by inverting the tube 4-6 times. Neutralization solution neutralizes the pH of the lysate-containing solution, therefore, plasmid DNA, thanks to its small size, is able to renaturalize, while genomic DNA does not, and associates to proteins and other cellular elements.
7. Centrifuge at maximum speed for 5 minutes, in order to sediment the cell debris and chromosomic DNA. Plasmid DNA remains in the supernatant.
8. Transfer the supernatant to the GeneJET column by means of decantation or pipetting. Avoid contact with the pellet.
9. Centrifuge the column for 1 minute at maximum speed. Discard the flow through and put again the column in its recollection tube.
10. Add 500 μl of washing solution. Centrifuge for 60 seconds at maximum speed and discard the flow through. Put again the column in its recollection tube.
11. Centrifuge the empty column for 1 minute at maximum speed, in order to eliminate the remaining ethanol from the washing solution.
12. Transfer the column to an eppendorf tube of 1.5 ml. Add 50 μl of elution solution in the center of the column membrane in order to elute plasmid DNA. Be careful not to touch the membrane. Maintain it 2 minutes at room temperature.
13. Centrifuge for 2 minutes at maximum speed.
14. Store the DNA at -20°C and discard the column.

10.7.2. Separation and purification of the genetic material: DNA electrophoresis

Agarose gel electrophoresis relies on the separation of DNA fragments submitted to an electric field in the presence of a porous gel, formed by polymerized agarose, that allows the migration of DNA to the positive pole. Electrophoretic mobility of nucleic acids is inversely proportional to the molecular weight of the molecule, but other variables have also to be taken into consideration, such as agarose concentration, electric current applied, and, in the case of plasmid DNA, the conformation of the plasmid.

This is a simple and effective method for separating DNA or RNA fragments of different size. The size of each band obtained is determined by comparing it to a molecular weight marker that contains DNA fragments of known sizes. This marker also allows the quantification of the genetic material obtained in function of the intensity of the band. Agarose gels at 1.5% (w/v) are obtained for separating DNA fragments of up to 1 kb, and agarose gels at 0.8% (w/v) for larger DNA fragments.

DNA fragments visualizing is performed using the SYBR Safe colorant (S33102, Invitrogen), which is a DNA intercalating agent that emits fluorescence when irradiated with blue light at 470 nm of wavelength.

In order to perform DNA electrophoresis, the following solutions are used:

- Tris-Acetate EDTA buffer (TAE) : 4 mM Tris (Panreac), 20 mM acetic acid (Panreac), 2 mM EDTA (Panreac)
- Loading buffer (6x) (R0611, ThermoScientific)
- SYBR Safe 1000X (S33102, Invitrogen)
- Top Vision Agarose (R0492, ThermoScientific)
- GeneRuler™ Mix, *Ready to use* (SM0334, ThermoScientific) molecular weight marker

Electrophoresis buffer is initially prepared at 10X and stored at room temperature.

When used, it is diluted 10 times with deionized water. Protocol:

1. The right amount of agarose for the gel preparation is weighted. For a standard 1% gel with 50 ml of TAE buffer, 0.5g agarose are used. Agarose is contained in a 250 ml Erlenmeyer, to which the TAE is added.
2. Agarose is melted in a microwave oven until no suspended particules are observed.
3. When the temperature of the melted agarose has decreased to 50-55°C, SYBR Safe is added at a ratio of 1 μ l for each 10 ml of gel.
4. The gel tray for the agarose gel is prepared with adhesive tape. The well comb is added to the gel in order to form the wells. Melted agarose is poured into the tray, and let there to solidify for 20-30 minutes.
5. The well comb and adhesive tape are removed from tray, which is placed into the gel box (electrophoresis unit), to which TAE buffer is added until it covers the surface of the gel.
6. Loading buffer is added to the DNA samples (1 μ l of loading buffer for each 5 μ l of DNA sample), and DNA samples are loaded to their corresponding well of the gel.
7. Electrophoresis is started, considering that a constant voltage not higher to 5 V/cm has to be applied (typically 90 V, for a 50 ml gel).
8. The electrophoresis is stopped when the colorant from the loading die (bromophenol blue) arrives to 2/3 of the gel length (normally it takes around 40 minutes).
9. DNA bands are observed using the device GelDoc EZ (Biorad), with a UV tray.

10.7.2.1. DNA purification from bands in agarose gels

In order to recover DNA fragments separated by electrophoresis, the portion of the gel that contains the band of interest is cut with a scalpel blade, and purified with

Chapter 11. Appendix

the GeneJet gel extraction kit (K0691, ThermoScientific), following manufacturer's instructions:

1. Remove the gel from the GelDoc EZ Imager and put it on the transilluminator (MaestroGen).
2. Switch off the light from the dark room and cut the band of interest with a scalpel blade and put it into a 1.5 ml eppendorf tube.
3. Add a 1:1 volume (i.e. 1 ml of buffer for 1 mg of band) of binding buffer into the tube that contains the band.
4. Incubate the fragment at 55°C for 10 minutes. Mix the solution by inversion each 2 minutes approximately, in order to facilitate agarose dissolution. Ensure that the gel is completely dissolved. Briefly vortex (5 seconds) before loading it into the column.
5. Check that the color of the solution is yellow, this indicates that the pH is optimal for DNA union to the column. If the color is orange or violet, add 10 µl of 3M sodium acetat, pH 5.2. The color will turn yellow.
6. Transfer up to 800 µl of the solution to the GeneJET purification column. Centrifuge for 60 seconds at 16000g. Discard the flow through.
7. Add 700 ml of washing buffer to the GeneJET purification column. Centrifuge for 60 seconds at 16000g. Discard the flow through and put the purification column back in the collection tube.
8. Centrifuge empty GeneJET purification column for an additional minute at 16000g in order to completely eliminate any remaining washing buffer trace.
9. Transfer the GeneJET purification column in a 1.5 ml Eppendorf tube. Add 30 µl of elution buffer to the center of the membrane of the purification column and centrifuge it at 16000g for 1 minute.
10. Discard the purification column and store the purified DNA at -20°C.

10.7.3. DNA quantification through spectrophotometry

DNA was quantified using an absorbance lecture at 260 nm (A_{260}) with a spectrophotometer (NanoDrop ND-1000, ThermoScientific) which provides the value of DNA concentration of the analyzed sample and also the purity of the sample, in terms of proportion A_{260}/A_{280} and A_{260}/A_{230} . Proteins and other contaminants absorb at 280 nm, while contaminants such as phenol, carbohydrates or guanidine chloride absorb at 230 nm. Values that indicate a good level purity for DNA are 1.8 or higher for A_{260}/A_{280} and 2 or higher for A_{260}/A_{230} .

10.7.4. Polymerase chain reaction (PCR)

PCR (Polymerase Chain Reaction) is a technology used in molecular biology for amplifying one or a few copies of a DNA fragment of known sequence, generating thousands or millions of copies (Saiki et al., 1988). This amplification can have several functions, including obtaining a high amount of a DNA sequence from a sample with low amount of this sequence, or assessing the presence of a specific DNA sequence in a sample.

PCR is based on cycles of heating and cooling, allowing DNA chains separation and DNA replication mediated by DNA polymerase. Other necessary elements for the PCR are the oligonucleotides or primers, which are short DNA sequences that allow the amplification of a specific region of interest of the initial DNA sample. DNA polymerase is thermally stable, and performs the amplification reaction using nucleotides, oligonucleotides, and template DNA. Along the reaction progression, the generated DNA also acts as a DNA template, thus, the region of interest is exponentially amplified.

Primers designed in this work are listed in the appendix II. Primers include, when necessary, restriction sites to the 5' end of the primer in order to allow the amplified sequence to be cloned in the expression vector of interest. Some extra nucleotides were added at the 5' of the restriction sites in order to allow the action of the

restriction enzymes. They also include, when necessary, the starting codon for mRNA translation (AUG) and the Stop codon (UGA, UAA, UAG). DNA polymerase Phusion (F531L, ThermoScientific) was used, since it is a polymerase with a low error rate.

The protocol performed for the PCR consisted in the following steps:

1. Thaw at room temperature the 2x Master Mix Phusion polymerase solution, the oligonucleotide solution and the DNA. Put them in ice.
2. Pipette in a PCR tube put in a box with ice, the following components in the indicated order:
 - a. 0.5 μ l of oligonucleotide Forward (10 μ M)
 - b. 0.5 μ l of oligonucleotide Reverse (10 μ M)
 - c. 2 μ l of template DNA (a 5 ng/ μ l)
 - d. 7 μ l of DEPC water
 - e. 10 μ l of 2x Master Mix Phusion
3. For the positive control, prepare a solution in the same way as described in step 2, but using oligonucleotides and a template DNA previously used from which it is known that it correctly performs the amplification. Annealing temperature of the positive control oligonucleotides should not be 5°C inferior to the annealing temperature of the oligonucleotides of the amplification of interest.
4. For the negative control (which has the function of checking that the oligonucleotide solution does not contain a DNA contamination), pipette in another tube:
 - a. 0.5 μ l of oligonucleotide Forward (10 μ M)
 - b. 0.5 μ l of oligonucleotide Reverse (10 μ M)
 - c. 2 μ l of template DNA (a 5 ng/ μ l)
 - d. 9.5 μ l of DEPC water
5. Insert inside the thermocycler the tubes that contain PCR reagents.

6. Start the i5 thermocycler and select the corresponding protocol (see the following table 10.6).

Table 10.6. PCR protocol

Cycle repetition	Steps	Time	Temperature
1x	Denaturalization	10 seconds	98°C
30x	Denaturalization	1 second	98°C
	Annealing	5 seconds	Temperature depending on the primer, generally between 45 and 65°C
	Elongation	15 s/kb of the amplified fragment	72°C
1x	Elongation	1 minute	72°C
1x	Preservation	Infinite	4°C

7. Once the PCR reaction is finished, the samples can be analyzed by means of an electrophoresis gel or be frozen at -20°C for posterior treatments.

10.7.4.1. Fusion of DNA fragments by means of splicing overlap extension PCR (SOE-PCR)

This PCR variant allows the fusion or splicing of DNA fragments using two pairs of oligonucleotides containing a partial overlap of their sequences. For each one of the molecules to be fused, two primer pairs are designed. The reverse primer of the sequence located in the 5' end of the fusion objective sequence must have an homology region with the forward primer of the sequence located in the 3' end of the fusion objective sequence, as observed in Figure 10.8.

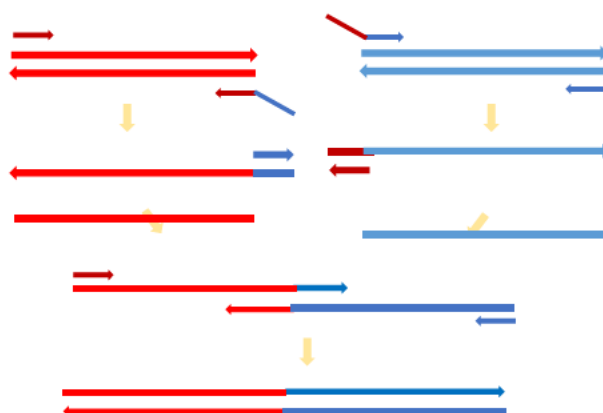


Figure 10.8. Scheme of a splicing overlap extension PCR.

The cycles sequence and temperatures are the same than in a conventional PCR, the only change is that it is performed in two steps: firstly, the two PCR reactions are independently performed, and, then, 1 μ L of each reaction are used as templates and incubated for 15 cycles. After that, the two most external oligonucleotides (forward 1 and reverse 2) are added and the PCR reaction is continued for 15-20 additional cycles. The final result is a PCR product consisting in the fusion of the sequence of interest. This technique has been used in this work for the construction of the Trastuzumab fused to a cytokine and the scFv fragments.

10.7.5. DNA enzymatic modifications

10.7.5.1. Digestion with restriction enzymes

The restriction endonucleases are enzymes that hydrolyze DNA in specific sites of its sequence. Type II enzymes, which are the most used, recognize sequences of 4 to 6 nucleotides (restriction sites), which are normally palindromic. Some of these enzymes cut the DNA sequence in the middle of the restriction site, generating blunt

ends, while other restriction enzymes generate cohesive or sticky ends. Most of the restriction enzymes have an optimal reaction temperature of 37°C.

The activity of the enzymes is measured in activity units. A restriction enzyme activity unit is defined as the necessary amount to completely digest 1 µg of DNA in 60 minutes, in the recommended conditions. The enzyme volume must be inferior to the 10% of the total reaction volume, since the glycerol present in the buffer of the enzyme solution can impair the enzyme activity if its concentration is higher than 5%. Enzymes are stored at -20°C and have to be contained in ice during their use. In this work, FastDigest restriction enzymes have been used (provided by ThermoScientific), since they allow a fast digestion of DNA (5-25'), and all enzymes can be used with the same restriction buffer.

The following procedure has been applied for performing restriction reactions:

1. Addition, in a 0.5 ml tube, the following amounts of reagents in the indicated order. The reagent amounts can be linearly scaled-up if more DNA is needed in the subsequent steps. Restriction enzymes should be kept in ice:
 - a) 2 µl of fast digest buffer
 - b) 1 µg of DNA
 - c) 1 µl of each restriction enzyme
 - d) 16 µl of DEPC (Diethyl Pyrocarbonate) H₂O
2. Incubate the restriction mixture at 37°C for 20 minutes and then for 20 minutes at 80°C in order to inactivate the restriction enzymes, in the thermocycler. If the used restriction enzyme cannot be inactivated by heating, the DNA will have to be purified with a PCR purification kit (GeneJET PCR purification kit (K0701 ThermoScientific) following manufacturer's instructions:
 - a) Add a 1:1 volume of binding buffer to the DNA solution. Mix vigorously by pipetting. Check the color of the solution, it should be yellow, indicating that the solution has the optimum pH for binding

the DNA to the column in the subsequent step. If the solution is not yellow, add 10 μl of a solution 3M sodium acetate, pH = 5.2.

- b) Transfer up to 800 μl of the solution to the purification column GeneJET. Centrifuge during 30-60s at 16000g. Discard the flow-through.
- c) Add 700 μl of washing buffer to the purification column GeneJET. Centrifuge for 30-60s at 16000g. Discard the flow-through and put the column back into the collection tube.
- d) Centrifuge the empty purification column for an additional minute in order to completely eliminate any washing buffer from the sample.
- e) Transfer the purification column into a clean microcentrifuge tube of 1.5 ml. Add 30 μl of elution buffer to the centre of the membrane of the purification column, and centrifuge it at 16000g for one minute.
- f) Discard the purification column and store the purified DNA at -20°C .

10.7.6. DNA dephosphorylation

The dephosphorylation of the 5' ends of DNA is performed in order to avoid the religation of plasmids that have been linearized with restriction enzymes. The dephosphorylation enzyme used in this work has been alkalyne phosphatase FastAP (EF0654, ThermoScientific) with its corresponding buffer. Each 1 μl of FastAP is able to dephosphorylize 1 μg of DNA in a volume of 20 ml, with 2 μl of dephosphorylation buffer. The solution has to be incubated at 37°C for 5 minutes and then at 80°C for another 5 minutes for performing the dephosphorylation and then inactivation reactions of the phosphatase.

10.7.7. Ligation of DNA fragments

DNA fragments ligation is a technique mainly used in order to clone inserts into plasmid vectors. The enzyme that has been used has been the T4 DNA Ligase (EL0014, ThermoScientific), which catalyzes the formation of a phosphodiester bond between 5-P' and 3-OH' ends in double-stranded DNA or RNA. This enzyme requires the presence of ATP for the reaction to take place. Ligation buffer used includes the necessary ATP amount. The DNA amount of needed insert to add is calculated using the following equation (10.4.):

$$ng\ insert = ng\ vector \cdot \frac{insert\ length\ (pb)}{vector\ length\ (pb)} \cdot molar\ proportion\ insert:vector$$

Figure 10.4. Map of pTRIpuro3 vector.

The following procedure has been applied for insert and vector ligation:

1. Addition in a 0.2 ml RNase-free tube of the following amounts of reagents:
 - X μ l of vector (the volume that corresponds to 30 ng of vector, up to a maximum of 4 μ l)
 - X μ l of insert DNA, containing a DNA amount in a molar relation of 3:1 (for ligations with cohesive ends) or 1:1 (for blunt ends) with respect to the amount of DNA (30 ng) of the vector (see equation 10.4), up to a maximum of 2 μ l
 - 1 μ l of T4 DNA ligase
 - 2 μ l of ligation buffer 10X
 - X μ l of DEPC water, in order to have a total volume of 20 μ l
2. As a negative control, in order to discard possible vector religations, a ligation reaction with the same conditions as in step 1 has to be prepared, substituting the insert volume for DEPC water.

3. Incubate the reaction at room temperature (22°C) for 120 minutes, alternatively it can be incubated for 16h at 4°C.
4. Proceed to transformation (see 10.7.7.1.) or store it at -20°C.

10.7.7. Introduction of genetic material into organisms

In this work, genetic material has been introduced in bacteria (transformation) and also in animal cells (transfection).

10.7.7.1. Bacteria transformation by means of heat shock process

The transformation process consists in the incorporation of exogenous plasmid DNA into competent *E. coli* DH5 α cells (12297016, ThermoScientific).

1. Thaw the competent cells by putting the vial in ice. Thaw 3 extra vials for controls.
2. Maintain the tubes in ice for 10 minutes.
3. Add 10 μ l of ligation mixture or up to 100 ng of circular plasmid to the cell suspension. Include a control adding 10 μ l of DEPC water, a second control with 1 μ l of a circular DNA plasmid (positive control) and another control consisting in adding the ligation without insert (negative control of the ligation reaction).
4. Maintain the tubes 10 minutes in ice.
5. Transfer the tubes to the thermocycler at 42°C and incubate for 60 seconds. It is very important to exactly incubate this amount of time.
6. Put the tubes in ice and maintain them 1-2'.
7. Add 390 μ l of sterile LB medium to each tube and incubate at 37°C at the thermocycler for 45 minutes. This allows the bacteria to express the antibiotic resistance protein (codified in the transformed plasmid). Gently invert the tube two or three times during the incubation.
8. Seed 200 μ l of each tube in a plate LB+Ampicillin mediating a Digrafsky spreader.

9. Incubate the plates for 16h at 37°C.

10.7.7.2. Animal cells transfection by means of lipofection

Lipofection (or transfection with liposomes) is a technique used for transferring genetic material to a cell mediating liposomes, which consist in vesicles that can easily fuse with the cell membrane, since both are formed by a fosfolipid bilayer. Lipofection is based on a positively charged lipid that forms a complex with the negatively charged genetic material. Cells then incorporate the formed complex mediating endocytosis. During the present work, the K2 Transfection kit (Biontexas) has been used, which contains the K2 Transfection reagent for forming the lipidic complexes and also the K2 Multiplier reagent, which is added in the first step of the process for decreasing the cells ability to recognize nucleic acids and therefore their ability to eliminate them, and improve the efficiency of the process.

The following protocol has been applied:

1. $1 \cdot 10^6$ cells are for each transfection to perform. A positive control should be included, consisting in transfecting the vector pIRESpuro3_eGFP (pIRESpuro3 vector containing the fluorescent protein eGFP), which will allow calculating the transfection efficiency and puromycin selection efficacy.
2. The cells are centrifuged (5 min at 800g) and washed with 900 μ l of SMF4Transfx medium.
3. 900 μ l are resuspended in fresh medium. The obtained cell suspension is homogeneously dispensed in each well in a 12-well plate.
4. 20 μ l of K2 Multiplier are added, the plate is gently homogenized.
5. Incubation for 2h at 37°C, 5% CO₂, 95% humidity.
6. Meanwnile, transfection solutions are prepared, which contain:
 - 1 μ g of plasmid DNA
 - 100 μ l of SFM4Transfx

- 4 μ l of K2 Transfection reagent
7. Homogenize the solutions by pipetting using DNase-free sterile filter tips.
 8. Incubate the solutions for 20 minutes.
 9. Add the solutions to the cell-containing well.
 10. Incubate for 24h. Check the transfection efficiency mediating fluorescence microscopy as indicated in the next section.
 11. In order to select the transfected cells, change the transfection medium with selective medium (see 10.2.1.1) 24h after the transfection of the cells.

10.7.7.2.1. Determination of transfection efficiency by fluorescence microscopy

The determination of the transfection efficiency is determined using an aliquot of the transfected cell culture of interest.

The phase contrast and epifluorescence microscope Olympus BH-2 has been used. This microscope allows irradiating the sample with UV light filtered with a dichroic DM500 filter and an excitation B-460 filter, irradiating a blue light with a wavelength of 460-520 nm. This allows the excitation and the observation of eGFP (excitation at 495 nm, emission at 520 nm). In order to calculate the transfection efficiency, cell counting can be performed with an hemacytometer in phase contrast (this will be the total cells amount), and then it can be repeated in epifluorescence. The transfection efficiency can then be determined through the following equation (eq. 10.5):

$$\%eGFP \text{ positive cells} = \frac{\text{Fluorescent cells number}}{\text{Total cells amount}} \cdot 100$$

10.7.8. Sequencing of DNA

The sequencing of the generated DNA constructs was performed at the Bioinformatics and Genomics Service of the Biotechnology and Biomedicine Institute

of UAB, using an ABI 3130XL analyzer (Applied Biosystems). DNA samples were prepared at 100 ng/ μ l (10 μ l) and were sequenced by the Sanger method, which is based on the selective incorporation of chain-terminating labelled dideoxynucleotides during in vitro DNA replication. Chromas Lite 2.3 software was used for the manipulation of the obtained sequencing chromatograms.

10.8. Antibody purification

In order to purify the produced Trastuzumab and Trastuzumab-derived molecules, a downstream sequence has been implemented consisting of several steps and depending on the production system employed: recovery of the product is not the same when produced with HEK293 or in the case of bacterial production (for scFv).

10.8.1. Solid-liquid separation

The first step of the recovery sequence consists in the separation of the biomass from the culture medium. When the product is secreted to the medium, as it is the case of the HEK293 production, the medium needs to be recovered. In the case of *E. coli* production, the product remains inside the cell, therefore, the biomass is the fraction of interest.

10.8.1.1. Centrifugation

Centrifugation is one of the most used ways to separate particles from a solution.

10.8.1.1.1. Centrifugation for small scale production with HEK293

For small scale production of Trastuzumab with HEK293 cells (see 3.3.2), the medium was recovered performing a centrifugation step at 3000g, for 15 minutes at 4°C (Avanti J20 XP, Beckman Coulter). Conical polypropylene 15 or 50 ml tubes (Corning)

were used. The supernatant was recovered and further purified following the downstream sequence.

10.8.1.1.2. Centrifugation for production with *E. coli*

For scFv production with *E. coli*, a centrifugation step at 5.000g for 10 minutes at 4°C (Avanti J20 XP, Beckman Coulter) was applied. The biomass was recovered and further purified following the downstream sequence. Centrifugation 500 ml tubes (Beckman Coulter, 355605) were used.

10.8.1.2. Depth filtration

Depth filtration consists in using a porous medium that is capable of retaining particulates throughout its matrix rather than just on its surface. In this work, it has been used for the clarification of the single use culture processes (wave and STR 50L bioreactors).

For the 5L wave process, a CS40MS filter (CS40MS02H1, MerckMillipore) of 0.027 cm² was used. The culture broth was pumped through the filter by means of a Watson Marlow 323 peristaltic pump (Watson Marlow). An analogic manometer was connected before the entry of the feed tube to the filter. The filter was first humidified with 550 ml of deionized water and then equilibrated with 550 ml of PBS (both at a flow of 60 ml/min). Then, the culture broth was pumped at a flow of 50 ml/min, avoiding the entry pressure to reach 2 bar.

For the 50L process, a CS40MS filter (CS40MS05F1) Merckmillipore) of 0.55 cm² was used. The filter was installed in a Pod filter holder (MPODPILLOT, MerckMillipore). Then, the filter is connected through silicone tubes to the P2500 pump of the Sartoflow Alpha Plus SU device (Sartorius). The filter was first humidified with 50 L of deionized water and then equilibrated with 50 L of PBS (both with the pump at a 20% potency). Then, the culture broth was pumped through the filter, with a 20% potency of the pump.

10.8.2. Cell disruption

Cell disruption was performed to release the scFv product contained inside the *E. coli* used for production. Mechanical disruption by the method of French press, which is one of the most used methods for cell disruption, was applied. In this method, the cells are submitted to high pressures through a narrow annular gap, and then released through a discharge valve to atmospheric pressure, the pressure change making them explode.

The pellet obtained from the centrifugation step (see 10.8.1.1.2.) was resuspended in 20 mM sodium phosphate, NaCl 0.15M, MgCl₂ 8 mM; pH = 7.2, and the DO₆₀₀ of the resuspended broth was adjusted to 100. Then, DNaseI (Roche) was added at a concentration of 50 µg/ml. The resuspended cells were disrupted through 2 cycles at 1.44 kbar, using a TS 5 4 kW disruptor (Constant Systems). Disrupted cells were then centrifuged at 8000g, 40 minutes, 4°C (Avanti J20 XP, Beckman Coulter). Aliquots of 50 ml of disrupted cultures were stored at -20°C.

10.8.3. Microfiltration

A microfiltration step is necessary in order to remove the solid particulates from the cell culture that have not been completely removed in the solid-liquid separation steps. Typical microfiltrations involve membranes with 0.45 or 0.2 µm of absolute pore size rating.

10.8.3.1. Small scale microfiltration

For small scale HEK293 culture and aliquots of *E. coli* disrupted culture, microfiltration was performed with 0.45 µm single use membrane filters (HAWP02500, MerckMillipore) of 25 mm of diameter. The medium to be filtered was passed through the filter by using a 50 ml syringe.

10.8.3.2. Microfiltration for HEK293 bioreactor cultures

Microfiltration of the broth recovered from depth filtration from the 5L wave bioreactor was performed using a 0.2 μm filter Millipore Express SHF Opticap XL300 of 480 cm^2 (KGEPG003HH3, Merck Millipore). The culture broth was pumped through the filter by means of a Watson Marlow 323 peristaltic pump (Watson Marlow). An analogic manometer was connected before the entry of the feed tube to the filter. The filtration was carried out at a maximum flow of 213 ml/min, lowering it when the entry pressure surpassed 2 bar. The filtrated broth was then stored overnight at 4°C. The filter was then washed with 1L of NaOH 0.5M and then with deionized water.

In the case of the 50L culture, the filtration was carried out using a 0.2 μm filter Millipore Express SHF Opticap of 5400 cm^2 (KGPA10TT1, Merck Millipore). The culture broth was pumped through the filter by means of a Watson Marlow 323 peristaltic pump (Watson Marlow). An analogic manometer was connected before the entry of the feed tube to the filter. The filtration was carried out at a maximum flow of 213 ml/min, lowering it when the entry pressure surpassed 2 bar. The filtrated broth was then stored overnight at 4°C in a single use bag (Sartorius).

10.8.4. Concentration

In order to reduce the volume of product to be loaded to the chromatography (last purification step), a concentration step was applied for the microfiltrated products produced with HEK293 bioreactor processes. The concentrations were performed through tangential flow ultrafiltration, in which the majority of the feed flow travels tangentially across the surface of the filter, washing away the filter cake during the filtration process, thus increasing the length of time that a filter unit can be operational.

In the case of the product produced with the 5L wave bioreactor, the filtration was performed using two 30 kDa membranes in Hydrosart ultrafiltration cassettes of 200 cm² (Sartorius), sustained in a Sartocon Slice 200 Holder (Sartorius). The membrane cassettes were installed on the holder and then a manometer was connected before the entry of the feed tube and after the outing of the retentate tube. First, 1L of deionized water and then 600 ml of PBS were pumped using a Watson Marlow 323 peristaltic pump (Watson Marlow), at a 20% of the potency of the bomb, or avoiding the feed pressure to reach values higher than 2 bar. Once the product volume had been reduced 10 times (obtaining approx. 500 ml of final volume), the concentration was stopped. The filters were cleaned by pumping 2L of deionized water and then 1L of 0.5M NaOH were recirculated overnight. Then, deionized water was passed again until outing pH was neutral.

In the case of the product produced with the 50L wave bioreactor, the filtration was performed using a 30 kDa membrane in Hydrosart ultrafiltration cassettes of 4200 cm² (Sartorius). Then, the filter is connected through silicone tubes to the P3000 pump of the Sartoflow Alpha Plus SU device (Sartorius). The filter was equilibrated by passing 10L of PBS. A holding volume of 9L was used. Once the product volume had been reduced 10 times (final volume obtained of approx. 4.5L), the concentration was stopped. The filters were cleaned by pumping 2L of deionized water and then 0.5M NaOH recirculating overnight. Then, deionized water was passed again until outing pH was neutral.

10.8.5. Chromatography

Chromatography is a technique employed for the separation of the components of a mixture, which are dissolved in a fluid stream called the mobile phase, which travels through a structure holding a material called the stationary phase. The interaction of the components of the mixture with the stationary phase makes them

travel at different speeds, causing them to separate. There are several chromatography types, depending on the nature of the stationary phase. In antibody purification, the most used chromatography is affinity chromatography, which is based in very specific non-covalent interaction between the molecule of interest of the mobile phase and the stationary phase. In this work, affinity chromatography has been used to purify Trastuzumab and Trastuzumab-derived molecules.

10.8.5.1. Trastuzumab and Trastuzumab-derived molecules purification with protein A and protein L affinity chromatography

The typical affinity chromatography for antibody purification employs protein A in the stationary phase. Protein A is a 42 kDa surface protein originally found in the cell wall of the bacteria *Staphylococcus aureus*, which has a high binding affinity for several immunoglobulins, having a particularly strong affinity for human IgG1, binding to the heavy chain of the Fc region.

For antibody fragments or light chain purification, Protein L has been used as the ligand of the stationary phase. Protein L was isolated from the surface of the bacteria *Peptostreptococcus magnus* and was found to bind to immunoglobulins through L chain interaction.

In this work, the MabSelect SuRe resin (GE Healthcare) has been used as a stationary phase. This resin contains an engineered Protein A ligand that is alkali-tolerant, having greater stability than Protein A affinity resins in the alkaline conditions used in cleaning-in-place (CIP) and sanitization protocols (GE Healthcare, 2019).

Typical chromatography purification runs include an equilibration step of the column with binding buffer, the loading of the sample to be purified, a wash step with binding buffer in order to wash away the molecules that have weakly interacted with the column, and an elution step with washing buffer. The protocol employed for Trastuzumab consisted in the following steps, performed using an ÄKTA Avant 150 chromatographer (GE Healthcare):

Chapter 11. Appendix

1. Install the column into the ÄKTA Avant chromatographer and pump binding buffer until the absorbance at 280 nm and pH values are stable (the column is stored in a 20% (v/v) ethanol solution, which has to be removed).
2. Equilibrate the column with 5 column volumes of binding buffer:
 - a. For Protein A chromatography: 20 mM phosphate, NaCl 150 mM, pH = 7.4
 - b. For Protein L chromatography: 50 mM sodium citrate, pH = 6.5
3. Load the sample to the column. Collect a sample of the flow-through for further analysis.
4. Wash the column with 10 column volumes of binding buffer. Collect a sample of the washed column for further analysis.
5. Elute with 5 column volumes of elution buffer:
 - a. For Protein A chromatography: 50 mM citrate, pH = 3.2
 - b. For Protein L chromatography: 50 mM sodium citrate, pH = 2.3
6. Dialyze the eluted product with PD-10 or PD Minitrap G-25 desalting columns (GE Healthcare), using 50 mM citrate, pH = 6.
7. Regenerate the column by passing another 5 column volumes of elution buffer and then wash it by passing 3 column volumes of binding buffer.
8. Perform a CIP of the column with 0.1M NaOH, 5 column volumes. Wash it with 3 column volumes of binding buffer.
9. Reequilibrate the column with 20% (v/v) ethanol solution and store it at 4°C.

For small scale and wave bioreactor production of Trastuzumab, Trastuzumab_cys114 or heavy chain, a HiScreen MabSelect SuRe Column (GE Healthcare) for was used. For light chain and scFv production, HiScreen Capto L (GE Healthcare) was used. For bioreactor pilot scale productions, a XK 26/40 column (GE Healthcare) packed with 55 ml of MabSelect SuRe resin was used. In Table 10.7. the column features are summarized, including the working flow rates for each column.

Table 10.7. Features of the columns used for antibody purification chromatography

Column	Resin volume	Operation flow for equilibration, wash and elution	Operation flow for sample loading
HiScreen MabSelect SuRe / CptoL	5 ml	3.9 ml/min	2.3 ml/min
XK 26/40 MabSelect SuRe	55 ml	25 ml/min	25 ml/min

10.9. Protein characterization

10.9.1. Molecular weight and purity: SDS-PAGE

Protein electrophoresis mediating polyacrilamide gel is a technique that allows the separation of proteins based on their molecular weight. Proteins from the sample are denaturalized with the detergent sodium dodecylsulfate (SDS), which is present in the loading dye, negatively charging the proteins with the same negative charge density. Proteins are then separated in a polyacrilamide gel to which an electric field is applied. The gels can be prepared in three main conditions:

- Native conditions: SDS is not added, proteins migrate depending on their native electric charge and tridimensional conformation.
- Denaturalizing conditions: SDS is added, breaking the weak interactions between protein subunits and eliminating the tertiary structure of the protein, except if it is hold together mediating disulfide bridges. Proteins will migrate depending on their molecular weight.

- Reducing denaturalizing conditions: β -mercaptoethanol or DTT are added to the samples (in addition to SDS), in order to break disulfide bridges of the protein of interest.

In this work, MiniProtean TGX StainFree gels (4568095, Biorad) have been used. These gels are precast gels and contain a trihalomethane compound that reacts with the tryptophan residue of the proteins. This compound allows the direct visualization of the proteins once the gels are irradiated with UV light.

Sample preparation protocol consists in:

1. Mix 7.5 μ l of sample with 7.5 μ l of Laemmli 2x loading dye (1610737, Biorad) in a 0.5 ml tube. Add 0.75 μ l of β -mercaptoethanol when performing a gel in reducing conditions. Add 10 μ l of molecular weight marker (Precision Plus Protein Unstained, Biorad, ref 1610363) to the most external wells.
2. Incubate the samples at 95°C for 5 minutes in a thermocycler.
3. Insert the gel into the electrophoresis box, and fill it with running buffer (Tris-glycine-SDS).
4. Load the samples in the gel, carefully avoiding disrupting the wells.
5. Apply a voltage of 250V for 20 minutes to the electrophoresis box.
6. Remove the gel from the electrophoresis box, remove the gel protection, and put the gel on a UV tray.
7. Put the tray with the gel inside the GelDocEZ imager (Biorad) and irradiate it with UV light for 90s.
8. Process the obtained image using the ImageLab software (Biorad).

10.9.2. Concentration determination: SDS-PAGE and spectrophotometry

Antibody concentration was determined using two different alternatives: densitometry analysis (from SDS-PAGE) and spectrophotometry analysis.

10.9.2.1. Concentration determination by densitometry analysis (SDS-PAGE)

Protein concentration of the band of interest was calculated using the ImageLab software (Biorad). The relative quantity tool of the software was used to obtain the amount of protein of a band with respect to a reference band of the molecular weight marker (Precision Plus Protein Unstained, Biorad, ref 1610363), which contained a known amount of protein. For whole antibody bands, the reference band of the molecular weight marker consisted in the 150 kDa band, which contains 150 ng of protein, while for antibody fragments, the 20 kDa band (150 ng) or the 50 kDa band (750 ng) were used as a reference.

10.9.2.2. Concentration determination by spectrophotometry

For pure samples of whole antibody, their concentration could also be calculated using the spectrophotometer NanoDrop (ND-1000, ThermoScientific). It uses an extinction molar coefficient in order to calculate the protein concentration from the absorbance of the sample. For whole IgG, it has a predetermined molar extinction coefficient.

10.9.3. Antigen binding assessment

10.9.3.1. Immobilized antigen binding: ELISA

The ability of the produced Trastuzumab and Trastuzumab-derived generated molecules to bind to their target HER2 antigen has been assessed with an ELISA (Enzyme Linked ImmunoSorbent Assay), which is a commonly used analytical biochemistry assay. In the applied assay, the target HER2 antigen (10004-HCCH, Sinobiological) is immobilized on the surface of a plate, and then it is recognized by Trastuzumab, which acts as a primary antibody. Trastuzumab is later recognized by a secondary antibody, a polyclonal anti-human IgG1 antibody (A00166, Genscript) conjugated to the enzyme Horse Radish Peroxidase (HRP), which generates colored

products from chromogenic substrates. For antibody fragments, instead of the previously described secondary antibody, a protein L protein conjugated to HRP (Genscript, ref M00098) was used.

The followed protocol consists of the following steps.

Prepare the following solutions:

- Anti-HER2 antigen solution (0.5 $\mu\text{g}/\text{ml}$) in PBS
 - Anti-human IgG1 conjugated to HRP (1 $\mu\text{g}/\text{ml}$) in PBS
 - Dilution PBS buffer (Hyclone)
 - Blocking solution: PBS-Tween20 0.05% (Sigma) + Skim Milk Powder 3% (LP0031, Oxoid)
 - Wash solution: PBS-Tween20 0.05% (Sigma)
1. Pipette 50 μl of HER2 antigen (1 $\mu\text{g}/\text{ml}$) in each well, cover the plate with a plastic cover and incubate at 4°C, 16h.
 2. Discard the content of the plate.
 3. Wash the plate three times with 200 μl of washing solution, discarding the content of the plate between wash steps.
 4. Gently dry the plate with a microfiber wiper.
 5. Pipette 100 μl of blocking solution into each well. Cover the plate and incubate at room temperature for 1h.
 6. Proceed as in step 4.
 7. Pipette 50 μl of dilution PBS buffer in each well.
 8. Pipette 50 μl of Trastuzumab sample to a well of row 1. Each different Trastuzumab sample to be analyzed will be added to a different well.
 9. Perform a serial dilution 1:2 in the plate from row 1 to 8, pipetting 50 μl between wells. Discard the final 50 μl .
 10. Pipette 50 μl of PBS in the blank wells.

Chapter 11. Appendix

11. Proceed as in step 2, 3 and 4.
12. Pipette 50 μl of a solution of secondary antibody diluted 1:10000 (0.1 $\mu\text{g}/\text{ml}$) in each well. Cover the plate and incubate at room temperature for 1h.
 - a. For antibody fragments, pipette 50 μl of a solution of Protein L-HRP diluted 1:20000 (0.025 $\mu\text{g}/\text{ml}$).
13. Proceed as in step 2, 3 and 4.
14. Pipette 50 μl of TMB solution. Incubate at room temperature during a maximum of 20 minutes. Shorter incubation times can be applied if the reaction occurs more rapidly than expected, in order to avoid saturation of the signal.
15. Stop the reaction by adding to each well 50 μl of H_2SO_4 , 20%.
16. Read the plate in a microplate reader. Absorbance at 405 nm and 600 nm wavelength has to be determined. Absorbance value of each well corresponds to the difference of both absorbances ($A_{405}-A_{600}$).

10.9.3.2. Cell surface antigen binding: Flow cytometry assay

Flow cytometer is a device that allows analyzing cell populations by separating individual cells in a laminar liquid flow. Individual cells pass through a detector that allows determining their size (Forward Scattering, FSC), their intracellular complexity (Side Scattering, SSC), and their fluorescence levels at different excitation and emission wavelengths. These parameters are represented in DotPlot graphs (Fig 10.9.), in which the cell population to be analyzed is delimited.

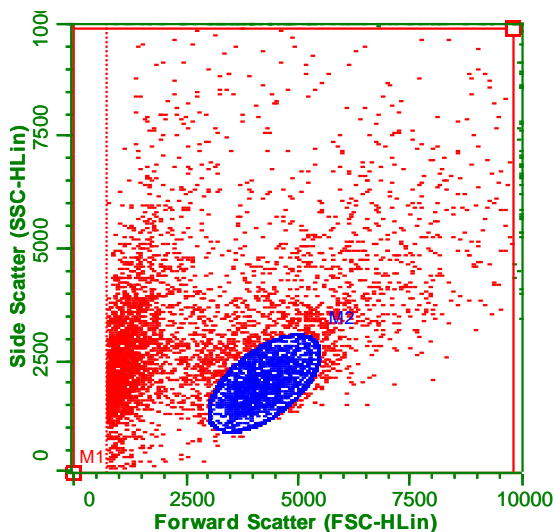


Figure 10.9. DotPlot of a SKBR3 cell population analyzed through the Guava EasyCyte.

In order to assess the ability of Trastuzumab or Trastuzumab-derived molecules to bind to its target antigen HER2 when found on the surface of a cell, Trastuzumab was incubated with the target cells and then a secondary anti-human IgG1 antibody conjugated to phycoerythrin was added. Therefore, cells with to which Trastuzumab is bound can be detected with the cytometer, through the emission of red light from phycoerythrin.

The analysis have been performed on unicellular population, excluding dead cells and aggregates. Guava easyCyte (Luminex) device was used for this assay.

The used protocol consisted in:

1. Centrifuge $5 \cdot 10^5$ cells of interest at 1000g for 3 minutes and discard the supernatant.
2. Wash the cells two times with PBS and resuspend them in 100 μ l of PBS.
3. Add 4 μ l of Trastuzumab antibody and incubate for 15 minutes.
4. Wash the cells two times with PBS and resuspend them in 100 μ l of PBS.

5. Add 1 μl of secondary antibody (anti-human IgG1 polyclonal antibody conjugated to phycoerythrin) and incubate for 15 minutes.
6. Wash two times with PBS and resuspend the cells in 500 μl of PBS.
7. Pass the cells to the flow cytometer. Excitation: 488 nm, emission: 583 nm (yellow light).

10.9.4. Aggregates determination and free drug determination: Size-Exclusion Chromatography-HPLC

High Performance Liquid Chromatography (HPLC) is a technique in analytical chemistry that can be used to separate, quantify and identify each component in a mixture. It relies on passing the sample mixture through a column containing a resin that interacts in a different way with each component of the sample, separating them. In this case, a Size-Exclusion Chromatography (SEC) column has been used: the components of the sample will be separated according to their size, with larger molecules being firstly eluted. In this case, aggregates will elute first, and, in the case of conjugated products, free drug will elute last.

In this work, SEC-HPLC experiments were performed in a Waters Alliance 2695 system using Zenix-C SEC-300 column (4,6 x 300 mm, Sepax, DE, USA). The mobile phase was PBS 1x (Sigma, MO, USA) at a flow rate of 0,35 ml/min. The absorbance of the eluted species was analyzed using UV light at a wavelength of 214 nm.

For free drug quantification in conjugated ADC products, drug at different concentrations was passed through the column in order to establish an area vs concentration calibration curve.

10.9.5. Mass and glycosylation pattern determination: Mass Spectrometry (MS)

In order to assess the mass of the produced antibody and its glycosylation pattern, a mass spectrometry (MS) assay was performed. Mass spectrometry is an analytical technique which ionizes chemical species and sorts the ions based on their mass-to-charge ratio.

In this thesis, the different MS assays were performed by the BioOrganic Mass Spectrometry Laboratory (LSMBO) at *Université de Strasbourg* (France). For deglycosylation, the enzyme IgGZero (Genovis) was used, at a ratio of 1 unit enzyme/1 µg IgG, applying an incubation of 30' at 37°C. Samples were manually desalted using a vivaspin 30 kDa ultracentrifugation device (Sartorius) exchanging buffer through five centrifugation cycles to AcONH₄ 150mM pH 6.9. Samples were then analyzed with an Exactive Plus EMR Orbitrap mass spectrometer (ThermoFisher), and data processing was performed using the MassLynx software (Waters).

10.9.6. Endotoxin content test: LAL method

An endotoxin content determination test based on the chromogenic end point method *Limulus* Amebocyte Lysate (LAL) has been used. The *Limulus* amebocyte lysate is an aqueous extract which contains a protein that causes the aggregation of endotoxins through an enzymatic reaction. Bacterial endotoxins catalyze the activation of the proenzyme present in the LAL to an active enzyme that liberates the p-nitroaniline (pNA) of the colorless substrate. The pNA has a color that can be detected at 405-410 nm wavelength when the reaction is stopped (see Fig. 10.10). The correlation between the absorbance and the endotoxin amount is lineal between 0.1-1,0 EU/ml, therefore, the endotoxin concentration of the sample can be calculated using a reference standard.

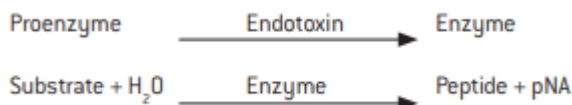


Fig. 10.10. LAL reaction scheme. Obtained from (Lonza 2015).

In this work, the LAL kit QCL-1000 (Lonza) has been used.

10.10. Antibody/fragment conjugations

Several whole antibody or antibody fragment conjugations to cytotoxic drugs have been performed in this work, with the drugs DM1 and vcMMAE, in heterogeneous and homogeneous ways.

10.10.1. Heterogeneous conjugation with DM1

Trastuzumab (whole antibody and scFv fragment) conjugation to DM1 has been performed heterogeneously, with the cytotoxic drug being conjugated to Lysine residues of the antibody, using the SMCC linker, with an aimed DAR of 3.1.

This has been the followed protocol:

- Solutions preparation:
 - Buffer A (50 mM potassium phosphate; 50 mM sodium chloride; 2 mM EDTA, pH 6.5). The following components are dissolved in 100 ml MilliQ ultrapure water and pH is adjusted with K₂HPO₄, if necessary (all the components from Sigma Aldrich):
 - 0.06072 g KH₂PO₄
 - 0.1609 g K₂HPO₄
 - 0.292 g NaCl
 - 0.058 g EDTA

Chapter 11. Appendix

- Antibody conjugation (example for conjugating 5 mg of Trastuzumab and scFv, and considering that the recovery percentage of dialyzing steps is 100%, for lower yields, escalate DM1 and reaction volumes accordingly):
 - Prepare the antibody to be contained at 20 mg/mL in buffer A
 - Dialyze it with Desalting G25 columns (GE Healthcare) equilibrated with Buffer A
 - Check the antibody concentration by spectrophotometry using Nanodrop (NanoDrop ND-1000, ThermoScientific).
 - Concentrate the antibody to 20 mg/ml using Amicon Tubes 30 or 3 kDa (GE Healthcare). Lower concentrations as low as 15 mg/mL have also been successfully tested.
 - Check the antibody concentration by spectrophotometry using Nanodrop (NanoDrop ND-1000, ThermoScientific).
 - Prepare stock solution of SMCC linker (at 20 mM): dissolve 5 mg of SMCC (Sigma Aldrich, 22360) in 747 μ l of DMSO (Sigma Aldrich, 472301) in an 1.5 ml Eppendorf tube.
 - Add the following volume of SMCC stock solution to the antibody/fragment solution, in both cases at a molar proportion of 7.5 of SMCC with respect to the antibody/fragment:
 - For whole Trastuzumab, add 12.88 μ l of SMCC stock solution.
 - For scFv, add 70.57 μ l of SMCC stock solution to the antibody solution. For lower DARs of scFv, the amount of SMCC was scaled down in a linear proportion (i.e. for an aimed DAR of 1.5, 34.15 μ l of SMCC stock solution was added).
 - Incubate for 2h at room temperature, at 300 rpm of mixing.
 - Prepare DM1 stock solution:

Chapter 11. Appendix

- All the DM1 and/or DMA manipulation steps have to be performed in a fume hood.
 - All the generated residues potentially containing DM1 have to be contained in safety containers and discarded.
 - Equilibrate the DM1 vial (Abcam, 146096) at room temperature for at least 1h.
 - Prepare the 10 mM DM1 stock solution: add 1.35 ml of DMA (Dimethyl Acetamide, Sigma Aldrich, ARK2190) with SolventSafe pipette tips (10470451, Fisher) to the DM1 vial (containing 10 mg of DM1), and homogenize very gently. SolventSafe pipette tips have a carbon fiber filter that blocks corrosive vapors generated when pipetting volatile organic solvents.
- Once the 2h of the linker conjugation have concluded, dialyze using a G25 desalting column (GE Healthcare) equilibrated with Buffer A, in order to eliminate the remaining SMCC linker. Measure the antibody/fragment concentration with Nanodrop and adjust the final volume with Buffer A obtaining a concentration of:
 - 10.6 mg/ml for whole Trastuzumab
 - 1.32 mg/mL for scFv
 - Transfer the antibody solution to a glass vial. The DM1 solution containing organic solvent (DMA) added in the following steps would have a corrosive effect on standard polypropylene Eppendorf tubes.
 - Add a volume of the stock DM1 solution to the antibody solution obtaining a molar proportion of 8.5 with respect to the antibody/fragment. Use Solvent Safe pipette tips. The volume of

DM1 solution cannot be higher than 6% of the total volume of the conjugation solution.

- For 5 mg of recovered Trastuzumab-SMCC, add 29.2 μ l of DM1 solution.
 - For 5 mg of recovered scFv-SMCC, add 240 μ l of DM1 solution. For lower DARs, the amount of DM1 was scaled down in a linear proportion (i.e. for an aimed DAR of 1.5, 116.13 μ l of DM1 stock solution was added).
-
- Incubate at room temperature for 16.5h at 300 rpm.
 - Dialyze with PBS using G25 desalting columns.
 - Store at 4°C.

10.10.2. Heterogeneous conjugation with vcMMAE

Heterogeneous Trastuzumab conjugation to vcMMAE has been carried out by means of a partial reduction with TCEP followed by a conjugation with vcMMAE, with an aimed DAR of 4. This has been the followed protocol:

- Solutions preparation:
 - TCEP: prepare stock solution at 0.5M in water, adjust pH with NaOH to 7. For 10 ml of stock preparation, dissolve 143.33 mg of TCEP (GEN-TCEP-1, Generon) in 10 ml of MilliQ water. Stock solution can be stored at -20°C.
 - PBS + DTPA 1.45 mM: dissolve 393 mg of DTPA (D6518, Sigma Aldrich) in 100 ml of PBS.
- Antibody conjugation (example for conjugating 5 mg of Trastuzumab):
 - Concentrate/dilute the antibody in order to have it at a concentration of 10 mg/ml in PBS (final volume of 486.2 μ l), in a 1.5 ml Eppendorf tube.

Chapter 11. Appendix

- Reduction step
 - Dilute a fraction of TCEP stock 1:50 with PBS and add 13.8 μl of it to the antibody solution (molar proportion of 4 with respect to the antibody).
 - Incubate 1h at 37°C.
- During the incubation step, prepare the vcMMAE stock solution:
 - All the vcMMAE manipulation steps have to be performed in a fume hood.
 - All the generated residues potentially containing vcMMAE have to be contained in safety containers and discarded.
 - Place a vcMMAE vial (MedChem Express, HY-15575) in ice, for approximately 30 minutes.
 - Add 76 μl of DMSO (dimethyl sulfoxide) to the vcMMAE vial, containing 1 mg of vcMMAE, in order to have a 10 mM vcMMAE stock solution.
 - Add, using Solvent Safe pipette tips, 382.13 μl of acetonitrile (Sigma Aldrich, 271004) in a glass vial. The organic solvent acetonitrile would have a corrosive effect on standard polypropylene Eppendorf tubes.
 - Add 17.86 μl of stock vcMMAE solution to the acetonitrile solution (final excess of 6x molar excess over Trastuzumab).
- Once the incubation at 37°C has ended, take a sample of 10 μl of the reduced antibody for checking on its reduction by means of a SDS-PAGE gel (10 μl).
- Add 1100 μl of PBS + DTPA 1.45 mM to the solution, up to a volume of 1.6 ml, in order to have the antibody at 2.5 mg/ml in the further conjugation step.
- Transfer the antibody solution in a glass vial.

- Add the prepared 0.4 ml of vcMMAE plus acetonitrile solution to the antibody solution, for a total 2 ml of solution, where 20% of the volume corresponds to vcMMAE plus acetonitrile.
- Incubate for 1h in ice.
- During the incubation, prepare a cysteine solution: dissolve 100 mg of cysteine (C7352, Sigma Aldrich) in 10 ml of PBS+DTPA 1.45 mM solution.
- Once the 1h of incubation has ended, perform the quenching step: add 43.3 μ l of cysteine solution, corresponding to a 20 molar proportion with respect to the added vcMMAE. Incubate for 30 minutes at room temperature.
- Dialyze with PBS using a G25 Desalting column (GE Healthcare).
- Store at 4°C.

10.10.3. Homogeneous conjugation with vcMMAE

Several homogeneous conjugations of Trastuzumab and scFv_cys111 fragment with vcMMAE have been attempted.

10.10.3.1. Trastuzumab DAR 8 conjugation

Homogeneous conjugation of Trastuzumab with the cytotoxic drug vcMMAE with a DAR of 8 has been carried out through applying a complete reduction with TCEP followed by conjugation. This has been the followed protocol:

- Solutions preparation:
 - TCEP: prepare stock solution at 0.5M in water, adjust pH with NaOH to 7. For 10 ml of stock preparation, dissolve 143.33 mg of TCEP (GEN-TCEP-1, Generon) in 10 ml of MilliQ water. Stock solution can be stored at -20°C.

Chapter 11. Appendix

- PBS + DTPA 1.45 mM: dissolve 393 mg of DTPA (D6518, Sigma Aldrich) in 100 ml of PBS.
- Antibody conjugation (example for conjugating 5 mg of Trastuzumab, and considering that the recovery percentage of dialyzing steps is 100%, for lower yields, escalate vcMMAE, acetonitrile and reaction volumes accordingly):
 - Concentrate/dilute the antibody in order to have it at a concentration of 10 mg/ml in PBS (final volume of 486.2 μ l), in a 1.5 ml Eppendorf tube.
 - Reduction step
 - Add 4.81 μ l of the TCEP stock solution to the antibody solution (molar proportion of 70 with respect to the antibody).
 - Incubate 1h at 37°C.
 - During the incubation step, prepare the vcMMAE stock solution:
 - All the vcMMAE manipulation steps have to be performed in a fume hood.
 - All the generated residues potentially containing vcMMAE have to be contained in safety containers and discarded.
 - Place a vcMMAE vial (MedChem Express, HY-15575) in ice, for approximately 30 minutes.
 - Add 76 μ l of DMSO (dimethyl sulfoxide) to the vcMMAE vial, containing 1 mg of vcMMAE, in order to have a 10 mM vcMMAE stock solution.
 - Add, using Solvent Safe pipette tips, 364.3 μ l of acetonitrile (Sigma Aldrich, 271004) in a glass vial. The organic solvent acetonitrile would have a corrosive effect on standard polypropylene Eppendorf tubes.

Chapter 11. Appendix

- Add 35.7 μl of stock vcMMAE solution to the acetonitrile solution (12x molar excess over Trastuzumab).
- Once the incubation at 37°C has ended, take a sample of 10 μl of the reduced antibody for checking on its reduction by means of a SDS-PAGE gel (10 μl).
- Dialyze with PBS + DTPA 1 mM using a G25 Desalting column (GE Healthcare). Measure the antibody concentration with Nanodrop ND-1000 (Thermofisher) and adjust its concentration to 3.13 mg/mL by dilution with PBS + DTPA 1mM, during the conjugation, or by concentration with 30 kDa Amicon Tubes in order to have it at 2.5 mg/mL.
- Transfer the antibody solution in a glass vial.
- Add the prepared 0.4 ml of vcMMAE + acetonitrile solution to the antibody solution, for a total 2 ml of solution, where 20% of the volume corresponds to vcMMAE + acetonitrile.
- Incubate for 1h in ice.
- During the incubation, prepare a cysteine solution: dissolve 100 mg of cysteine (C7352, Sigma Aldrich) in 10 ml of PBS+DTPA 1.45 mM solution.
- Once the 1h of incubation has ended, perform the quenching step: add cysteines in a 20 molar proportion with respect to the added vcMMAE: add 34.6 μl of cysteine solution. Incubate for 30 minutes at room temperature.
- Dialyze with PBS using a G25 Desalting column (GE Healthcare).
- Store at 4°C.

10.10.3.2. Trastuzumab_cys114 DAR 2 conjugation

The site-directed conjugation of the cysteine-engineered Trastuzumab_cys114 to the cytotoxic drug vcMMAE includes a first reduction step followed by a reoxidation and then conjugation. The applied protocol consists in the following:

- Solutions preparation:
 - DTT: prepare stock solution at 0.5M in water. For 10 ml of stock preparation, dissolve 7213 mg of DTT (Sigma) in 10 ml of MilliQ water. Stock solution can be stored at -20°C.
 - dhAA: prepare stock solution at 10 mg/ml. For 1 ml, dissolve 10 mg in 1 ml of PBS.
 - PBS + DTPA 1.45 mM: dissolve 393 mg of DTPA (D6518, Sigma Aldrich) in 100 ml of PBS.
- Antibody conjugation (example for conjugating 5 mg of Trastuzumab_cys114, and considering that the recovery percentage of dialyzing steps is 100%, for lower yields, escalate vcMMAE, acetonitrile and reaction volumes accordingly):
 - Concentrate/dilute the antibody in order to have it at a concentration of 10 mg/ml in PBS (final volume of 496.33 μ l), in a 1.5 ml Eppendorf tube.
 - Reduction step
 - Add 3.67 μ l of the DTT stock solution to the antibody solution (molar proportion of 50 with respect to the antibody: for other DTT molar excesses, add the DTT stock solution volume accordingly).
 - Incubate 1h at 37°C.
 - Dialyze with PBS + DTPA 1 mM using a G25 Desalting column (GE Healthcare).
 - Reoxidation:

Chapter 11. Appendix

- Add 52.2 μl of the stock solution of dhAA, for a molar excess of 2 with respect to the previously added reducing agent. Incubate at room temperature for 3 hours.
- During the incubation step, prepare the vcMMAE stock solution:
 - All the vcMMAE manipulation steps have to be performed in a fume hood.
 - All the generated residues potentially containing vcMMAE have to be contained in safety containers and discarded.
 - Place a vcMMAE vial (MedChem Express, HY-15575) in ice, for approximately 30 minutes.
 - Add 76 μl of DMSO (dimethyl sulfoxide) to the vcMMAE vial, containing 1 mg of vcMMAE, in order to have a 10 mM vcMMAE stock solution.
 - Add, using Solvent Safe pipette tips, 389.7 μl of acetonitrile (Sigma Aldrich, 271004) in a glass vial. The organic solvent acetonitrile would have a corrosive effect on standard polypropylene Eppendorf tubes.
 - Add 10.31 μl of stock vcMMAE solution to the acetonitrile solution (3x molar excess over Trastuzumab_cys114).
- Dialyze with PBS + DTPA 1 mM using a G25 Desalting column (GE Healthcare). Measure the antibody concentration with Nanodrop ND-1000 (Thermofisher) and adjust its concentration to 3.13 mg/mL with PBS + DTPA 1mM, in order to have it at 2.5 mg/mL during the conjugation, or by concentration with 30 kDa Amicon Tubes.
- Transfer the antibody solution in a glass vial.
- Add the prepared 0.389 ml of vcMMAE + acetonitrile solution to the antibody solution, for a total 2 ml of solution, where 20% of the volume corresponds to vcMMAE + acetonitrile.
- Incubate for 1h in ice.

- During the incubation, prepare a cysteine solution: dissolve 100 mg of cysteine (C7352, Sigma Aldrich) in 10 ml of PBS+DTPA 1.45 mM solution.
- Once the 1h of incubation has ended, perform the quenching step: add cysteines in a 20 molar proportion with respect to the added vcMMAE: add 24.9 μ l of cysteine solution. Incubate for 30 minutes at room temperature.
- Dialyze with PBS using a G25 Desalting column (GE Healthcare).
- Store at 4°C.

10.10.3.3. Construction and conjugation of an homogeneous Trastuzumab ADC without genetic modification: conjugation and assembly of independently produced heavy and light antibody chains

The construction and conjugation of this homogeneous ADC was achieved through the conjugation of the light chain and its assembly to the heavy chain, both chains being independently produced.

10.10.3.3.1. Chain assembly

Two different strategies for chain assembly were assessed: chain assembly through a reduction-oxidation approach and through a spontaneous assembly approach.

10.10.3.3.1.1. Chain assembly through reduction-oxidation approach

The reduction-oxidation mAb assembly approach consists of mixing HC and LC at an equivalent molar proportion and applying a reduction of the disulfide bonds of the mixed chains, with dcHC at a concentration of around 4.5 mg/mL and dcLC at around 1.7 mg/mL. This was achieved by adding a 16:1 molar proportion of DTT (Sigma) with respect to dcHC (heavy chain dimers), and the mixture was incubated at 37°C for 1h. Next, a dialyzing step was performed with G25 columns and 50 mM citrate buffer pH = 6, allowing the removal of the reducing agent. Finally, a 2:1 molar proportion of

dhAA (Sigma) with respect to DTT was added to promote disulfide bonds reoxidation for 3 hours at room temperature.

10.10.3.3.1.2. Chain assembly through spontaneous assembly approach

This assembly strategy consisted in an equimolar mixture of dcLC and dcHC in 50 mM citrate buffer (pH = 6) for 3h at room temperature, with dcHC at around 4.5 mg/mL and dcLC at around 1.7 mg/mL.

10.10.3.3.2. LC / scFv_cys111 conjugation

The conjugation of the LC consisted in a reduction step in order to free the capped cysteines, followed by a dialyzing step and the conjugation with vcMMAE. The scFv_cys111 conjugation consists in the same procedure, only modifying the protein concentration and reducing agent proportion. Protocol:

- Solutions preparation:
 - TCEP: prepare stock solution at 0.5M in water, adjust pH with NaOH to 7. For 10 ml of stock preparation, dissolve 143.33 mg of TCEP in 10 ml of MilliQ water. Stock solution can be stored at -20°C.
 - Sodium citrate + DTPA 1.45 mM: dissolve 393 mg of DTPA (D6518, Sigma Aldrich) in 100 ml of sodium citrate 50 mM, pH = 6.
- Antibody conjugation (example for conjugating 5 mg of LC and scFv_cys111, and considering that the recovery percentage of dialyzing steps is 100%, for lower yields, escalate vcMMAE, acetonitrile and reaction volumes accordingly):
 - Concentrate/dilute the LC/scFv_cys111 in order to have it at a concentration of around 5 mg/ml in sodium citrate buffer (pH = 6) (final volume of 1 ml), in a 1.5 ml Eppendorf tube. In the case of scFv_cys111, reduction at lower concentrations (as low as 1 mg/mL) can also be performed.
 - Reduction step

Chapter 11. Appendix

- For LC: Add 32 μl of the TCEP stock solution to the antibody solution (molar proportion of 100 with respect to the antibody).
- For scFv_cys111: Add 7.2 μl of the TCEP stock solution to the antibody solution (molar proportion of 20 with respect to the antibody).
- Incubate 1h at 37°C.
- During the incubation step, prepare the vcMMAE stock solution:
 - All the vcMMAE manipulation steps have to be performed in a fume hood.
 - All the generated residues potentially containing vcMMAE have to be contained in safety containers and discarded.
 - Place a vcMMAE vial (MedChem Express, HY-15575) in ice, for approximately 30 minutes.
 - Add 380 μl of DMSO (dimethyl sulfoxide) to the vcMMAE vial, containing 5 mg of vcMMAE, in order to have a 10 mM vcMMAE stock solution.
 - Add, using Solvent Safe pipette tips, 498.75 μl of acetonitrile (Sigma Aldrich, 271004) in a glass vial. The organic solvent acetonitrile would have a corrosive effect on standard polypropylene Eppendorf tubes.
 - Add 80 μl of stock vcMMAE solution to the acetonitrile solution (5x molar excess over LC/scFv_cys111).
- Once the incubation at 37°C has ended, take a sample of 5 μl of the reduced antibody fragment for checking on its reduction by means of a SDS-PAGE.
- Dialyze with sodium citrate 50 mM (pH = 6) + DTPA 1 mM using a G25 Desalting column (GE Healthcare). Measure the LC concentration with Nanodrop ND-1000 (Thermofisher) or SDS-PAGE

and adjust its concentration to 3.13 mg/mL with PBS + DTPA 1mM, in order to have it at 2.5 mg/mL during the conjugation, or by concentration with 30 kDa Amicon Tubes. The conjugation can be carried out at lower LC/scFv_cys111 concentrations (as low as 1.6 mg/mL for LC and 0.6 mg/mL for scFv_cys111), to which the acetonitrile volume and total conjugation volume should be adapted.

- Transfer the antibody solution in a glass vial.
- Add the prepared 0.579 ml of vcMMAE + acetonitrile solution to the antibody solution, for a total 2 ml of solution, where 20% of the volume corresponds to vcMMAE + acetonitrile.
- Incubate for 1h in ice.
- During the incubation, prepare a cysteine solution: dissolve 100 mg of cysteine (C7352, Sigma Aldrich) in 10 ml of PBS+DTPA 1.45 mM solution.
- Once the 1h of incubation has ended, perform the quenching step: add cysteines in a 20 molar proportion with respect to the added vcMMAE: add 34.6 μ l of cysteine solution. Incubate for 30 minutes at room temperature.
- Dialyze with sodium citrate 50 mM (pH = 6) using a G25 Desalting column (GE Healthcare).
- Store at 4°C.

10.11. Characterization drug-antibody ratio (DAR) in conjugated ADCs

In order to assess the DAR of the produced ADCs, different techniques have been employed, mainly: UV/Vis for heterogeneous conjugation to Lysines with DM1,

HPLC-HIC for conjugations to cysteines with vcMMAE, and mass spectrometry (MS) as a more precise validation method.

10.11.1 DAR determination: UV spectroscopy

DAR determination mediating ultraviolet spectroscopy was carried out by measuring the absorbance of the naked antibody and the conjugated ADC at the wavelength of the maximum of absorption of the antibody (280 nm) and the drug (252 nm) and, using these values and the extinction coefficients of each molecule (antibody and drug) at each wavelength, determining the concentration of both antibody and drug in the ADC product. Then, the DAR can be obtained by simply dividing the drug concentration by the antibody concentration, both in molar concentrations.

The absorbance measurements were carried out at an antibody and ADC concentration of 0.3 mg/ml, with a Cary 50 (Varian) spectrophotometer, and with product samples in quartz cuvettes (6030-UV, Hellma).

The extinction coefficients for DM1 and Trastuzumab were obtained bibliographically (Fishkin, 2015; Kim et al., 2014), except for the extinction coefficient of 252 nm for Trastuzumab, which was empirically determined. Used extinction coefficients are summarized in Table 10.8.

Table 10.8. Extinction coefficients of Trastuzumab and DM1

Wavelength (nm)	Extinction coefficients (ϵ) (M^{-1}/cm^{-1})	
	Trastuzumab	DM1
280	103774	5700
252	210863	26350

The used equation for DAR determination consists in the following one (eq. 10.6):

$$[Trastuzumab] = [A_{280} * \epsilon_{DM1(252 \text{ nm})} - A_{252} * \epsilon_{DM1(280)}] / [\epsilon_{Tzmb(280)} * \epsilon_{DM1(252)} - \epsilon_{Tzmb(252)} * \epsilon_{DM1(280)}]$$

$$[DM1] = [A_{280} * \epsilon_{Tzmb(252 \text{ nm})} - A_{252} * \epsilon_{Tzmb(280)}] / [\epsilon_{DM1(280)} * \epsilon_{Tzmb(252)} - \epsilon_{DM1(252)} * \epsilon_{Tzmb(280)}]$$

$$DAR = [DM1] / [Trastuzumab]$$

Where:

- $A_{(\text{wavelength})}$ = absorbance of the molecule at the indicated wavelength
- $\epsilon_{\text{molecule}(\text{wavelength})}$ = extinction coefficient (M^{-1}/cm^{-1}) of the corresponding molecule at the indicated wavelength (nm)

The DAR value was calculated for both the ADC and the unconjugated Trastuzumab. The final DAR value consisted in the obtained DAR value for the ADC minus the obtained DAR value for the naked Trastuzumab.

10.11.2. DAR determination: Hydrophobic Interaction Chromatography

DAR for Trastuzumab-vcMMAE heterogeneous products was determined by using a Hydrophobic Interaction Chromatography (HIC-HPLC). In this type of chromatography, the molecules of interest are separated depending on their hydrophobicity. Applied to ADCs, antibodies loaded with a higher number of drug molecules will be more hydrophobic due to the hydrophobicity of the drug. Therefore, ADC species can be separated depending on the drug molecules number to which they are linked. Hydrophobicity of the ADC specie, and therefore its interaction with the HIC column, will depend not only on the number of drug molecules attached to it, but also on their location on the antibody.

In this case, the column used was a Proteomix HIC Butyl NP5 (4.6x50 mm) (Sepax). Conjugated products were analysed with the following protocol:

Solvents used:

- Solvent A was 2M ammonium sulphate in 25 mM sodium phosphate (pH 7)
- Solvent B was isopropanol 100%
- Solvent C was 25 mM sodium phosphate (pH 7)

The method consisted of the following:

- A flow rate of 0.8 ml/min at room temperature is applied.
- The column is equilibrated with 75% of solvent A and 25% of solvent C.
- Apply a lineal gradient to 25% B and 75% C for 15 min, isocratic gradient of 25% B and 75% C for 5 minutes, lineal gradient to 75% A and 25% C for 10 minutes.
- An injection volume of 10 µl with 1 mg/ml of product was applied.

Drug-loaded antibody species were assigned to the different peaks obtained using information of the manufacturer (Chen, 2015). See the reference example in Figure 10.9, where several ADC species of a cysteine-conjugated Herceptin (Trastuzumab) are depicted, particularly, species of Trastuzumab molecules conjugated to 0, 2, 4, 6 or 8 drug molecules. In the case of the species conjugated to 2, 4 or 6 molecules, more than one species can appear in the HIC profile, due to the location of the conjugated drug (see Fig. 10.12). In the case of the reference profile (Fig. 10.11), two different species of ADC loaded with 4 drug molecules are observed.

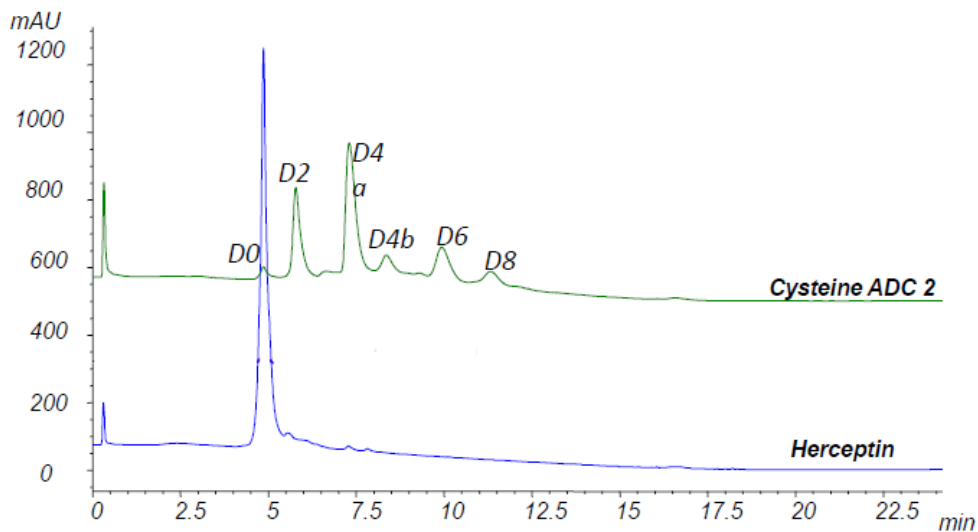


Figure 10.11. HPLC-HIC profiles of Herceptin (Trastuzumab) and an Herceptin derived ADC conjugated to cysteines. Modified from (Chen, 2015). D0 corresponds to unconjugated mAb, D2 to ADC specie with 2 drugs linked; D4a to an ADC specie with 4 drugs linked; D4b to an ADC specie with 4 drugs linked, but in a different position of D4a; D6 corresponds to an ADC specie with 6 drugs linked, and D8 to an ADC specie with 8 drugs linked.

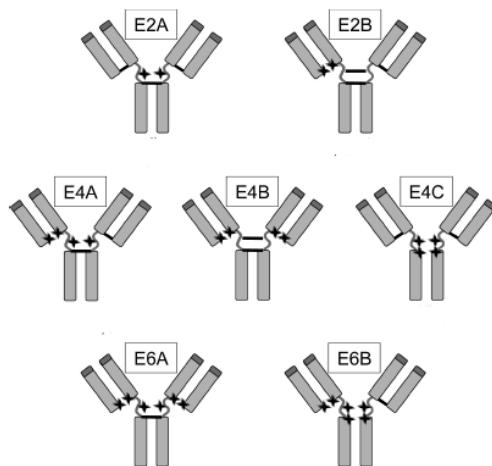


Fig. 10.12. Species of a cysteine conjugated ADC with the payload located on different cysteines, therefore generating species that can run differently in a HIC-HPLC. Modified form (Sun et al., 2005).

The peak area percentage of each specie was used to calculate the weighted average DAR for each molecule (see eq. 10.7, corresponding to the case of the profile depicted in Figure 10.9):

$$DAR = \frac{(2 * Area D2 + 4 * Area D4 + 6 * Area D6 + 8 * Area D8)}{Total\ peak\ area}$$

10.11.3. DAR determination: Mass Spectrometry assay (MS)

In order to assess the DAR of the produced ADCs in a more precise way, mass spectrometry assays were carried out. These were performed in the same way as for the naked Trastuzumab antibody, described in section 10.9.4.

Therefore, the MS assays were performed by the BioOrganic Mass Spectrometry Laboratory (LSMBO) at *Université de Strasbourg* (France). For deglycosylation, the enzyme IgGZero (Genovis) was used, at a ratio of 1 unit enzyme/1 µg IgG, applying an incubation of 30' at 37°C. Samples were manually desalted using a vivaspin 30 kDa ultracentrifugation device (Sartorius) exchanging buffer through five centrifugation cycles to AcONH₄ 150mM pH 6.9. Samples were then analyzed with an Exactive Plus EMR Orbitrap mass spectrometer (ThermoFisher), and data processing was performed using the MassLynx software (Waters).

ADC species were identified taking into account the mass of the naked Trastuzumab antibody or antibody chains, and the linker and drug (see Table 10.9). The relative abundance of each specie was obtained from deconvoluted spectrum profiles (see Fig. 10.13 as an example for the obtained Trastzumab-DM1).

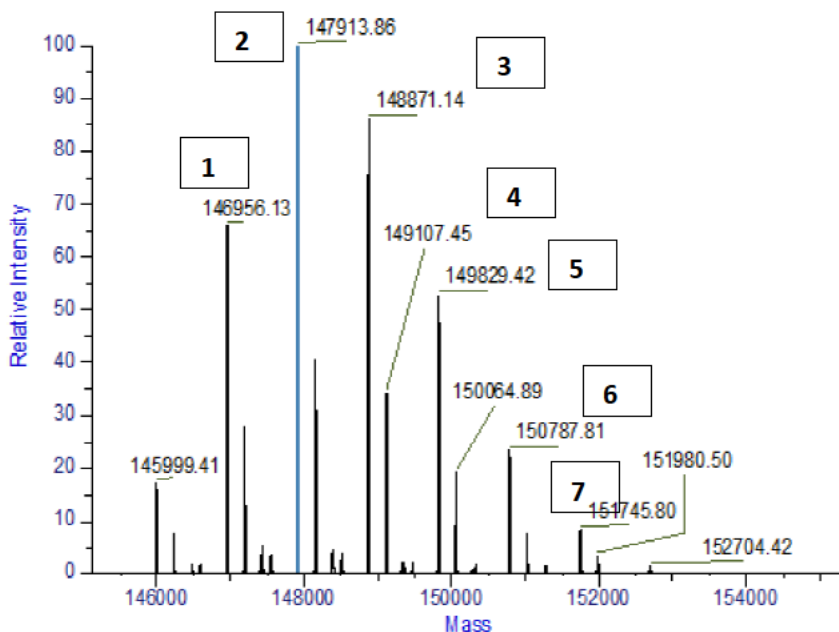


Fig. 10.13: deconvoluted mass spectrum of the analyzed Trastuzumab-DM1 molecule, where the peak with a mass of 145999.41 Da corresponds to the unconjugated Trastuzumab, and the following peaks have their number of conjugated molecules indicated.

Then, the relative intensity percentage of each specie was used to calculate the weighted average DAR for each molecule (see equation 10.8, corresponding to the case of the profile depicted in Figure 10.11):

$$DAR = \frac{(1 * RI1 + 2 * RI2 + 3 * RI3 + 4 * RI4 + 5 * RI5 + 6 * RI6 + 7 * RI7)}{100}$$

Where RI = relative intensity (percentage) of each specie.

10.12. Biological activity assessment of protein and ADC products

Several tests have been used for assessing the in vitro and in vivo activity of the different immunocytokine and ADCs developed.

10.12.1. MTS antiproliferation assay

Microplate assays based on tetrazolium salts are used to investigate activation and damage cellular mechanisms. They are colorimetric assays based on the bioreduction of the tetrazolium salt (MTS) to formazan: the MTS reagent enters the mitochondria of the cells, where succinate dehydrogenase enzyme reduces it to formazan. This reduction is possible only in metabolically active cells: the amount of produced formazan is directly proportional to the number of viable cells in the well. Formazan can then be detected at a wavelength of 492 nm.

In this work, commercial CellTiter 96 Aqueous Non-Radioactive Cell Proliferation Assay MTS (Promega) was used.

This protocol has been followed:

- Define the assay and prepare the cells:
 1. Define the number of products to be tested, and their concentration rang and number of different concentrations tested, in order to establish how many wells of a 96 well plate will be needed. Take into account that 6 replicates of each concentration will performed, as well as an extra 6 wells for medium without product (positive control).
 2. Trypsinize the cells (see 10.3.1.4) and count them (see 10.5.1), and adjust their concentration to $2 \cdot 10^5$ cells/mL by dilution with culture medium.

Chapter 11. Appendix

3. Add 50 μl of cell suspension (10.000 cells) per well. Incubate the plate for 24h at 37°C, 95% humidity and 5% CO₂ (Steri-cult 2000 Incubator, Forma Scientific).
- Prepare the drug sample to be analyzed:
 1. Define the concentration rang of the product to be tested and dilute the product in culture medium accordingly. The product volume in the initial dilution cannot be higher than 10% of the total volume. If the initial product is too diluted, dialyze the sample with Amicon tubes of 4mL.
 2. Product solutions have to be prepared two times more concentrated than the assay final concentration, so as to, when the culture volume is added to the well (see next steps), the final product concentration in the well corresponds to the wanted concentration.
 3. Filter the prepared initial solution with a 0.22 μm filtration with Sterivex filters (10411741, Millipore) in a laminar flow hood (Telstar AV-100).
 4. In the same hood, perform serial dilutions of the prepared concentrated solution with culture medium, accordingly to the concentration rang to be tested, in a 24 well plate (Corning).
 5. Add 50 μl of each product concentration solution to the wells containing the target cells prepared 24h before. Incubate in the same conditions as before, for 72h.
 6. After 72h of incubation, add 20 ml of the MTS reagent to each well and incubate again in the same conditions for 3 hours.
 7. Analyze the plate with the microplate analyzer Labtech LT-4000, recording absorbance at 492 nm.

8. Represent the results as the proliferation percentage, using the proportional absorbance of each condition with respect to the absorbance of the positive control wells.

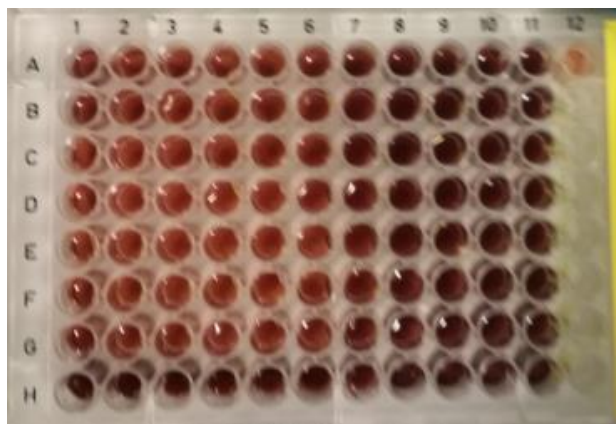


Figure 10.14. 96 well plate of SKBR3 cells treated with Trastuzumab-vcMMAE with MTS added and incubated for 3h.

10.12.2. Lymphocyte proliferation assay

Lymphocyte proliferation assessment serves to analyze the immunomodulation effect of a product of interest. The assay performed in this work had been previously developed at Advanced Therapies Group of the Blood and Tissues Bank (*Banc de Sang i Teixits* (BST), Barcelona). The assay consists in human peripheral blood mononuclear cells (PBMNC, they consist of mononuclear cells: lymphocytes and monocytes) being stained with a fluorescent compound (Carboxy-Fluorescein Diacetate Succinimidyl Ester, CFSE) that is incorporated into the cytoplasm of the cells, therefore allowing to detect the cells that have proliferated, since they have a diminished content of CFSE with respect to the cells that have not proliferated. The detection of the cells was performed by flow cytometry. This test had been previously developed by the Advanced Therapies group, aiming at measuring the impact of mesenchymal stromal cells (MSC) on the proliferation of lymphocytes

(Oliver-Vila et al., 2018). In this case, it was adapted to the assessment of IFN α 2 activity, by replacing the PBMNC incubation with IFN α 2 instead of MSC.

The applied protocol consisted of:

- Isolation of PBMNC cells:
 1. Perform all the blood or cell manipulation test in sterile conditions, in a laminar flow hood.
 2. Dilute 80 ml of blood with 80 ml of PBS in a flask. Blood samples were obtained from donors following the ethical and quality requirements of BST.
 3. Add 15 ml of Lymphoprep density gradient (Stemcell Technologies) to 4 SepMate tubes (Stemcell Technologies).
 4. Add 40 ml of the diluted sample on the density gradient of the SepMate tubes.
 5. Centrifuge the tubes at 1200g for 20 minutes at room temperature.
 6. Collect the supernatant (which contains the mononuclear fraction) of each SepMate tube in a sterile 50 ml tube, by decanting, avoiding the contamination of the supernatant with the erythrocyte fraction.
 7. Add PBS to each of the previous 50 ml tubes with the mononuclear fraction, until it reaches a volume of 50 ml.
 8. Centrifuge at 340-400 g for 10 minutes at room temperature.
 9. Eliminate the supernatant by decanting. Resuspend each pellet with 5-10 ml of PBS and unite the pellets in a single tube. Add again PBS, until reaching 50 ml of volume, and repeat the centrifugation step.
 10. Again, decant the supernatant and resuspend the pellet in 15 ml of PBS.
 11. Take a sample for determining the cell concentration and phenotypic characterization by means of flow cytometry. Dilute it 1:50 with PBS. Cell concentration can alternatively be assessed as

explained in section 10.5.1. This procedure has also been used to determine the viability of the cells.

- Cell concentration and phenotypic characterization with flow cytometry:
 1. Prepare the cell sample to be analyzed, dilute it 1:50 with PBS.
 2. Add, in a cytometer tub:
 - 100 μ l of PBS
 - 50 μ l of sample
 - 50 μ l of Perfect-Count Microsphere solution (Cytognos)
 3. Homogenize the mixture by vortexing for 5 seconds.
 4. On the FACS Calibur cytometer software (BD Biosciences), open the cell counting template and load the related settings.
 5. Acquire 20.000 events (between cells and microspheres).
 6. Define the gates for the cell population and the microspheres population, on the size vs complexity DotPlot. The size is determined with the forward scatter (FSC), while the side scatter (SSC) determines the complexity of the cell.
 7. The number corresponding to cells and microspheres of the total events counted appear in a statistical box. From these numbers, the cell concentration can be determined using the following equation (eq. 10.9):

$$\frac{\text{cell}}{\text{mL}} = \frac{\text{number of cell events}}{\text{number of microsphere events}} \cdot \text{microsphere concentration}$$

- Cell staining with CFSE:
 1. Prepare the CFSE: reconstitute a CFSE vial (from Cell Trace CFSE Cell Proliferation Kit, Thermofisher) with 18 μ l of DMSO, in order to obtain the solution at 5 mM.

Chapter 11. Appendix

2. It is recommended to stain the double of the necessary cells for the assay. Take the necessary suspension volume into a 50 ml tube, add PBS until the total volume is 50 ml and centrifuge it at 340g, 10 minutes, at room temperature.
 3. Eliminate the supernatant by decanting and resuspend the pellet with PBS in the volume that allows obtaining a cell concentration of $1 \cdot 10^7$ cell/ml.
 4. Prepare the CFSE at 4 μ M from the previous stock at 5 mM, prepare at least the same volume in which cells have been resuspended in the previous step.
 5. Mix the cell suspension with the CFSE, and maintain 5 minutes at room temperature gently swirling.
 6. Add 5 volumes of DMEM+10% human serum B pre heated at 37°C.
 7. Centrifuge at 340g, 10 minutes, room temperature.
 8. Resuspend the pellet with 5 ml of the same DMEM+10% human serum B pre heated at 37°C and incubate for 10 minutes at room temperature.
 9. Add 5 volumes of the same medium and centrifuge at 340 g, 10 minutes, room temperature.
 10. Resuspend the pellet with the same medium, use a volume in which the cells will be at $2 \cdot 10^6$ cell/ml.
 11. Incubate the cell suspension at 37°C, 5% CO₂, 95% humidity overnight.
- IFN α 2 and controls addition:
 1. The assay will be carried out in 24 well plates. It is recommended to perform a duplicate for each condition and use $5 \cdot 10^5$ mononuclear cells per well. Take into account that a positive control (stimulation medium) and a negative control (basal medium) need to be considered.

Chapter 11. Appendix

2. The positive control consists in a solution of PMA + ionomycin. PMA is a phorbol ester used as a mitogen for PBMNC; ionomycin is a ionophore which can stimulate the intracellular production of cytokines that result in an activation of lymphocytes.
 3. Take a sample of the PBMNC suspension and count them using the flow cytometer as previously stated. Represent them in a FL1-H histogram. FL1-H is the channel that detects CFSE fluorescence, in order to check that the cells are correctly stained (>90% of the cells between 10^3 - 10^4 of FL1-H, otherwise, the assay must be aborted). Centrifuge at 340g for 10', room temperature, the necessary volume of PBMNC that allows for obtaining the total cell number required ($5 \cdot 10^5 \cdot$ number of conditions), and resuspend the pellet with culture medium at $2 \cdot 10^6$ cell/ml.
 4. Add 0.25 ml of PBMNC suspension to each well of interest of the 24 well plate.
 5. Prepare PMA + ionomycin solution: PMA at 50 ng/ml and ionomycin at 1 μ M. Prepare 0.25 ml for each well of the positive control (for two wells, prepare 0.5 ml). Prepare the solution in culture medium.
 6. Prepare the IFN α 2 solution at the different concentrations to be tested, with 0.25 ml per well.
 7. Add the PMA + ionomycin solution and IFN α 2 solutions at each corresponding well, 0.25 ml per well. Use culture medium as basal medium (negative control).
 8. Incubate the cell suspension at 37°C, 5% CO₂, 95% humidity for 5 days.
- Proliferation determination:
 1. After 5 days, take a sample of each condition and pass it through the flow cytometer, at 20.000 events per condition.

- The cells are represented in a FSC-SSC DotPlot, as well as a FL1-H histogram, in order to determine the proportion of proliferated cells. The threshold for proliferation is indicated using the equivalent condition without stimulation (see Fig. 10.15):

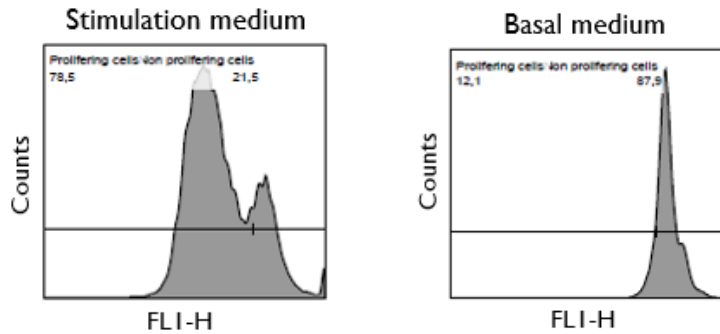


Fig. 10.15: histogram of PBMNC treated with PMA+Ionomycin (stimulation medium) and treated with basal medium.

- The proliferation percentage can be calculated by using equation 10.10:

$$proliferation (\%) = \frac{proliferated\ cells\ (left\ of\ the\ threshold)}{total\ cells} \cdot 100$$

10.12.4. 3D Model generation

Different 3D culture model methodologies have been attempted in this work, including scaffold-free and scaffold-dependent approaches.

10.12.4.1. Hanging drop

The method consists in the trypsinization of the cells and their subsequent resuspension in culture medium and display being pipetted forming a drop on a lid:

Chapter 11. Appendix

- Trypsinize (10.3.1.4) the cells (grown in a T-flask) and resuspend them in culture medium (10.2.1.2) at a concentration of $0.25 \cdot 10^6$ cell/mL.
- Add 5 ml of sterile PBS in the bottom of a tissue culture dish, in order to ensure the hydration of the cells.
- Pipette drops of 20 μ l in the inner side of the lid of the dish. At least 20 drops can be applied on the lid.
- Put again the lid onto the dish and incubate at 37°C, 95% humidity, 5% CO₂.
- After 3 days, transfer the drops into a 96-well plate and observe them with a contrast phase inverted microscope (Nikon, TMS).

Protocol adapted from (Foty, 2011).

10.12.4.2. Culture in Ultra Low Attachment plate

This method relies in the use of ultra-low attachment (ULA) plates, which impair the cellular attachment to the plate surface, forcing the cells to aggregate or form a spheroid.

Protocol:

- Trypsinize the cells from a monolayer to a single-cell suspension.
- Adjust cell concentration to $1 \cdot 10^5$ cells/ml with culture medium.
- Add 50 μ l of cell suspension to each corresponding well of the 96-well ULA plate (4515, Corning).
- Incubate at 37°C, 95% humidity, 5% CO₂ for 24h.
- Observe the cultures with a contrast phase inverted microscope (Nikon, TMS) in order to check the morphology of the spheroid. Pictures of the wells of interest were taken with a Nikon Coolpix 4500 camera.
- Add 50 μ l of culture medium with or without drug content and incubate for 72h.
- Observe the cultures with a contrast phase inverted microscope (Nikon, TMS).

- Perform the corresponding biological activity test (MTS assay (10.12.1) or viability assay with PI (10.12.5)).

10.12.4.3. Embedded seeding

In this approach, the cells grow in a culture medium that contains the extracellular matrix hydrogel Matrigel, which allows the formation of 3D structures. Protocol:

- Thaw Matrigel (E1270, Sigma) at 4°C overnight. Matrigel can only be manipulated at low temperatures, since it starts to form a gel above 10°C.
- Prechill the 96-well plate and the pipette tips to be used (with ice or by putting them in the freezer for example).
- Coat the wells of interest of the prechilled 96-well plate, each well with 5 µl of Matrigel. Spread the solution evenly with a pipette tip or by gently swirling the plate.
- Incubate for 15-30' at 37°C to allow Matrigel to solidify (but do not let it overdry).
- Trypsinize cells from a monolayer to a single-cell suspension.
- Aliquot $N \cdot 45000$ cells, where N corresponds the number of wells to be seeded, into a 1.5 ml microcentrifuge tube and gently pellet the cells by centrifugation at 115g for 1 minute. Add another $0.135 \cdot 10^6$ cells, in a separate tube, for growth culture without matrix (control, 3 wells). Eliminate the supernatant medium pipetting, not decanting.
- On ice, resuspend the cells into the appropriate volume of Matrigel: 75 µl per well ($N \cdot 75$ µl). Resuspend the control cells with 135 µl of volume for each well (405 µl).
- Pipette the mixture of cells and Matrigel onto the precoated wells, add 75 µl to each well. Incubate 30' at 37°C to allow Matrigel to solidify. Then, add 60 µl of culture medium per well.
- Maintain the culture for 10 days, changing medium every 2 days.

Protocol adapted from (Lee et al., 2010).

10.12.4.4. On top seeding

In this culture method, cells grow on top of an hydrogel coating. Protocol:

- Thaw EHS (Matrigel) at 4°C overnight.
- Prechill the 96-well plate and the pipette tips to be used (with ice or by putting them in the freezer for example).
- Coat the prechilled 96-well plate, each well with 15 µl of Matrigel. Coat 3 wells. Spread the solution evenly with a pipette tip.
- Incubate for 15-30' at 37°C to allow Matrigel to solidify (but do not let it overdry).
- Trypsinize cells from a monolayer to a single-cell suspension.
- Aliquot N·7000 cells, where N corresponds the number of wells to be seeded, into a 1.5 ml microcentrifuge tube and gently pellet the cells by centrifugation at 115g. Add $2.1 \cdot 10^4$ cells, in a separate tube, for growth culture without matrix (control, 3 wells).
- Resuspend the cells, in N·30 µl, and seed them on the previously coated wells. Allow the cells to settle and attach to the Matrigel for 10-30' at 37°C.

- Chill the remaining medium on ice and add to it Matrigel to 10% v/v. Necessary medium: 60 µl per well (54 µl + 6 µl Matrigel). Gently add the Matrigel-medium mixture to the each well of interest of the plate.
 - The medium must be thoroughly chilled before addition of Matrigel to ensure homogeneous mixing and even deposition of Matrigel onto cells in culture. Pipette the Matrigel-medium mixture down the side of the well to avoid disturbance of the cells or the Matrigel coating.

- Maintain culture for 4 days, replacing Matrigel-medium mixture every 2 days.

Protocol adapted from (Weigelt et al., 2010).

10.12.4.5. Culture with ULA plate with Matrigel and centrifugation

Combining the culture with ultra-low attachment plates, with Matrigel and a centrifugation in order to promote the aggregation of the cells, results in an alternative strategy to generate spheroids. Protocol:

- Thaw Matrigel at 4°C overnight.
- Prechill the plates and the pipette tips to be used (with ice or by maintaining them in the freezer). Prechill also the media by putting it in the fridge at 4°C.
- Trypsinize SKBR3 cells from a monolayer to a single-cell suspension.
- Adjust cell concentration to $2 \cdot 10^5$ cells/ml with culture medium. Chill the cell suspension by putting them in ice or in the fridge for 10-15'.
- Add 25 µl of cell suspension to each well of interest of the 96-well ULA plate.
- Prepare a 5% (v/v) Matrigel solution with culture medium and add 25 µl of Matrigel solution to each corresponding well. Use chilled pipette tips and maintain chilling conditions. For 2D controls, add 25 µl of culture medium to the well.
- Centrifuge at 1000 g for 10'.
- Incubate at 37°C, 95% humidity and 5% CO₂ for 24 h.
- Observe the cultures with a contrast phase inverted microscope (Nikon, TMS) in order to check the morphology of the spheroid. Pictures of the wells of interest were taken with a Nikon Coolpix 4500 camera.
- Add 50 µl of culture medium with or without drug content and incubate for 72h.
- Observe the cultures with a contrast phase inverted microscope (Nikon, TMS).

- Perform the corresponding biological activity test (MTS assay (10.12.1) or viability assay with PI (10.12.5)).

Protocol adapted from (Ivascu et al., 2007).

10.12.4.6. Confocal microscopy: images and 3D models viability assessment with PI assay

Confocal microscopy uses fluorescence optics, in which laser light is focused onto a spot at a specific depth within the sample, leading to the emission of fluorescent light. A pinhole inside the optical pathway eliminates signals that are out of focus, therefore allowing only the fluorescence signals from the illuminated spot to enter the light detector. This type of microscopy is broadly used to resolve the detailed structure of specific objects inside the cell, which can be specifically labeled using dyes or immunofluorescence, among others. By stacking several images from different optical planes, 3D structures can be analyzed.

In this work, the microscope Leica SP5 has been used at the Microscopy Service of UAB.

The viability determination of the cells relied on their staining with Hoechst dye and with propidium iodide. Hoechst dyes are benzimidazoles that stain the DNA of the total cell population (viable and dead cells), having an emission spectrum at around 461 nm, generating blue light. Propidium iodide is a fluorescent intercalating agent that binds to DNA, but, since it is not membrane-permeable, it only stains the DNA of non-viable cells (necrotic and apoptotic). Therefore, the combination of Hoechst and propidium iodide stainings allows the determination of the viability of the cellular population of a sample.

Protocol:

Chapter 11. Appendix

- Generate the spheroids as described in previous section 10.12.4.5. Proceed with the next step at the moment of viability determination.
 - For the 2D controls, seed 140.000 cells in a MatTek plate. Use one MatTek plate for each condition to be applied.
- For the microscopy observation, transfer the generated spheroids in MatTek plates: with a cut cut 1000 μ L pipette tip, gently aspire the spheroid from the ULA plate and transfer it to the bottom of a 35mm petri dish MatTek plate (P35G-1.5-14-C, MatTek).
- Add 20 μ L of Matrigel on top of the spheroid/s in order to fix it to the plate. Then, add 100 μ L of medium in order to avoid the spheroid drying.
- Before staining it with propidium iodide/Hoechst, gently add 2 ml of culture medium and the usual amount of propidium iodide/Hoechst to the MatTek plate. If the spheroid detaches from the surface, remove the medium until the spheroids remains attached again.
- Staining with propidium iodide and Hoechst:
 - Propidium iodide: add 0.2 μ L of a 1.5 mg/mL stock solution (ThermoFisher), in the 2 mL of culture medium containing the spheroids.
 - Hoechst: add 1 μ L of a 0.5 mg/mL stock solution (ThermoFisher), in the 2 mL of culture medium containing the spheroids
 - Incubate for 15' at 37°C.
- Imaging conditions with Leica SP.5:
 - Z stack: 1.5 μ m between slides, 3 μ m of thickness each slide.
 - 1024x1024 resolution.
 - 10x objective.

The images were then analyzed with the Imaris software. For the 2D control conditions, at least 3 fields were counted.

10.12.6. *In vivo* assay

All the *in vivo* experiments and assays realized have been performed by the Functional Validation and Preclinical Research (FVPR) area of the Vall d'Hebron Institute of Research (VHIR), at Vall d'Hebron hospital, Barcelona.

10.12.6.1. Used mice strains

Several mice strains have been used for the performed *in vivo* assays. All of them were female and of 6-8 weeks old. The strains consist of:

- Nude: they have a mutation consisting in the disruption of the gene *FOXN1*, which is involved in the thymus development, being deficient for T cell activity, and therefore providing a model for tumor engraftment of human cell lines derived from solid tumors. The nude mutation (*Foxn1^{nu}*) also affects the mouse hair growth, giving way to its naming as “nude”.
 - For the SKBR3 cells mice generation model experiment, BALB/c nude mice were employed, from the breeder Charles River.
 - For the BT474 cells mice generation model experiment, Hsd:Athymic nude mice were used, from the breeder Envigo.
- NOD-SCID: mice homozygous for the severe combined immunodeficiency (SCID) mutation are deficient for both T and B cells and are thus characterized by an absence of both innate and adaptative immune response. The NOD strain background provides intrinsic defects in innate immunity, including lowered NK cell activity, reduced levels of macrophage activation, abnormal dendritic cell. This strain was used for the SKBR3 cell line mice generation model experiment, from the breeder Charles River.
- Rag: they are a class of SCID mice which present the advantage of not generating any T and B cell, whereas SCID mice with the *Pkrdc^{SCID}* mutation are “leaky”, meaning that they can generate low amounts of T and B cells.

This strain was used for the SKBR3 cell line mice generation model experiment, from the breeder Charles River.

10.12.6.2. Mice housing

The animals were randomly housed under Specific Pathogen Free (SPF) conditions in autoventilated racks.

- Habitat: animals were housed in groups of five, in Innocage® IVC mouse type II 523 cm² cages (Innovive). Two enrichment elements were included, a cardboard tube and a square nestlet for nesting and thermoregulation.
- Cage litter: sterile corn cob bedding was used (Innovive). The provider guarantees that the litter was analyzed according to the regulations of the manufacturer for contaminants.
- Feed: maintenance 14% protein rodent irradiated diet, in cases of 10 kg vacuum packs (Capsumlab, Spain) *ad libitum*. The provider guarantees that the feed was analyzed according to the regulations of the manufacturer for contaminants.
- Drink: disposable water bottles decalcified and sterile (Innovive) *ad libitum*. The provider guarantees that the water was regularly analyzed microbiologically, physico-chemically and chemically; and the analytical results proved that the limits set by the Spanish regulations for human drinking water have been observed (drinking: Real Decreto 140/2003).
- Temperature and relative humidity: temperature and relative humidity is continuously recorded in the animal housing. The temperature ranged from 23°C to 25°C. Relative humidity ranged between 10% and 42%.
- Lighting: lighting was artificial, from an automatic controlled supply. The cycle gradually stimulates twilight and sunset from 7:30 to 8:00 am and from 19:30 to 20.00 pm respectively, giving 12h of light with an intensity of 300 Lux and 12h of darkness for each 24h period.

10.12.6.3. Mice model generation: tumor engraftment

For both SKBR3 and BT474 cells, they were confirmed to be negative for viral, bacterial (mycoplasma, among others) and parasite pathogens prior to inoculation.

Cells were trypsinized, and viability prior to inoculation was checked to be higher than 97%.

Cells were resuspended with sterile PBS at a concentration of $200 \cdot 10^6$ cell/ml, and then mixed in a 1:1 proportion with Matrigel. 100 μ l of the mixture was then orthotopically injected (into the mammary fat pad) to each mouse ($10 \cdot 10^6$ cells per mouse).

Tumor measure was carried out each 3-7 days, tumor volume was measured by caliper measurements and calculated according to the formula $Dxd^2/2$, where D is the larger diameter of the tumor and d the smaller one.

10.12.6.4. Mice ADC treatment

In the case of mice engrafted with BT474 cells, when the tumors reached a volume of 75-125 mm³, the activity assay of the ADC was started.

Mice were randomized according to the tumor volume in two groups: one of 8 mice for the vehicle (sodium citrate 50 mM, pH = 6), and another of 10 mice for the ADC (contained in the same sodium citrate buffer). Administrations of the vehicle or the ADC were performed in the tail of the mice, intravenously. Both groups were treated with the same frequency, and body weight, tumor volume and physical appearance of the animals were monitored during all the study until the end of the experiment.

At the end time point, animals were euthanized by cervical dislocation, and mammary primary tumors were obtained. The animals were euthanized following the defined euthanasia standard operating procedure when reached the established

ethical criteria's (in accordance with the protocol approved by Vall d'Hebron's Experimental Animal Ethics Committee (CEEA), 05/16). Whenever possible, tumors were weighted and measured *ex vivo* using a caliper.

10.13. References

- BT-474 ATCC[®] HTB-20[™] Homo sapiens mammary gland; breast/duc. (2016). Retrieved March 20, 2019, from <https://www.atcc.org/products/all/HTB-20.aspx>
- Chen, H. (2015). *Sepax HIC hydrophobic interaction separation*. Retrieved from www.sepax-tech.com
- Clontech. (2008). *pIRESneo3 Vector Information*. Retrieved from www.clontech.com
- Clontech. (2010). pIRESpuro3 Vector Map and Multiple Cloning Site (MCS). Retrieved March 13, 2019, from www.clontech.com
- Fishkin, N. (2015). Maytansinoid–BODIPY Conjugates: Application to Microscale Determination of Drug Extinction Coefficients and for Quantification of Maytansinoid Analytes. *Molecular Pharmaceutics*, 12(6), 1745–1751. <https://doi.org/10.1021/mp500843r>
- Foty, R. (2011). A simple hanging drop cell culture protocol for generation of 3D spheroids. *Journal of Visualized Experiments: JoVE*, (51). <https://doi.org/10.3791/2720>
- Ivascu, A., & Kubbies, M. (2007). Diversity of cell-mediated adhesions in breast cancer spheroids. *International Journal of Oncology*, 31(6), 1403–1413. <https://doi.org/10.3892/ijo.31.6.1403>
- Kim, M. T., Chen, Y., Marhoul, J., & Jacobson, F. (2014). Statistical Modeling of the

Chapter 11. Appendix

Drug Load Distribution on Trastuzumab Emtansine (Kadcyla), a Lysine-Linked Antibody Drug Conjugate. *Bioconjugate Chemistry*, 25(7), 1223–1232. <https://doi.org/10.1021/bc5000109>

Lee, G. Y., Kenny, P. a, Lee, E. H., & Bissell, M. J. (2010). Three-dimensional culture models of normal and malignant breast epithelial cells. *Nature Methods*, 4(4), 359–365. <https://doi.org/10.1038/nmeth1015>. Three-dimensional

Liste-Calleja, L. (2015). *Study and characterisation of human HEK293 cell line as a platform for recombinant protein production*. Universitat Autònoma de Barcelona.

MabSelect SuRe antibody purification resin - GE Healthcare Life Sciences. (2019). Retrieved April 2, 2019, from <https://www.gelifesciences.com/en/ro/shop/chromatography/resins/affinity-antibody/mabselect-sure-antibody-purification-resin-p-00700#overview>

Oliver-Vila, I., Ramírez-Moncayo, C., Grau-Vorster, M., Marín-Gallén, S., Caminal, M., & Vives, J. (2018). Optimisation of a potency assay for the assessment of immunomodulative potential of clinical grade multipotent mesenchymal stromal cells. *Cytotechnology*, 70(1), 31–44. <https://doi.org/10.1007/s10616-017-0186-0>

pET System Manual Novagen 1. (1992). Retrieved from <https://research.fhcrc.org/content/dam/stripe/hahn/methods/biochem/pet.pdf>

Pinsach i Boada, J. (2009). *Development of recombinant aldolase production process in Escherichia coli*. TDX (Tesis Doctorals en Xarxa). Universitat Autònoma de Barcelona. Retrieved from <https://www.tdx.cat/handle/10803/5325>

QCL-1000™ Endpoint Chromogenic LAL Assay| Lonza. (2015). Retrieved April 1, 2019, from https://bioscience.lonza.com/lonza_bs/PR/en/Endotoxin-

Chapter 11. Appendix

Detection/p/000000000000182374/QCL-1000-Endpoint-Chromogenic-LAL-Assay

Saiki, R. K., Gelfand, D. H., Stoffel, S., Scharf, S. J., Higuchi, R., Horn, G. T., ... Erlich, H. A. (1988). Primer-directed enzymatic amplification of DNA with a thermostable DNA polymerase. *Science (New York, N.Y.)*, 239(4839), 487–491. <https://doi.org/10.1126/SCIENCE.239.4839.487>

SK-BR-3: Human Breast Cancer Cell Line (ATCC HTB-30). (2018). Retrieved March 19, 2019, from <https://www.mskcc.org/research-advantage/support/technology/tangible-material/human-breast-cell-line-sk-br-3>

Soule, H. D., Vazquez, J., Long, A., Albert, S., & Brennan, M. (1973). A Human Cell Line From a Pleural Effusion Derived From a Breast Carcinoma 2. *JNCI: Journal of the National Cancer Institute*, 51(5), 1409–1416. <https://doi.org/10.1093/jnci/51.5.1409>

Subik, K., Lee, J.-F., Baxter, L., Strzepek, T., Costello, D., Crowley, P., ... Tang, P. (2010). The Expression Patterns of ER, PR, HER2, CK5/6, EGFR, Ki-67 and AR by Immunohistochemical Analysis in Breast Cancer Cell Lines. *Breast Cancer : Basic and Clinical Research*, 4, 35–41. Retrieved from <http://www.ncbi.nlm.nih.gov/pubmed/20697531>

Sun, M. M. C., Beam, K. S., Cervený, C. G., Hamblett, K. J., Blackmore, R. S., Torgov, M. Y., ... Alley, S. C. (2005). Reduction–Alkylation Strategies for the Modification of Specific Monoclonal Antibody Disulfides. *Bioconjugate Chemistry*, 16(5), 1282–1290. <https://doi.org/10.1021/bc050201y>

Thermo Scientific. (2010). Thermo Scientific™ pUC57 DNA 50µg Ver productos. Retrieved March 27, 2019, from <https://www.fishersci.es/shop/products/fermentas-puc57-dna/10765071>

Chapter 11. Appendix

- Thomas, P., & Smart, T. G. (2005). HEK293 cell line: A vehicle for the expression of recombinant proteins. *Journal of Pharmacological and Toxicological Methods*, 51(3), 187–200. <https://doi.org/10.1016/J.VASCN.2004.08.014>
- Uphoff, C. C., & Drexler, H. G. (2014). Detection of Mycoplasma Contamination in Cell Cultures. In *Current Protocols in Molecular Biology* (Vol. 106, p. 28.4.1-28.4.14). Hoboken, NJ, USA: John Wiley & Sons, Inc. <https://doi.org/10.1002/0471142727.mb2804s106>
- Weigelt, B., Lo, A. T., Park, C. C., Gray, J. W., & Bissell, M. J. (2010). HER2 signaling pathway activation and response of breast cancer cells to HER2-targeting agents is dependent strongly on the 3D microenvironment. *Breast Cancer Research and Treatment*, 122(1), 35–43. <https://doi.org/10.1007/s10549-009-0502-2>

Chapter 11. Appendix

11.1 Appendix I. Genetic and protein sequences

11.1.1 Trastuzumab heavy chain (HC)

ATGGACTGGACCTGGAGATTCTCTTTGTGGTGGCTGCAGCCACAGGTGTCCAGAGTGAAGTGCAGCTG
GTAGAGTCAGGAGGAGGTCTTGTTCAGCCCGGTGGCTCCCTGAGGCTCAGCTGTGCTGCTTCTGGTTTC
AACATCAAGGATACCTATATCCACTGGGTTCAGGCAGGCTCCTGGCAAAGGCCTGGAATGGGTGGCCAGG
ATCTACCCACCAACGGCTACACCAGATATGCTGATTCTGTCAAGGGCCGCTTACCATTTCTGCTGAC
ACCTCTAAGAATACAGCCTACCTGCAGATGAACAGTCTGAGAGCTGAGGACACTGCAGTGTACTACTGC
AGCCGCTGGGGTGGAGATGGCTTCTATGCCATGGATTACTGGGGCCAGGGCACTCTGGTTACTGTTTCT
TCTGCCAGCACAAAGGGTCCCAGTGTTTTCCCCTGGCCCCTAGCAGCAAAGCACTTCTGGAGGCACA
GCTGCCCTGGGCTGTCTGGTGAAGACTACTTCCCAGAACCCTGTGACTGTCTCCTGGAACAGCGGTGCC
TTGACCAGTGGAGTGCACACCTTCCCTGCTGTCTTCAGAGCAGTGGCCTCTACTCCCTCTCTCTGTT
GTGACAGTCCCCCTCCAGCCTTGGCACCAGACCTACATCTGCAATGTCAATCACAAGCCCAGCAAC
ACCAAGGTGGATAAGAAGGTTGAGCCACCCAAGTCCCTGTGACAAAACCTCACACATGTCCTCCCTGCCA
GCTCCAGAGCTGCTGGGTGGTCTTCAGTCTTCTTGTTCCTCCAAAGCCTAAGGACACACTGATGATC
AGCAGGACTCCTGAAGTACCTGTGTGGTTGTTGATGTGTCTCATGAAGATCCCAGGTGAAGTTAAC
TGGTATGTGGATGGTGTGGAAGTTCACAATGCCAAAACCAAAGGGAGGAGCAGTACAACCTCCACA
TACAGAGTGGTCAAGTGTGCTCACAGTGTGCACCAGGACTGGCTGAATGGCAAGGAGTACAAGTGCAAA
GTGTCCAACAAGGCTGTGCTGCCCCATTGAGAAGACCATCTCCAAGGCCAAGGGACAGCCAAGAGAG
CCCCAGGTGTATACACTTCCCTCCTTCCAGAGATGAGCTCACCAAGAACCAGGTGAGCCTGACCTGCCCTG
GTCAAAGGATTCTACCCAAGTGACATTGCTGTGGAGTGGGAGAGCAATGGGCAGCCTGAGAACAACACTAC
AAAACAACCTCCACCTGTCTGGCAGTGTGGAAGCTTCTTCTGTACAGCAAGCTGACTGTGGACAAG
AGCAGATGGCAGCAGGGAATGTCTTCTCCTGTCTGTGATGCATGAGGCCCTCCACAACCACTACACA
CAGAAGTCACTGTCTCTGAGCCCTGGGAAGTGA

11.1.2. Trastuzumab light chain (LC)

ATGGACATGAGAGTTCCTGCCAGCTGCTGGGGCTGCTTCTCTGTGGCTGTCTGGTGGCCGCTGTGAC
ATCCAGATGACCCAGAGCCCCCTCCTCCCTGAGTGCCAGTGTGGGAGACAGAGTGACCATCACCTGCAGA
GCTTCTCAGGATGTGAACACAGCTGTGGCCTGGTACCAGCAGAAGCCTGGCAAGCCCCCAAGCTGCTC
ATCTACTCTGCCTCCTTCCCTGTACAGTGGTGTGCCAGCCGCTTCTCTGGAAGCAGAAGTGGCACAGAC
TTCACCCTGACCAATTTCTTCTTTCAGCCTGAAGATTTGCCACATACTACTGCCAGCAGCACTACACC
ACCCCTCCCACCTTTGGCCAGGGAACCAAAGTGGAGATCAAGAGGACTGTGGCTGCTCCTTCTGTCTTC
ATCTTCCCACCCAGTGTATGAGCAACTGAAGTCTGGGACAGCCTCTGTGGTGTGCTGCTCAACAACCTT
TACCCAAGAGAGGCCAAGGTGCAAGTGGAAAGTGGACAATGCCCTGCAGTCTGGCAACAGCCAGGAGAGC
GTGACAGAGCAGGACTCCAAGGACAGCACCTACAGCCTGAGCAGCACACTGACTCTCAGCAAGGCTGAC
TATGAGAAGCACAAAGTCTATGCCTGTGAGGTGACTCACAGGCCTGTCCAGCCCAGTCACCAAGAGC
TTCACAGAGGAGAGTGTAA

11.1.3. Trastuzumab heavy chain with A114C mutation (Trastuzumab_cys114)

ATGGACTGGACCTGGAGATTCTCTTTGTGGTGGCTGCAGCCACAGGTGTCCAGAGTGAAGTGCAGCTG
GTAGAGTCAGGAGGAGGTCTTGTTCAGCCCGGTGGCTCCCTGAGGCTCAGCTGTGCTGCTTCTGGTTTC
AACATCAAGGATACCTATATCCACTGGGTTCAGGCAGGCTCCTGGCAAAGGCCTGGAATGGGTGGCCAGG
ATCTACCCACCAACGGCTACACCAGATATGCTGATTCTGTCAAGGGCCGCTTACCATTTCTGCTGAC
ACCTCTAAGAATACAGCCTACCTGCAGATGAACAGTCTGAGAGCTGAGGACACTGCAGTGTACTACTGC

Chapter 11. Appendix

AGCCGCTGGGGTGGAGATGGCTTCTATGCCATGGATTACTGGGGCCAGGGCACTCTGGTTACTGTTTCT
TCTTGCAGCACAAAAGGGTCCCAGTGTTTTCCCCCTGGCCCCTAGCAGCAAAGCACTTCTGGAGGCACA
GCTGCCCTGGGCTGTCTGGTGAAAGACTACTCCCAGAACCCTGTGACTGTCTCCTGGAACAGCGGTGCC
TTGACCAGTGGAGTGCACACCTTCCCTGCTGTCTTCCAGAGCAGTGGCCTCTACTCCCTCTCCTCTGTT
GTGACAGTCCCCCTCCAGCCTTGGCACCCAGACCTACATCTGCAATGTCAATCACAAGCCCAGCAAC
ACCAAGGTGGATAAGAAGGTTGAGCCACCCAAGTCTGTGACAAAACCTCACACATGTCTCCTCCCTGCCCA
GCTCCAGAGCTGCTGGGTGGTCCCTCAGTCTTCTTGTTCCTCCAAAGCCTAAGGACACACTGATGATC
AGCAGGACTCCTGAAGTACCTGTGTGGTTGTTGATGTGTCTCATGAAGATCCCAGGTTGAAGTTAAC
TGGTATGTGGATGGTGTGGAAGTTCACAATGCCAAAACCAAGGGAGGAGCAGTACAACCTCCACA
TACAGAGTGGTCAGTGTGCTCACAGTGTGCACCAGGACTGGCTGAATGGCAAGGAGTACAAGTGCAAA
GTGTCCAACAAGGCTCTGCCTGCCCCATTGAGAAGACCATCTCCAAGGCCAAGGGACAGCCAAGAGAG
CCCCAGGTGTATACTTCCCTCCTCCAGAGATGAGCTCACCAAGAACCAGGTCAGCCTGACCTGCCTG
GTCAAAGGATTCACCCAAGTGACATTGCTGTGGAGTGGGAGAGCAATGGGCAGCCTGAGAACAACCTAC
AAAACAACCTCCACCTGTCTGGACAGTGTGGAAGCTTCTTCTGTACAGCAAGCTGACTGTGGACAAG
AGCAGATGGCAGCAGGGAAATGTGTTCTCTCTGCTCTGTGATGCATGAGGCCCTCCACAACCACTACACA
CAGAAGTCACTGTCTCTGAGCCCTGGGAAGTGA

11.1.4. scFv DNA sequence

ATGGACATCCAGATGACCCAGAGCCCCTCCTCCCTGAGTGCCAGTGTGGGAGACAGAGTGACCATCACC
TGCAGAGCTTCTCAGGATGTGAACACAGCTGTGGCCTGGTACCAGCAGAAGCCTGGCAAGGCCCCCAAG
CTGCTCATCTACTCTGCCTCCTTCTGTACAGTGGTGTGCCAGCCGCTTCTCTGGAAGCAGAAGTGGC
ACAGACTTCACCTGACCATTTCTTCTTTCAGCCTGAAGATTTTGCCACATACTACTGCCAGCAGCAC
TACACCACCCCTCCACCTTTGGCCAGGGAACCAAAGTGGAGATCAAGAGGACTGGCTCTACTTCCGGT
AGCGGTAACCCGGATCAGGCCAAGGATCGACTAAAGGCCAAGTGCAGCTGGTAGAGTCAGGAGGAGGT
CTTGTTTCAGCCCGTGGCTCCCTGAGGCTCAGCTGTGCTGCTTCTGGTTTCAACATCAAGGATACCTAT
ATCCTACTGGGTACGCAGGCTCCTGGCAAAGCCTGGAATGGGTGGCCAGGATCTACCCACCAACGGC
TACACCAGATATGCTGATTCTGTCAAGGGCCGCTTACCATTTCTGCTGACACCTCTAAGAATACAGCC
TACCTGCAGATGAACAGTCTGAGAGCTGAGGACACTGCAGTGTACTACTGCAGCCGCTGGGGTGGAGAT
GGCTTCTATGCCATGGATTACTGGGGCCAGGGCACTCTGGTTACTGTTTCTTCT

11.1.5. scFv_cys111 DNA sequence

ATGGACATCCAGATGACCCAGAGCCCCTCCTCCCTGAGTGCCAGTGTGGGAGACAGAGTGACCATCACC
TGCAGAGCTTCTCAGGATGTGAACACAGCTGTGGCCTGGTACCAGCAGAAGCCTGGCAAGGCCCCCAAG
CTGCTCATCTACTCTGCCTCCTTCTGTACAGTGGTGTGCCAGCCGCTTCTCTGGAAGCAGAAGTGGC
ACAGACTTCACCTGACCATTTCTTCTTTCAGCCTGAAGATTTTGCCACATACTACTGCCAGCAGCAC
TACACCACCCCTCCACCTTTGGCCAGGGAACCAAAGTGGAGATCAAGAGGACTGGCTCTACTTCC
GGTAGCGGTAACCCGGATCAGGCCAAGGATCGACTAAAGGCCAAGTGCAGCTGGTATGTGAGTCAGGA
GGAGGTCTTGTTCAGCCCGTGGCTCCCTGAGGCTCAGCTGTGCTGCTTCTGGTTTCAACATCAAGGAT
ACCTATATCCACTGGGTACAGGCAGGCTCCTGGCAAAGCCTGGAATGGGTGGCCAGGATCTACCCACC
AACGGCTACACCAGATATGCTGATTCTGTCAAGGGCCGCTTACCATTTCTGCTGACACCTCTAAGAAT
ACAGCCTACCTGCAGATGAACAGTCTGAGAGCTGAGGACACTGCAGTGTACTACTGCAGCCGCTGGGGT
GGAGATGGCTTCTATGCCATGGATTACTGGGGCCAGGGCACTCTGGTTACTGTTTCTTCT

In yellow, the inserted cys111 codon.

11.1.6. Mature scFv protein sequence

DIQMTQSPSSLSASVGDRVTITCRASQDVNTAVAWYQQKPGKAPKLLIYSASFLYSGVPSRFS
 GSRSGTDFLTISLQPEDFATYYCQQHYTTPPTFGQGTKVEIKRTGSTSGSGKPGSGEGSTKG
 EVQLVESGGGLVQPGGSLRLSCAASGFNIKDTYIHWVRQAPGKGLEWVARIYPTNGYTRYAD
 SVKGRFTISADTSKNTAYLQMNSLRAEDTAVYYCSRWGGDGFYAMDVWGQGLTVVSS

In blue, variable light chain sequence; in grey, 218 linker; in green, variable heavy chain sequence. In the case of the expression in *E. coli*, an extra methionine (M) residue was added at the beginning of the mature protein sequence in order to allow its expression.

11.1.7. Mature scFv_cys111 protein sequence

DIQMTQSPSSLSASVGDRVTITCRASQDVNTAVAWYQQKPGKAPKLLIYSASFLYSGVPSRFS
 GSRSGTDFLTISLQPEDFATYYCQQHYTTPPTFGQGTKVEIKRTG^CSTSGSGKPGSGEGSTKG
 GEVQLVESGGGLVQPGGSLRLSCAASGFNIKDTYIHWVRQAPGKGLEWVARIYPTNGYTRYA
 DSVKGRFTISADTSKNTAYLQMNSLRAEDTAVYYCSRWGGDGFYAMDVWGQGLTVVSS

In blue, variable light chain sequence; in grey, 218 linker; in green, variable heavy chain sequence; in red, the added cysteine at the 111 location.

11.1.8. Mature human Interferon- α 2 sequence

TGTGATCTGCCTCAAACCCACAGCCTGGGTAGCAGGAGGACCTTGATGCTCCTGGCACAGATGAGGAGA
 ATCTCTCTTTTCTCCTGCTTGAAGGACAGACATGACTTTGGATTTCCCCAGGAGGAGTTTGGCAACCAG
 TTCAAAAGGCTGAAACCATCCCTGTCTCCATGAGATGATCCAGCAGATCTTCAATCTCTTCAGCACA
 AAGGACTCATCTGCTGCTTGGGATGAGACCCCTCTAGACAAATCTACACTGAAGTCTACCCAGCAGCTG
 AATGACCTGGAAGCCTGTGTGATACAGGGGTGGGGGTGACAGAGACTCCCCGTGATGAAGGAGGACTCC
 ATCTGGCTGTGAGGAAATACTTCCAAAGAATCACTCTCTATCTGAAAGAGAAGAAATACAGCCCTTGT
 GCCTGGGAGGTTGTCAGAGCAGAAATCATGAGATCTTTTCTTGTCAACAAACTTGCAAGAAAGTTTA
 AGAAGTAAGGAATGA

11.2. Appendix II. Oligonucleotides

11.2.1. Oligonucleotides for Trastuzumab-IFN α 2 fusion protein construction

Description	Sense	DNA sequence
Tzmb	Fw	ATTAGGAATTCATGGACTGGACCTGGA
Tzmb- IFN α 2	Rv	ATCACATGAACCACCTCCTCCCTTCCCAGGGCTCAGAGACAG
Tzmb- IFN α 2	Fw	GGAAGGGAGGAGGTGGTTCATGTGATCTGCCTCAAACCCAC
IFN α 2	Rv	AATGGATCCTCATTCTTACTTCTTAA

In yellow, restriction sites indicated. In blue, in green, the sequence corresponding to Trastuzumab is highlighted, in blue, the sequence corresponding to IFN α 2, and in violet, the sequence corresponding to the GGS linker.

11.2.2. Oligonucleotides for Trastuzumab_cys114 construction

Sense	DNA sequence
Fw	CGAATTCGGATCCATGGACTGGA
Rv	ACTGGGACCTTTGTGCTGCAAGAA

In yellow, restriction sites indicated. In green, the two mutated nucleotides that generate the A114C mutation.

11.2.3. Oligonucleotides for scFv construction

Description	Sense	DNA sequence
LC (<i>E. coli</i>)	Fw	ATACCATGGACATCCAGATGAC
LC (HEK293)	Fw	ATAGCTAGCATGGACATGAGAGTTCCTGC
LC-Linker	Rv	CTGATCCGGGTTTACCGCTACCGGAAGTAGAGCCAGTC CTCTTGATCTCCACTTTGGTTC
HC-Linker	Fw	GTA AACCCGGATCAGGCGAAGGATCGACTAAAGGCCGA AGTGCAGCTGGTAGAGTCAGG
HC	Rv	ATTAAGAATTCCTAAGAAGAAACAGTAACC

In yellow, restriction sites indicated. In light green, the sequence corresponding to variable LC region is highlighted; in blue, the sequence corresponding to variable HC region; in grey, the stop codon; and in red and violet, the sequence corresponding to the 218 linker. The sequence of the 218 linker highlighted in red corresponds to the overlapping sequence.

11.2.4. Oligonucleotides for scFv_{cys111} construction

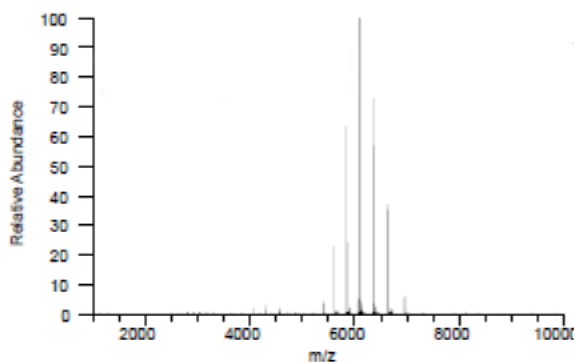
Description	Sense	DNA sequence
LC	Fw	ATAGCTAGCATGGACATGAGAGTTCCTGC
LC-Linker	Rv	CCGCTACCGGAAGTAGAACAGCCAGTCCTCTTGATCT
HC-Linker	Fw	AGATCAAGAGGACTGGCTGTTCTACTTCCGGTAGCGG
HC	Rv	ATTAAGAATTCCTAAGAAGAAACAGTAACC

In yellow, restriction sites indicated. In light green, the sequence corresponding to variable LC region is highlighted; in blue, the sequence corresponding to variable HC

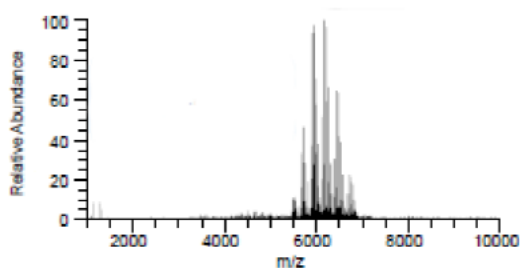
region; in grey, the stop codon; in red, the sequence corresponding to the 218 linker, and in dark blue, the codon codifying for cys111.

11.3 Appendix III. Mass Spectrometry profiles

11.3.1. Full mass spectrum of Trastuzumab



11.3.2. Full mass spectrum of Trastuzumab-DM1



11.3.3. Full mass spectrum of Trastuzumab-vcMMAE DAR 8

